

https://dspace.org/

Ecdysone receptor knockdown: implications on longevity, reproductive success and plasmodium susceptibility in the malaria vector anopheles funestus

Maharaj, Surina

2021

https://hdl.handle.net/10539/32553

Downloaded from a DSpace repository. https://dspace.org/



Ecdysone Receptor Knockdown: Implications on Longevity, Reproductive Success and *Plasmodium* Susceptibility in the Malaria Vector *Anopheles funestus.*

Surina Maharaj

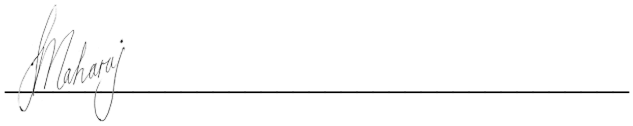
A Dissertation submitted to the Faculty of Health Sciences, University of the Witwatersrand, Johannesburg, in fulfilment of the requirements for the degree of Master of Science in Medicine.

Johannesburg, 2021

Declaration

I, Surina Maharaj declare that this Dissertation is my own, unaided work. It is being submitted for the Degree of Masters of Science at the University of Witwatersrand, Johannesburg.

It has not been submitted before for any degree or examination at any other University.



Surina Maharaj

28 day of June 2021 in Johannesburg

Publications arising from this study

1. Ekoka, E., **Maharaj, S.,** Nardini, L., Dahan-Moss, Y., Koekemoer, L.L. (2021) **20-Hydroxyecdysone (20E) signalling as a promising target for the chemical control of malaria vectors.** Parasites and Vectors, 14 (86).

https://doi.org/10.1186/s13071-020-04558-5

(Supplementary file 1)

Role in publication: Co-wrote the first draft of manuscript and critically read all its subsequent versions.

2. **Maharaj, S.,** Ekoka, E., Erlank, E., Nardini, L., Koekemoer, L.L. (2021) **The Ecdysone receptor regulates several key physiological factors in malaria vector *Anopheles funestus*.** Manuscript in Preparation.

Role in publication: Wrote the first draft and contributed to all subsequent versions of the manuscript, contributed to the study design, performed the experiments, interpreted and analysed the data.

Presentations arising from this research

Maharaj, S., Ekoka, E., Nardini, L., Koekemoer, L.L. (2020). **Ecdysone receptor knockdown reduces longevity in the malaria vector *Anopheles funestus*.** Wits Faculty of Health Sciences Biennial Research Day, 15 October 2020.

Role in presentation: Conducted research, analysed and interpreted data and wrote first and subsequent drafts of presentation.

Abstract

Malaria is a devastating disease in humans, transmitted by female *Anopheles* mosquitoes infected with *Plasmodium* parasites. Current insecticide-based strategies exist to control the spread of malaria by targeting vectors. Unfortunately, the effectiveness of these vector control methods is declining due to increasing insecticide resistance in vector populations. It is therefore essential to develop novel vector control methods that can efficiently target transmission reducing factors such as vector density (influenced by vector survival and reproduction) and competence (influenced by transmission ability). A possible vector control candidate gene, the ecdysone receptor (EcR) regulates longevity, reproduction, immunity, as well as many other physiological processes in several insects and malaria vectors. The malaria vector, *Anopheles funestus* (*An. funestus*) is responsible for the majority of malaria outbreaks in South Africa, however, the function of *EcR* in this vector has not previously been studied. This study therefore aimed to determine the extent of *EcR* regulation on longevity, reproduction and susceptibility to *Plasmodium falciparum* (*P. falciparum*) in *An. funestus*. In this study, RNA interference was used to reduce *EcR* expression levels in *An. funestus* females and investigate how it impacted their longevity, reproduction and susceptibility to *P. falciparum* infection. Additionally, the expression levels of *EcR*, and reproduction genes lipophorin (*Lp*) and vitellogenin receptor (*VgR*) as well as the immune gene, leucine rich immune molecule 9 (*LRIM9*) were determined using qPCR and relative expression analysis was performed. *EcR*-depleted mosquitoes had a shorter lifespan, were less fecund, less fertile, and had reduced *P. falciparum* infection intensity. Moreover, gene expression analyses revealed that mosquitoes with reduced *EcR* expression also had depleted *Lp, VgR* and *LRIM9* expression levels. As EcR regulates processes affecting vector density and competence, this study provides the first experimental evidence that supports EcR as a novel target in the development of vector control measures targeting *An. funestus*.

Acknowledgements

I would like to express my sincere appreciation to my supervisors Prof Lizette Koekemoer and Ms Elodie Ekoka for the endless guidance, support and extensive knowledge they have provided to me throughout this project. Thank you for all the encouragement and helpful advice given to me and all the skills you've taught me.

I would also like to extend my deepest gratitude to Dr Luisa Nardini for her invaluable contribution towards the technical aspects of my project and for teaching me new and fundamental laboratory skills. Thank you for all your insightful suggestions and advice.

I very much appreciate the help of Ms Erica Erlank, Mr Nelius Venter and Dr Luisa Nardini in several aspects of the *Plasmodium* infection work. The completion of my work would have been very difficult without your assistance.

I'm extremely grateful for the assistance of Mrs Clowey Stevenson with day to day tasks in and around the lab.

I'd also like to gratefully acknowledge Prof Lizette Koekemoer and the National Research Foundation for providing me with financial support.

Table of contents

Declaration i
Publications arising from this study ii
Presentations arising from this research iii
Abstract iv
Acknowledgements v
Table of contents vi
List of figures x
List of tables xiv
Abbreviations xv

1 INTRODUCTION 1

1.1 Background 1

1.2 The malaria parasite cycle and the manifestation of clinical symptoms in humans 4

1.3 Malaria treatment 6

1.4 Current vector control methods 7

1.5 Limitations of vector control methods 9

1.6 Genetically based vector control strategies 12
1.6.1 Gene drives 12
1.6.2 Transmission blocking vaccines 14
1.6.3 Paratransgenesis 15

1.7 The identification of putative genes for genetically based vector control strategies 16
1.7.1 RNA interference 16
1.7.2 The mechanism of RNAi 17
1.7.3 Administering dsRNA to adult mosquitoes 18

1.8 A new potential for malaria vector control 19
1.8.1 The 20E signalling pathway 20
1.8.2 The ecdysone receptor 22
1.8.3 20E signalling regulates longevity in insects 24
1.8.4 20E signalling regulates several processes essential for reproduction 26
1.8.5 20E signalling regulates immunity to *Plasmodium* in *Anopheles* mosquitoes 28

1.9 Aim 32

1.10 Objectives 32

2 MATERIALS AND METHODS 33

2.1 Biological material 33

2.2 Optimisation of experimental methods 33
2.2.1 Design of quantitative PCR (qPCR) and RNAi primers 33
2.2.2 Total RNA (tlRNA) extraction 36
2.2.3 DNase treatment 36
2.2.4 RNA quality control 37
2.2.5 Complementary DNA (cDNA) synthesis 37
2.2.6 Quantitative PCR 38
2.2.7 Optimisation of PCR and qPCR conditions using RNAi and qPCR primers 38
2.2.8 Sequencing analysis 40
2.2.9 Double stranded RNA synthesis 40
2.2.10 Nanoinjection 45
2.2.11 Determination of the optimal age for nanoinjection of *An. funestus* 46
2.2.12 Determination of time point to confirm *EcR* knockdown after nanoinjection 46

2.3 *Anopheles funestus* longevity 47
2.3.1 Longevity assay 47

2.4 *Anopheles funestus* reproductive success 48
2.4.1 Optimisation of reproduction parameters 48
2.4.1.1 Determining the time for the optimal mating success rate in *An. funestus* 48
2.4.1.2 Determining if *An. funestus* requires one or two blood meals to oviposit 49
2.4.1.3 Optimisation of oviposition for fecundity assay 50
2.4.1.4 Determining if older mosquitoes are more susceptible to mortality after nanoinjection 51
2.4.2 Fecundity assay 52
2.4.3 Fertility assay 53

2.5 *P. falciparum* infection assay 53

3 RESULTS 56

3.1 Optimisation of experimental procedure 56
3.1.1 Total RNA extraction and cDNA synthesis 56
3.1.2 Synthesis of ds*GFP* and ds*EcR* 58
3.1.2.1 Preparation of *EcR* dsDNA template 58
3.1.2.2 Incorporation of T7 promoter sequences in the dsDNA templates 60
3.1.2.3 Double stranded RNA synthesis and purification 61
3.1.3 Optimisation of qPCR conditions 63
3.1.3.1 Optimisation of qPCR conditions for target genes 63
3.1.3.2 Optimisation of qPCR conditions for reference genes 66
3.1.4 Selection of the most stable reference genes 69
3.1.5 Agarose gel electrophoresis and sequencing analysis confirmed identity of qPCR amplicons 70
3.1.6 Optimisation of RNAi parameters 72

3.1.6.1 Determining the age for nanoinjection of *An. funestus* females that results in minimal mortality....72
3.1.6.2 Normalised *EcR* expression was significantly decreased in ds*EcR* injected mosquitoes 24 to 72 hours after injection....73
3.1.6.3 *EcR* expression was equal when normalised with the *RPS7* and *RPL19* reference genes respectively....75

3.2 Longevity....77
3.2.1 The *EcR* was significantly knocked down in *An. funestus* females injected with ds*EcR*....77
3.2.2 *Anopheles funestus* survival decreased when *EcR* was knocked down....78
3.2.3 *Anopheles funestus* survival was reduced at the infectious stage when *EcR* was knocked down....79

3.3 Fecundity and fertility....80
3.3.1 The optimal mating success rate was achieved after allowing mating for 12 days in laboratory reared *An. funestus*....80
3.3.2 Oviposition in *An. funestus* was not affected by the number of blood meals ingested....82
3.3.3 Nanoinjection induced mortality was not influenced by *An. funestus* age. 83
3.3.4 The *EcR* was significantly knocked down in *An. funestus* females injected with ds*EcR*....84
3.3.5 Lipophorin and vitellogenin receptor genes involved in mosquito reproduction were downregulated when *EcR* was knocked down....86
3.3.6 Ecdysone receptor knockdown reduced total fecundity in *An. funestus*....87
3.3.7 Fertility was reduced when *EcR* was knocked down in *An. funestus*....90
3.3.8 The blood feeding rates did not influence the reductions in fecundity and fertility in female *An. funestus*....91

3.4 *Anopheles funestus* susceptibility to *P. falciparum*....92
3.4.1 The *EcR* was significantly knocked down in ds*EcR* injected *An. funestus* females 92
3.4.2 Immune gene: *LRIM9* was downregulated when *EcR* was knocked down....94
3.4.3 Ecdysone receptor knockdown decreased oocyst numbers in *P. falciparum* infected *An. funestus* females....94
3.4.4 *Anopheles funestus* TBA and TRA differed between ds*EcR* treated *An. funestus* females and control *An. funestus* females....97
3.4.5 The blood feeding rate did not contribute to changes in phenotype in infected *An. funestus* females....98

4 DISCUSSION....100

4.1 Decreased longevity in ds*EcR* treated *An. funestus*....100

***4.2* Decreased fecundity and fertility in ds*EcR* treated *An. funestus*....104**

***4.3* Decreased intensity of *P. falciparum* in ds*EcR* treated *An. funestus*....109**

5 CONCLUSION AND FUTURE PERSPECTIVES 115

6 REFERENCES 118

7 APPENDIX 143

7.1 Appendix 1: RNAi and qPCR primer information 143

7.2 Appendix 2: Chromatograms of all genes sequenced to confirm primer specificity to respective genes 145

7.3 Appendix 3: Agarose gel electrophoresis and spectrophotometry confirm tlRNA integrity and purity from ds*EcR*, ds*GFP* and uninjected *An. funestus* females used in Objective 1 148

7.4 Appendix 4: Quantitative PCR results demonstrate specific amplification amongst samples amplified for longevity assay 150

7.5 Appendix 5: Agarose gel electrophoresis and spectrophotometry confirm tlRNA integrity and purity from ds*EcR*, ds*GFP* and uninjected *An. funestus* females used in Objective 2 151

7.6 Appendix 6: Quantitative PCR results demonstrate specific amplification amongst samples amplified for fecundity and fertility assays 153

7.7 Appendix 7: Agarose gel electrophoresis and spectrophotometry confirm tlRNA integrity and purity from ds*EcR*, ds*GFP* and uninjected *An. funestus* females used in Objective 3 154

7.8 Appendix 8: Quantitative PCR results demonstrate specific amplification amongst samples amplified for *P. falciparum* infection assay 156

7.9 Appendix 9: *Anopheles funestus* fecundity assay data 157

7.10 Appendix 10: *Anopheles funestus* infection with *P. falciparum* data 158

7.11 Appendix 11: Ethics waiver 159

7.12 Appendix 12: Bioethics clearance certificate 160

7.13 Appendix 13: Certificate for registration of facility 161

7.14 Appendix 14: Turnitin report 162

List of figures

Figure 1.1: Worldwide malaria incidence rate per 1,000 people in 2018. 1

Figure 1.2: The WHO goals for a malaria free world and current malaria situation. 2

Figure 1.3: Schematic diagram outlining the three phases of the malaria parasite cycle. 4

Figure 1.4: Insecticide resistance status of *An. funestus* to four classes of WHO approved insecticides in Africa from 2000 to 2017. 10

Figure 1.5: Genetically based vector control methods focus on population suppression or replacement using genetically modified mosquitoes. 12

Figure 1.6: The double-stranded RNA pathway in a mosquito cell. 18

Figure 1.7: Schematic diagram representing the 20E signalling pathway in insects. 21

Figure 1.8: Schematic diagram of EcR. 22

Figure 1.9: The functional EcR-USP complex regulates transcriptional activation as well as transcriptional repression of EcR induced genes. 24

Figure 1.10: Schematic diagram of the involvement of 20E in oogenesis and vitellogenesis. 27

Figure 1.11: Schematic diagram outlining *P. falciparum* infection and development in the mosquito vector. 29

Figure 2.1: An outline of all steps taken into account to design and validate primers for PCR and qPCR. 35

Figure 2.2: Positions of the ds*EcR* target region and the qPCR amplification region on both transcripts of the *An. funestus EcR*. 35

Figure 2.3: Overview of the ds*RNA* synthesis process. 41

Figure 2.4: Nanoinjection of *An. funestus*. 45

Figure 2.5: Determination of mating status in female *An. funestus*. 49

Figure 2.6: Different methods assessed as an oviposition medium for blood fed *An. funestus* females. 51

Figure 2.7: Determination of mating status and egg development in ovaries of female *An. funestus*. 53

Figure 2.8: Determination of *P. falciparum* infection status in female *An. funestus*.....55

Figure 3.1: RNA gel electrophoresis confirms the presence of intact and good quality 18S RNA. 57

Figure 3.2: Unsuccessful amplification of the *EcR* dsDNA template with *Taq* DNA polymerase. 59

Figure 3.3: Successful amplification of the *EcR* dsDNA template with Q5 DNA polymerase. 60

Figure 3.4: Incorporation of the T7 promoter region into dsDNA templates. 61

Figure 3.5: Double stranded RNA synthesis.....62

Figure 3.6: Average efficiencies of primer pairs tested indicate the best primer pairs with efficiency values closest to 100%. 64

Figure 3.7: Standard curves and melt peaks of selected primer pairs indicate good efficiency, correlation coefficient values and specificity respectively. 65

Figure 3.8: Reference gene primer efficiency values (%) of reference genes *GAPDH, RPS7, 18S, RPL19* and *RPS26.*.....67

Figure 3.9: Standard curves and melt peaks of selected primer pairs indicate good efficiency, correlation coefficient values and specificity respectively. 68

Figure 3.10: Reference gene stability plot of reference genes *RPL19*, *RPS7*, *GAPDH* and *RPS26*.....69

Figure 3.11: Agarose gel electrophoresis of qPCR products confirm amplification of the correctly sized fragments. 71

Figure 3.12: Kaplan-Meier survival curve of *An. funestus* mosquitoes injected at various ages. 73

Figure 3.13: Relative *EcR* expression levels in ds*EcR* injected *An. funestus* females compared to ds*GFP* injected *An. funestus* females. 74

Figure 3.14: Relative expression levels of *EcR* in ds*EcR* and ds*GFP* (control) injected *An. funestus* females were constant when normalised with reference genes *RPL19* and *RPS7*.....76

Figure 3.15: Relative *EcR* expression in ds*EcR* treated females was significantly downregulated when compared with ds*GFP* and uninjected treated females. 78

Figure 3.16: Kaplan Meier survival curve indicates decreased survival in ds*EcR* injected *An. funestus* females when compared with ds*GFP* and uninjected *An. funestus* females.....79

Figure 3.17: Percentage survival of *An. funestus* when *EcR* is knocked down is considerably lower than controls 16 days post injection.....80

Figure 3.18: Differences in the spermatheca of mated and virgin *An. funestus* females. 81

Figure 3.19: The highest mating success rate was achieved when *An. funestus* males and females are combined for 12 days after which no further increases are observed. 82

Figure 3.20: Oviposition in *An. funestus* females was not dependent on the number of blood meals ingested.....83

Figure 3.21: Mortality of *An. funestus* females at different age groups was not influenced by nanoinjection.....84

Figure 3.22: Relative *EcR* expression in ds*EcR* injected *An. funestus* females was reduced when compared to ds*GFP* injected and uninjected *An. funestus* females.....85

Figure 3.23: Relative *Lp* and *VgR* expression in ds*EcR* injected *An. funestus* females was reduced when compared to ds*GFP* injected and uninjected *An. funestus* females. 86

Figure 3.24: Fecundity was reduced in ds*EcR* injected females by their ability to develop eggs but not by their oviposition ability. 89

Figure 3.25: The development of eggs differed between mated uninjected and ds*GFP* controls and mated ds*EcR* treated *An. funestus* females. 90

Figure 3.26: Reduced fertility was observed in *An. funestus* females treated with ds*EcR*. 91

Figure 3.27: Blood feeding rates did not differ between treatment groups 92

Figure 3.28: Relative *EcR* expression in ds*EcR* injected *An. funestus* females was reduced when compared to ds*GFP* injected and uninjected *An. funestus* females.....93

Figure 3.29: Relative *LRIM9* expression in ds*EcR* injected *An. funestus* females was significantly reduced when compared to ds*GFP* injected and uninjected *An. funestus* females. 94

Figure 3.30: Reduced oocyst intensity was observed in *An. funestus* females treated with ds*EcR*. 96

Figure 3.31: Oocyst size appeared to differ between ds*EcR* treated and ds*GFP* and uninjected control groups. 97

Figure 3.32: Blood feeding rates were similar between ds*EcR* treated and ds*GFP* and uninjected control groups.....99

Figure 4.1: Schematic diagram showing the pleiotropic functions of the *EcR* gene. 115

Figure S1: Chromatograms of all *An. funestus* qPCR products sequenced. 147

Figure S2: RNA gel electrophoresis confirms the presence of intact and good quality 18S RNA. 148

Figure S3: Melt curve and no template controls confirm specific amplification in qPCR....150

Figure S4: RNA gel electrophoresis confirms the presence of intact and good quality 18S RNA. 151

Figure S5: Melt curve and no template controls confirm specific amplification in qPCR....153

Figure S6: RNA gel electrophoresis confirms the presence of intact and good quality 18S RNA. 154

Figure S7: Melt curve and no template controls confirm specific amplification in qPCR....156

List of tables

Table 1.1: Resistance mechanisms recorded in *An. funestus*. 11

Table 2.1: Optimal annealing temperatures for primers used in qPCR. 40

Table 3.1: A_{260}/A_{280} Purity ratios of RNA extracted from *An. funestus* females used in downstream reactions for optimisation purposes. 58

Table 3.2: Decreasing expression stability of reference genes indicated by M values calculated using the GeNorm algorithm. 70

Table 3.3: BLAST results obtained after sequencing *EcR*, *Lp*, *LRIM9*, *VgR*, *RPS7* and *RPL19* genes. 72

Table 3.4: The TBA and TRA of ds*EcR* treated *An. funestus* females compared to ds*GFP* control and uninjected control *An. funestus* females. 98

Table S1: RNAi and qPCR primer information. 143

Table S2: A_{260}/A_{280} Purity ratios of total RNA samples extracted from ds*EcR* treated, ds*GFP* treated and uninjected *An. funestus* females used in downstream reactions for objective one. 149

Table S3: A_{260}/A_{280} Purity ratios of total RNA samples extracted from ds*EcR* treated, ds*GFP* treated and uninjected *An. funestus* females used in downstream reactions for objective two. 152

Table S4: A_{260}/A_{280} Purity ratios of all RNA samples used in downstream reactions for objective three. 155

Table S5: Raw data obtained from *An. funestus* fecundity assay. 157

Table S6: Raw data obtained from *An. funestus* infection with *P. falciparum*. 158

Abbreviations

20E	20-hydroxyecdysone
An.	*Anopheles*
APL	*Anopheles-Plasmodium* responsive leucine rich repeat
ATSB	Attractive toxic sugar bait
bp	Base pairs
CEC	Cecropin
CLIPs	CLIP domain serine proteases
CRISPR	Clustered regularly interspaced short palindromic repeats
DNA	Deoxyribonucleic acid
dsRNA	Double-stranded RNA
EcR	Ecdysone receptor
EcRE	Ecdysone response elements
EIP	Extrinsic incubation period
GAPDH	Glyceraldehyde 3 phosphate dehydrogenase
GFP	Green fluorescent protein
HPX15	Heme peroxidase 15
ILP3	Insulin like peptide 3
IRS	Indoor residual spraying
JH	Juvenile hormone
LLIN	Long lasting insecticidal nets
Lp	Lipophorin
LRIM	Leucine rice immune molecule
MISO	Mating induced stimulator of oogenesis
mRNA	Messenger RNA
OEH	Ovary ecdysteroidogenic hormone
P. falciparum	*Plasmodium falciparum*
PAMP	Pathogen associated molecular protein
PBS	Phosphate buffered saline
PCR	Polymerase chain reaction
PPO	Prophenoloxidases
PRR	Pathogen recognition receptors

qPCR	Quantitative polymerase chain reaction
RISC	RNA induced silencing complex
RNA	Ribonucleic acid
RNAi	RNA interference
RPL19	Ribosomal protein L19
RPS26	Ribosomal protein S26
RPS7	Ribosomal protein S7
siRNA	Small interfering RNA
TAE	Tris-acetate-EDTA
TBA	Transmission blocking activity
TBE	Tris-borate-EDTA
TBV	Transmission blocking vaccines
TEP	Thioester containing protein
TRA	Transmission reducing activity
tlRNA	Total RNA
USP	Ultraspiracle protein
Vg	Vitellogenin
VgR	Vitellogenin receptor
YPP	Yolk protein precursor

1 INTRODUCTION

1.1 Background

Malaria is a severe disease transmitted by female *Anopheles* mosquitoes infected with protozoan *Plasmodium* parasites. With 228 million cases reported in 2018 and a mortality of 405,000, this parasitic disease is without a doubt, a cause for concern (Figure 1.1) (WHO, 2019b).

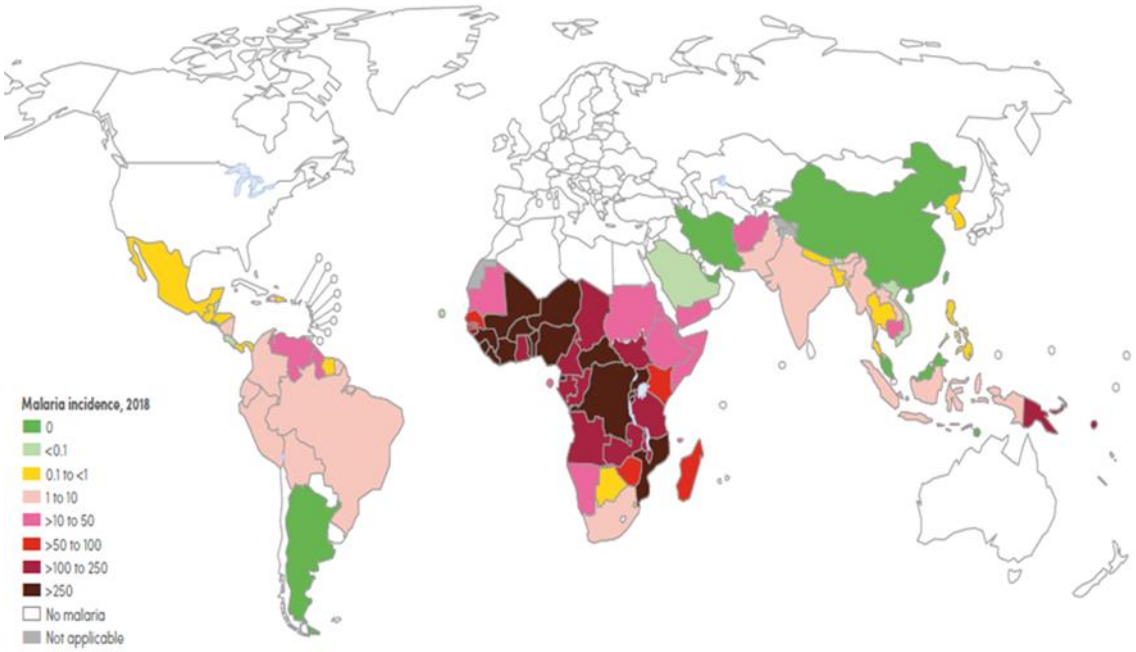


Figure 1.1: Worldwide malaria incidence rate per 1,000 people in 2018. Malaria cases are endemic to countries with warmer, more tropical climates where cases range from 10,000 to more than 250,000. Areas most affected by malaria are the upper region of South America, sub-Saharan Africa, the Eastern Mediterranean region, South-East Asia and the Western pacific area. On the contrary, countries with colder climates are free of malaria. Taken from World Malaria Report 2019 (WHO, 2019b).

In 2019, malaria cases increased to 229 million and deaths to 409,000 (WHO, 2020). Children younger than five years have the greatest risk as it was responsible for 67% of deaths in this age group (WHO, 2020). Malaria is endemic to tropical and sub-tropical regions of the world as this climate is ideal for mosquito and *Plasmodium* survival and reproduction, two factors contributing to its transmission. Africa is therefore the worst affected with more than 90% of cases and mortalities occurring in this continent annually (WHO, 2020). Due to the malaria

socio-economic impact, the World Health Organization (WHO) has set in place milestones and targets aimed at creating a world free of malaria such as eliminating 90% of malaria by the year 2030, especially in countries that were most affected in 2015 (Figure 1.2A) (WHO, 2015). While much progress has been achieved with several countries already classified as malaria-free (Figure 1.2B), the ultimate goal of a malaria-free world still requires intensified efforts in malaria parasite and vector control.

A

VISION – A WORLD FREE OF MALARIA

GOALS	MILESTONES		TARGETS
	2020	2025	2030
1. Reduce malaria mortality rates globally compared with 2015	At least 40%	At least 75%	At least 90%
2. Reduce malaria case incidence globally compared with 2015	At least 40%	At least 75%	At least 90%
3. Eliminate malaria from countries in which malaria was transmitted in 2015	At least 10 countries	At least 20 countries	At least 35 countries
4. Prevent re-establishment of malaria in all countries that are malaria-free	Re-establishment prevented	Re-establishment prevented	Re-establishment prevented

B

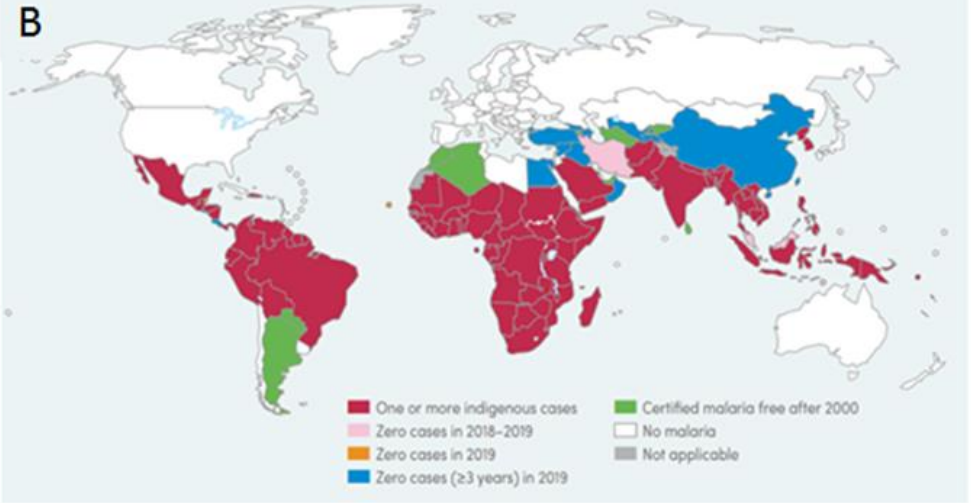


Figure 1.2: The WHO goals for a malaria free world and current malaria situation. The outline of WHO goals for achieving a world free of malaria over the years (A). Taken from Global Technical Strategy for Malaria 2016-2030, Global Malaria Programme (WHO, 2015). A map of regions free of malaria with magenta coloured regions indicating those countries still affected by malaria (B). Taken from World Malaria Report 2020 (WHO, 2020).

The causative agent of malaria, the *Plasmodium* parasite, consists of four major species that attribute to the majority of malaria cases in humans: *Plasmodium falciparum* (*P. falciparum*), *P. vivax*, *P. ovale* and *P. malariae* (Sinden and Gilles, 2002). A fifth species *P. knowlesi* that causes zoonotic malaria has recently been recorded to cause malaria in humans (Ahmed and Cox-Singh, 2015; Cooper *et al.*, 2020). *Plasmodium falciparum* located largely in sub-Saharan Africa and *P. vivax* located in Asia and South America are the two deadliest species among their counterparts as they are accountable for the majority of malaria cases (Snow *et al.*, 2005; Gething *et al.*, 2012). In 2018, it was found that *P. falciparum* was responsible for 99.7% of cases in Africa and the majority of cases worldwide, earning the title of the most lethal malaria parasite (WHO, 2019b). It also causes more severe malaria often resulting in organ dysfunction, which is possible but rarely seen in *P. vivax* cases (Luxemburger *et al.*, 1997; Patil *et al.*, 2015). *Plasmodium* species require two hosts to complete their lifecycle: a vertebrate host and the invertebrate vector, a female anopheline mosquito.

The main malaria vectors in Africa consist of two *Anopheles* groups: the *Anopheles gambiae* (*An. gambiae*) complex and the *Anopheles funestus* (*An. funestus*) group (Gillies and De Meillon, 1968). Mosquitoes within each group are morphologically similar but molecularly distinct (Gillies and Coetzee, 1987). The *An. funestus* group comprises eleven African species but contains only a single significant malaria vector— *An. funestus* (Gillies and Coetzee, 1987; Cohuet *et al.*, 2003; Spillings *et al.*, 2009). Due to its highly anthropophilic (preference for a human host) and endophilic (preference to rest indoors) nature, *An. funestus* is one of the main vectors that are located primarily in sub Saharan Africa (Gillies and De Meillon, 1968; Wiebe *et al.*, 2017). Furthermore, *An. funestus* is a major vector in Mozambique, from which the bulk of imported malaria cases in South Africa emerge (Moonasar *et al.*, 2013). Strikingly, some studies have found that the vector competence (the ability of a vector to transmit malaria) of *An. funestus* has been increased substantially as these mosquitoes have adapted to diurnal feeding indoors and some biting outdoors as opposed to their normal pattern of nocturnal feeding indoors (Moiroux *et al.*, 2012; Sougoufara *et al.*, 2014). Additional studies are needed to confirm the extent of behavioural change. This new behavioural adaptation has been attributed to the evasion of the current vector control method, long lasting insecticidal nets (LLINs) that prevent mosquitoes from indoor nocturnal feeding (Moiroux *et al.*, 2012; Sougoufara *et al.*, 2014). Adaptations like these highlight the importance of the development of novel vector control methods to reduce malaria transmission and ultimately eradicate malaria.

1.2 The malaria parasite cycle and the manifestation of clinical symptoms in humans

The malaria parasite cycle can be divided into three stages: the exoerythrocytic stage, the erythrocytic stage and the sporogonic cycle (CDC, 2019) (Figure 1.3). The exoerythrocytic stage begins when an infected mosquito releases sporozoites into the bloodstream of the vertebrate host during a blood meal (Figure 1.3). The sporozoites migrate to and invade the liver, maturing into schizonts in the hepatic cells. After a period of growth, the schizonts rupture to release merozoites that are able to infect erythrocytes, initiating the erythrocytic phase.

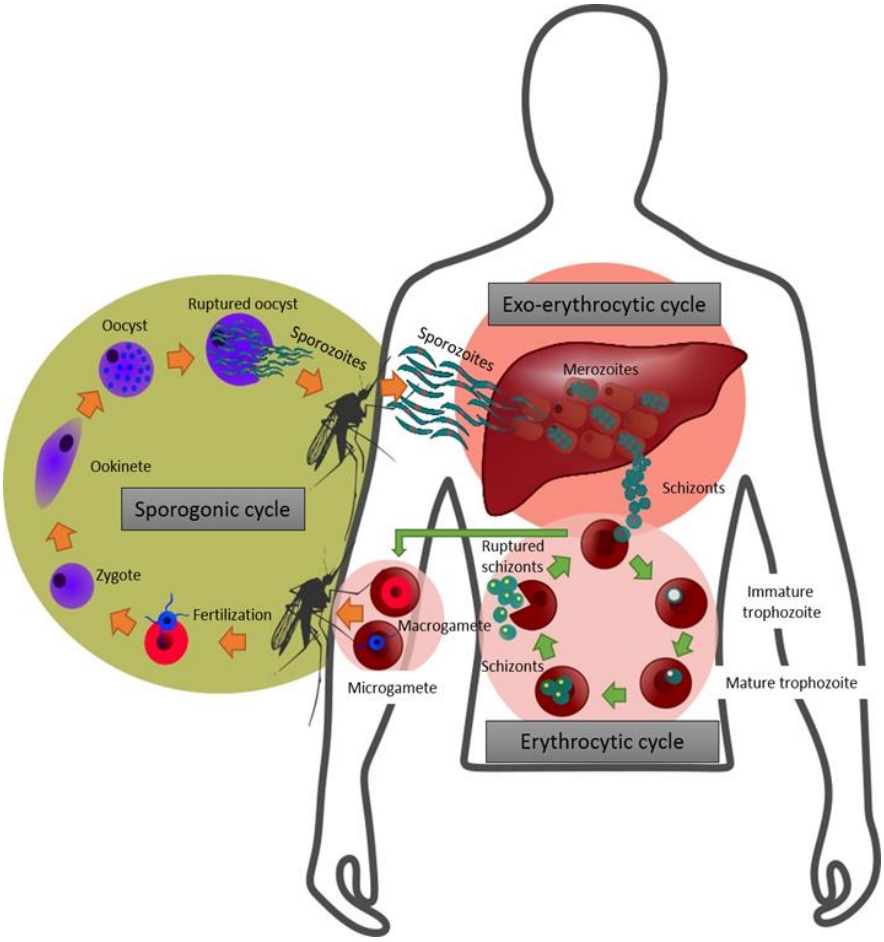


Figure 1.3: Schematic diagram outlining the three phases of the malaria parasite cycle. The malaria parasite cycle begins when an infected mosquito injects sporozoites into the human bloodstream during ingestion of blood. The manifestation of the exoerythrocytic cycle begins in the hepatic cells. As the disease progresses, growth of the parasite proceeds in the erythrocytes in either an asexual phase, destroying erythrocytes and manifesting symptoms or a sexual phase which is transferred to the mosquito when a blood meal is ingested. This initiates the sporogonic cycle in which the parasite reproduces and develops inside the mosquito until it matures into sporozoites which can then be transferred to another person, initiating a new malaria parasite cycle.

The merozoites in the erythrocytes are now known as immature ring stage trophozoites. Once matured, the schizonts rupture to release merozoites similar to the exoerythrocytic stage. This cycle results in the asexual reproduction of the parasite. As asexual reproduction in the vertebrate host progresses, symptoms of malaria begin to manifest. Sexual reproduction of *Plasmodium* begins concurrently during the erythrocytic stage when immature ring trophozoites mature into macrogametocytes (female counterpart) and microgametocytes (male counterpart) (CDC, 2019).

The sporogonic cycle commences with the ingestion of blood containing gametocytes from the vertebrate host by the female *Anopheles* mosquito. Within one hour the macrogametocytes are fertilized by the microgametes resulting in formation of zygotes in the mosquito. Over the next 24 hours zygotes mature into motile ookinetes and after 10 to 25 hours are capable of infecting the mosquito midgut. Once inside the midgut, ookinetes mature into oocysts. As oocysts develop they produce sporozoites; a process taking approximately 10 to 12 days. The oocyst ruptures upon the growth of sporozoites, releasing thousands of them into the mosquito haemocoel. The infectious sporozoites then migrate to the mosquito salivary gland where they remain until the mosquito ingests another blood meal and consequently infects another vertebrate host, restarting this lethal cycle (CDC, 2019).

During the erythrocytic stage of the malaria cycle, parasite metabolism results in the production of toxic waste products such as glycosylphosphatidylinositol (GPI), hemozoin and several others (reviewed by Weatherall *et al.*, 2002). Once schizonts are ruptured during the erythrocytic phase, merozoites as well as toxins such as GPI and hemozoin are released into the bloodstream. The release of these toxins stimulate localization of pro-inflammatory cytokines such as interferon gamma (IFN-γ) which in turn activates macrophages (reviewed by Arango Duque and Descoteaux, 2014). Macrophage activation marks the start of an immune response in the vertebrate host and cytokines such as tumour necrosis factor (TNF) are released into the bloodstream (Kwiatkowski *et al.*, 1989). Consequently, an inflammatory response is elicited resulting in fever, chills, malaise, lethargy, headaches, nausea, vomiting and other flu-like symptoms (Kwiatkowski *et al.*, 1989; reviewed by Urquhart, 1994).

More critical symptoms such as seizures and coma (cerebral malaria) as well as severe anaemia, haemoglobinuria, acute respiratory distress syndrome (ARDS), jaundice and renal damage among others are evident of a more severe lethal form of malaria, (reviewed by Bartoloni and Zammarchi, 2012). These symptoms are brought about by an increase of cytokines as well as

other lethal parasite by-products. Heightened concentrations of IFN-γ and TNF contribute to apoptosis of infected erythrocytes as well as limit erythropoiesis causing symptoms such as anaemia and haemoglobinuria (Tarumi *et al.*, 1995; Dufour *et al.*, 2003; Lamikanra *et al.*, 2009). Additionally, a rhoptry protein in *Plasmodium* (RSP2) has also been linked to apoptosis of erythrocytes (Layez *et al.*, 2005). Cerebral malaria, caused by hypoxia and induced by sequestration of infected erythrocytes blocking cerebral blood vessels is triggered by increased expression of intercellular adhesion molecule-1 (ICAM-1) due to the upregulation of cytokines (MacPherson *et al.*, 1985; Wong and Dorovini-Zis, 1992). Blockage of blood vessels as well as a cytokine enhanced increase in reactive oxygen species is thought to contribute to renal failure whereas ARDS is due to excess cytokines in the lungs (reviewed by Urquhart, 1994). Both uncomplicated and severe cases of malaria are treatable, however, severe cases require a higher degree of treatment.

1.3 Malaria treatment

There are three classes of antimalarial drugs targeting the parasite that are currently available: aryl aminoalcohol, antifolate and artemisin (reviewed by Arrow *et al.*, 2004). The first class, aryl aminoalcohol interferes with haeme dimerisation in the parasite, preventing accumulation of the toxic hemozoin by-product (reviewed by Arrow *et al.*, 2004). Unfortunately, several mutations in the parasite have caused resistance to this group of compounds (Price *et al.*, 1999; Djimdé *et al.*, 2001; Durand *et al.*, 2001; Warhurst, 2001). The antifolate mechanism of action is as per name; drugs disrupt the folic acid pathway in the parasite resulting in inefficient DNA synthesis (reviewed by Arrow *et al.*, 2004). However, the development of resistance to this drug hampered efforts to treat malaria (Peters, 1970; White, 2004). The third class of antimalarials, artemisin, exhibits the broadest range of action and affects all stages of asexual parasite forms (Ter Kuile *et al.*, 1993). Artemisin compounds combined with cellular haem hinders the parasitic enzyme calcium ATPase thus reducing the efficacy of the parasite (Meshnick *et al.*, 1991; Eckstein-Ludwig *et al.*, 2003). Resistance to artemisin based compounds has also been recorded due to mutations in the parasite's genome (Hunt *et al.*, 2010; Saralamba *et al.*, 2011; Tucker *et al.*, 2012). Due to resistance to current antimalarials, other methods such as vector control must be employed concurrently to help alleviate the worldwide burden of malaria.

1.4 Current vector control methods

Current vector control methods largely target the adult population with insecticides. Presently, there are only five classes of insecticides that have been approved for use by the WHO, namely organochlorines, organophosphates, carbamates, pyrethroids and neonicotinoids (WHO, 2011; WHO, 2018b). Two primary insecticide-based control interventions: indoor residual spraying (IRS) and LLINs are widely employed and their popularity is attributed to their efficiency, cost-effectiveness and ease of implementation (WHO, 2012). Indoor residual spraying involves spraying the inside of houses with insecticides. This vector control method kills any vectors resting on the sprayed surfaces (e.g. walls), thus reducing vector lifespan, vector density (the number of vectors in a certain area) and contact with humans (Pluess *et al.*, 2010; WHO, 2011). All five classes of insecticides can be used in IRS and their efficacy ranges from two to twelve months depending on the class (WHO, 2011; WHO, 2019a). On the other hand, LLINs prevent human-vector contact and when used in conjunction with pyrethroids, act as a chemical barrier thus reducing malaria transmission and vector density (Lengeler, 2004). Increasingly, synergists (compounds that when used in conjunction with others, increase the action of the latter) to boost the efficacy of LLINs are being used (WHO, 2017). These synergists include piperonyl butoxide (Gleave *et al.*, 2018) and insect growth regulators (Tiono *et al.*, 2018). The LLINs remain efficacious for three to five years, however may still act as a physical barrier after this time (WHO, 2007). Both IRS and LLINs are highly effective against anthropophilic, endophilic and nocturnal vectors such as *An. funestus* (Brooke *et al.*, 2013).

Additional chemically based interventions currently being optimised for use in malaria vector control include eave tubes, attractive toxic sugar baits (ATSB), endectocides and larvicides. Eave tubes, a novel control method, involves reducing vector biting and density by placing tubes lined with insecticide laced mesh on one end leaving the other end open for mosquitoes to enter (Knols *et al.*, 2016). Eave tubes are located in gaps between the roofs and walls of houses and are specially designed to attract mosquitoes with human scent emanating from houses. Contact with insecticidal mesh consequently results in the death of mosquitoes (Knols *et al.*, 2016). Studies have shown promising results of eave tubes being used as control interventions (Sternberg *et al.*, 2016; Waite *et al.*, 2016) with the potential of controlling those mosquitoes even resistant to existing insecticides (Andriessen *et al.*, 2015). Similarly, ATSB which is a sugar solution containing insecticides such as boric acid are designed to attract mosquitoes and subsequently kill them as they ingest the insecticides. Several studies have

revealed the effectiveness of ATSB as a control method for malaria vectors, including those resistant to current insecticides (Xue *et al.*, 2006; Xue *et al.*, 2008; Müller *et al.*, 2010; Xue *et al.*, 2011; Beier *et al.*, 2012; Stewart *et al.*, 2013). Another strategy exploiting vector sustenance comprises the use of blood containing ivermectin as an endectocide. Ivermectin is a compound that paralyses the somatic muscles in insects eventually leading to their death (reviewed by Õmura and Crump, 2004). Results have been promising as a reduction in both malaria vectors (Chaccour *et al.*, 2010; Kobylinski *et al.*, 2010; Khaligh *et al.*, 2021) and parasites (Kobylinski *et al.*, 2011) have been observed.

Targeting the larval stage of the vector is another way of reducing malaria vector density. Larvicides are insecticides added to vector oviposition sites that function to kill or impair the growth of vector aquatic stages. Compounds approved for larvicides by the WHO include insect growth regulators and organophosphates; pyrethroids and organochlorines are however excluded due to their environmental toxicity to aquatic life (WHO, 2006). Besides larvicides, the use of biological agents to control vector aquatic stages are employed. Biological control of vectors refers to the use of natural organisms that reduce vector population. Interestingly, bacterial species *Bacillus thuringiensis israelensis* and *Bacillus sphaericus* have demonstrated larvicidal activity with low environmental toxicity and are also recommended by the WHO (reviewed by Mittal, 2003; WHO, 2006). Other forms of larval control include other bacterial and viral species as well as natural aquatic predators including fish and amphibians (reviewed by Raghavendra *et al.*, 2011).

Apart from biological control in larvae, biological control of adult vectors is also an intervention that is implemented. The Sterile Insect Technique (SIT) aims to reduce vector density by targeting vector reproduction. This technique involves the mass rearing of male mosquitoes which are sterilised using radiation (Knipling, 1955). Sterilised males are released and compete with wild fertile males for a mate. The result of a mating between a sterile male and a wild female is a decrease in vector density through impaired reproduction over time (Knipling, 1955). Some limitations of SIT include the need for mass scale production of sterile males, the cost of this process, the fact that it is a species-specific control method and that it requires approval from the community before implementation (reviewed by Alphey *et al.*, 2010). Due to these reasons, SIT is not yet as widely implemented as malaria control interventions like LLINs and IRS.

1.5 Limitations of vector control methods

Although LLIN and IRS have proved to be very effective forms of vector control, preventing malaria transmission in Africa by 68% and 13% between the years 2000 and 2015 respectively (Bhatt *et al.*, 2015), vectors have undergone adaptations that have hindered efforts in malaria eradication. The emergence of resistance in vector populations has been sustained by several factors (reviewed by Riveron *et al.*, 2018). Firstly, the overuse of insecticides in both the agricultural and health sectors has resulted in the selection and development of resistant strains. Secondly, the long term use of LLINs and IRS allows for growing development of resistance to a certain class of insecticide over time. Thirdly, the short life cycle of the mosquito (approximately 10- 30 days) (Gillies and De Meillon, 1968) allows for the rapid development and spread of resistance mechanisms throughout the population. In Africa, *An. funestus* has developed resistance to four of the approved insecticide classes (Figure 1.4) (WHO, 2018a).

The genetic, physical and behavioural adaptations that are responsible for this widespread resistance in *An. funestus* are outlined below (Table 1.1). Briefly, genetic target site resistance is caused by mutations in the mosquito genome that alter the binding site of the insecticide which results in a decreased efficiency of the insecticide to bind to the target site (Okoye *et al.*, 2008). Another genetically initiated mutation is metabolic resistance which arises due to overexpression of detoxification enzymes that metabolise the insecticide before it exhibits any lethal effects in the mosquito (Amenya *et al.*, 2008). Physical resistance mechanisms are brought about by any changes to the mosquitoes exterior that limit the uptake of insecticides (Wood *et al.*, 2010). Lastly, behavioural resistance is a change in the mosquito's normal behaviour that allows it to evade existing vector control strategies (Moiroux *et al.*, 2012; Sougoufara *et al.*, 2014).

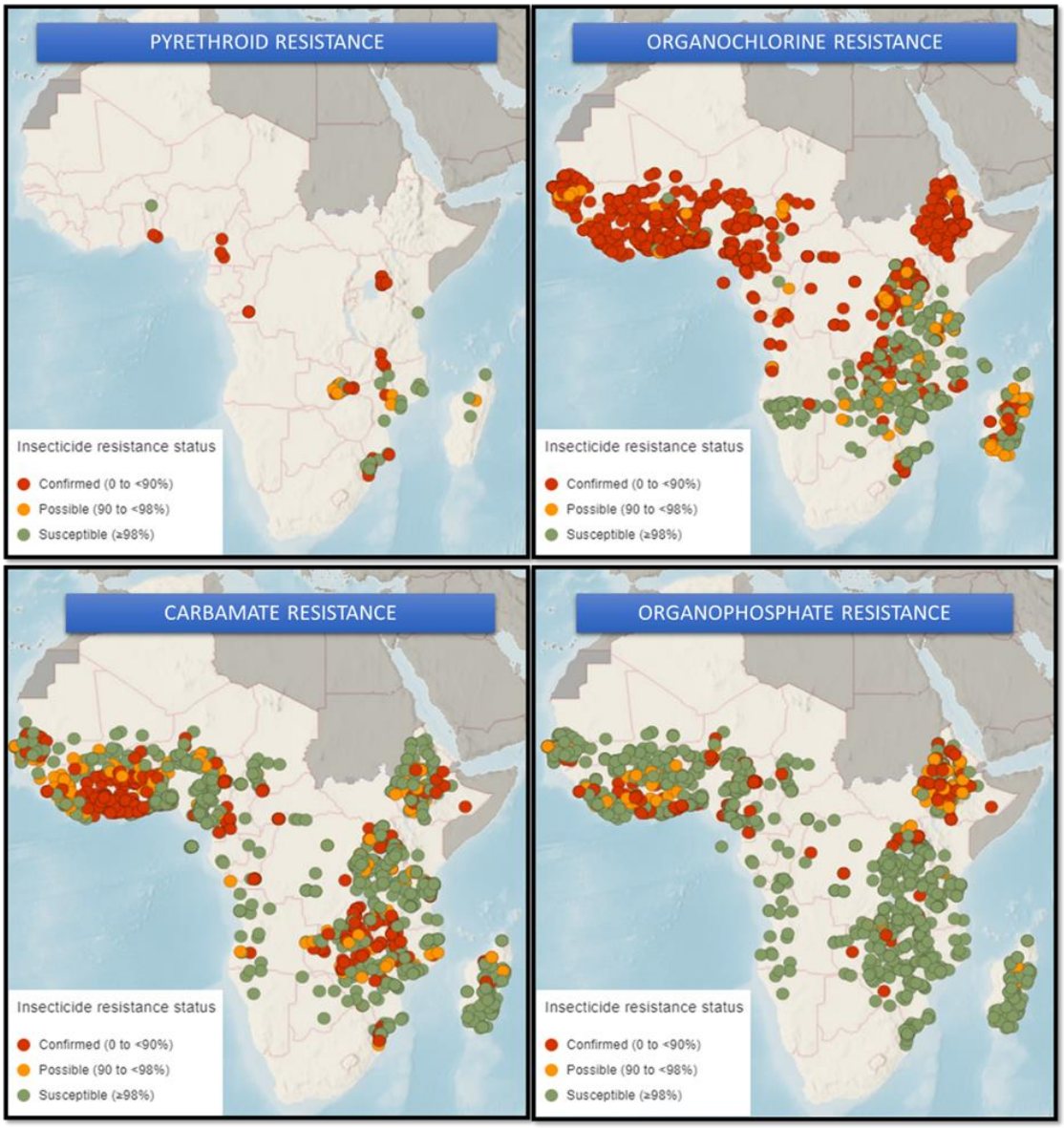


Figure 1.4: Insecticide resistance status of *An. funestus* to four classes of WHO approved insecticides in Africa from 2000 to 2017. The confirmed cases of *An. funestus* resistance to all classes of insecticides indicate the importance of novel vector control mechanisms to reduce the vector population as a means to curb the spread of malaria (Note: Map may not fully represent the extent of pyrethroid resistance throughout Africa). Malaria threat map created on http://apps.who.int/malaria/maps/threats/ by the World Health Organization.

Table 1.1: Resistance mechanisms recorded in *An. funestus*.

Type of resistance	Mechanism	Effect	Insecticide(s) affected	Reference
Genetic: Target site	Dieldrin resistance (rdl) to GABA receptor	Rdl mutation in GABA receptor gene decreases organochlorine binding	Organochlorines	(Wondji *et al.*, 2011)
	Insensitivity to Acetylcholinesterase (AChE)	Duplication of Acetylcholine (*ACh*) gene reducing activity of AChE	Carbamates	(Okoye *et al.*, 2008; Ibrahim *et al.*, 2016)
Genetic: Metabolic	Cytochrome P450 monooxygenases	Upregulation of and mutations in *CYP6P9a* and *CYP6P9b* genes increases insecticide metabolism	DDT; Pyrethroids; Carbamates	(Amenya *et al.*, 2008; Christian *et al.*, 2011; Riveron *et al.*, 2013; Riveron *et al.*, 2014b; Ibrahim *et al.*, 2015)
	Glutathione S transferases	Mutation and upregulation of *GSTe2* gene increases insecticide metabolism	DDT; Pyrethroids	(Riveron *et al.*, 2014a)
Physical	Cuticle thickening	Reduced uptake of insecticides	Pyrethroids	(Wood *et al.*, 2010)
Behavioural	Exophagic and diurnal feeding	Evasion of indoor control interventions (LLINs and IRS)	All classes used in LLINs and IRS	(Moiroux *et al.*, 2012; Sougoufara *et al.*, 2014)

1.6 Genetically based vector control strategies

As an alternative to chemical vector control methods, the manipulation of genes in the vector has also emerged as a promising strategy to target malaria vectors. Coupled with existing control methods, these strategies described below have the potential to reduce the malaria transmission to a greater extent and possibly even lead to its eradication. Interest in genetic control methods has grown with the availability of several *Anopheles* genomes (Neafsey *et al.*, 2013) including the *An. funestus* genome (Ghurye *et al.*, 2019) as well as novel genome editing techniques such as the genome CRISPR (clustered regularly interspaced short palindromic repeats) (Doudna and Charpentier, 2014) and TALENs (transcription activator-like effector nucleases) (reviewed by Joung and Sander, 2013) to name a few.

1.6.1 Gene drives

Genome editing is a key component of gene drives. Gene drives can be defined as a genetic engineering technique aimed at spreading a particular gene through populations more rapidly than normal Mendelian inheritance, thus resulting in the suppression or replacement of a population over time (reviewed by Hammond and Galizi, 2017) (Figure 1.5).

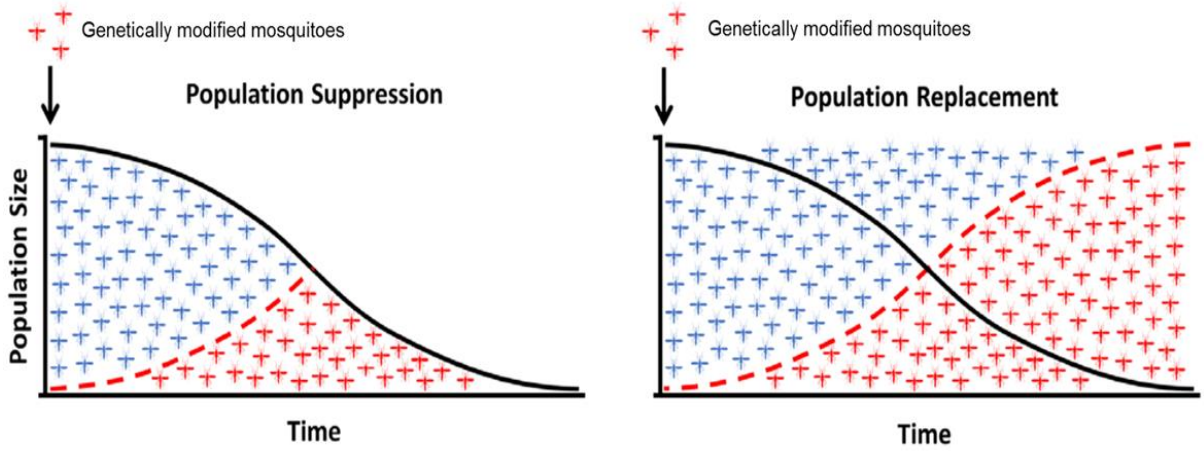


Figure 1.5: Genetically based vector control methods focus on population suppression or replacement using genetically modified mosquitoes. Population suppression involves diminishing the vector population over time. Contrastingly, population replacement involves replacing the original population with genetically modified organisms carrying a beneficial trait resulting from gene manipulation. Figure adapted from Hammond and Galizi (2017).

Population suppression is a self-limiting strategy in which the modified gene is reduced over time and needs to be continuously renewed with the release of new genetically modified organisms (reviewed by Alphey, 2014). On the other hand, population replacement is a self-sustaining strategy in which the modified gene spreads through a population over time until it replaces the wild type gene (reviewed by Alphey, 2014). Taking into account characteristics of all gene editing tools, the most suitable candidate for a gene drive would be the CRISPR-Cas9 system as opposed to other endonucleases such as TALENs, homing endonuclease genes (HEG) or Zinc finger nucleases (ZFN) (reviewed by Hammond and Galizi, 2017). This is because of the simplicity of design and the fact that inheritance is biased towards the modified gene in the CRISPR-Cas 9 system (reviewed by Doudna and Charpentier, 2014; Hammond and Galizi, 2017).

The CRISPR-Cas9 system was first discovered as an adaptive immune response to bacteriophages (Makarova *et al.*, 2006). After a viral infection, regions of the viral genome would be incorporated into repetitive sequences in the bacterial genome known as CRISPR. Simply put, the CRISPR and CRISPR associated (Cas) genes i.e. sequences coding for endonucleases and helicases are then transcribed into a guide RNA sequence which contains an RNA sequence complementary to a specific DNA sequence as well as a binding site for the Cas9 nuclease (Mojica *et al.*, 2005; Makarova *et al.*, 2006). A complex of the guide RNA and Cas9 endonuclease is formed and upon base pairing of the guide RNA to the DNA the Cas9 nuclease introduces blunt double-stranded breaks into the DNA (Jinek *et al.*, 2012). Cellular DNA repair mechanisms try to repair the cleaved DNA using either non-homologous end joining (NHEJ) or if a homologous sequence is available, homology directed repair (HDR) (reviewed by Doudna and Charpentier, 2014). The former method results in DNA damage due to the loss of nucleotides whereas the latter can successfully repair the DNA with a sequence homologous to the cleaved sequence. This is where gene drives and genome editing can be exploited, guide RNA can be synthesised against any gene of interest with the addition of a homologous template designed to modify the gene of interest. Upon cleavage by the Cas9 endonuclease, the homologous template will be inserted into the break by HDR, thereby editing the gene (reviewed by Doudna and Charpentier, 2014).

For vector control purposes, it would be strategic to modify genes involved in vector survival, reproduction or anti-parasitic genes using genome editing technology such as CRISPR Cas9. In this way the gene would spread through a population, eventually achieving an end goal of vector population suppression or replacement. Studies using the CRISPR-cas9 system in

malaria vectors have shown promising results for gene drives by reducing factors that affect vector competence. Silencing of the immune Fibrinogen related protein 1 (*FREP1*) in *An. gambiae* results in decreased infection rates in mosquitoes infected with *P. falciparum* and *P. berghei* as well as reduced reproductive success, longevity and blood feeding rate (Dong *et al.*, 2018). The doublesex gene (*Agdsx*) in *An. gambiae* is responsible for differentiation into the two sexes; silencing of this gene in a female specific region resulted in females that were intersex and sterile, eventually resulting in population suppression of the laboratory colony (Kyrou *et al.*, 2018).

1.6.2 Transmission blocking vaccines

As the name suggests, malaria transmission blocking vaccines (TBVs) aim to prevent transmission of the malaria parasite between the vector and host. Transmission blocking vaccines function by inhibiting or impairing the sexual stage parasite in the mosquito midgut after ingestion of an infected blood meal (reviewed by Carter, 2001). This result is achieved by stimulating the synthesis of or designing antibodies against a mosquito antigen such as a protein essential for parasite development or survival (reviewed by Nikolaeva *et al.*, 2015). These antibodies, present in humans, are ingested by the mosquito along with a blood meal where they induce their effects on the sexual stages of the parasite within the midgut (reviewed by Carter, 2001 and Nikolaeva *et al.*, 2015). The first instance of transmission blocking was identified in poultry, which had previously been immunised with *P. gallinaceum* gametes. When mosquitoes ingested a blood meal from immunised poultry, *P. gallinaceum* development was impaired, preventing subsequent infections in mosquitoes (Carter and Chen, 1976; Gwadz, 1976). Several targets have shown promising results for the development of TBVs. Antibodies directed against *An. gambiae* and *An. stephensi* mosquito midgut proteins resulted in decreased oocyst prevalence (the number of mosquitoes containing oocysts in their midgut) along with a decrease in longevity and fecundity in these mosquitoes (Lal *et al.*, 2001). Decreased oocyst prevalence was also observed in *An. gambiae* and *An. stephensi* when antibodies against *Anopheles gambiae* aminopeptidase N 1 (AgAPN1) were introduced into the vectors following a blood meal (Dinglasan *et al.*, 2007). Successful oocyst inhibition when antibodies against *Plasmodium* post fertilisation antigen (Pfs25) are introduced into mosquitoes are currently in trials for a TBV (Stowers *et al.*, 2000; Kapulu *et al.*, 2015; Chaturvedi *et al.*, 2016; Menon *et al.*, 2018). Recently, greater oocyst inhibition was observed with Pfs30 when compared to

Pfs25, making this a promising target for a TBV (Healy *et al.*, 2020). Identification of antiplasmodial mosquito antigens such as the ones mentioned above are important for further research and development of a TBV. If localised to malaria endemic areas and are higher than the current malaria transmission rate, TBVs can adequately reduce transmission by vectors (reviewed by Carter, 2001).

1.6.3 Paratransgenesis

The genetic modification of vector symbionts such as bacteria, fungi or viruses to bring about an effect in the vector is defined as paratransgenesis: a population replacement strategy. (reviewed by Wilke and Marrelli, 2015). Paratransgenesis in mosquito populations can be used to induce effects such as a reduction in vector lifespan, impaired vector reproduction, a decrease in vector competence as well as a disturbance in parasite growth or survival (reviewed by Wilke and Marrelli, 2015 and Wang and Jacobs-Lorena, 2017). Mosquito symbionts are genetically modified with effector molecules that bring about a change in the mosquito (e.g. express antiplasmodial proteins) when they are introduced into the mosquito (reviewed by Wilke and Marrelli, 2015). Paratransgenesis is seen as a promising approach to vector control because of its simplicity; one bacterial, viral or fungal strain could be genetically modified to be effective against several vector species (reviewed by Riehle and Jacobs-Lorena, 2005). Moreover, the fact that *Plasmodium* and symbionts both reside in the midgut and the symbionts are known to increase after a blood meal, makes this strategy an encouraging one to impede *Plasmodium* infection (Whitten *et al.*, 2006; Drexler *et al.*, 2008). The development of paratransgenic strategies has progressed greatly. One example is the synthesis of a densonucleosis virus (DNV) with a plasmid capable of expressing any gene of interest and affecting both adult and larval stages of *An. gambiae* with the ability to be passed to offspring (Ren *et al.*, 2008). Another example includes a bacterial strain of *Pantoea agglomerans* capable of producing and expressing antiplasmodial proteins that decrease *P. falciparum* and *P. berghei* in the midgut of vectors *An. gambiae* and *An. stephensi* by up to 98% (Wang *et al.*, 2012). Identification of target genes that can be incorporated into the abovementioned vector control strategies can yield a successful transgenic system to replace the current malaria vector population with mosquitoes less capable of transmitting malaria.

1.7 The identification of putative genes for genetically based vector control strategies

The elucidation of gene functions forms part of many molecular scientific techniques described as functional genomics. The purpose of functional genomics is to identify and categorise phenotypes according to their respective genotypes by exploring changes such as DNA mutations, translational or transcriptional changes, variations in gene expression and molecular interactions (Bunnik and Le Roch, 2013). Many molecular techniques have been classified under functional genomics, one such method is RNA interference (RNAi).

1.7.1 RNA interference

RNAi which involves post transcriptional gene silencing, is a method that can be used to determine gene function. RNA interference comprises the silencing of genes with double-stranded RNA (dsRNA) (Fire *et al.*, 1998). The dsRNA, complementary to its messenger RNA (mRNA) target, acts by degrading or repressing the translation of the target mRNA when bound which consequently interferes with protein synthesis (Fire *et al.*, 1998). This results in a new phenotype characterised by a loss of function that provides evidence for the functioning of a gene. Therefore, by silencing a particular gene, researchers may determine and study its function. In malaria vector control research, RNAi has been used to identify the genes mediating mosquito immunity, insecticide resistance, haematophagy and *Plasmodium* susceptibility amongst others (reviewed by Airs and Bartholomay, 2017 and Pillai *et al.*, 2017). Moreover, RNAi studies have allowed researchers to unravel which genes and pathways affect *Plasmodium* development in malaria vectors. For example, silencing the thioester containing protein 1 (*TEP1*) (Blandin *et al.*, 2004), leucine rich repeat molecule 1 (*LRIM1*) (Osta *et al.*, 2004) and *Anopheles-Plasmodium* responsive leucine-rich repeat 1 (*APL1*) genes (Riehle *et al.*, 2006) has led to the discovery that the proteins regulated by these genes are all involved in immunity against the *Plasmodium* parasite and functioned to lyse or melanise them in the vector. Exploitation of RNAi can thus help to identify putative target pathways for vector control methods based on vaccines, insecticides, larvicides, and genetically modified mosquitoes.

1.7.2 The mechanism of RNAi

Once introduced, the post transcriptional silencing mechanism of dsRNA acts on the gene of interest in the organism being studied (Figure 1.6). In the cell, the endoribonuclease DICER cleaves the dsRNA into small interfering RNA (siRNA) molecules approximately 19 to 21 base pairs in length (Bernstein *et al.*, 2001). Composed of a sense and an antisense strand, the siRNA is integrated into a multiprotein RNA induced silencing complex (RISC). RISC is composed of enzymes Dicer, transactivation response RNA binding protein (TRBP), and argonaute 2. The sense strand is degraded by RISC while the antisense strand remains due to its lower thermodynamic stability, higher flexibility and weaker base pairing at the 5' end which facilitates easier unwinding and incorporation into RISC (Khvorova *et al.*, 2003; Schwarz *et al.*, 2003). Guided by RISC, the antisense strand then binds to its complementary mRNA target. The argonaute 2 protein in the RISC cleaves the target mRNA, which is recognised as a foreign entity (Filipowicz, 2005). The cleaved mRNA can no longer be used as a template for translation, resulting in a decrease in the abundance of the protein that is normally expressed by the gene. Phenotypical changes arise from silencing the gene of interest which therefore allows for its function to be determined.

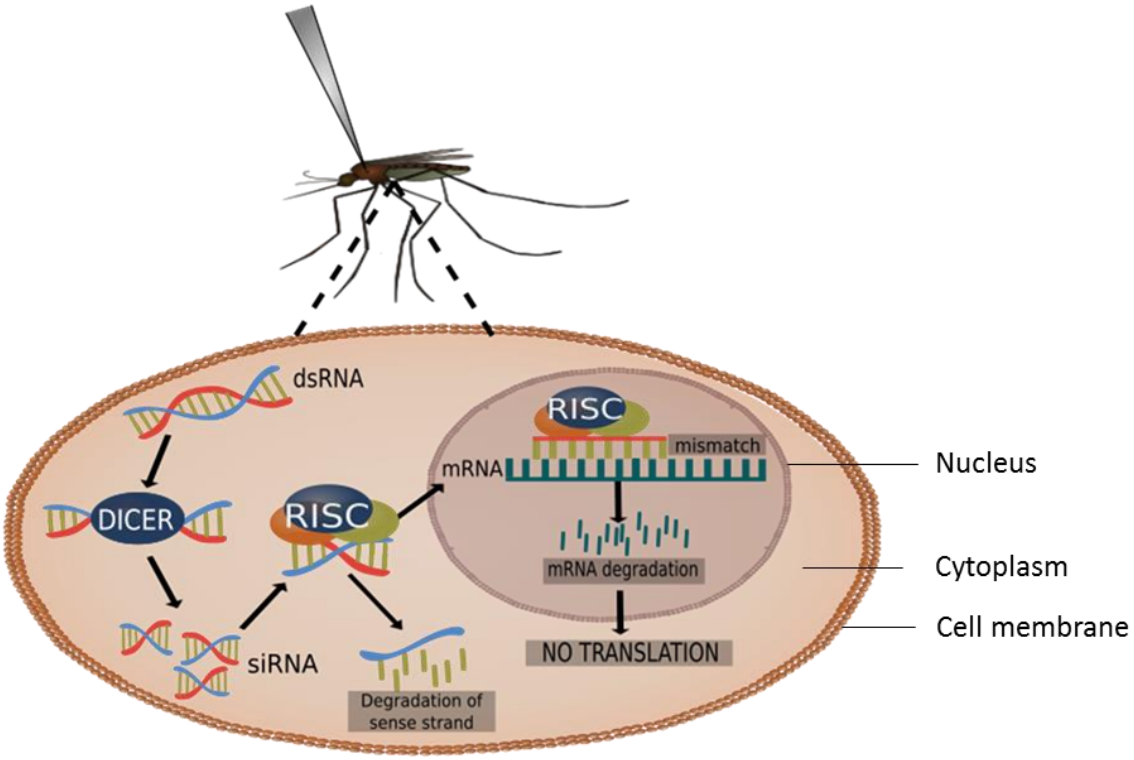


Figure 1.6: The double-stranded RNA pathway in a mosquito cell. Double-stranded RNA is introduced into the cell. An endonuclease DICER cleaves the dsRNA into siRNA molecules which are approximately 19 to 21 base pairs long. The siRNA is incorporated into the RISC containing DICER (blue oval), TRBP (orange oval) and argonaute 2 (green oval) where degradation of the sense strand occurs while the antisense strand is transported to the nucleus. It is in the nucleus that the antisense strand binds to complementary mRNA forming a double-stranded complex. Recognised as foreign, the mRNA is cleaved by argonaute 2 in the RISC, thus preventing translation of the gene.

1.7.3 Administering dsRNA to adult mosquitoes

The introduction of exogenous dsRNA into adult mosquitoes can be done in several ways, each with their own advantages and limitations. Other methods such as transfection or bacterial and viral expression systems are also ways of introducing dsRNA into a cell, however in mosquitoes these methods are more suitable for use in larvae or cell lines (reviewed by Airs and Bartholomay, 2017). In adult mosquitoes, ingestion of dsRNA is possible through incorporation of the dsRNA with a blood or sucrose meal. Various methods have resulted in the successful knockdown of genes through the ingestion of dsRNA in *Aedes aegypti* (Coy *et al.*, 2012; Van Ekert *et al.*, 2014), *Caenorhabditis elegans* (Timmons and Fire, 1998) and

Glossina morsitans (Walshe *et al.*, 2009). The ease, cost effectiveness and good subject survivability (Walshe *et al.*, 2009) of this method make it a promising method for RNAi however the concentration and volume of dsRNA ingested cannot be controlled, adding inconsistency into this method.

Microinjection, also known as nanoinjection involves the injection of a fixed amount of dsRNA into the mosquito through a capillary tube pulled into a needle. Several studies have successfully silenced genes and observed changes in the phenotypes associated with gene silencing in *Anopheles* mosquitoes (Blandin *et al.*, 2004; Baldini *et al.*, 2013; Werling *et al.*, 2019). In addition, the introduction of dsRNA through injection results in a higher and lengthier transcript knockdown than ingestion (Walshe *et al.*, 2009). Limitations of nanoinjection include high mortality, optimisation and training as well the need for a standardised protocol (Walshe *et al.*, 2009; Sampath and Puttaraju, 2012).

Another method of delivery involves the topical application of dsRNA onto the subject. In *Aedes aegypti*, dsRNA topically applied to the thorax resulted in a 1 to 8 fold knockdown and mortality associated with gene silencing (Pridgeon *et al.*, 2014). Additionally, efficient knockdown correlated with the concentration of dsRNA and dsRNA induced susceptibility to insecticides was observed in *Diaphorina citri* when dsRNA was applied to the thorax (Killiny *et al.*, 2014). This method however may have some issues with absorbability through the mosquito cuticle, also making it subject to inconsistency.

1.8 A new potential for malaria vector control

Recently, much attention has been given to the 20-hydroxyecdysone (20E) signalling pathway and its pleiotropic effects on insects (reviewed by Ekoka *et al.*, 2021). The 20E signalling pathway is generally responsible for growth and development in insects (reviewed by Yamanaka *et al.*, 2013). For example, Yu *et al.* (2014) demonstrated the effects of the 20E signalling pathway as a method of pest control; reduced longevity and decreased offspring was observed after RNAi in *Nilaparvata lugens* (*N. lugens*). Interestingly in mosquitoes, this pathway has been implicated in survival (Childs *et al.*, 2016), egg development (Attardo *et al.*, 2005), oviposition (Childs *et al.*, 2016), refractoriness to mating (Gabrieli *et al.*, 2014), blood feeding behaviour (Beach, 1979) and susceptibility to *Plasmodium* (Werling *et al.*, 2019). All these behaviours in mosquitoes influence vector density and competence and thus malaria

transmission. It would therefore be fascinating to intensively study the 20E signalling pathway using RNAi to determine its function(s) in malaria vectors and how these functions could ultimately affect malaria transmission.

1.8.1 The 20E signalling pathway

20-hydroxyecdysone signalling in insects is facilitated by the ecdysone receptor complex (Figure 1.7). This complex consists of the nuclear ecdysone receptor (EcR) and Ultraspiracle protein (USP) (homologous to mammalian retinoid x receptor) which form a heterodimer known as the EcR-USP complex (Oro *et al.*, 1990; Yao *et al.*, 1993). The functional EcR-USP complex is completed upon binding of the transcription regulatory 20E hormone to EcR (Wang *et al.*, 2000). Together the functional EcR-USP complex binds to a region of DNA either in the form of an inverted or direct repeat, termed the ecdysone response element (EcRE) which is located upstream of genes that are regulated by 20E signalling (Koelle *et al.*, 1991; Wang *et al.*, 1998). The EcREs consist of palindromic DNA sequences consisting of the sequence 5'AGGTCA3' (Cherbas *et al.*, 1991). Once bound to the EcRE, the functional EcR-USP complex activates transcription of the target gene whereas the EcR-USP complex excluding 20E represses transcription of the target gene in insects (Cherbas *et al.*, 1991; Dobens *et al.*, 1991; Koelle *et al.*, 1991).

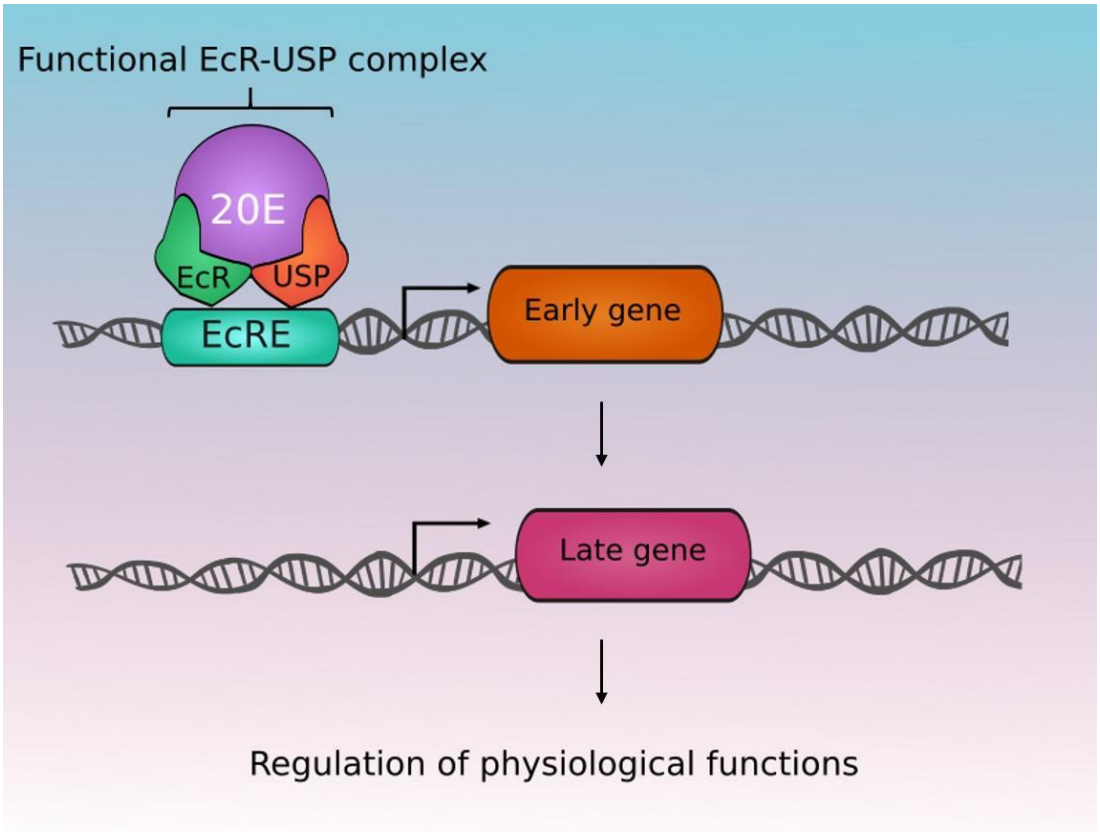


Figure 1.7: Schematic diagram representing the 20E signalling pathway in insects. The functional EcR-USP complex binds to the EcRE region upstream of the EcR regulated early gene and activates transcription of this gene. Subsequently, the early gene which acts as a transcription factor activates the transcription of late genes which induce physiological changes in insects.

Genes that are first activated by the 20E signalling pathway include *EcR*, *BR-C*, *E74*, *E75*, *E78*, *HR3*, *HR4*, *HR39* and *ftz-f1*— these are known as early genes (DiBello *et al.*, 1991; Koelle *et al.*, 1991; Pierceall *et al.*, 1999; Sun *et al.*, 2002; King-Jones and Thummel, 2005). These early genes subsequently activate the transcription of several late genes which are involved in physiological roles in the mosquito. One such late gene is Vitellogenin (*Vg*) which is involved in regulating reproduction in mosquitoes (Martín *et al.*, 2001). Furthermore, several immune related genes such as several prophenoloxidases (*PPO*s) and the leucine rich repeat immune molecule 9 (*LRIM9*) which play a role in immunity to *Plasmodium* are regulated by 20E and may function as late genes (Ahmed *et al.*, 1999; Upton *et al.*, 2015). Since EcR is a key component of the 20E signalling pathway, mediates hormone and DNA binding and is the focus of this dissertation, it will be discussed in more detail.

1.8.2 The ecdysone receptor

The ecdysone receptor is a ligand controlled transcription factor present in the nucleus of insects (reviewed by Mangelsdorf *et al.*, 1995). This receptor forms part of the nuclear receptor family and shares structural features with other receptors in this family (Koelle *et al.*, 1991). Such features include highly conserved DNA and ligand binding domains (Koelle *et al.*, 1991; reviewed by Mangelsdorf *et al.*, 1995) (Figure 1.8).

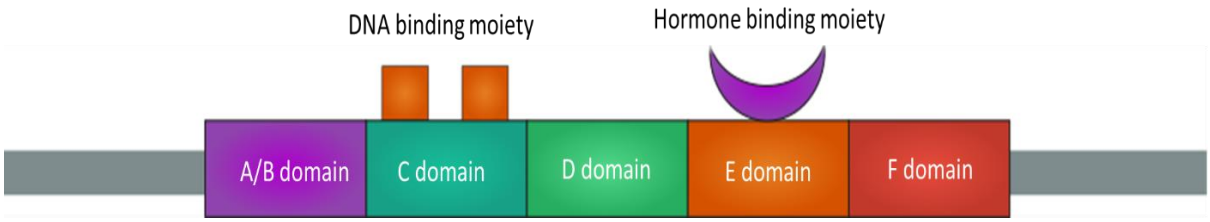


Figure 1.8: Schematic diagram of EcR. The five domains of EcR are shown above: each with different functions. Playing a role in EcR transactivation is the A/B domain as well as the D and F domains. The C domain is responsible for binding to EcRE on DNA and consists of two zinc fingers (represented by orange boxes) that assist in EcR binding to DNA. The D domain links the C and E domain and also facilitates localisation in the nucleus. Lastly, the E domain provides a site for 20E binding (represented by the purple crescent).

The DNA binding domain of EcR is located towards the N terminus and consists of two conserved zinc fingers containing the proximal and distal boxes that are involved in DNA binding and dimerization (Berg, 1989; Koelle *et al.*, 1991; Jayachandran and Fallon, 2000; Devarakonda *et al.*, 2003). Located towards the C terminus is the ligand or hormone binding domain that recognises and binds the 20E hormone (Koelle *et al.*, 1991; Cho *et al.*, 1995; Jayachandran and Fallon, 2000). Other less conserved domains identified in the EcR include the A/B domain, the D domain and the F domain (Koelle *et al.*, 1991; Cho *et al.*, 1995; Jayachandran and Fallon, 2000). The A/B domain is involved in transcriptional activation and contains a sequence termed activation function 1 that is responsible for this as it facilitates binding to coactivators (Cruz *et al.*, 2000; Hu *et al.*, 2003). The D domain connects the DNA and ligand binding domains and is involved in nuclear localisation and transactivation (Cho *et al.*, 1995; Jayachandran and Fallon, 2000). Also involved in transactivation is the F domain (Cho *et al.*, 1995; Jayachandran and Fallon, 2000). Currently, two isoforms of EcR (EcR-A and EcR-B) have been identified in mosquitoes (Wang *et al.*, 2000; Wang *et al.*, 2002). These isoforms differ in their N terminal domains, are responsible for different functions in

mosquitoes and are expressed in tissues and life stages accordingly (Wang *et al.*, 2000; Wang *et al.*, 2002).

The regulation of EcR is mediated by the 20E hormone in a dose dependent manner (Koelle *et al.*, 1991; Karim and Thummel, 1992; Fujiwara *et al.*, 1995). An increase in 20E in mosquitoes is brought about by the ingestion of either a blood or sugar meal which serves as a source of cholesterol (Karlson, 1963; Clayton, 1964). Through a series of enzymatic reactions, cholesterol is converted to 20E (Gilbert *et al.*, 2002). Prior to obtaining a blood or sugar meal both EcR and USP are present at low levels in the fat body, however a heterodimer of USP and the orphan receptor HR38 exists, preventing the heterodimerization of EcR and USP (Zhu *et al.*, 2003b). As the 20E hormone is synthesised, both EcR RNA and protein levels begin to increase (Talbot *et al.*, 1993; Fujiwara *et al.*, 1995). An increase in EcR levels in the fat body results in the dislocation of the HR38-USP complex which allows for the heterodimerization of EcR and USP (Zhu *et al.*, 2003b). A decline in 20E results in reduced EcR levels and therefore reduced or non-existent transcriptional regulation by this receptor (Talbot *et al.*, 1993; Fujiwara *et al.*, 1995). The regulation of EcR and the regulation of transcription by 20E both demonstrate the interplay between the EcR and 20E hormone and their importance for the others functioning.

Functioning as a transcription factor, EcR regulates transcription in several ways. The 20E hormone binds to the hormone binding domain on EcR to activate transcription of early genes and subsequently late genes that induce phenotypic changes (Koelle *et al.*, 1991). The EcR however, must already be present in a heterodimer with USP in order for 20E binding to occur as USP is involved in allosteric control and alters the conformation of EcR to favour hormone binding (Yao *et al.*, 1993; Hu *et al.*, 2003). This has also been found true for DNA, as the affinity of the EcR DNA binding domain to EcRE is increased upon heterodimerization with USP (Yao *et al.*, 1993; Hu *et al.*, 2003). Once 20E is bound to the EcR-USP complex, it binds coactivators such as FISC p160/SRC, CREB binding protein (CBP) or NURF with histone acetyltransferase activity that uncoil and make DNA readily available for binding by the complex (Rosenfeld and Glass, 2001; Hu *et al.*, 2003; Badenhorst *et al.*, 2005; Zhu *et al.*, 2006; Gaddelapati *et al.*, 2020). This in turn allows for the transcriptional activation of EcR regulated genes (Figure 1.9). Conversely, repression of transcription occurs during the absence of the 20E hormone (Figure 1.9). The EcR-USP complex binds to co-repressor proteins such as SMRTER, Svp or Bonus (Zelhof *et al.*, 1995; Tsai *et al.*, 1999; Beckstead *et al.*, 2001). This complex subsequently interacts with histone deacetylases such as mSin3A that condense DNA

and reduce the ability of the EcR-USP complex to bind, thereby repressing transcription (Tsai *et al.*, 1999; reviewed by Milazzo *et al.*, 2020). The EcR regulates several physiological functions in insects and mosquitoes, some of these will be discussed further.

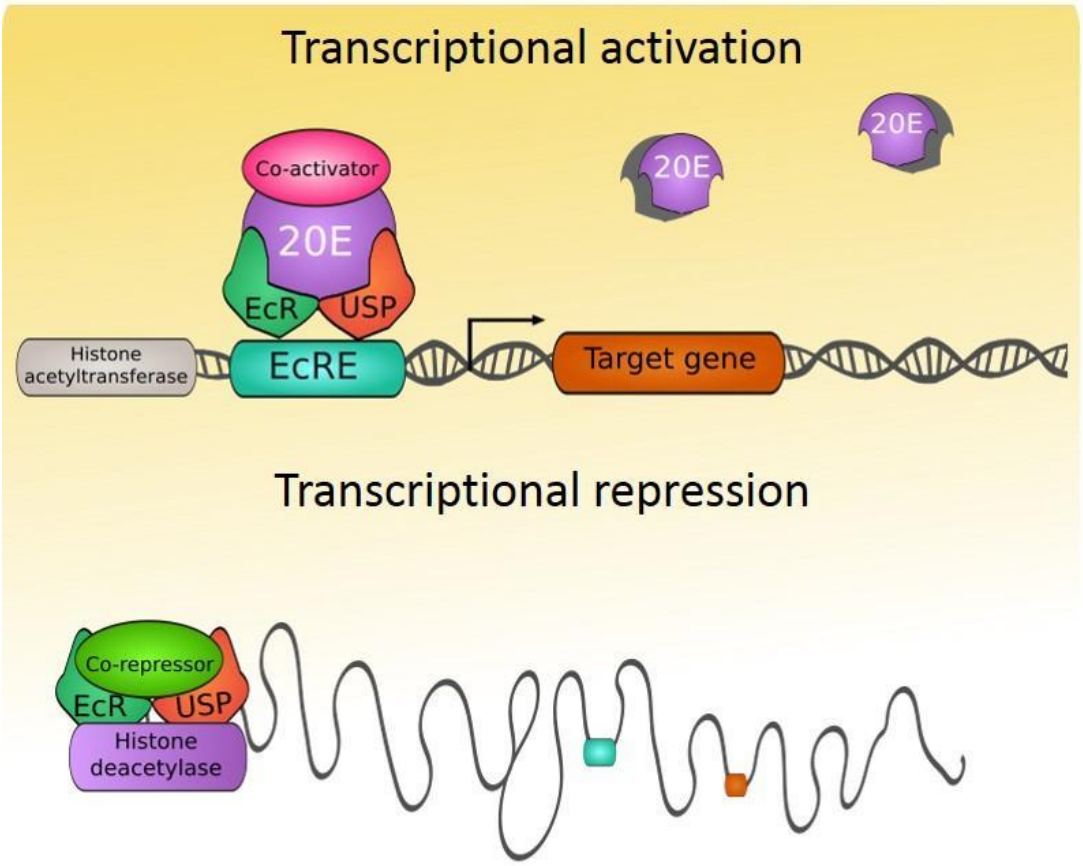


Figure 1.9: The functional EcR-USP complex regulates transcriptional activation as well as transcriptional repression of EcR induced genes. The EcR-USP complex in conjunction with 20E binds coactivators that have histone acetyltransferase activity. These coactivators uncoil and make DNA available for binding and transcriptional activation by the complex. Contrastingly, transcriptional repression occurs in the absence of 20E. The EcR-USP complex binds co-repressors with histone deacetylase activity. Consequently, DNA condenses, preventing binding of the EcR-USP complex to EcREs, thereby repressing transcription.

1.8.3 20E signalling regulates longevity in insects

The 20E signalling pathway has been implicated in the longevity and aging of many insects, recently including major malaria vectors, *An. gambiae* and *An. funestus* (Childs *et al.*, 2016; Werling *et al.*, 2019; Brown *et al.*, 2020). However, the effect that EcR has on *An. funestus* longevity has not yet been characterised. The effect of the EcR on longevity in the model organism *Drosophila melanogaster* (*D. melanogaster*) has been well studied and forms the

bulk of information available. In *D. melanogaster* mutants with a deletion in the *EcR* gene, both males and females average lifespans increased significantly (Simon *et al.*, 2003). Furthermore, resistance to oxidative, heat and dry starvation stresses in *EcR* mutants as well as heightened performance measured by *D. melanogaster's* fast response to phototaxis was observed (Simon *et al.*, 2003). In a subsequent study by Simon *et al.* (2006), slower aging was observed in *D. melanogaster EcR* mutants compared to the control. Tricoire *et al.* (2009) also witnessed slower aging of male *D. melanogaster* adults when *EcR* was slightly inactivated, however a stronger inactivation of *EcR* increased mortality. Moreover *EcR* that was inactivated in female *D. melanogaster* adults resulted in decreased longevity (Tricoire *et al.*, 2009). This decrease in longevity was also observed in *Nilaparvata lugens*; ingestion of dsRNA targeting *EcR* resulted in a concentration dependent decrease in lifespan (Yu *et al.*, 2014).

Importantly, the 20E signalling pathway has also been discovered to affect lifespan in the malaria vectors *An. gambiae* and *An. funestus*. The ectopic application of a 20E agonist, which is structurally similar to the hormone and therefore results in heightened 20E signalling significantly reduced *An. gambiae* adult female lifespan (Childs *et al.*, 2016). A greater reduction in lifespan was observed when higher doses were administered (Childs *et al.*, 2016). Promising results have recently been observed in *An. funestus* where tarsal, but not topical application of a 20E agonist resulted in a significantly decreased survival (Brown *et al.*, 2020). However, the effect of EcR on *An. funestus* longevity was not examined in the abovementioned study. These results are promising as they show that longevity is regulated by 20E signalling in malaria vectors and could be used as a basis for the development of future vector control methods.

Although the EcR regulated genes affecting longevity in malaria vectors have not yet been identified, understanding the importance of EcR regulation of vector longevity is important as it can ultimately affect malaria transmission. A decrease in the longevity of vectors and consequently a decrease in vector density can result in a cascade effect. Decreased vector density may result in decreased transmission of malaria due to a reduction in the mosquito to human ratio (reviewed by Shaw and Catteruccia, 2018). The inability to ingest a second blood meal to transmit malaria or not surviving long enough for *Plasmodium* to become infectious and of course a decrease in reproduction may also lead to a further decrease in vector density (reviewed by Shaw and Catteruccia, 2018). All of the above consequences of 20E signalling substantiate the further study of the EcR to more deeply understand its mechanisms and functions regarding malaria vector longevity.

1.8.4 20E signalling regulates several processes essential for reproduction

Anopheline reproductive output —as measured by fecundity and fertility, is a key component of malaria transmission. It increases both the vector to host ratio as well as enables the transmission of *Plasmodium* pathogens to hosts through a blood meal (which is requirement for mosquito reproduction) (reviewed by Shaw and Catteruccia, 2018). Ingestion of a blood meal initiates two important reproductive processes in the mosquito. Firstly, vitellogenesis which involves the synthesis of yolk precursor proteins (YPPs) that are deposited in the developing oocytes and are essential for embryo nutrition and secondly, oogenesis which is the maturation of underdeveloped oocytes into mature egg cells (Pierceall *et al.*, 1999; Raikhel *et al.*, 1999; Carney and Bender, 2000). 20-hydroxyecdysone signalling is essential for the successful completion of vitellogenesis and oogenesis in mosquitoes.

Upon emergence, juvenile hormone (JH) in the adult female mosquito regulates the first maturation of oocytes which then experience a "resting" stage until blood meal ingestion. Juvenile hormone simultaneously regulates the βFTZ-F1 receptor and together they function to make the mosquito fat body responsive to 20E (Li *et al.*, 2000; Zhu *et al.*, 2003a). Ingestion of a blood meal represses JH activity and subsequently signals the brain to release ovary ecdysteroidogenic hormone (OEH) and insulin-like peptide 3 (ILP3) (Lea, 1967; Hagedorn *et al.*, 1975; Readio *et al.*, 1988; Brown *et al.*, 1998; Brown *et al.*, 2008). In developing egg cells, OEH and ILP3 then bind to the OEH receptor and insulin receptor respectively which subsequently initiates insulin signalling and ecdysone (a precursor of 20E) production by the ovaries (Figure 1.10) (Riehle and Brown, 2002; Dhara *et al.*, 2013; Vogel *et al.*, 2015). The hormone ecdysone is then hydroxylated to it functional form: 20E, in the mosquito fat body (Hagedorn and Fallon, 1973). The 20E signalling pathway is initiated by the binding of 20E to EcR and DNA of early genes, *E74B* and *E75A*, which peak around 24 hours post blood meal (Raikhel *et al.*, 1999, 2002). Binding of these early genes activate the transcription of several late YPP genes involved in vitellogenesis, namely Vitellogenin (*Vg*), Vitellogenic carboxypeptidase (*VCP*), Cathepsin B-like protease (*VCB*) and Lipophorin (*Lp*) (Hays and Raikhel, 1990; Cho *et al.*, 1991; Cho *et al.*, 1999; Sun *et al.*, 2000). Concurrently, digestive enzymes, trypsin, aminopeptidases, glycosidases and lipases facilitate blood meal digestion into amino acids and other constituents respectively. These amino acids are further incorporated in the synthesis of YPPs in the fat body (Briegel, 1975; Geering, 1975; Geering and Oberlin, 1975; Lemos *et al.*, 1996). Post the synthesis of YPPs, these proteins are

incorporated into developing oocytes by receptor mediated endocytosis and stored until required for embryogenesis (Raikhel, 1992).

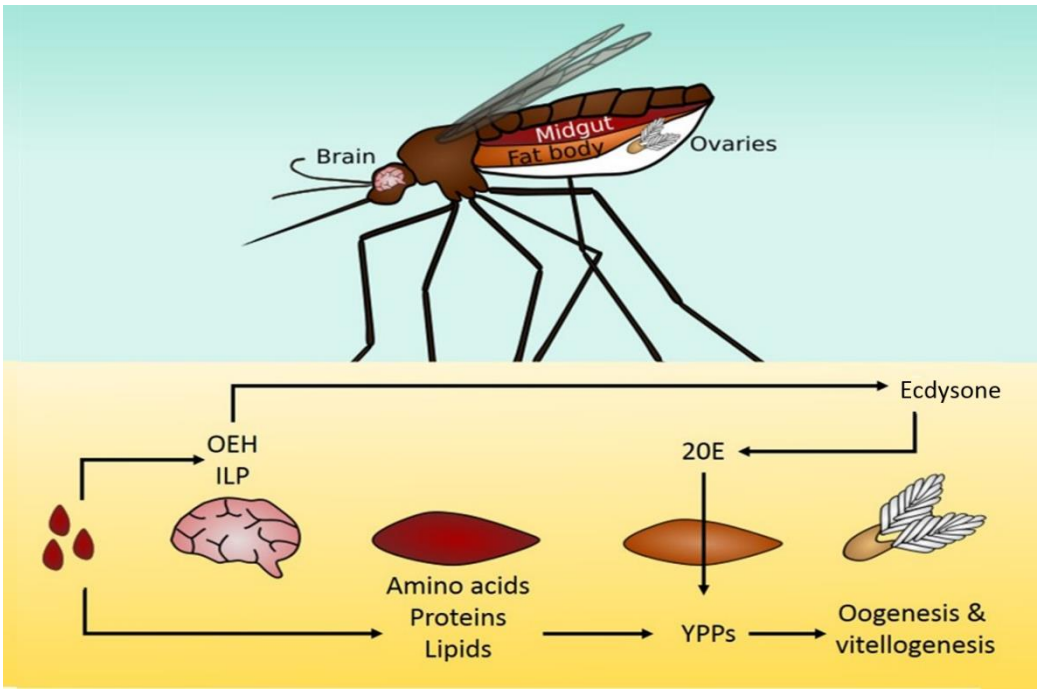


Figure 1.10: Schematic diagram of the involvement of 20E in oogenesis and vitellogenesis. Ingestion of a blood meal stimulates the brain to produce OEH and ILP. Additionally, in the midgut, the blood is digested into constituents such as amino acid, proteins and lipids required for nutrition and egg maturation. In the ovaries, OEH and ILP stimulate the production of ecdysone which is then hydroxylated to its active form 20E in the fat body and is involved in YPP transcription. The blood constituents are incorporated into the YPPs and then travel to the ovaries where they are taken up into developing oocysts and function to regulate oogenesis and vitellogenesis. Figure adapted from Hansen *et al.* (2014).

Oogenesis requires a constant and elevated supply of amino acids following a blood meal (Uchida, 1998). In addition to this, lipids are essential for oocyte development and are transported by the lipid transporter Lp (Sun *et al.*, 2000). An EcR induced gene, mating induced stimulator of oogenesis (*MISO*) ensures nutrients are transported towards developing oocytes by controlling *Lp* expression (Baldini *et al.*, 2013). Combined with amino acids and yolk proteins in the developing oocyte, RNA and proteins from nurse cells along with a chorion secreted by follicle cells complete the composition of the matured egg (Valzania *et al.*, 2019).

The termination of oogenesis and vitellogenesis occurs at approximately 30 hours post blood meal, when the 20E titre begins to decline (Bohm *et al.*, 1978). The HR38 binds USP in the absence of EcR resulting in the downregulation of YPP genes (Zhu *et al.*, 2003b). Simultaneously, *βFTZ-F1* is activated which transforms the fat body into its pre-vitellogenic

state (White *et al.*, 1997; Zhu *et al.*, 2003a). This leaves the ovaries and fat body ready to complete another cycle of vitellogenesis and oogenesis once the next blood meal is ingested.

Besides 20E synthesised after a blood meal, the male mosquito also contributes to 20E synthesis and resulting behavioural changes influencing reproduction in females. Male mosquitoes are able to synthesise and store 20E in male accessory glands (MAGs) (Pondeville *et al.*, 2008). The 20E is transferred to female mosquitoes by males after mating takes places (Pondeville *et al.*, 2008). The transfer of this hormone initiates a series of behavioural changes in the mosquito that includes the refractoriness to further mating, increased egg production and the induction of oviposition (Gabrieli *et al.*, 2014). Moreover, 20E transferred by males is involved in oogenesis as it regulates the expression of *MISO* which increases *Lp* expression and thereby facilitates the transfer of nutrients to the developing egg (Baldini *et al.*, 2013).

As mentioned previously, reproduction in mosquitoes plays an important role in malaria transmission through increasing the vector density as well as spreading *Plasmodium* parasites when ingesting a blood meal required for vitellogenesis and oogenesis. A reduction in the mating capability or a decrease in the fecundity or fertility of female vectors by investigating the role of EcR in these parameters will be of great advantage. Firstly, it will widen the knowledge of what is already known about EcR and reproduction and secondly, it will provide a path for the research and development of novel EcR based control methods. Interfering with mosquito reproduction and 20E signalling could potentially decrease malaria transmission by reducing vector density through manipulating vitellogenesis and oogenesis or through behavioural changes such as oviposition or a refractoriness to mating.

1.8.5 20E signalling regulates immunity to *Plasmodium* in *Anopheles* mosquitoes

The sporogonic cycle in mosquitoes begins upon ingestion of gametes from an infected blood meal. This cycle progresses in the mosquito until infectious sporozoites develop and can be transmitted to vertebrates (Figure 1.11). Once gametes infect the mosquito the innate immune system is activated to suppress *Plasmodium* infection. Strikingly, there is evidence that several immune processes in the mosquito are regulated by the 20E signalling cascade or are influenced by EcR regulated products. These immune processes are discussed below.

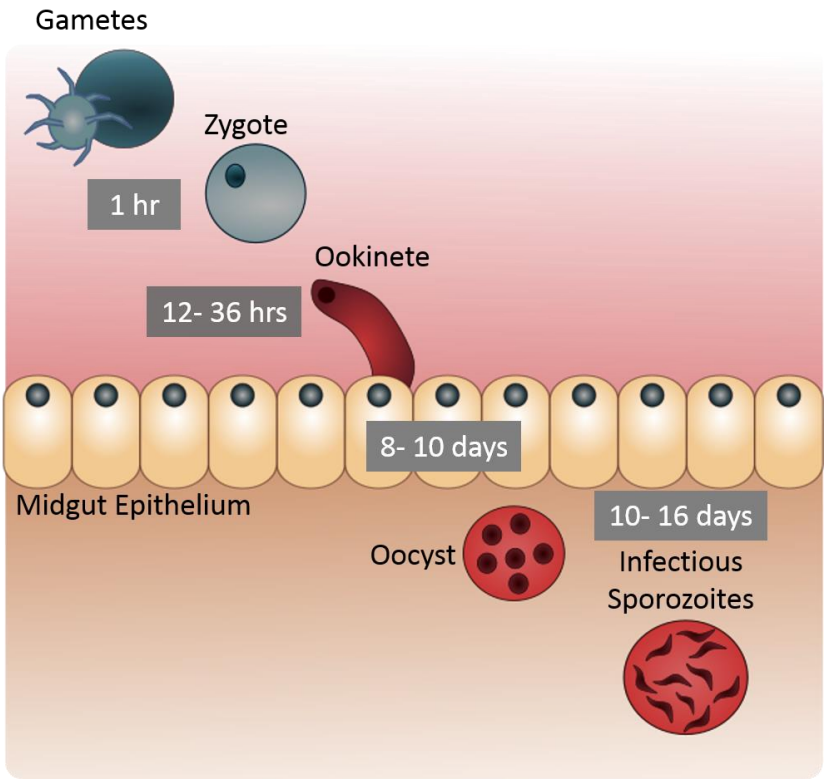


Figure 1.11: Schematic diagram outlining *P. falciparum* infection and development in the mosquito vector. Male and female gametes are contained within an infected blood meal ingested by the vector. In approximately one hour the male microgamete fertilises the female microgamete to form a zygote. The zygote can take from 12 to 36 hours to mature into an ookinete. The ookinete then transverses the midgut epithelium and develops into mature oocysts, a process taking 8 to 10 days. Ten to sixteen days later, sporozoites are mature and travel to the salivary glands of the mosquito with the potential to be transmitted to a vertebrate host during a subsequent blood meal.

Recognition of foreign and infectious bodies comprises the first step of innate immunity in the mosquito (reviewed by Christophides *et al.*, 2004). This involves the binding of pathogen recognition receptors (PRRs) in the mosquito to pathogen-associated molecular patterns (PAMPs) in the *Plasmodium* parasite. One such PRR is the thioester containing protein (TEP) family (Christophides *et al.*, 2002). To date, 15 TEPs have been identified in the *An. gambiae* genome (Christophides *et al.*, 2002). Interestingly, infection with *Plasmodium* results in the upregulation of TEP1 in the malaria vector and silencing of TEP1 increases anopheline susceptibility to *P. yoelii* confirming that TEP1 is involved in the immune response (Blandin *et al.*, 2004; Jaramillo-Gutierrez *et al.*, 2009). The TEPs contain a thioester motif which is responsible for binding to the ookinete that is then killed by mechanisms independent of TEP1 (Christophides *et al.*, 2002; Blandin *et al.*, 2004). Binding to the ookinete is facilitated by the

leucine rich repeat proteins, LRIM1 and APL1C which stabilises and keeps TEP1 in the haemolymph of the mosquito (Blandin *et al.*, 2004; Fraiture *et al.*, 2009; Povelones *et al.*, 2009). Confirming TEP1 is an immune regulator of *Plasmodium*, Blandin *et al.* (2004) and Dong *et al.* (2006) observed an increase in oocysts concurrent with TEP1 knockdown. Strikingly, two EcR induced genes, *Lp* and *Vg* influence the action but not the expression of TEP1 (Rono *et al.*, 2010). The YPPs *Lp* and *Vg* hinder the binding efficiency of TEP1 to ookinetes as observed by an increase in oocyst numbers under typical conditions, whereas silencing of *Lp* and *Vg* reduces *P. berghei* oocyst intensity (the number of oocysts present in the mosquito midgut) (Rono *et al.*, 2010). Vitellogenin appeared to effect TEP1s function to a greater extent to Lp, as when silenced, a higher reduction in oocysts were observed (Rono *et al.*, 2010). Other studies have shown similar results where the silencing of *Lp* resulted in reduced infection levels with *Plasmodium* parasites (Vlachou *et al.*, 2005; Mendes *et al.*, 2008). These results suggest that increased Lp and Vg caused by elevated EcR levels hinder the binding efficiency and parasite killing mechanism of TEP1. Moreover, Lp was discovered to regulate oocyst size; silencing of *Lp* resulted in reduced oocyst size due to a decrease in nutrients (Rono *et al.*, 2010; Costa *et al.*, 2018; Werling *et al.*, 2019).

Another PRR involved in the recognition of infectious bodies are the LRIM9 proteins. *LRIM9* is directly regulated by EcR and is similarly upregulated after a blood meal (Upton *et al.*, 2015). Unlike LRIM1, LRIM9 does not interact and is not involved in the functioning of TEP1 (Upton *et al.*, 2015). An increase in the intensity of oocysts after *LRIM9* knockdown suggests its function as an immune regulator of *Plasmodium* (Upton *et al.*, 2015). Moreover, knockdown of *LRIM9* resulted in a decrease in the number of melanised parasites which suggests that LRIM9 plays a role in the melanisation cascade (Upton *et al.*, 2015). Melanisation in mosquitoes either directly destroys or clears melanised parasites from the mosquito. LRIM9 was found to be involved in the clearing process of melanised parasites and hence is not directly responsible for the melanisation of parasites, but instead their recognition (Volz *et al.*, 2006).

Following the recognition of parasites, signal modulation and amplification either allow for an immune response by intensifying the signal or prevent an immune response by diminishing the signal (reviewed by Christophides *et al.*, 2002). The signal intensification is carried out by CLIP domain serine proteases (CLIPs) that subsequently activates an effector response of parasite killing molecules (reviewed by Christophides *et al.*, 2002). Focusing on the CLIPs that are influenced by 20E signalling to elicit immune responses, the most involved are *CLIPA14* and *CLIPA2*. Along with modulating an immune response in *An. gambiae*, CLIPA14 regulates

the TEP1 dependent recognition and melanisation of parasites (Volz *et al.*, 2006; Nakhleh *et al.*, 2017). Silencing of *CLIPA14* resulted in a high level of melanisation in ookinetes, suggesting that *CLIPA14* negatively regulates TEP1 functioning (Volz *et al.*, 2006). A striking comparison was made in *CLIPA2* which prevents TEP1 from becoming active; knockdown of *CLIPA2* resulted in increased TEP1 activity (Yassine *et al.*, 2014; Kamareddine *et al.*, 2016). Moreover, CLIPA14 controls the activation of EcR induced pro-phenoloxidases (*PPO*s) that function to melanise and kill parasites (Volz *et al.*, 2006). Knocking down *CLIPA14* resulted in increased phenoloxidase (PO) activity in the mosquito (Volz *et al.*, 2006).

Succeeding signal modulation and amplification, signal transduction pathways initiate the transcriptional activation of immune genes. Effector response systems are responsible for the transcription of their specific genes (reviewed by Christophides *et al.*, 2002). Ecdysone receptor induced genes that are activated by effector response systems include *PPO*s and cecropins (*CEC*). Currently, 9 PPOs and 4 cecropins have been identified in *An. gambiae* and specifically *PPO1*, *PPO3*, *PPO8*, *CEC1* and *CEC3* are regulated by 20E signalling (Ahmed *et al.*, 1999; Christophides *et al.*, 2004; Reynolds *et al.*, 2020). Additionally an EcRE has been identified on the *An. gambiae PPO1* gene, suggesting that it might be an EcR induced gene (Ahmed *et al.*, 1999). Prophenoloxidases are present in the haemolymph of mosquitoes, and upon signal modulation are converted to their active form POs (reviewed by Christophides *et al.*, 2002). The function of POs is to form melanotic capsules containing lethal free radicals and quinone intermediates, a process termed melanisation (reveiwed by Michel and Kafatos, 2005). Foreign bodies such as parasites are subsequently encapsulated and killed with the aid of the free radicals and quinone intermediates (reveiwed by Michel and Kafatos, 2005). This phenomenon was confirmed by Collins *et al.* (1986). Cecropins are antimicrobial peptides providing immunity against bacteria, fungi and yeast in mosquitoes (Vizioli *et al.*, 2000). Interestingly, *CEC* expression was increased in a mosquito vector after being infected with *P. berghei* (Vizioli *et al.*, 2000). Gwadz *et al.* (1989) demonstrated a decrease in the number of oocysts when mosquitoes were exposed to CEC. Additionally, silencing *CEC3* resulted in an increase in *Plasmodium* intensity in several studies (Kim *et al.*, 2004; Dong *et al.*, 2009; Kokoza *et al.*, 2010).

Once an *Anopheles* mosquito becomes infected with *Plasmodium*, it depends on the competence of the vector to determine if the malaria transmission cycle will continue. Vector survival and immune system responses can influence *Plasmodium* survival and development into infectious sporozoites. Since the 20E signalling pathway regulates and is involved in many

aspects of the innate immune system, modifications, e.g. transgenic mosquitoes or gene drives involving the modification of EcR induced genes should be explored to determine if they could reduce vector competence. The reduction of vector competence could ultimately decrease malaria transmission rates by killing parasites or prevent them from maturing to their infectious forms.

1.9 Aim

Since each vector-parasite interaction is unique, it is necessary that further studies on EcR be conducted using different parasite and vector species to uncover the potential of this hormone receptor as a target in malaria vector control strategies. One ideal system to work on would be *An. funestus* mosquitoes as well as malaria parasite *P. falciparum*, as both are major species involved in malaria transmission in Africa. Moreover, the effects of *EcR* knockdown on *An. funestus* longevity, reproduction and susceptibility to *P. falciparum* have not been investigated to date. This study therefore aims to determine the effects of *EcR* knockdown on *An. funestus* longevity, reproductive success and susceptibility to *P. falciparum*.

1.10 Objectives

1. Determine the effect of *EcR* knockdown on *An. funestus* longevity.
2. Determine the effect of *EcR* knockdown on *An. funestus* reproductive success.
3. Determine the effect of *EcR* knockdown on *An. funestus* susceptibility to *P. falciparum*.

2 MATERIALS AND METHODS

2.1 Biological material

A laboratory strain of *An. funestus* mosquitoes originating from Mozambique (FUMOZ) was used in this study. Female FUMOZ mosquitoes were used for all data collection purposes and were aged accordingly. The FUMOZ strain was reared in the Maureen Coetzee insectary at the Wits Research Institute for Malaria (WRIM) under standard insectary conditions at ± 26°C with ± 80% humidity and a 12:12 day: night cycle (Hunt *et al.*, 2005).

The *P. falciparum* NF54 strain was used to infect *An. funestus*. Infected blood was provided by Prof Lyn-Marie Birkholtz from the University of Pretoria, Institute for Sustainable Malaria Control (UP ISMC).

2.2 Optimisation of experimental methods

The methods presented in the following section were conducted to ensure all techniques were optimal and resulted in accurate and reliable data collection for all three objectives i.e. *An. funestus* longevity, reproductive success and susceptibility to *P. falciparum*.

2.2.1 Design of quantitative PCR (qPCR) and RNAi primers

For qPCR analyses, gene-specific primers targeting *An. funestus EcR*, *Lp*, *VgR*, and *LRIM9* were designed (Figure 2.1). First, the nucleotide sequences of these four genes were obtained from VectorBase (https://vectorbase.org/vectorbase/app). For each target gene, the corresponding nucleotide sequence was imported to PrimerQuest (https://www.idtdna.com/pages/tools/primerquest) where it served as template for the design of sense and antisense primers meeting the following criteria: a GC content of 40% to 60%, a length of 18 to 25 nucleotides and a melting temperature (T_m) of 55˚C to 65˚C and the ability to amplify a 75-150 base pair (bp) region (Taylor *et al.*, 2010). Notably, similar to previous reports in *Aedes aegypti* (Wang *et al.*, 2002), two *EcR* isoforms were also detected in the transcriptome of *An. funestus* available on VectorBase, namely *EcR-A* (AFUN020231-RA) and

EcR-B (AFUN020231-RB). Thus, to quantify *EcR* expression, primers that could amplify a 130 bp region common to both isoforms were selected (Figure 2.2). To confirm that the primers designed were specific to the gene of interest, primer-BLAST was used (https://www.ncbi.nlm.nih.gov/tools/primer-blast/) (Ye *et al.*, 2012). All primers were synthesised by Inqaba Biotechnical Industries (South Africa). *Anopheles funestus* reference gene primers (*GAPDH*, *RPS7*, *18S*, *RPL19* and *RPS26*) previously designed in the WRIM laboratory were used in qPCR analyses.

For RNAi, two gene-specific primers targeting *An. funestus EcR* were designed (Figure 2.2, Table S1). The first set, which was designed according to Figure 2.1, comprised gene-specific primers that could amplify a 484 bp region common to both *An. funestus EcR* transcripts. The second set of primers contained the same sequences as the first, but in addition, they were flanked by the T7 promoter minimal sequence on the 5' end of each primer to allow for subsequent *in-vitro* transcription (Table S1). The nucleotide sequence for *An. funestus EcR* was obtained from VectorBase (https://vectorbase.org/vectorbase/app) and input as a template in PrimerQuest (https://www.idtdna.com/pages/tools/primerquest). Primers targeting a 484 bp region from both transcripts of the *An. funestus EcR* coding sequence (AFUN020231-RA and AFUN020231-RB) were designed. A region of approximately 500 bp was targeted as this results in the most efficient silencing (Tuschl *et al.*, 1999) and was similar to the length of the ds*EcR* region targeting the *An. gambiae EcR* (Baldini *et al.*, 2013). Care was taken to ensure that the 484 bp region targeted by the *EcR* dsRNA primers would not overlap with the 130 bp region targeted by *EcR* qPCR primers (Figure 2.2) so that qPCR primers would not amplify any regions targeted by dsRNA. To confirm that the primers designed were specific to the gene of interest, primer-BLAST was used (Ye *et al.*, 2012). All primers were synthesised by Inqaba Biotechnical Industries (South Africa). As a negative control, double-stranded green fluorescent protein (*GFP*) primers were designed by Ms. Elodie Ekoka from the WRIM laboratory to amplify a 492 bp region from the *GFP* clone (Table S1).

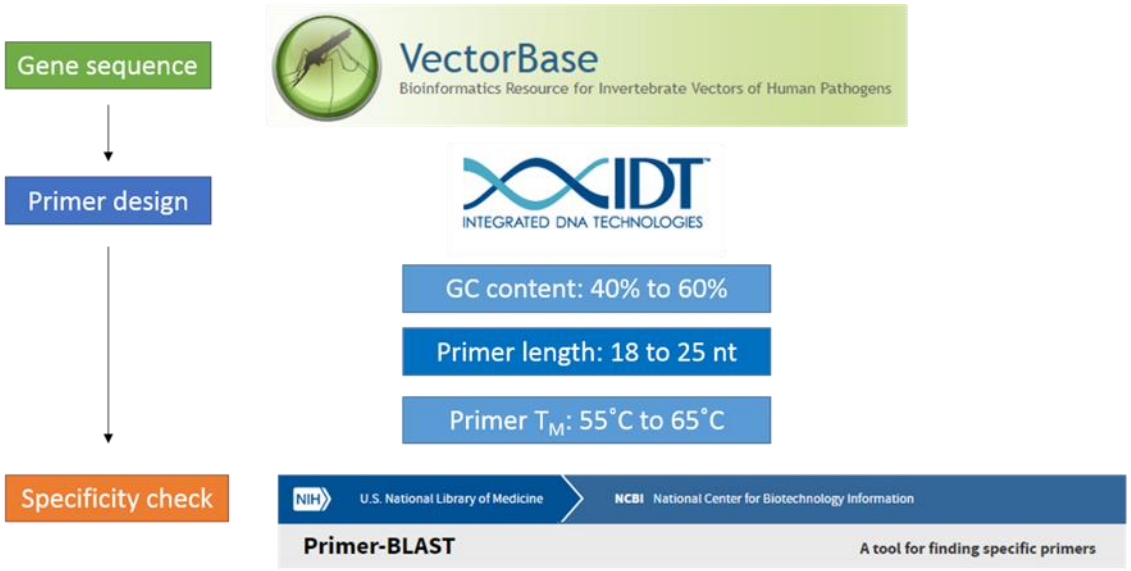


Figure 2.1: An outline of all steps taken into account to design and validate primers for PCR and qPCR. Concisely, primer design consisted of acquisition of the gene sequence for a particular gene followed by primer design composed of several criteria. Primers were lastly tested for specificity to the target gene in *An. funestus*.

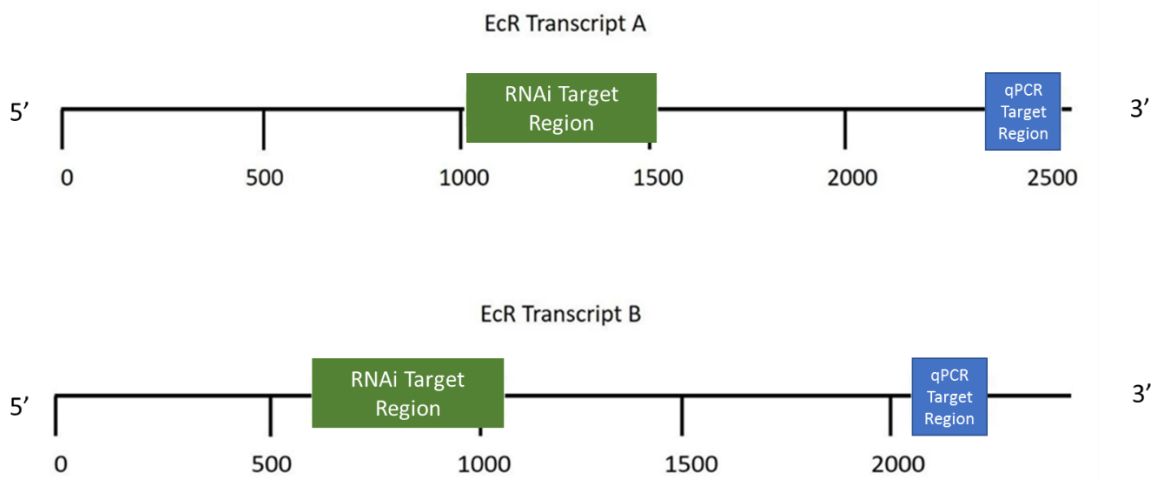


Figure 2.2: Positions of the ds*EcR* target region and the qPCR amplification region on both transcripts of the *An. funestus EcR*. The *EcR* ds*RNA* was designed to target a 484 base pair region on both transcripts of EcR. The qPCR primer pair was designed to amplify a 130 base pair region on the *An. funestus EcR* gene towards the 3' end of the gene to prevent amplification of products cleaved by ds*EcR*.

2.2.2 Total RNA (tlRNA) extraction

Total RNA was extracted from approximately 15 mosquitoes in each replicate according to the TRIzol™ Plus RNA Purification Kit (Catalogue number: 12183555, Invitrogen, CA, USA) with a modification in the homogenisation step. Mosquitoes were immobilised at -80˚C for 30 seconds and were placed in 1.5 ml microcentrifuge tubes. A pestle was used to homogenise the mosquitoes in 500 µl of TRIzol reagent™ and the remaining 500 µl of TRIzol™ was added subsequently as this ensures a more efficient homogenisation. The manufacturer's instructions were followed for the remainder of the RNA purification. The homogenised mosquito samples were incubated in the TRIzol™ reagent for 5 minutes at room temperature. Subsequently 200 µl of chloroform was added to the mixture and was incubated at room temperature for 2 minutes. The sample was centrifuged for 15 minutes at 12,000 x*g* at 4°C. After centrifugation, a colourless aqueous phase containing RNA was present at the top of the tubes. Six hundred microliters of this phase was transferred to a new tube and the old tube discarded. Six hundred microliters of 70% (v/v) ethanol was then added to the tube and briefly vortexed. To bind RNA to the membrane, the RNA sample was added to a spin cartridge and centrifuged for 15 seconds at 12,000 x*g* at 4°C, and the flow through discarded. This was repeated until the entire sample had been processed. The RNA sample was washed with 700 µl of wash buffer I™ supplied with the kit and was then centrifuged for 15 seconds at 12,000 x*g* and 4°C. The flow through was discarded and 500 µl of wash buffer II™ was added to the RNA and subsequently centrifuged for 15 seconds at 12,000 x*g* and 4°C, after which this step was repeated once. Once the flow through had been discarded, the sample was centrifuged at 12,000 x*g* and 4°C for 1 minute to dry the membrane. The spin column was inserted into a new collection tube and 50 µl of elution solution was added to the middle of the column. The tube was then centrifuged for 2 minutes at 14,000 x*g* and 4°C. The eluted RNA present in the tube was stored at -80˚C until further use.

2.2.3 DNase treatment

To remove any contaminating genomic DNA carried over from RNA extraction, a DNase treatment was conducted with the TURBO DNA-*free*™ Kit (Catalogue number: AM1907, Ambion, TX, USA) according to manufacturer's instructions. To the tlRNA, 0.1 volumes of 10X TURBO DNase™ buffer was added, followed by 1 µl of TURBO DNase™ Enzyme. This

was mixed by vortexing. This solution was incubated at 37˚C for 30 minutes. DNase inactivation reagent was added at 0.1 volumes of the initial RNA volume to the solution. The solution was then incubated at room temperature for 5 minutes with gentle mixing during this period. The samples were thereafter centrifuged at 10,000 x*g* for 1.5 minutes and the supernatant containing DNA-free RNA was transferred to a new microcentrifuge tube at stored at -80˚C until further use.

2.2.4 RNA quality control

RNA quality control consisted of spectrophotometry with the Nanodrop One (Catalogue number: ND-ONE-W, Thermo Scientific, MA, USA) and agarose gel electrophoresis to determine RNA integrity. Spectrophotometry was used to assess concentration and purity. One microliter of RNA from each biological replicate was tested. All RNA subsequently used had an A_{260}/A_{280} ratio above 1.7 indicating purity. For electrophoresis, an aliquot of RNA from each biological replicate was mixed with an equal amount of 2X RNA loading dye (Catalogue number: R0641, Thermo Scientific™, MA, USA) and incubated at 70˚C for 10 minutes. RNA was then loaded into a 1% (w/v) agarose/Tris-borate-EDTA (TBE) gel which was electrophoresed at 100V for 50 minutes in TBE buffer. The RiboRuler High Range RNA Ladder (Catalogue number: SM1821, Thermo Scientific, MA, USA) was used to size RNA fragments. The gel was thereafter viewed using an ultraviolet (UV) gel documentation system.

2.2.5 Complementary DNA (cDNA) synthesis

First strand cDNA synthesis was conducted with the iScript™ cDNA Synthesis Kit (Catalogue number: 1708891, Bio-Rad, CA, USA). Reactions consisted of 1 µg of tlRNA (extracted as above), 1X reaction mix containing oligo dT and random hexamer primers, 1X reverse transcriptase and nuclease free water to make up a total reaction volume of 20 µl. The cDNA cycling conditions consisted of 5 minutes at 25˚C followed by 30 minutes at 42˚C and finally 5 minutes at 85˚C. The cDNA was stored at -20˚C until further use.

2.2.6 Quantitative PCR

All gene expression studies were performed with qPCR. Each 1X qPCR reaction consisted of 5 µl of IQ™ SYBR super-mix (Catalogue number: 1708880, Bio-Rad, CA, USA), 300 nM of each primer, 1 µl of cDNA and nuclease free water to make up a 10 µl reaction. Cycling conditions consisted of an initial denaturation at 94˚C for 3 minutes, 35- 39 cycles of denaturation at 94˚C for 20 seconds, annealing for 25 seconds and extension at 72˚C for 30 seconds with a final extension step at 72˚C for 10 minutes. The annealing temperatures were previously determined by optimisation. A melt peak analysis and a no-template control excluding cDNA were included to assess for specificity and contamination, respectively. Quantitative PCR products were stored at -20˚C until agarose gel electrophoresis to confirm product presence and size and sequencing analysis to confirm that the correct gene had amplified. Agarose gel electrophoresis to confirm product size was conducted at 120V for 120 minutes on a 2.5% (w/v) agarose/Tris-acetate-EDTA (TAE) gel. The GeneRuler 100 bp DNA Ladder (Catalogue number: SM0234, Thermo Scientific, MA, USA) was used to size qPCR amplicons. Relative gene expression analysis was calculated manually using the ΔΔCt method where

$$Ratio = 2^{-(\Delta\Delta Ct)}$$

$$and\ \Delta\Delta Ct = [Ct(target\ test) - Ct(target\ calibrator)] - [Ct(reference\ test) - Ct(reference\ calibrator)]$$

(Livak and Schmittgen, 2001). All significance tests were calculated using an unpaired student's t-test for two samples or a one way ANOVA with Tukey's test for multiple comparisons for more than two samples.

2.2.7 Optimisation of PCR and qPCR conditions using RNAi and qPCR primers

Optimisation of *EcR* primers for RNAi applications consisted of testing the efficacy of the *Taq* DNA Polymerase (Catalogue number: R011, Takara, Shiga, Japan) and the Q5 DNA Polymerase (Catalogue number: M0491S, New England Biolabs, MA, USA) using an array of various PCR conditions to produce *EcR* amplicons as well as a temperature gradient PCR to determine the optimal annealing temperature. The Q5 DNA polymerase that produced a single *EcR* amplicon with a high yield was used in further experiments. The optimal annealing

temperature of 56.9˚C was determined from annealing temperatures that ranged between 43˚C to 68˚C.

Optimisation of qPCR primers consisted of a temperature gradient qPCR to determine the optimal annealing temperature of *EcR, Lp, LRIM9* and *VgR* primers and primer selection based on efficiency. Optimisation of qPCR reference gene primers (*RPS7, RPL19, RPS26* and *GAPDH*) included primer selection using efficiency, specificity and expression stability as parameters. Prior to optimisation, RNA was extracted as previously described (section 2.2.2) from *An. funestus* females who had ingested a blood meal less than 24 hours prior to extraction as this increases expression of *EcR* (Cho *et al.,* 1995). Complementary DNA was synthesised as above (section 2.2.5) and used as is to assess annealing temperature or used to create a twofold diluted standard curve to assess primer efficiency. The temperature gradient qPCR tested annealing temperatures ranging from 50˚C to 59˚C for all primer pairs. The temperatures that resulted in the lowest Cq values for each primer pair were selected as the optimal annealing temperatures. The standard curve was used to assess all primer pairs and the pair with the best efficiency (closest to 100%) and the correlation coefficient (R^2) value closest to 1 was selected. The standard curve was also used to assess reference gene efficiency and specificity as well as determine the optimal annealing temperature as described above. Reference genes with efficiency values closest to 100% were chosen to be used in subsequent qPCRs and any reference genes showing nonspecific amplification were excluded from further analysis.

Subsequently, the most stable reference genes were selected by evaluating their expression in samples injected with ds*EcR* and ds*GFP*. One day old *An. funestus* females were nanoinjected with either 10 µg/µl of ds*EcR* or ds*GFP* (section 2.2.10). This experiment was conducted in 2 replicates with 35 females in each replicate. Two days after nanoinjection, RNA was extracted from mosquitoes according to the protocol (section 2.2.2). Complementary DNA was subsequently synthesised with the iScript™ cDNA Synthesis Kit (Catalogue number: 1708891, Bio-Rad, CA, USA) according to the manufacturer's instructions (section 2.2.5). Quantitative PCR was conducted to determine which reference genes Ribosomal protein S7 (*RPS7*), Ribosomal protein L19 (*RPL19*), Ribosomal protein S26 (*RPS26*) and glyceraldehyde 3 phosphate dehydrogenase (*GAPDH*) were the most stable across samples (section 2.2.6). Analysis was conducted with the reference gene selection tool on the Bio-Rad CFX Maestro software which is based on the geNorm software (Vandesompele *et al.,* 2002). This software functions on the assumption that reference genes are uniformly expressed across all samples, producing high stability. Any variation in the expression of reference genes decreases the

stability of the reference gene, making it more unsuitable for analysis. The most stably expressed reference genes were selected for analysis based on the above assumption.

Table 2.1: Optimal annealing temperatures for primers used in qPCR.

Primer	Optimal annealing temperature (˚C)
EcR	55
RPS7	55
RPL19	55
Lp	58.5
VgR	57
LRIM9	58.8

2.2.8 Sequencing analysis

To confirm primers were amplifying the correct gene, Sanger sequencing of qPCR products was conducted. Prior to sequencing *EcR*, *Lp*, *LRIM9*, *VgR*, *RPS7* and *RPL19* products were electrophoresed on a 2.5% (w/v) agarose/TAE gel to confirm amplification of the correct size products had occurred. The gel was electrophoresed at 120V for 90 minutes. Once amplicons were confirmed to be the expected size, products were prepared for sequencing. Sanger sequencing in the forward and reverse direction was conducted by Inqaba Biotec™ (Pretoria). Consensus sequences were subsequently entered into BLAST (https://vectorbase.org/vectorbase/app/search/transcript/UnifiedBlast) to compare sequence similarity and E values with the actual gene sequences obtained from VectorBase.

2.2.9 Double stranded RNA synthesis

Double-stranded RNA molecules targeting *EcR* or *GFP* were designed as described below (Figure 2.3). Double-stranded *GFP* was synthesised to act as a control as it is not naturally expressed in mosquitoes, and should not affect the expression of *EcR*. The synthesis of dsRNA

can be divided into three steps, namely (i) the production of a DNA template (PCR amplicon or plasmid) containing the target region, (ii) incorporation of the promoter sequences in this DNA template, and (iii) dsRNA synthesis and purification.

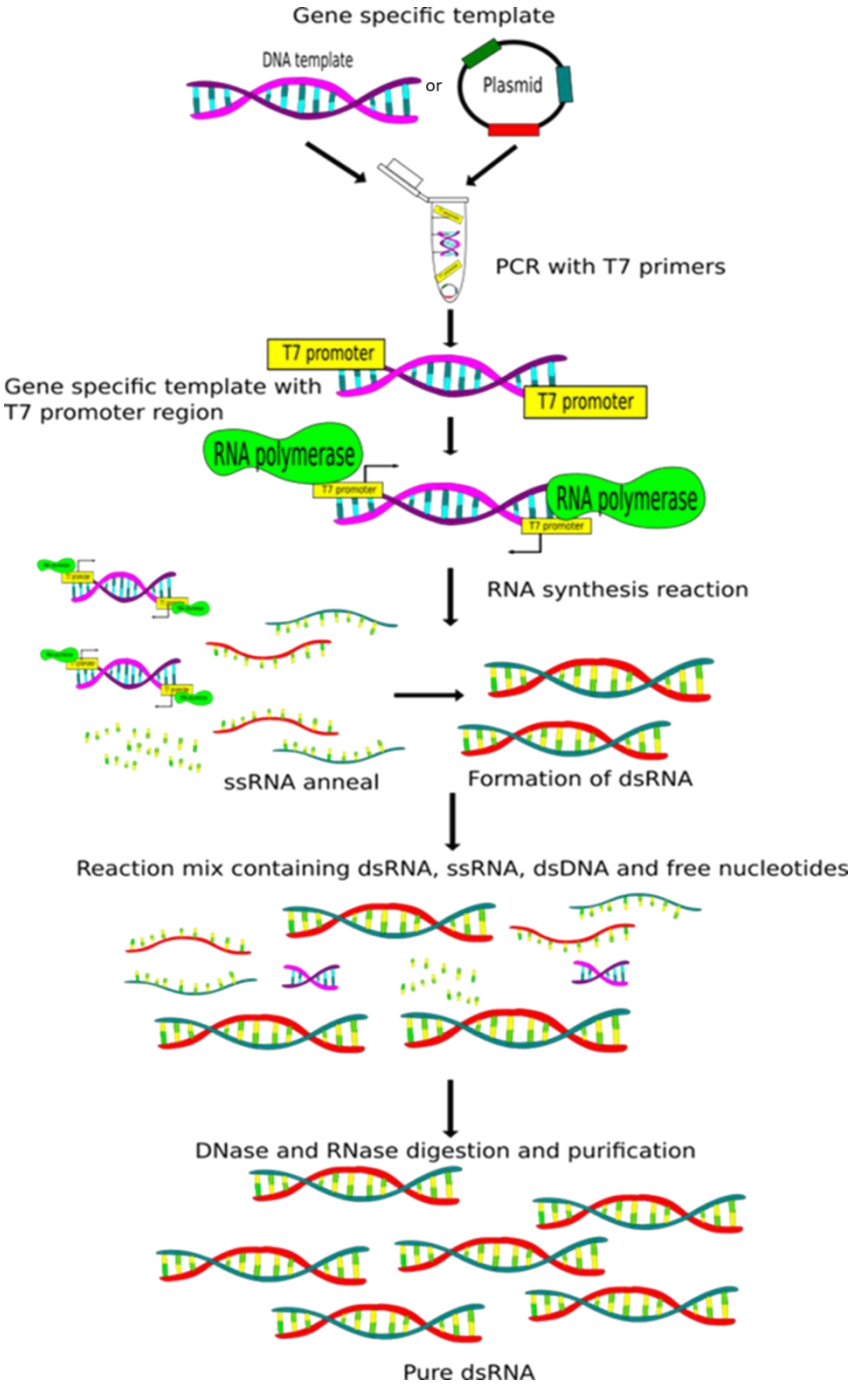


Figure 2.3: Overview of the ds*RNA* synthesis process. The DNA template for the gene of interest is in the form of a PCR amplicon or a plasmid. A template is created with a PCR step to attach the T7 promoter region to the gene of interest. The T7 promoter region is recognised by the RNA polymerase enzyme, which when combined with ribonucleotides produce single stranded RNA. The ssRNA anneals to dsRNA upon cooling in a reaction mix still containing DNA, ssRNA and free nucleotides. The dsRNA is then isolated with a purification step containing DNase I and RNase I.

(i) The production of a DNA template

The starting material for the production of dsRNA molecules consisted of a plasmid containing the gene of interest (*GFP*) or a PCR amplicon of the target gene (*EcR*) (Figure 2.3). While the *GFP* clone was provided by Prof Patrick Arbuthnot's laboratory (Antiviral Gene Therapy Research Unit, University of the Witwatersrand), the *EcR* amplicon was produced as follows. Total RNA was extracted from female *An. funestus* mosquitoes at 24 hours post-blood meal (as described in section 2.2.2), since this is the peak of *EcR* expression (Cho *et al.*, 1995). This was followed by DNase I treatment and cDNA synthesis (section 2.2.3- 2.2.5). The cDNA was used as template in a PCR reaction to amplify a 484 bp region on *EcR*. The PCR mastermix consisted of a 1X Q5 reaction buffer, 1X high GC enhancer, 0.4 mM of dNTPs, 0.5 µM of each *An. funestus EcR* primer, 0.5 µl of Q5 DNA polymerase (Catalogue number: M0491S, New England Biolabs, MA, USA), 2 µl cDNA and deionised water to make up a total volume of 50 µl. Cycling conditions were composed of initial denaturation at 98˚C for 30 seconds and 40 cycles of denaturation at 98˚C for 10 seconds, annealing at 57˚C for 30 seconds and extension at 72˚C for 30 seconds, which was followed by a final extension at 72˚C for 5 minutes. The integrity of the *EcR* templates was checked with agarose gel electrophoresis. Ten microlitres of each product was electrophoresed on a 2.5% (w/v) agarose/TAE gel at 120V for 90 minutes.

To remove all contaminants (unincorporated dNTPs, excess primers, etc.), the remaining *EcR* templates were subsequently pooled and purified with the PureLink® PCR Purification Kit (Catalogue number: K310002, Invitrogen, CA, USA) according to manufacturer's instructions. Briefly, 4 volumes of binding buffer B2 were added to 1 volume of the *EcR* PCR product. This solution was then transferred to a spin column and centrifuged at 10,000 x*g* for 1 minute. The flow through was discarded and the spin column was placed back into the collection tube. To the spin column 650 µl of wash buffer™ was added and was centrifuged at 10,000 x*g* for 1 minute. The flow through was discarded and the spin column was centrifuged at 14,000 x*g* for 3 minutes to dry the membrane. The spin column was subsequently placed into an elution tube and 50 µl of Elution Buffer (10 mM Tris-HCl, pH 8.5) was added to it. This was incubated at room temperature for 1 minute and then centrifuged at 14,000 x*g* for 2 minutes. The purified product was stored at -20˚C until further use.

(ii) Incorporation of T7 promoter sequences in the *GFP* and *EcR* DNA templates

To add T7 promoter sequences to the 5' end of the DNA templates, a PCR reaction was conducted using the T7-containing RNAi primers, and either the *GFP* clone or the above *EcR* amplicon as templates. At least 15 of these PCR reactions were conducted to ensure sufficient T7-containing dsDNA template would be obtained for the next phase.

To produce *GFP* DNA templates flanked with T7 promoter sequences at both 5' ends (thereafter called T7-*GFP* dsDNA templates), a 1X PCR mastermix consisted of the T7-*GFP* primer pair at a final concentration of 0.2 µM, 1X buffer, 0.2 mM of dNTPs, 1.5 mM of $MgCl_2$, 0.25 µl of *Taq* polymerase (Catalogue number: R011, Takara, Shiga, Japan), 1 µl of a 1:100 dilution of the *GFP* clone and deionised water to make up a final reaction volume of 50 µl. PCR cycling conditions consisted of an initial denaturation step at 94˚C for 30 seconds, 5 cycles of denaturation at 94˚C for 30 seconds, annealing at 53˚C for 5 seconds and extension at 72˚C for 40 seconds. This was followed by 25 cycles of denaturation at 94˚C for 30 seconds and annealing and extension combined at 72˚C for 45 seconds. A final extension step at 72˚C for 30 seconds completed the PCR. The integrity of the T7-*GFP* dsDNA templates were analysed with agarose gel electrophoresis. Ten microliters of each product was electrophoresed on a 2.5% (w/v) agarose/TAE gel at 120V for 90 minutes. The remaining PCR products were pooled and purified with the PureLink® PCR Purification Kit (Catalogue number: K310002, Invitrogen, CA, USA) according to manufacturer's instructions.

To produce *EcR* DNA templates flanked with T7 promoter sequences at both 5' ends (thereafter called T7-*EcR* dsDNA templates), a 1X PCR mastermix consisted of 1X Q5 reaction buffer, 1X high GC enhancer, 0.2 mM of dNTPs, 0.1 µM of each *An. funestus* T7-*EcR* primer, 0.5 µl of Q5 DNA polymerase (Catalogue number: M0491S, New England Biolabs, MA, USA), 1 µl *EcR* DNA template and deionised water to make up a total volume of 50 µl. Cycling conditions consisted of an initial denaturation step at 98˚C for 30 seconds, 5 cycles of denaturation at 98˚C for 10 seconds, annealing at 62˚C for 5 seconds and extension at 72˚C for 40 seconds. This was followed by 25 cycles of denaturation at 98˚C for 10 seconds and annealing and extension combined at 72˚C for 45 seconds. A final extension step at 72˚C for 2 minutes completed the PCR. To determine the integrity and specificity, the T7-*EcR* dsDNA products were electrophoresed in a 2.5% (w/v) agarose/TAE gel at 120V for 90 minutes. The remaining T7-*EcR* dsDNA templates were pooled to obtain a final concentration of 1 µg/µl, and the final concentrated products were purified with ethanol precipitation.

Ethanol precipitation was conducted as follows: to the pooled T7-*EcR* templates, 0.1 volumes of 3 M sodium acetate (pH 5.5) (Catalogue number: AM9740, Invitrogen, CA, USA) and 2.5 volumes of ice cold 100% (v/v) ethanol were added. This mixture was vortexed briefly and then placed at -80˚C for 1 hour. After incubation the mixture was centrifuged at 13,000 x*g* at 4˚C for 30 minutes. This was followed by 2 wash steps with 500 µl ice cold 75% (v/v) ethanol being added and centrifugation at 13,000 x*g* and 4˚C for 10 minutes each time. The template was allowed to air dry and subsequently suspended in nuclease free water.

(iii) Synthesis and purification of ds*GFP* and ds*EcR*

Double stranded RNA molecules homologous to the *EcR* and *GFP* templates (thereafter called ds*EcR* and ds*GFP*) were synthesised with the MEGAscript® RNAi Kit (Catalogue number: AM1626, Thermo Scientific, MA, USA). The transcription reaction mixtures contained 1 µg template (either T7-*EcR* or T7-*GFP* dsDNA templates from step ii), 4 µl each of T7 enzyme buffer, ATP, GTP, CTP, UTP and T7 RNA polymerase, and nuclease-free water to a final volume of 40 µl. These were incubated at 37˚C overnight as this is the optimal temperature for RNA polymerase activity. Transcription was stopped with 5 min incubation at 75˚C, and the synthesised single-stranded RNA molecules (ssRNA) were allowed to anneal to form dsRNA by cooling the solutions at room temperature. To remove any contaminants (ssRNA or dsDNA template) from the 40 µl dsRNA solution, 42 µl nuclease-free water, 10 µl of 10X digestion buffer, 4 µl of DNase I and 4 µl of RNase were added to the mixture, which was then incubated for 1 hour at 37˚C for nuclease digestion. This was followed by a column purification step (Catalogue number: AM1626, Thermo Scientific, MA, USA) to remove proteins, free ribonucleotides, ssRNA and dsDNA from the dsRNA. Each reaction mixture consisted of 50 µl of dsRNA, 50 µl of 10X binding buffer, 150 µl of nuclease free water and 250 µl of 100% (v/v) ethanol. The reaction mix was mixed by briefly pipetting and was then placed in a filter cartridge in a collection tube, after which the reaction mix was centrifuged at 14,000 x*g* for 2 minutes. The flow through was discarded and 500 µl of wash solution was added to the filter cartridge and centrifuged at 14,000 x*g* for 2 minutes. The flow through was discarded and the wash solution and centrifugation step was repeated once. After the flow through was discarded the filter cartridge was centrifuged at 14,000 x*g* for 1 minute to dry the membrane. The cartridge was subsequently placed in a new collection tube and 100 µl of elution buffer was added onto the filter and incubated in a water bath at 65˚C for 2 minutes. The filter cartridge

was then centrifuged at 14,000 x*g* for 2 minutes. Another 100 µl of elution buffer was added onto the filter and again incubated in the water bath at 65˚C for 2 minutes. The filter cartridge was finally centrifuged at 14,000 x*g* for 2 minutes with the elution containing purified ds*RNA*. One percent (w/v) agarose/TBE gels containing ds*GFP* and ds*EcR* products were electrophoresed in TBE buffer after the transcription and purification steps to ensure that the ds*RNA* produced was specific and no spurious products were present. Specific ds*RNA* products were then precipitated (as described in step ii above) to a final concentration of 10 µg/µl and stored at – 20˚C until further use.

2.2.10 Nanoinjection

To deliver ds*RNA* molecules to mosquitoes, the following method was used. All mosquitoes were fed on a 10% (w/v) sucrose solution prior to nanoinjection. Mosquitoes were immobilised at -20°C for 30 seconds before being transferred to a glass test tube placed on ice until nanoinjection. *Anopheles funestus* females were nanoinjected with 10 µg/µl of ds*RNA* in a volume of 51 nl at a speed of 46 nl/second on the Nanoject II (Catalogue number: 3-000-204, Drummond, AL, USA). The volume of 51 nl was selected as opposed to the largest volume 69 nl used on larger mosquitoes such as *An. gambiae* (Figure 2.4A). Mosquitoes were injected in the thorax (Figure 2.4B). After nanoinjection, mosquitoes were placed in recovery cages where they were provided with a 10% (w/v) sucrose solution and kept under standard insectary conditions to be used for further assays.

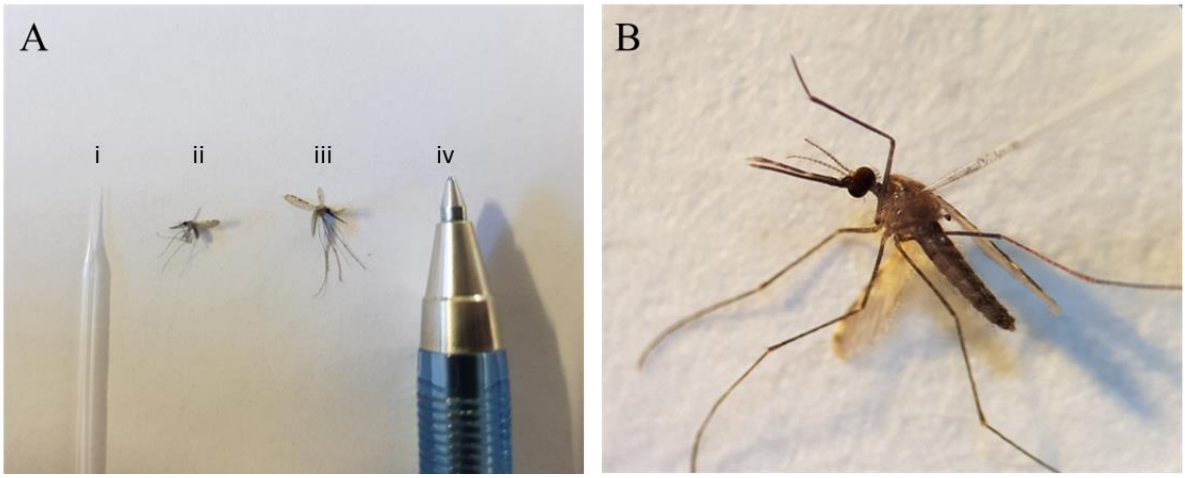


Figure 2.4: Nanoinjection of *An. funestus*. Size comparison of *An. funestus* (ii) to nanoinjection needle (i), *An. gambiae* (iii) and a pen (iv) (A). Nanoinjection in the thorax of a female *An. funestus* mosquito (B).

2.2.11 Determination of the optimal age for nanoinjection of *An. funestus*

As younger mosquitoes may be more susceptible to nanoinjection induced injuries such as cuticle damage, survival analysis was conducted to determine the age that would result in minimal mortality after injection with ds*EcR* or ds*GFP*. Fifteen mosquitoes from each age group (newly emerged, 1 day old, 2 days old and 3 days old) were nanoinjected (section 2.2.10) with phosphate buffered saline (PBS). Since PBS does not affect mosquito survival (Liu *et al.*, 2010), this procedure ensured that only the effect of injection would be measured. Three biological replicates were conducted. After nanoinjection mosquitoes were placed in 250 ml paper cups and given access to a 10% (w/v) sucrose solution. Mosquitoes were kept under standard insectary conditions and were observed for a period of 10 days after nanoinjection. Mortality was recorded daily and a Kaplan-Meier survival curve was used to represent survival. Statistical analysis was conducted with the Log Rank test on GraphPad Prism 8 (https://www.graphpad.com/scientific-software/prism/).

2.2.12 Determination of time point to confirm *EcR* knockdown after nanoinjection

To confirm that *EcR* was knocked down after nanoinjection, *EcR* expression was measured to determine at which time point *EcR* depletion was prominent. To this end, 1 day old *An. funestus* females were nanoinjected with either 10 µg/µl of ds*EcR* or ds*GFP* in a volume of 51 nl to confirm *EcR* knockdown. All mosquitoes were fed on a 10% (w/v) sucrose solution prior to nanoinjection. Two biological replicates consisting of 35 females in each replicate were used. Mosquitoes were immobilised at -20°C for 30 seconds before being transferred to a petri dish placed on ice until nanoinjection. Mosquitoes were nanoinjected as per method described previously (section 2.2.10). After nanoinjection mosquitoes were placed in 2 L recovery cages where they had access to a 10% (w/v) sucrose solution and kept under standard insectary conditions. RNA was extracted from approximately 7 mosquitoes at 24, 48 and 72 hours after nanoinjection according to the protocol (section 2.2.2). Complementary DNA was subsequently synthesised with the iScript™ cDNA Synthesis Kit (Catalogue number: 1708891, Bio-Rad, CA, USA) according to the manufacturer's instructions (section 2.2.5). To confirm *EcR* knockdown after nanoinjection with ds*EcR*, qPCR was conducted as described previously (section 2.2.6). To express percentage knockdown in ds*EcR* samples compared to control samples the following formula was used:

$$\frac{Average\ relative\ expression\ of\ dsGFP\ and\ uninjected\ samples - relative\ expression\ of\ dsEcR\ samples}{Average\ relative\ expression\ of\ dsGFP\ and\ uninjected\ samples} \text{ x } 100$$

Additionally, qPCR results from RNA extracted 48 hours after nanoinjection were used to determine if *EcR* expression was equal when normalised with *RPS7* and *RPL19* reference genes (section 3.1.6.3).

2.3 *Anopheles funestus* longevity

2.3.1 Longevity assay

One day old female *An. funestus* mosquitoes were administered with either 10 µg/µl of ds*EcR* or ds*GFP* according to the nanoinjection method described previously. An uninjected control was included to account for any mortality arising from nanoinjection. Mosquitoes were provided with a 10% (w/v) sucrose solution and maintained under standard insectary conditions after injection. Mortality in mosquitoes was recorded each day until all the mosquitoes had died. The survival assay was carried out using 3 biological replicates. The Kaplan Meier survival curve was used to represent findings and the Log Rank test was used to calculate statistical significance using GraphPad Prism 8.

Quantitative PCR was used to confirm *EcR* knockdown in mosquitoes used in the longevity assay. Fifteen mosquitoes were randomly selected from each treatment group in each biological replicate. These mosquitoes were subject to RNA extraction, RNA quality control, DNase treatment and cDNA synthesis as described previously (section 2.2.2- 2.2.5) 48 hours post injection (when *EcR* knockdown is most pronounced). Quantitative PCR was conducted using the *EcR* primer pair and normalised with the *RPS7* and *RPL19* reference gene primer pairs (section 2.2.6). Mastermix reactions and cycling conditions were conducted as per previous method. A melt peak analysis and a no-template control excluding cDNA were included to assess for specificity and contamination respectively. Relative expression analysis was calculated using the $\Delta\Delta Ct$ method. Data were subsequently analysed using a one way ANOVA with Tukey's test for multiple comparisons on GraphPad Prism 8. The hazard ratio used to represent results in the longevity assay indicates the probability of survival in ds*EcR* treated

females compared to control females at a certain time point and is calculated using the following formula:

$$Hazard\ ratio\ = \frac{Average\ \%\ deaths\ in\ dsGFP\ and\ uninjected\ control\ groups\ at\ a\ certain\ time\ point}{\%\ deaths\ in\ dsEcR\ group\ at\ a\ certain\ time\ point}$$

2.4 *Anopheles funestus* reproductive success

2.4.1 Optimisation of reproduction parameters

2.4.1.1 Determining the time for the optimal mating success rate in *An. funestus*

To determine the effect of *EcR* knockdown on *An. funestus* reproductive output, ds*RNA* had to be injected after the majority (if not all) mosquitoes were mated. Therefore, to determine the time period in which the highest mating success rate is achieved, male and female *An. funestus* mosquitoes were combined together for either 4, 8, 12, 16 or 20 days. The mating success rate in females was thereafter determined. Briefly, newly emerged adults were combined into 2 L cages each containing 30 males and 30 females. This was conducted for each time frame and repeated in three biological replicates. The adults were maintained under standard insectary conditions with a diet of 10% (w/v) sucrose solution. On days 5, 9, 11, 13, 17 and 21 females were immobilised at –20˚C and subsequently placed in 70% (v/v) ethanol. The females were then transferred to PBS. Female mosquitoes were placed on a microscope slide in PBS and dissected to isolate the spermatheca by placing dissecting needles at mid abdomen and at the cercus (end of abdomen) and pulling apart under a compound microscope (Figure 2.5). The mating status was subsequently determined using a dissecting microscope at 100X magnification. Mated females were identified by the presence of spermatozoa in their spermatheca which appear as thread-like structures around the perimeter of the spermatheca (Clements and Potter, 1967; Munhenga *et al.*, 2011). The mating success rate was determined by calculating the percentage of mated females from the total females. Statistical analysis was conducted with a one way ANOVA and Tukey's test for multiple comparisons on GraphPad Prism 8.



Figure 2.5: Determination of mating status in female *An. funestus*. Dissection of mosquito using dissection needles placed at the cercus and the middle of the abdomen to isolate the spermatheca (A). Isolated spermatheca indicated by arrow (B).

2.4.1.2 Determining if *An. funestus* requires one or two blood meals to oviposit

Certain species of *Anopheles* require several blood meals as a prerequisite of oviposition (Briegel and Hörler, 1993). To identify the number of blood meals required for *An. funestus* to oviposit, 10 female and 10 male mosquitoes were combined into 17.5 cm cubic BugDorm cages (Catalogue number: BD41515, MegaView Science, Taiwan, China) for each treatment group. Each treatment group consisted of mosquitoes that would ingest one (T1) or two (T2) blood meals and this was conducted in three biological replicates. When T2 were 10 days of age they were offered the first blood meal with the Hemotek membrane feeding system for 30 minutes. Mosquitoes that did not ingest a blood meal were discarded into ethanol. Two days later both treatment groups (T1 and T2) were offered either their first or second blood meal with the Hemotek membrane feeding system for 30 minutes and those that did not feed were discarded into ethanol. Black oviposition plates lined with filter paper were placed into cages three days later to allow for *en masse* egg counting. Two days later, the total number of eggs from each cage were counted and females were subsequently dissected and their spermathecae were examined for the presence of sperm indicating their mating status. The total number of eggs per cage was then divided by the number of mated females per cage to determine the average amount of eggs oviposited by each female. Statistical analysis conducted using an unpaired student's t test with GraphPad Prism 8.

2.4.1.3 Optimisation of oviposition for fecundity assay

Three different oviposition methods were evaluated for their efficiency to encourage oviposition in gravid *An. funestus* females (Figure 2.6). The first method utilised an oviposition vial that was lined with filter paper with approximately 1ml of water at the bottom of the vial. Subsequent to ingesting a blood meal, females were placed into individual oviposition vials to induce oviposition (Munhenga *et al.*, 2011). This method however was not ideal as *An. funestus* did not oviposit in these vials. Secondly, the black oviposition plates (used commonly in mosquito rearing) were tested as a potential method of oviposition. These oviposition plates are only suitable for use with several mosquitoes due to their size which results in *en masse* egg count. *Anopheles funestus* females preferred this medium to oviposition vials as several eggs were oviposited after ingestion of a blood meal. This method is however unreliable as it produces an average egg count and leaves one unable to differentiate between mosquitoes that oviposited and those that did not. Taking into account the differences between the oviposition vials and oviposition plates that may have encouraged oviposition, the black background of the oviposition plates stood out as a factor that could have influenced oviposition as laboratory reared *An. funestus* are known to prefer a dark background for oviposition (Bates, 1940; Huang *et al.*, 2005). The third method therefore utilised this black background which was formed by using black coloured paper to fit the bottom of 250 ml disposable paper cups. Filter paper was placed over the black background and approximately 10 ml of distilled water was added to the cups to encourage oviposition. Individual mosquitoes were placed into these cups subsequent to the ingestion of a blood meal. The majority of eggs oviposited in this study was observed in the oviposition cups lined with black filter paper therefore this method was preferential over the others. It was decided that the oviposition cups lined with black paper would be used as the subsequent medium of oviposition as it allows for the individual egg count per female and was favoured by *An. funestus* over the other methods.

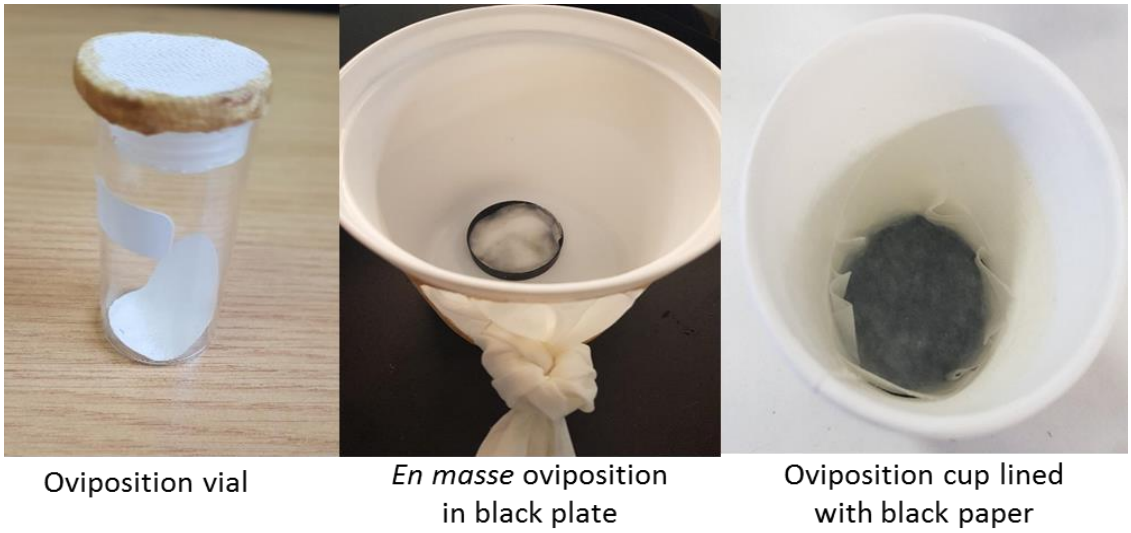


Figure 2.6: Different methods assessed as an oviposition medium for blood fed *An. funestus* females. Glass oviposition vials with moistened filter paper, *en masse* black oviposition plates and oviposition cups lined with moistened filter paper and a dark background were all trialled as oviposition mediums.

2.4.1.4 Determining if older mosquitoes are more susceptible to mortality after nanoinjection

As *EcR* knockdown was to be conducted when the optimal mating success rate was achieved, older females had to be injected. The purpose of this study was to determine if the survival of older mosquitoes after nanoinjection was adequate for experimental purposes and a high mortality did not result due to decreased fitness in older mosquitoes. This method was designed to maintain the optimal mating success rate of 12 days and the peak knockdown effect achieved at 48 hours post injection whilst obtaining the largest sample size possible for experiments. To this end, *An. funestus* females aged 5, 10 and 12 days old with a 1 day old control were injected in the thorax with 51 nl of PBS at a speed of 46 nl/second on the Nanoject II (3-000-204, Drummond, AL, USA) (section 2.2.10). The mosquitoes were thereafter transferred to 250 ml paper cups, covered with a net and allowed to recover. Mosquitoes were kept under standard insectary conditions and provided with a 10% (w/v) sucrose solution. Mosquito mortality was observed daily until all mosquitoes had succumbed and was used to determine the age at which mosquitoes would subsequently be nanoinjected (section 3.3.3). Three biological replicates were conducted which included 10 mosquitoes in each treatment group. Statistical analysis was conducted with the Log rank test on GraphPad Prism 8.

2.4.2 Fecundity assay

To determine if *EcR* knockdown has an impact on *An. funestus* fecundity, 40 newly emerged males and 40 newly emerged females were combined into 17.5 cm cubic BugDorm cages (Catalogue number: BD41515, MegaView Science, Taiwan, China) and allowed to mate for 12 days. Mosquitoes were maintained on a 10% (w/v) sucrose solution under standard insectary conditions for the duration of this experiment. When females were 10 days old they were isolated and were administered with 51 nl of ds*GFP* or ds*EcR* through nanoinjection at a speed of 46 nl/second as described previously (section 2.2.10), 40 female mosquitoes remained as an uninjected control. After injection, the females were placed back with males for the remaining two days to fulfil the 12 day period in which the optimal mating success rate is obtained. On day 11 and approximately 24 hours before blood feeding, the 10% (w/v) sucrose solution was removed and replaced with distilled water to encourage blood feeding. On day 12, fifteen females from each treatment group were removed for RNA extraction and qPCR (section 2.2.2-2.2.6) to confirm *EcR* knockdown and determine if *Lp* and *VgR* are regulated by EcR in *An. funestus*. Subsequently, the remaining females were blood fed for 1 hour on bovine blood with the Hemotek artificial membrane feeding system. Fully engorged females were thereafter removed and placed into individual 250 ml oviposition cups containing approximately 10 ml of distilled water and lined with filter paper over a black background whereas unfed or mosquitoes not fully engorged were discarded. The number of eggs oviposited by mated females were counted by microscopy to determine fecundity. Females that had oviposited were dissected after oviposition and their spermathecae observed by microscopy at 200X magnification to determine mating status; virgin females were subsequently excluded from the study. If mosquitoes had not oviposited seven days post blood meal, they were dissected to determine their mating status and observe if eggs were retained in ovaries to calculate total fecundity (Figure 2.7). Total fecundity refers to the total eggs developed (both oviposited and retained). Statistical analysis was conducted using the Kruskal Wallis test for number of eggs oviposited, and total number of eggs per mated female and the one way ANOVA for percentage oviposition with GraphPad Prism 8.

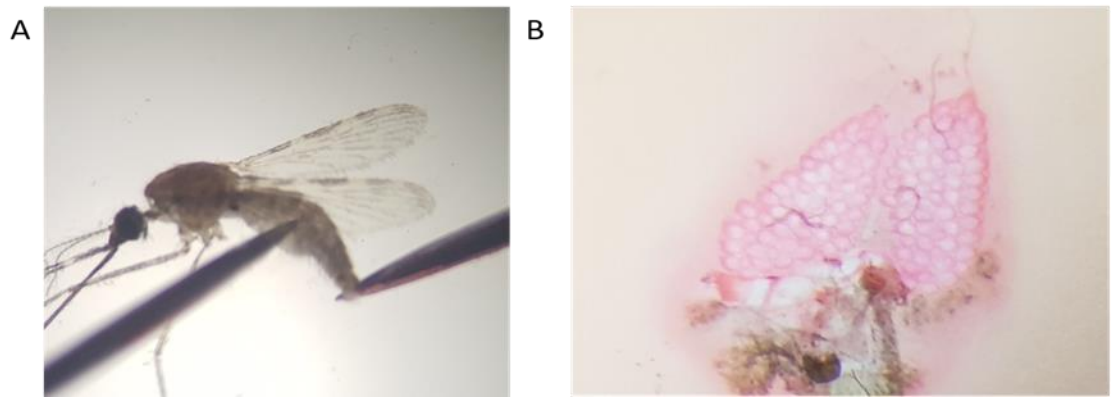


Figure 2.7: Determination of mating status and egg development in ovaries of female *An. funestus*. Dissection of mosquito using dissection needles placed at the cercus and the middle of the abdomen to isolate the spermatheca and ovaries (A). Isolated spermatheca identified by round brown shape and ovaries identified by the presence of immature or mature egg follicles stained with 0.4% (v/v) mercurochrome for visualisation purposes (B).

2.4.3 Fertility assay

To determine if *EcR* knockdown affects fertility, eggs that were oviposited during the fecundity assay were immersed in distilled water and kept under standard insectary conditions. Egg hatch rates were observed daily for 10 days and thereafter unhatched eggs were considered infertile and discarded. Statistical analysis was conducted with the Kruskal Wallis test on GraphPad Prism8.

2.5 *P. falciparum* infection assay

To determine if knocking down *EcR* influences *An. funestus*' susceptibility to *P. falciparum,* mosquitoes were either injected with 51 nl of 10 µg/µl ds*EcR* or ds*GFP* or remained as an uninjected control (section 2.2.10). Thirty mosquitoes were included per technical replicate and five technical replicates per treatment group were conducted. An additional 15 mosquitoes from each treatment group in each biological replicate were used for RNA extraction 24 hours post injection to determine *EcR* and *LRIM9* expression with qPCR (section 2.2.2- 2.2.6) at the time of infection with *P. falciparum*. Mosquitoes were aged prior to injection until approximately seven to ten days old (as mosquitoes of this age are more likely to ingest a blood meal) and were thereafter injected. After injection and 24 hours before blood feeding, the 10% (w/v) sucrose solution was removed and replaced with distilled water to

encourage blood feeding. During infection, mosquitoes were allowed to feed on an infected blood meal for 40 minutes with a glass feeder. The feeding rate was recorded and unfed mosquitoes or mosquitoes that were not fully engorged were discarded while fully engorged mosquitoes were maintained on a 10% (w/v) sucrose solution for 8 days post feeding. Eight days post feeding mosquitoes were aspirated into ethanol to immobilise them and subsequently transferred to 1X PBS. Mosquito midguts were dissected by placing dissecting needles on the thorax and fifth abdominal segment to isolate the midgut (Figure 2.8). Midguts were removed and separated from other organs and stained on a microscope slide using 0.4% (v/v) mercurochrome (Catalogue number: M7011, Sigma, MO, USA) (BEI, 2015). Midguts were subsequently viewed under a compound microscope at 400X magnification and the intensity and prevalence of oocysts in each midgut was counted and recorded. The Shapiro-Wilk test was conducted to determine if the data is normally distributed. As the data was not normally distributed, statistical analysis for intensity and prevalence data was conducted with the Mann-Whitney test where each control was individually compared with the ds*EcR* treatment group and controls were compared with each other. The transmission reducing activity (TRA) and transmission blocking activity (TBA) for ds*EcR* treatment was calculated using infection intensity and prevalence respectively and statistical analysis was conducted with the Mann-Whitney test thereafter. The TRA represents the percentage inhibition of mean oocyst intensity and the TBA represents the percentage inhibition of oocyst prevalence in mosquitoes (Miura *et al.*, 2016). The TRA is calculated with the following formula:

$$TRA = 100 \times \{1 - \frac{Mean\ number\ oocysts\ in\ test\ group}{Mean\ number\ oocysts\ in\ control\ group}\}$$ (Miura *et al.*, 2016).

Additionally, the TBA is calculated with the following formula:

$$TBA = 100 \times \{1 - \frac{Proportion\ of\ mosquitoes\ with\ any\ oocysts\ in\ test\ group}{Proportion\ of\ mosquitoes\ with\ any\ oocysts\ in\ control\ group}\}$$ (Miura *et al.*, 2016).

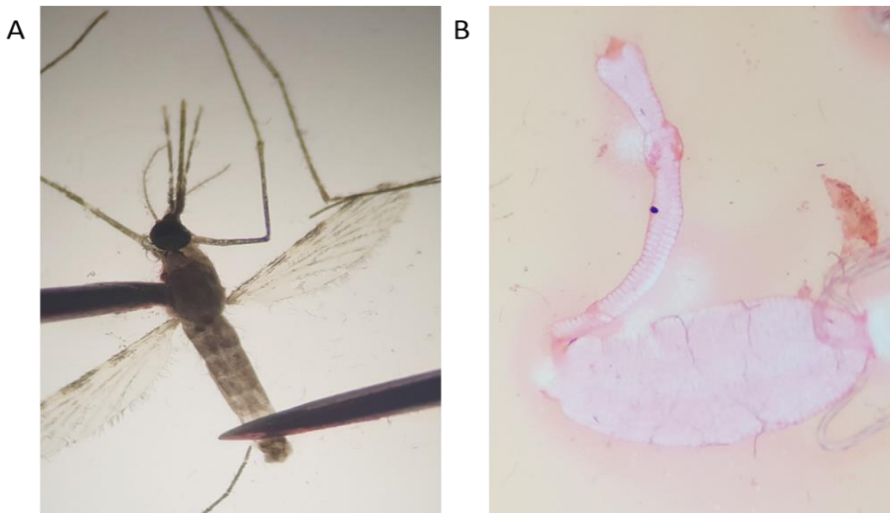


Figure 2.8: Determination of *P. falciparum* infection status in female *An. funestus*. Dissection of mosquito using dissection needles placed at the fifth abdominal segment and the thorax to isolate the midgut (A). Isolated midgut stained with 0.4% (v/v) mercurochrome for visualisation purposes (B).

3 RESULTS

3.1 Optimisation of experimental procedure

Various techniques had to be optimised before data could be generated for the specific objectives i.e. *An. funestus* longevity, reproductive success and susceptibility to *P. falciparum*. Optimisation experiments included extraction of tlRNA, cDNA synthesis and amplification of dsDNA templates used for the synthesis of ds*EcR* and ds*GFP* prior to nanoinjection. In addition, primers and conditions for the qPCR analyses were optimised using two biological replicates. Following this, sequencing was conducted to confirm specificity of gene products amplified during qPCR. Finally, optimisation of the RNAi procedure was conducted to confirm decreased *EcR* expression after ds*EcR* treatment and to confirm gene expression analysis using qPCR was accurate.

3.1.1 Total RNA extraction and cDNA synthesis

Quality control to ensure extracted tlRNA was intact and pure was of utmost importance as it affects downstream reactions such as cDNA synthesis and qPCR. The inhibition of these downstream reactions occurs with RNA samples that are contaminated with carryover protein, phenol or ethanol from previous extraction steps (Taylor *et al.*, 2010). Moreover, poor quality RNA can greatly influence the accuracy of gene expression analyses. Complementary DNA synthesised from degraded RNA is usually incomplete and fragmented (Fleige and Pfaffl, 2006). Consequently, gene expression analyses are more varied when poor quality RNA samples are used as opposed to more uniform expression when all RNA samples are of good quality (Huch *et al.*, 2005). RNA quality control is therefore integral to detect small changes in gene expression between samples.

RNA extracted from blood fed *An. funestus* females was intact, observed by a single distinct ribosomal RNA 18S fragment of 1,923 base pairs for each sample (Figure 3.1). Typically in eukaryotes, RNA is considered intact when two distinct fragments (28S and 18S) are observed after agarose gel electrophoresis, however this is not always the case with insect RNA samples. Heat denaturation prior to agarose gel electrophoresis of insect RNA results in the dissociation of the 28S RNA into two similarly sized fragments (approximately 1,900 and 2,000 base pairs)

that co-migrate concurrently with the 18S RNA (1,923 base pairs) and appear as one RNA fragment (Winnebeck *et al.*, 2010). It can therefore be confirmed that RNA extracted had good integrity and was not denatured. The single intact mosquito RNA fragment that results after heat denaturation was also confirmed by Macharia *et al.* (2015).

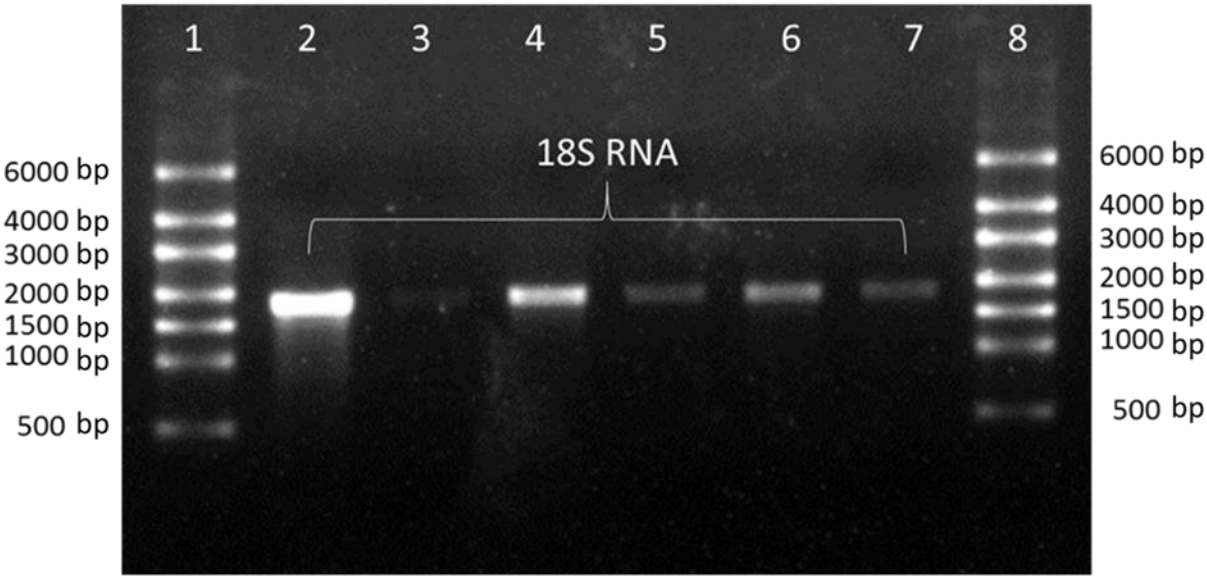


Figure 3.1: RNA gel electrophoresis confirms the presence of intact and good quality 18S RNA. RNA fragments sized with RiboRuler™ High Range RNA ladder SM 1821 (Lanes 1 and 8). RNA extracted from *An. funestus* females (Lanes 2 to 7) were confirmed to have integrity, observed by a single intact fragment of 1,923 base pairs in size. This indicated that the RNA extracted was suitable for use in downstream reactions.

To assess the purity of RNA samples, spectrophotometry was conducted using the Nanodrop™ one (ND-ONE-W, Thermo Scientific, MA, USA). RNA samples are considered pure and free of contaminants with an A_{260}/A_{280} ratio of ~1.80 (Fleige and Pfaffl, 2006). In the current study RNA samples above 1.70 were considered acceptable. All RNA samples extracted from *An. funestus* for optimisation purposes had A_{260}/A_{280} ratios above 1.8, indicating that samples were pure (Table 3.1). All RNA samples were therefore considered acceptable and subsequently used downstream for the synthesis of cDNA. First strand cDNA synthesis allows for the reverse transcription of only mRNA from tlRNA due to the use of an oligo-dT and random hexamer primers that specifically bind to the poly-adenylated tail on mRNA. The transcription of cDNA from mRNA thereby allows for the study of gene transcripts.

Table 3.1: A_{260}/A_{280} Purity ratios of RNA extracted from *An. funestus* females used in downstream reactions for optimisation purposes.

RNA sample	A_{260}/A_{280}
Sample 1	2.31
Sample 2	2.17
Sample 3	2.33
Sample 4	2.46
Sample 5	2.20
Sample 6	2.26

3.1.2 Synthesis of ds*GFP* and ds*EcR*

To efficiently knockdown the *EcR* gene, ds*EcR* was synthesised. In addition, ds*GFP* was synthesised to act as a control as it is not naturally expressed in mosquitoes and should not affect the expression of *EcR*. As described earlier (section 2.2.9), dsRNA synthesis occurs in 3 steps: (i) preparation of template (either PCR amplicon or plasmid containing the gene of interest), (ii) incorporation of T7 promoter sequences in the DNA templates, and (iii) dsRNA synthesis and purification.

3.1.2.1 Preparation of *EcR* dsDNA template

Complementary DNA was synthesised from good quality tlRNA to create a gene specific template (dsDNA-*EcR*). No amplification of *EcR* occurred after testing a range of primers, annealing temperatures (48˚C to 55˚C) and cDNA concentrations with Takara *Taq* polymerase in conventional PCR (Figure 3.2). Due to this, the Q5 DNA polymerase (Catalogue number: M0491S, New England Biolabs, MA, USA) with a fidelity 280 times higher than *Taq* polymerase was tested for its efficiency in amplifying *EcR* with conventional PCR. A range of annealing temperatures (43˚C to 68˚C) were tested with the Q5 polymerase using two primers

targeting the *EcR* transcript. Annealing temperatures (Ta) of the Q5 polymerase tested were higher than that of the *Taq* polymerase due to differences in calculations, with Ta of Q5 being the lowest Tm + 1˚C and the Ta of *Taq* polymerase being the lowest Tm - 5˚C (https://tmcalculator.neb.com/#!/main). Successful amplification was evident for annealing temperatures 60.6˚C and 59.6˚C for primer pair one and 67.1˚C, 63.3˚C and 56˚C for primer pair two when Q5 DNA polymerase was used (Figure 3.3). Primer pair one with an annealing temperature of 59.6˚C was subsequently selected for further amplification of dsDNA-*EcR* due to the higher yield it produces after amplification. Amplification of the correct sized *EcR* dsDNA template (± 484 bp) from *An. funestus* cDNA was therefore successful (Figure 3.3). This *EcR* dsDNA template together with the *GFP* dsDNA template (originating from a plasmid containing the *GFP* gene) obtained from Prof Patrick Arbuthnot's laboratory were subsequently used to generate dsDNA templates flanked by the T7 promoter region.

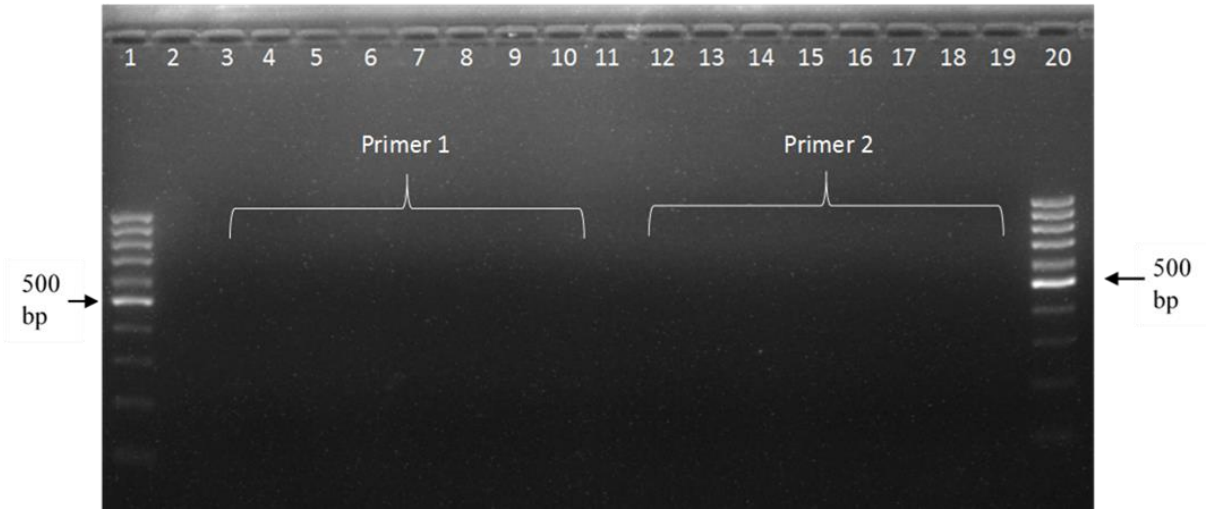


Figure 3.2: Unsuccessful amplification of the *EcR* dsDNA template with *Taq* DNA polymerase. PCR products were resolved on a 2.5% (w/v) agarose/TAE gel (Lanes 3-10 and 12-19). Amplification of *EcR* cDNA was unsuccessful due to the presence of no fragments on the gel. Annealing temperatures ranged from 48˚C to 55˚C for both primer pairs. The GeneRuler™ 100 bp DNA ladder was included to size any fragments that might have been present (Lanes 1 and 20). No template controls were included for each primer pair (Lanes 2 and 11).

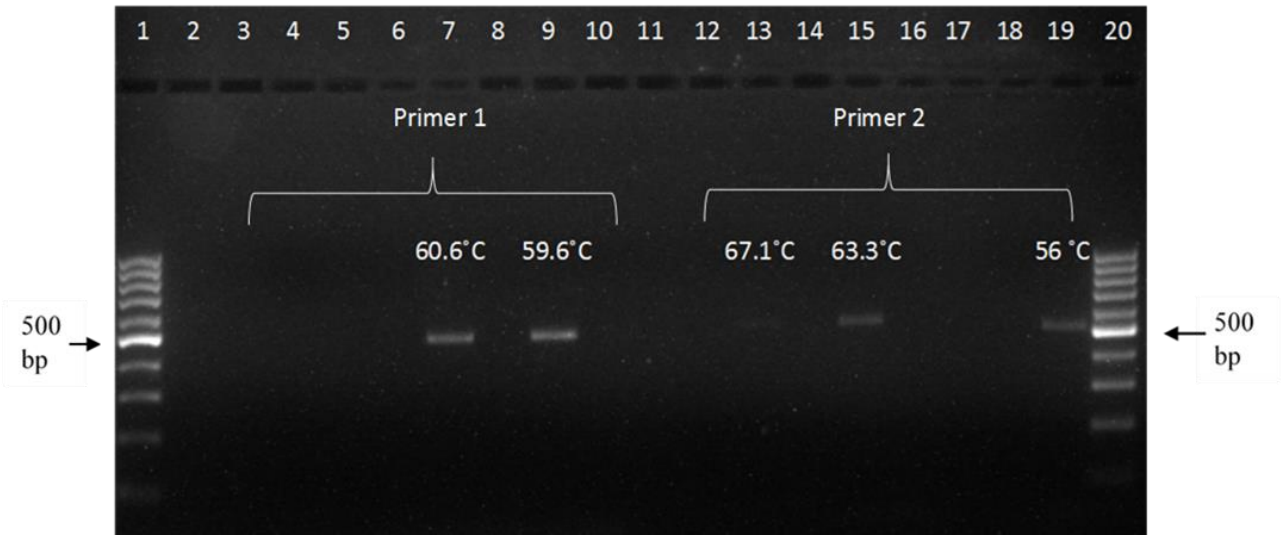


Figure 3.3: Successful amplification of the *EcR* dsDNA template with Q5 DNA polymerase. PCR products were resolved on a 2.5% (w/v) agarose/TAE gel after amplification with Q5 polymerase (Lanes 3-10 and 12-19). Annealing temperatures tested ranged from 68˚C to 56˚C for products resolved on this gel. Amplification of *EcR* occurred successfully, visible by fragments sized to 484 bp for primer 1 (annealing temperatures 60.6˚C and 59.6˚C) and 507 bp for primer 2 (annealing temperatures 67.1˚C, 63.3˚C and 56˚C). The GeneRuler™ 100 bp DNA ladder was used to size fragments (Lanes 1 and 20). No template controls were included for each primer pair and indicated no contamination (Lanes 2 and 11). Specific annealing temperatures were 68˚C (Lanes 3 and 12), 67.1˚C (Lanes 4 and 13), 65.5˚C (Lanes 5 and 14), 63.3˚C (Lanes 6 and 15), 60.6˚C (Lanes 7 and 16), 58.3˚C (Lanes 8 and 17), 56.9˚C (Lanes 9 and 18) and 56˚C (Lanes 10 and 19).

3.1.2.2 Incorporation of T7 promoter sequences in the dsDNA templates

The *EcR* dsDNA amplicon (Figure 3.3) and the *GFP* plasmid were used as templates in PCR reactions with T7 promoter containing primers to incorporate the T7 sequences into the dsDNA templates. The synthesis of *GFP* and *EcR* dsDNA templates flanked with the T7 promoter sequences was successful, as specific fragments of ± 544 bp (Figure 3.4A) and ± 530 bp (Figure 3.4B) were obtained for *GFP* and *EcR*, respectively.

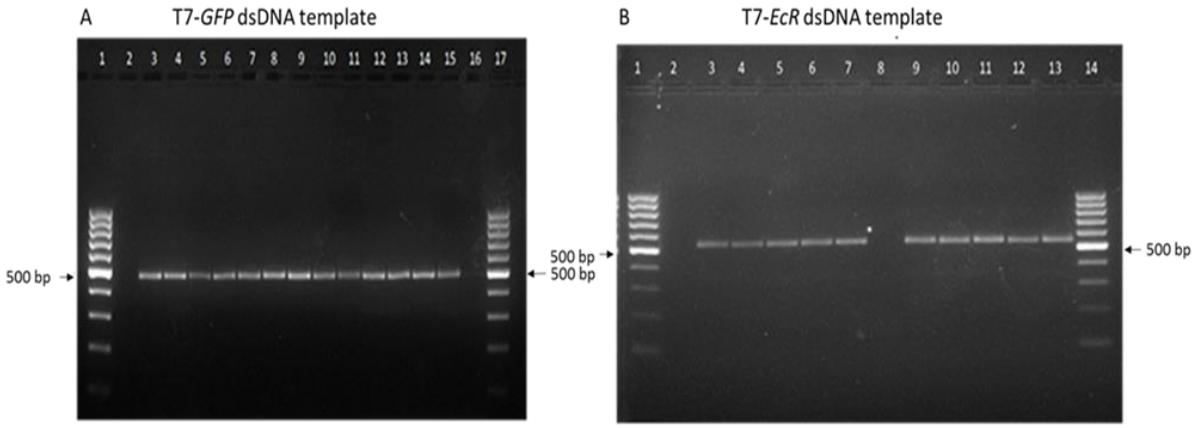


Figure 3.4: Incorporation of the T7 promoter region into dsDNA templates. Synthesis of T7-*GFP* dsDNA template (A). *GFP* templates flanked by the T7 promoter region were successfully amplified by PCR (± 544 bp) and resolved on a 2.5% (w/v) agarose/TAE gel (Lanes 3-16). These products served as a template for dsRNA transcription. A no template control confirmed no contamination was present (Lane 2). The GeneRuler™ 100 bp DNA ladder was used to size fragments (Lanes 1 and 17). Synthesis of T7-*EcR* dsDNA template (B). *EcR* templates flanked by the T7 promoter region (± 530 bp) were successfully amplified by PCR and resolved on a 2.5% (w/v) agarose/TAE gel (Lanes 3-7, 9-13). These products served as a template for dsRNA transcription. No template controls confirmed no contamination was present (Lanes 2 and 8). The GeneRuler™ 100 bp DNA ladder was used to size fragments (Lanes 1 and 14).

3.1.2.3 Double stranded RNA synthesis and purification

In the last step, the T7-dsDNA products (Figure 3.4) were used as templates in transcription reactions to synthesise dsRNA targeting *EcR* (ds*EcR*) and dsRNA targeting *GFP* (ds*GFP*). Double stranded RNA fragments of the correct sizes were obtained for ds*GFP* (± 498 bp) (Figure 3.5A) and for ds*EcR* (± 484 bp) (Figure 3.5 C). The dsRNA purification step successfully removed contaminants, such as single-stranded RNA or any DNA template/ primers remaining from ds*GFP* (± 498 bp) (Figure 3.4B) and ds*EcR* (± 484 bp) reaction mixes (Figure 3.4D). Therefore the ds*GFP* and ds*EcR* products synthesised were of good quality and were subsequently used in the longevity, reproductive success and *Plasmodium* susceptibility assays.

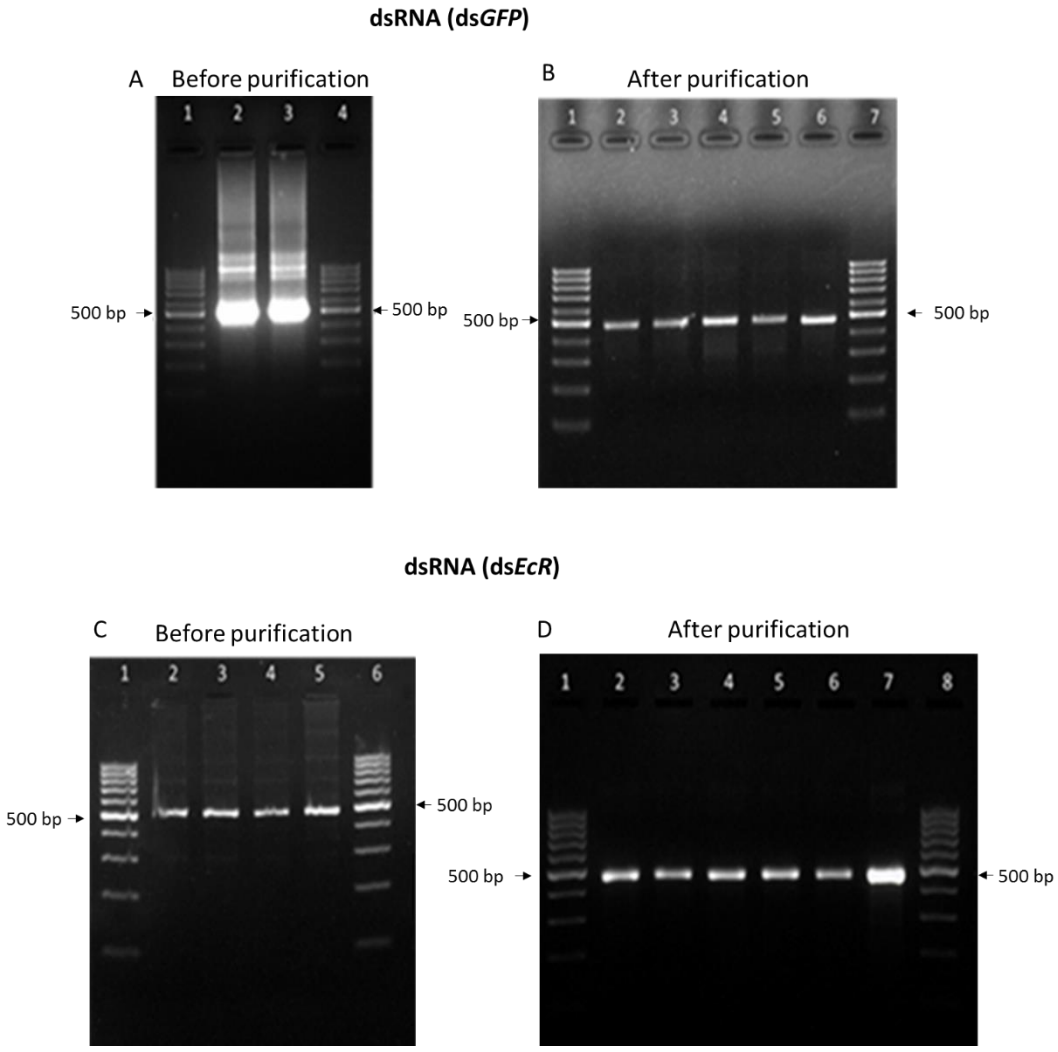


Figure 3.5: Double stranded RNA synthesis. Double-stranded RNA (ds*GFP*) before (A) and after (B) purification resolved on 1% (w/v) agarose/TBE gels. A large yield of ds*GFP* was produced before purification as observed by the prominent fragment (± 498 bp), fragments observed close to 1 kb are recognized as secondary structure as it is double the size of the specific product (Lanes 2 and 3). The GeneRuler™ 100 bp DNA ladder was used to size fragments (Lanes 1 and 4). Purification of ds*GFP* products resulted in specific dsRNA fragments of the expected size (± 498 bp) (Lanes 2- 6). The GeneRuler™ 100 bp DNA ladder was used to size fragments (Lanes 1 and 7). Double-stranded RNA (ds*EcR*) before (C) and after purification (D) resolved on 1% (w/v) agarose/TBE gels. Double stranded *EcR* before purification is seen as the most prominent fragment (± 484 bp) (Lanes 2- 5). The GeneRuler™ 100 bp DNA ladder was used to size fragments (Lanes 1 and 6). Specific ds*EcR* products of the correct size (± 484 bp) are observed after the purification step indicating successful ds*EcR* synthesis (Lanes 2- 7). The GeneRuler™ 100 bp DNA ladder was used to size fragments (Lanes 1 and 8).

3.1.3 Optimisation of qPCR conditions

Quantitative PCR was used in all objectives to measure the impact of knocking down *EcR* on various transcripts. Optimisation of qPCR conditions was therefore vital to ensure accurate quantification of transcripts. Transcripts that were measured included *EcR*, those involved in vitellogenesis (*Lp* and *VgR*) and immunity (*LRIM9*) as well as the reference genes (*GAPDH*, *RPS7*, *18S*, *RPL19* and *RPS26*). The optimisation procedures are provided in more detail below.

3.1.3.1 Optimisation of qPCR conditions for target genes

To determine the optimal annealing temperature for selection of *EcR*, *LRIM9*, *Lp* and *VgR* primers to be used in subsequent qPCRs, annealing temperatures were evaluated ranging from 50˚C to 59˚C for two primer pairs designed to target each gene. Average annealing temperatures that produced the lowest C_q value and hence the fastest amplification were chosen as the optimal annealing temperatures for primers. To aid in the selection of primers, efficiency values, specificity and correlation coefficient values (R^2) were considered. Efficiency values should range from 90% to 110% for results to be acceptable, with the best efficiency being the closest value 100% whereas R^2 values should be closest to 1 (Taylor *et al.*, 2010). Primers with the best efficiency values and lowest standard deviations from each group were determined to be *EcR* primer pair 2 with an average efficiency of 94 ± 3.1%, *LRIM9* primer pair 2 with an average efficiency of 94.1 ± 4.9%, *Lp* primer pair 2 with an average efficiency of 95.5 ± 5.5% and *VgR* primer pair 2 with an average efficiency of 99.4 ± 5.3% (Figure 3.6). All primers mentioned above had correlation coefficient (R^2) values close to 1 and not below 0.980. Correlation coefficient values of these primer pairs were 0.996, 1.000, 0.992 and 0.996 for *EcR*, *LRIM9*, *VgR* and *Lp* respectively (Figure 3.7). Annealing temperatures that produced the lowest C_q values for primers selected based on efficiency were 55˚C for *EcR*, 58.8˚C for *LRIM9*, 58.5˚C for *Lp* and 57˚C for *VgR* (Figure 3.7) (Table 2.1 [only selected primer annealing temperatures shown]). Specificity was confirmed with melt curves showing one distinct peak for each *EcR*, *LRIM9*, *VgR* and *Lp* primer pair (Figure 3.7). These primers are therefore the most suitable primers out of all primer pairs tested to use in subsequent qPCRs.

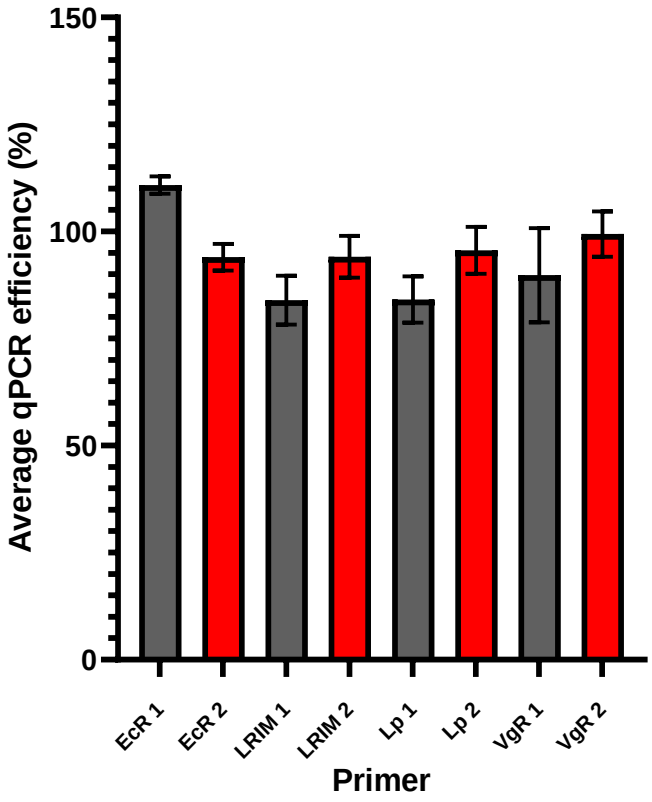


Figure 3.6: Average efficiencies of primer pairs tested indicate the best primer pairs with efficiency values closest to 100%. Represented by red bars, the *EcR* primer pair 2, *LRIM9* primer pair 2, *Lp* primer pair 2 and the *VgR* primer pair 2 produced the best efficiencies with the lowest standard deviations. These primer pairs are therefore validated to be used in subsequent qPCRs. Error bars represent standard deviation of means. Data is representative of two biological replicates.

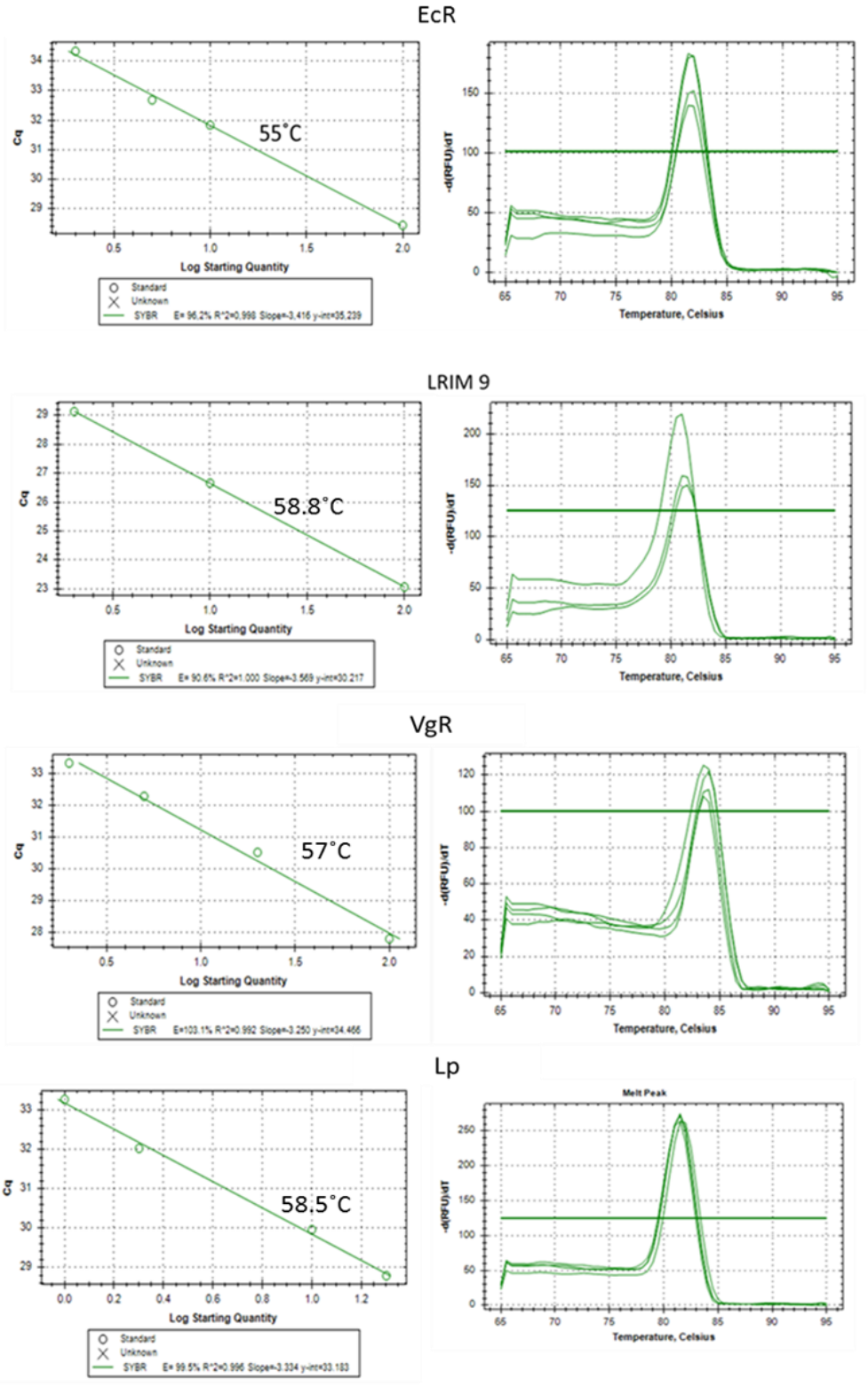


Figure 3.7: Standard curves and melt peaks of selected primer pairs indicate good efficiency, correlation coefficient values and specificity respectively. The *EcR*, *LRIM9*, *VgR* and *Lp* primer pairs all had efficiency percentages between 90% and 110%, making them suitable for use in subsequent qPCRs. All R^2 values were close to 1. Optimized annealing temperatures for each gene are indicated on the standard curve graph. Melt peaks of all primer pairs showed one distinct peak, suggesting amplification of a single specific product. Data is representative of two biological replicates.

3.1.3.2 Optimisation of qPCR conditions for reference genes

To determine which reference gene primer pairs produced the best efficiency, qPCR was conducted to evaluate five reference gene primer pairs with a standard curve. Efficiency values should range from 90% to 110% for results to be suitable for analysis, with the best efficiency being the closest value 100% (Taylor *et al.*, 2010). The reference gene primer efficiency values were 97.7 ± 6.6% for *RPS7*, 94.6 ± 5.9% for *18S*, 93.6 ± 3.0% for *RPS26*, 92.8 ± 4.0% for *RPL19* and 91.9 ± 17.4% for *GAPDH* (Figure 3.8). All reference gene primers fell within the acceptable efficiency range. Furthermore, all reference gene primers had correlation coefficient (R^2) values close to 1 and not below 0.980 and were considered acceptable for use. Correlation coefficient values of reference gene primer pairs were 0.988 for GAPDH, 0.992 for RPS7, 0.990 for 18S, 0.999 for RPL19 and 0.994 for RPS26 (Figure 3.9). To determine primer specificity, melt curves were observed. *GAPDH*, *RPS7*, *RPL19* and *RPS26* primers amplified specific products observed by the presence of one distinct peak, however, the *18S* reference gene primer was excluded from subsequent use as it produced non-specific products on multiple instances (Figure 3.9). The non-specific products produced were most probably due to primer dimer formation or primer self-annealing. This was observed in multiple instances and suggested that the *18S* primer was not suitable for subsequent qPCRs as the formation of nonspecific products may produce inaccurate results and interfere with further analysis. The four remaining reference gene primers were used for further analysis to make an improved selection using the GeNorm algorithm (Figure 3.10).

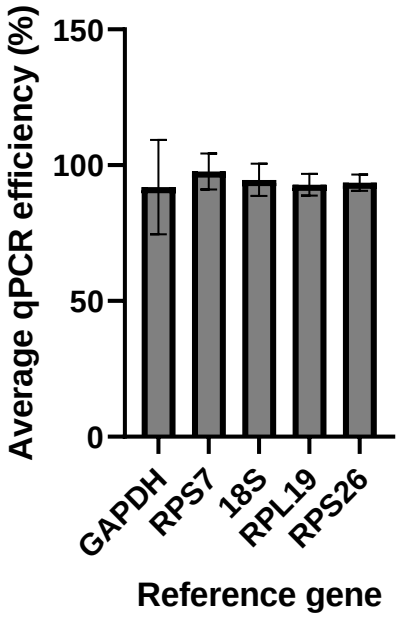


Figure 3.8: Reference gene primer efficiency values (%) of reference genes *GAPDH, RPS7, 18S, RPL19* and *RPS26.* The reference genes with the best efficiency values (90% to 110%, closest to 100%) were most suitable for subsequent use in qPCR as amplification doubles after each cycle. All reference genes fell within the acceptable range and were therefore all suitable for use. The reference gene primers closest to 100% efficiency in descending order and therefore with the best efficiency were *RPS7* followed by *18S, RPS26, RPL19* and finally *GAPDH*. Data is representative of 3 biological replicates. Error bars represent standard deviation of means.

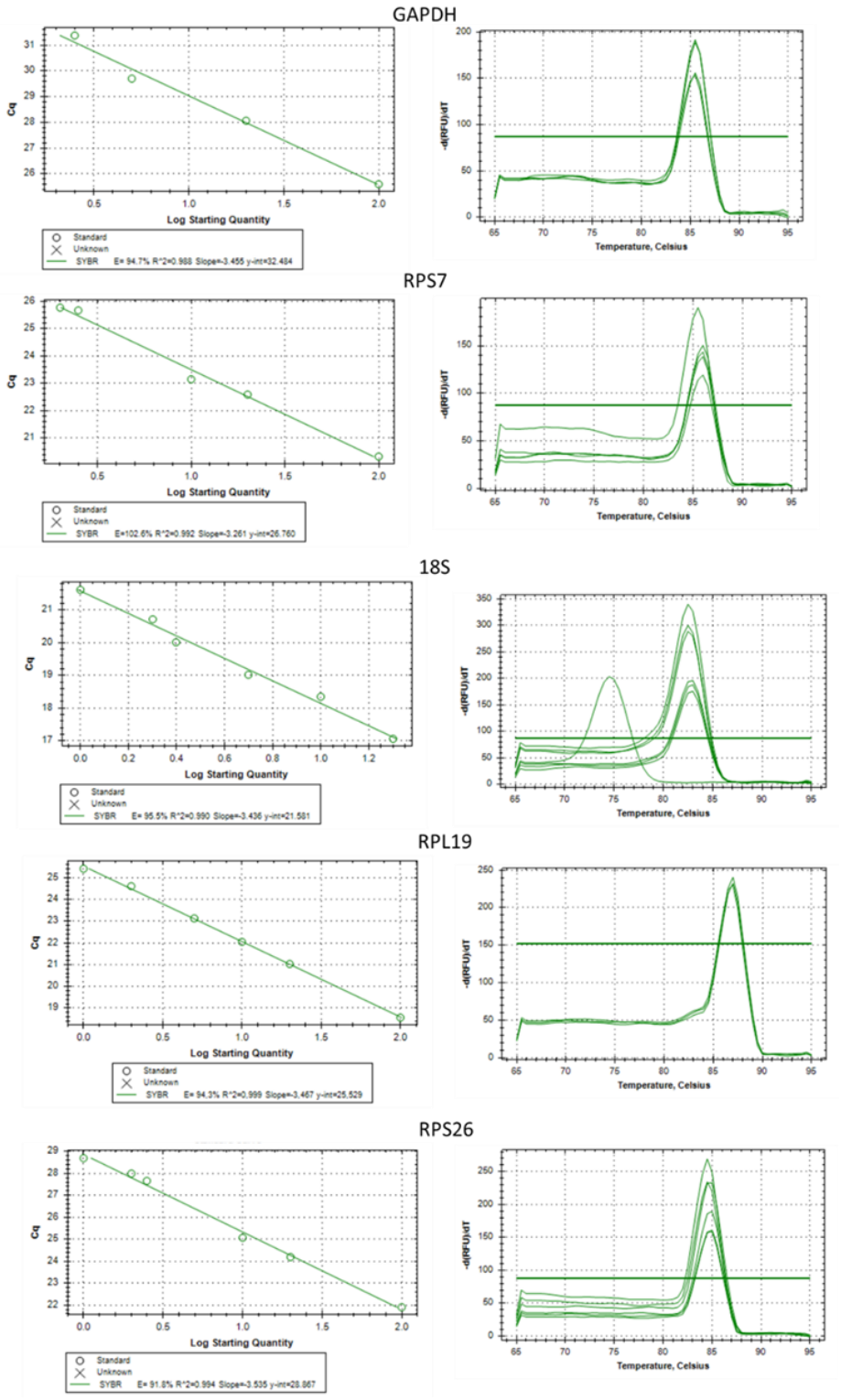


Figure 3.9: Standard curves and melt peaks of selected primer pairs indicate good efficiency, correlation coefficient values and specificity respectively. All primers had good efficiency values between 90% to 110%. Correlation coefficient values were all above 0.98 and therefore primers were suitable for use. Melt curves of *GAPDH, RPS7, RPL19* and *RPS26* had one distinct peak suggesting primers produce specific gene products. Melt curve of *18S* reference gene primer showed nonspecific amplification observed by the presence of two different melt peaks.

3.1.4 Selection of the most stable reference genes

To determine the reference genes most suitable for expression analysis, four reference genes were evaluated to determine which were expressed uniformly in ds*EcR* and ds*GFP* treated *An. funestus* females for reliable gene expression analysis. Three reference genes were ideal for use (*RPL19*, *RPS7* and *GAPDH*) due to their high stability values (Figure 3.10). Stability values represent variation in expression amongst samples, where ideal reference genes have minimal variation across samples. The reference gene *RPS26* had an acceptable stability value, meaning that it had some variation in expression amongst samples. Stability values are calculated based on the GeNorm algorithm where reference genes with the lowest M value, preferably under 1, are the most stable (Vandesompele *et al.*, 2002). As per figure 3.10, Table 3.2 indicates the reference gene M values in order of most stable to least stable (*RPL19*, *RPS7*, *GAPDH* and *RPS26*). The two reference genes with the highest stability values will be used for subsequent analysis i.e. *RPL19* and *RPS7*.

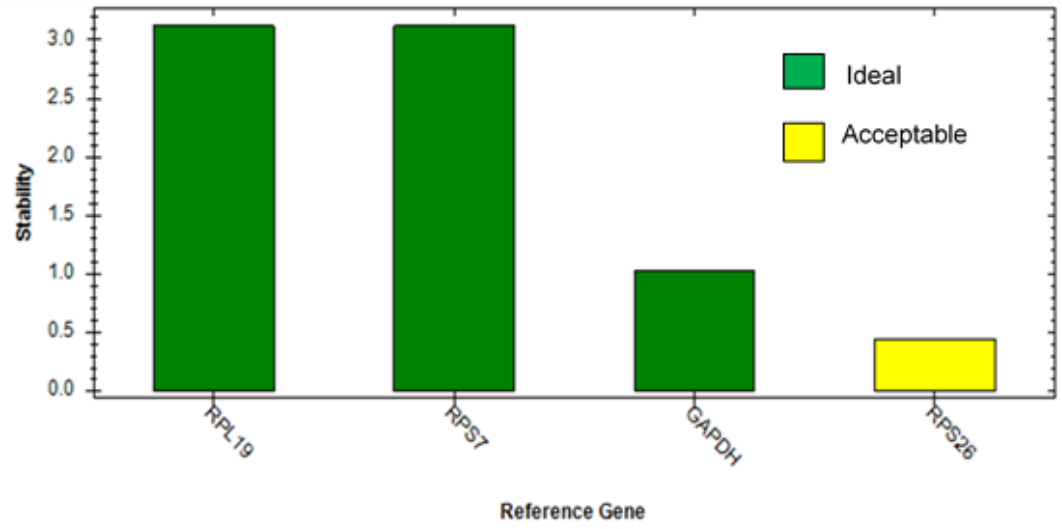


Figure 3.10: Reference gene stability plot of reference genes *RPL19, RPS7, GAPDH* and *RPS26*. The reference genes *RPL19*, *RPS7* and *GAPDH* were classified as ideal as they showed minimal variation in expression across samples. The reference gene *RPS26*, however, was classified as acceptable for use due to its lower stability value and higher degree of variation in expression across samples. *RPL19* and *RPS7* had the highest stability values and were therefore the best possible reference genes to use for qPCR. Data is indicative of two biological replicates.

Table 3.2: Decreasing expression stability of reference genes indicated by M values calculated using the GeNorm algorithm.

Reference gene(s)	M value
RPL19; RPS7	0.044
GAPDH	0.358
RPS26	0.644

3.1.5 Agarose gel electrophoresis and sequencing analysis confirmed identity of qPCR amplicons

Agarose gel electrophoresis confirmed the amplification of correctly sized gene products for *EcR* (130 base pairs), *Lp* (104 base pairs), *LRIM9* (117 base pairs), *VgR* (147 base pairs), *RPS7* (134 base pairs) and *RPL19* (223 base pairs) (Figure 3.11). Sanger sequencing of amplicons in the forward and reverse direction was subsequently used to confirm the identity of the products. Consensus sequences generated from the forward and reverse sequences of all genes were inserted into BLASTn against the *An. funestus* genome to confirm sequence similarity to each target gene- indicated with accession numbers (Table 3.3). The target gene with the highest percentage similarity (i.e. closest to 100%) and lowest expected-value or E-value (closest to zero) was considered as the gene amplified by our primers as these parameters would indicate high sequence homology and unlikeliness that this similarity occurred by chance, respectively (Pearson, 2013). Chromatograms were examined to determine the quality of the sequences (Figure S1). Sequences containing bad reads were excluded from BLASTn analyses for accurate results. The *EcR* product had a 99% similarity to the *An. funestus EcR* sequence, with an E value of $3x10^{-60}$. The *Lp* amplicon and *An. funestus Lp* sequence shared a similarity of 99% with an E value of $9x10^{-46}$. The *LRIM9* amplicon and *LRIM9 An. funestus* sequence was 100% similar with $5x10^{-55}$ as an E value. The *RPL19* gene product and *An. funestus RPL19* had a similarity of 100%, sharing an E value of $7x10^{-54}$. *Anopheles funestus RPS7* and the *RPS7* gene amplified during qPCR shared a 96.1% sequence similarity and an E value of $3x10^{-112}$. Lastly, the *VgR* amplicon shared a 99% similarity with the *An. funestus VgR* gene and had an E value of $4x10^{-47}$. All sequence similarities to the *An. funestus* genes were high. Additionally,

E values for all gene products were low which indicated high sequence homology. Taken together these results confirm that the correct gene products were amplified using the respective primer pairs.

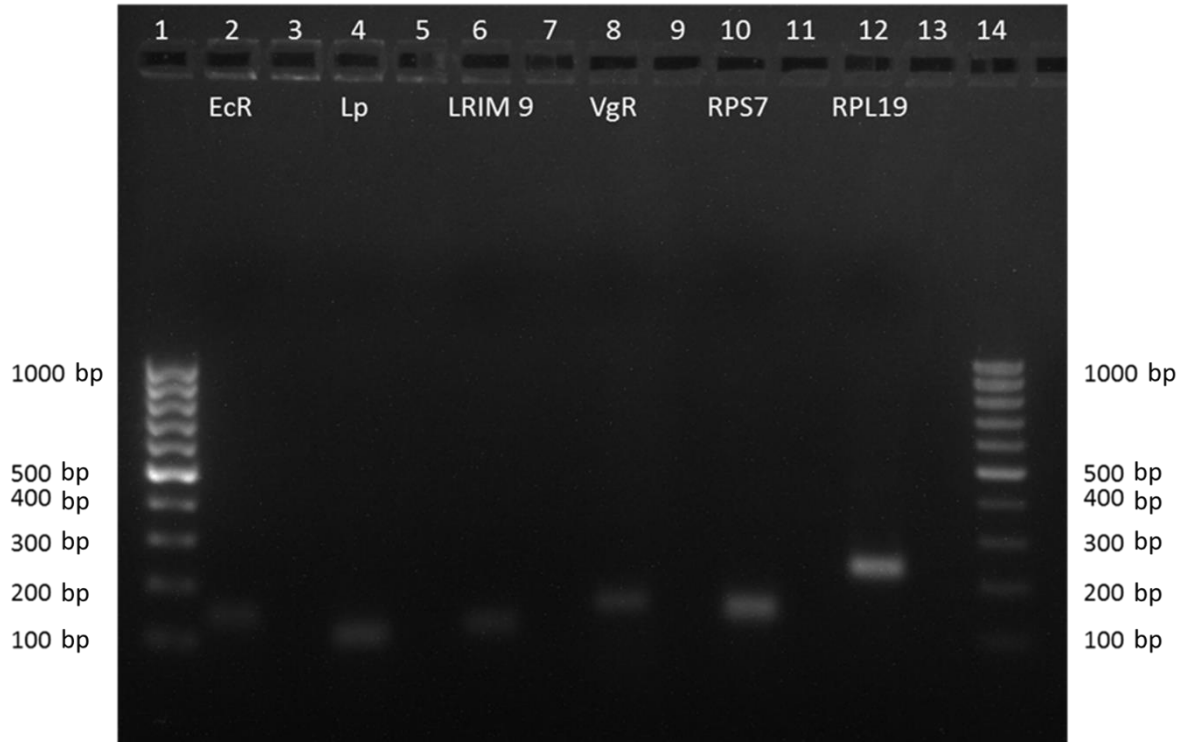


Figure 3.11: Agarose gel electrophoresis of qPCR products confirm amplification of the correctly sized fragments. The *EcR* gene products were all correctly sized at 130 base pairs (Lane 2). The *Lp* gene was of the expected size at 104 base pairs (Lane 4). *LRIM9* was the expected size of 117 base pairs (Lane 6). The *VgR* gene was of the correct size at 147 base pairs (Lane 8). Gene products of *RPS7* were all sized as expected 134 base pairs (Lane 10) and all products of *RPL19* were correctly sized at 223 base pairs in length (Lane 12). No template controls containing *EcR*, *Lp*, *LRIM9*, *VgR*, *RPS7* and *RPL19* primer pairs did not amplify, indicating no contamination in qPCR reagents (Lanes 3, 5, 7, 9, 11, 13). The GeneRuler™ 100 bp DNA ladder was used to size fragments (Lanes 1 and 14).

Table 3.3: BLAST results obtained after sequencing *EcR*, *Lp*, *LRIM9*, *VgR*, *RPS7* and *RPL19* genes.

Sample name	Percentage similarity (%)	E value	Accession number
EcR	99.2	$3x10^{-60}$	AFUN020231
Lp	99	$9x10^{-46}$	AFUN008000
LRIM9	100	$5x10^{-55}$	AFUN014990
RPL19	100	$7x10^{-54}$	AFUN005878
RPS7	96.1	$3x10^{-112}$	AFUN007153
VgR	99	$4x10^{-47}$	AFUN021786

3.1.6 Optimisation of RNAi parameters

Nanoinjection is an invasive procedure and can lead to high mortality. Therefore, to minimise mortality, the ideal age of the female for nanoinjection had to be determined. In addition, it was important to confirm that *EcR* knockdown (measured by reduced *EcR* expression levels) was achieved after nanoinjection with ds*EcR* to provide evidence that the ds*EcR* delivery system functioned. To this end, *EcR* expression was measured up to 72 hours post nanoinjection. Furthermore, *EcR* expression normalised against each selected reference gene was compared in ds*EcR* and ds*GFP* treated samples to validate that gene quantification was accurate.

3.1.6.1 Determining the age for nanoinjection of *An. funestus* females that results in minimal mortality

As younger mosquitoes may be more susceptible to nanoinjection induced injuries such as cuticle damage, survival analysis was conducted to determine the age that would result in minimal mortality after injection with ds*EcR* or ds*GFP*. This ensured that a suitable number of

mosquitoes would be available for use in the various assays. Analysis was conducted with *An. funestus* females injected with PBS at various ages. Uninjected mosquitoes consisting of mixed ages (0-3 days) were used as a control group. Mosquito survival one week after nanoinjection was as follows; uninjected control mosquitoes 76.9%, newly emerged and 1 day old mosquitoes 66.7%, 2 day old mosquitoes 53.9% and 3 day old mosquitoes 56% (Figure 3.12). Results were determined to be non-significant with the Log Rank test ($p>0.05$). Consequently, 1 day old mosquitoes were selected for nanoinjection as they have had the chance to imbibe a sucrose meal which provides sustenance prior to nanoinjection as well as to increase the sample size before age related mortality occurs.

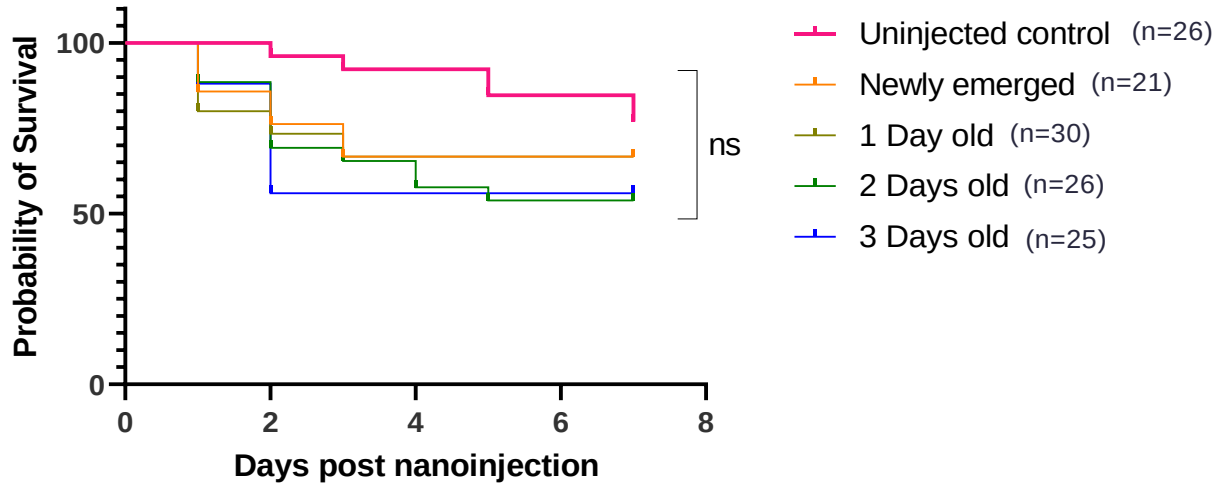


Figure 3.12: Kaplan-Meier survival curve of *An. funestus* mosquitoes injected at various ages. From the different age groups nanoinjected, probability of survival was not significant after 7 days of observation. Furthermore, the survival of injected mosquitoes did not differ from the uninjected control. Statistical analysis conducted with log rank test ($\chi 2 = 4.25$, DF = 4, $p>0.05$). Data is indicative of 3 biological replicates, with n representing the number of mosquitoes across all biological replicates. ns= not statistically significant ($p>0.05$).

3.1.6.2 Normalised *EcR* expression was significantly decreased in ds*EcR* injected mosquitoes 24 to 72 hours after injection

Ecdysone receptor expression was measured across 3 time points after nanoinjection to determine the time point to confirm that *EcR* was knocked down (when the *EcR* transcript was depleted) post nanoinjection for the various assays. Relative quantitative expression analysis

was conducted using 1 day old *An. funestus* females injected with ds*EcR* and a ds*GFP* control. RNA was extracted at 24, 48 and 72 hours after nanoinjection and qPCR was conducted to confirm *EcR* expression levels. Relative expression analysis (Bio-Rad CFX Maestro) was conducted and reference genes *RPS7* and *RPL19* were used for normalisation. Ecdysone receptor knockdown was observed 24 to 72 hours after nanoinjection as indicated by *EcR* expression values below 0.2 when compared to the *GFP* control value of 1 (Figure 3.13). Percentage *EcR* knockdown values 24, 48 and 72 hours after nanoinjection with ds*EcR* were all significant and calculated to be 90% ($p<0.05$), 99% ($p<0.01$) and 80% ($p<0.05$) respectively. This suggested that efficient knockdown was achieved when *EcR* was targeted using ds*RNA*. These results therefore demonstrated that relative expression analysis can be conducted from 24 to 72 hours after nanoinjection to confirm *EcR* knockdown.

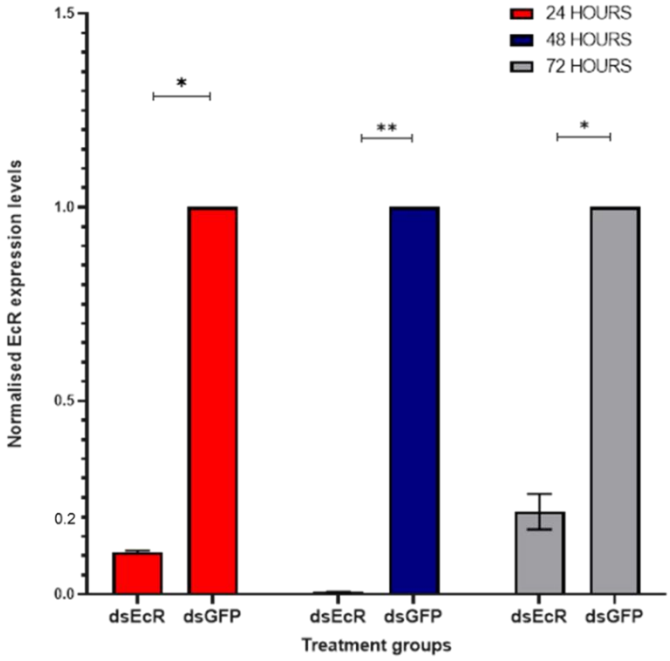


Figure 3.13: Relative *EcR* expression levels in ds*EcR* injected *An. funestus* females compared to ds*GFP* injected *An. funestus* females. The *EcR* gene was knocked down in ds*EcR* injected *An. funestus* females as *EcR* expression levels were drastically reduced compared to the *GFP* control. Statistically significant knockdown was evident in ds*EcR* injected *An. funestus* females 24, 48 and 72 hours after injection as *EcR* expression in ds*EcR* injected *An. funestus* females was 0.11 ± 0.006 ($P<0.05$), 0.01 ± 0.001 ($P<0.01$) and 0.2 ± 0.06 ($P<0.05$) respectively when compared to the *GFP* injected control of 1. This data confirmed *EcR* knockdown in *An. funestus* females injected with ds*EcR*. Data is representative of 2 biological replicates and normalised using an average of *RPS7* and *RPL19* reference genes. Expression levels calculated using relative quantification method ($\Delta\Delta$Ct). At each time point statistical significance was assessed with the unpaired student's t-test. *$p<0.05$, **$p<0.01$. Error bars represent standard deviation.

3.1.6.3 *EcR* expression was equal when normalised with the *RPS7* and *RPL19* reference genes respectively

When using two or more references genes it is important that they are equally expressed in samples during gene expression analysis. The uniformity of *EcR* expression in both ds*EcR* and ds*GFP* treated samples was confirmed by normalising each sample to *RPS7* or *RPL19* individually 48 hours post nanoinjection. Relative expression analysis (Bio-Rad CFX Maestro) was conducted and *EcR* expression levels in ds*EcR* treated samples were determined to be 0.00336 when normalised with *RPL19* and 0.00886 when normalised with *RPS7* compared to *EcR* expression of 1 in the ds*GFP* control (Figure 3.14). Efficient and equal expression was observed when reference genes *RPL19* ($p<0.01$) and *RPS7* ($p<0.01$) were used to normalise *EcR* expression levels in different treatment groups. Furthermore, no significant difference was observed in *EcR* expression in ds*EcR* and ds*GFP* treatment groups among *RPS7* and *RPL19* reference genes used to normalise data ($p>0.05$), indicating that both reference genes can be used for analysis. These results validate the accuracy of subsequent gene expression analyses.

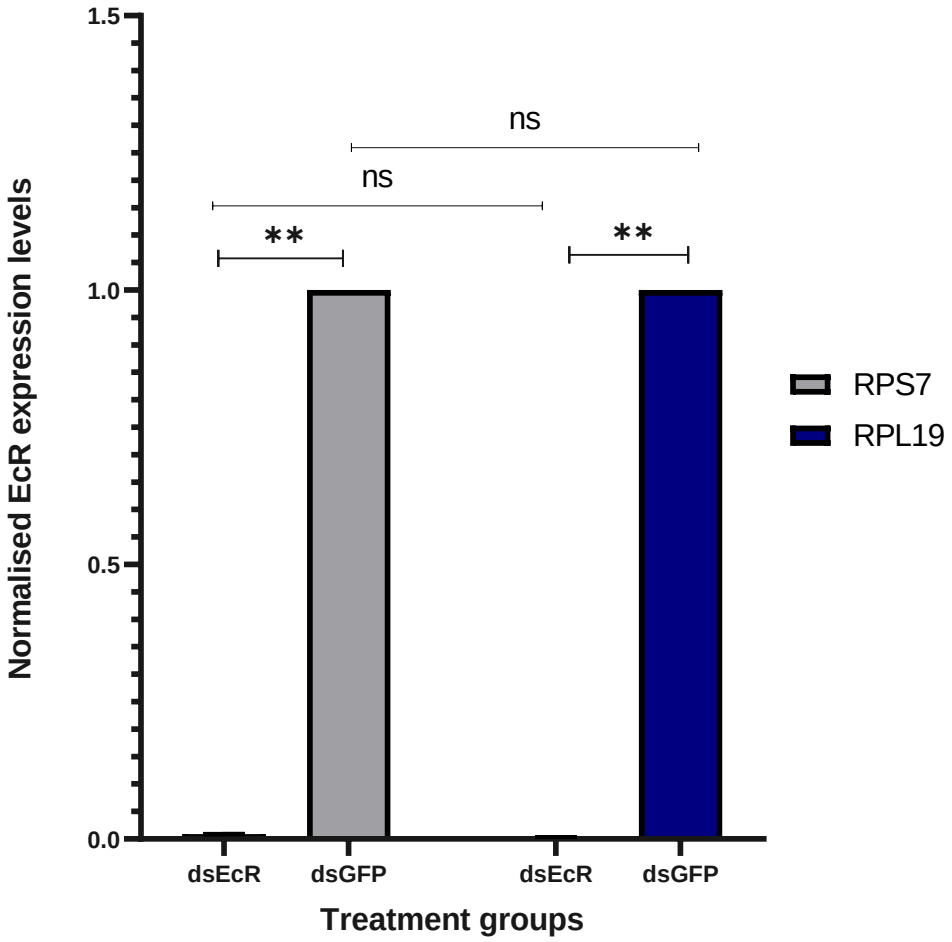


Figure 3.14: Relative expression levels of *EcR* in ds*EcR* and ds*GFP* (control) injected *An. funestus* females were constant when normalised with reference genes *RPL19* and *RPS7*. The relative expression of *EcR* after knockdown was statistically significant when normalised with reference gene *RPL19* ($p<0.01$). A statistically significant knockdown ($p<0.01$) was also observed in *EcR* when normalised with reference gene *RPS7*. No significant difference in *EcR* expression was observed between ds*EcR* treatment groups normalised with *RPS7* and *RPL19* and ds*GFP* treatment groups normalised with *RPS7* and *RPL19* ($p>0.05$). Data represents 2 biological replicates. Expression levels calculated using relative quantification. Statistical significance was calculated using the unpaired student's t-test. Error bars represent standard deviation of means. **=$p<0.01$; ns= not statistically significant.

3.2 Longevity

To determine the effect that EcR has on longevity in *An. funestus*, *EcR* was knocked down and longevity was measured in ds*EcR* treated and ds*GFP* and uninjected control *An. funestus* females.

3.2.1 The *EcR* was significantly knocked down in *An. funestus* females injected with ds*EcR*

Anopheles funestus females were injected with ds*EcR* and compared with ds*GFP* and uninjected controls to determine the impact of *EcR* knockdown on *An. funestus* longevity. A subset of *An. funestus* females was used from the longevity assay to confirm *EcR* knockdown. Total RNA was extracted from these females in each treatment group for the longevity assay. All tlRNA samples extracted from *An. funestus* treatment groups for objective one were intact (Figure S2) and had A_{260}/A_{280} ratios above 1.8, indicating that samples were pure (Table S2). All RNA samples were therefore considered acceptable for use in downstream reactions such as cDNA synthesis and qPCR. Additionally, a quality control measure for qPCR included observing melt peaks and no template controls to confirm specific amplification of gene products. Melt peaks contained a single specific peak and the no template controls did not amplify, indicating specificity of the qPCR (Figure S3).

Relative *EcR* expression in ds*EcR*, ds*GFP* and uninjected treatment groups was confirmed using qPCR. Data indicated that *EcR* was significantly downregulated in ds*EcR* injected mosquito samples with an expression of 0.04 ± 0.01 ($p<0.0001$) when compared to *EcR* expression in ds*GFP* injected (normalised expression of 1) and uninjected control samples (normalised expression of 1) (Figure 3.15). This translated to a 96% knockdown of *EcR* in ds*EcR* injected *An. funestus* females. No significant difference in *EcR* expression was observed between the ds*GFP* and uninjected treatment groups ($p>0.05$), showing that the injection procedure does not affect *EcR* expression. Therefore the administration of ds*EcR* resulted in a significant knockdown of *EcR* in *An. funestus* and survival analysis was subsequently monitored in ds*EcR*, ds*GFP* and uninjected treatment groups.

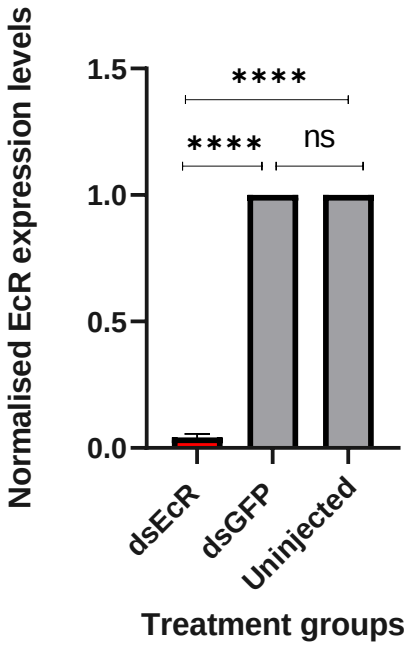


Figure 3.15: Relative *EcR* expression in ds*EcR* treated females was significantly downregulated when compared with ds*GFP* and uninjected treated females. Expression of *EcR* in ds*EcR* injected *An. funestus* females was significantly reduced compared to ds*GFP* and uninjected control samples ($p<0.0001$). No significant difference in *EcR* expression was observed between ds*GFP* and uninjected control samples. Relative expression analysis was conducted using ΔΔ Ct method. Statistical significance calculated using one way ANOVA. Error bar indicates standard deviation. ****= $p<0.0001$; ns= not statistically significant.

3.2.2 *Anopheles funestus* survival decreased when *EcR* was knocked down

To determine if EcR regulates survival in *An. funestus*, mosquito mortality was monitored in ds*EcR* treated *An. funestus* females and compared with ds*GFP* and uninjected control groups until all *An. funestus* females had succumbed. Controls included a cohort of *An. funestus* females injected with ds*GFP* and a cohort of uninjected *An. funestus* females. The median survival time was 20 days in the ds*EcR* injected group compared to 37 days and 33 days for the ds*GFP* and uninjected controls respectively (Figure 3.16). Significantly, the data showed a 57% decrease in longevity in the ds*EcR* injected *An. funestus* females when compared to an average of ds*GFP* and uninjected controls ($p<0.0001$). No significant difference was observed between survival times of dsGFP and uninjected control samples ($p>0.05$), suggesting that the injection procedure does not influence the survival in injected mosquitoes. Overall these results indicate that *EcR* regulates longevity in *An. funestus* and when knocked down, *EcR* has deleterious effects, reducing *An. funestus* female survival.

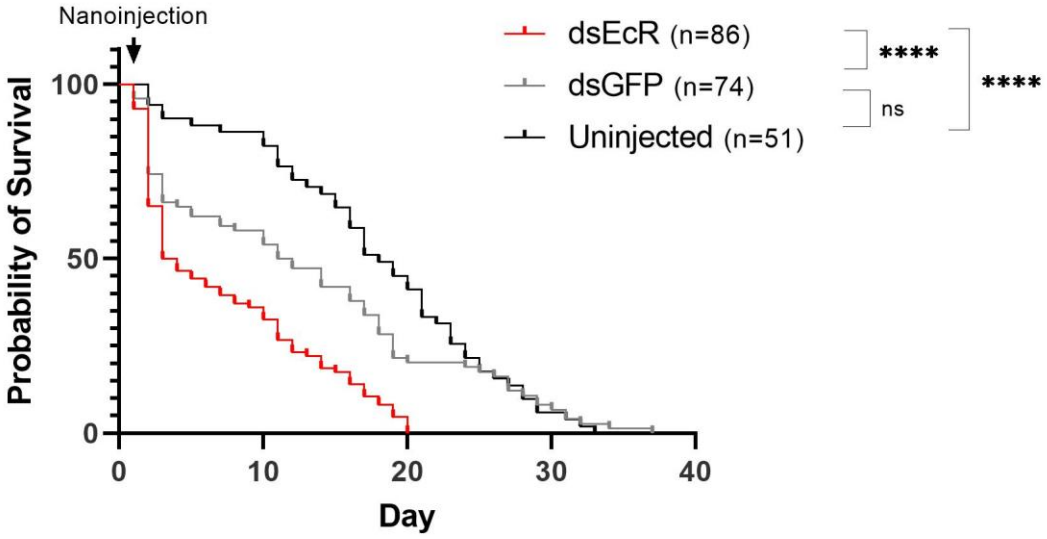


Figure 3.16: Kaplan Meier survival curve indicates decreased survival in ds*EcR* injected *An. funestus* females when compared with ds*GFP* and uninjected *An. funestus* females. *An. funestus* females injected with ds*EcR* had the lowest survival time when compared to ds*GFP* and uninjected control groups. This translated to a 57% decrease in longevity of ds*EcR* injected *An. funestus* females (Log rank test, $\chi_2 = 46.30$, DF = 2, $p<0.0001$). No significant difference was observed between ds*GFP* injected and uninjected control groups (Log rank test, $\chi_2 = 2.0$, DF = 1, $p>0.05$). ****= $p<0.0001$; ns= not statistically significant $p>0.05$.

3.2.3 *Anopheles funestus* survival was reduced at the infectious stage when *EcR* was knocked down

As *An. funestus* females begin to become infectious approximately 16 days after ingestion of an infected blood meal with *P. falciparum*, the percentage survival was calculated in all treatment groups at 16 days post injection. A percentage survival of 14% was observed in ds*EcR* injected *An. funestus* females compared to 38% ($p>0.05$) in ds*GFP* injected *An. funestus* females and 59% ($p<0.01$) in uninjected *An. funestus* females (Figure 3.17). Valuably, a significant decrease was observed between ds*EcR* and uninjected mosquitoes which is more representative of field conditions using treated and untreated mosquitoes. It is also interesting to note that at 16 days post nanoinjection, ds*EcR* treated *An. funestus* females had a hazard ratio of 1.7: 1. This indicates that 1.7 more adults die when treated with ds*EcR* 16 days post treatment than control mosquitoes. Together these results confirm a very low survival rate in ds*EcR* treated *An. funestus* during the potential infectious period, decreasing the likelihood of infection substantially as fewer *An. funestus* females will survive to transmit the parasite.

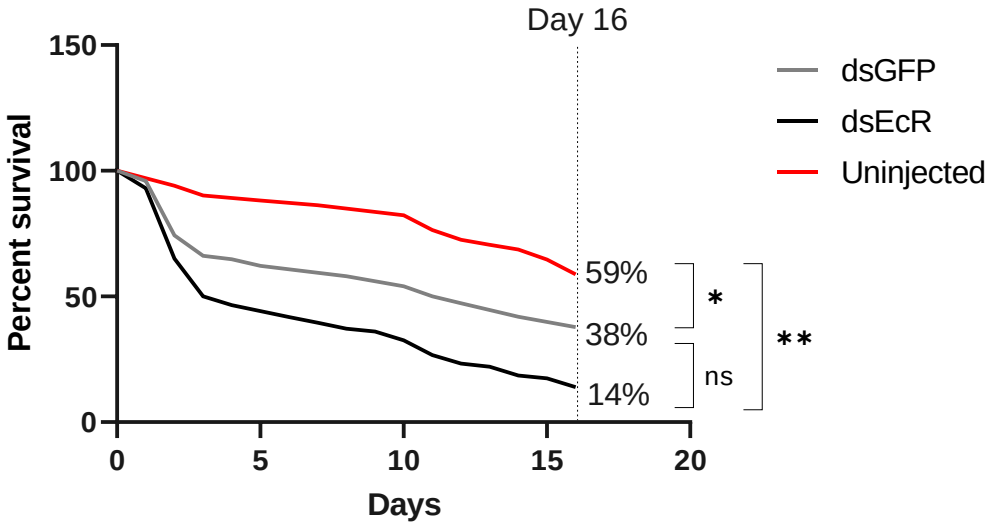


Figure 3.17: Percentage survival of *An. funestus* when *EcR* is knocked down is considerably lower than controls 16 days post injection. Only 14% of ds*EcR* treated *An. funestus* females survived 16 days post injection compared to 38% ds*GFP* treated (Log rank test, $\chi_2 = 0.56$, DF = 1, $p>0.05$) and 58% uninjected (Log rank test, $\chi 2 = 2.0$, DF = 1, $p<0.01$) *An. funestus* females. Data is representative of 3 biological replicates. ns= not statistically significant $p>0.05$; *=$p<0.05$;**$p<0.01$.

3.3 Fecundity and fertility

Fecundity and fertility assays were conducted to determine if the phenotypes of ds*EcR* treated females differed from those of control females. However, to measure these phenotypic parameters, females needed to be inseminated. Due to challenges of mating and reproduction of *An. funestus* under laboratory conditions, it was essential to determine the optimal mating time (duration of mating measured as the number of days males and females were allowed to mate) to determine fecundity and fertility. In addition to this, the number of blood meals required before oviposition and the influence of nanoinjection on older mosquitoes' survival had to be determined.

3.3.1 The optimal mating success rate was achieved after allowing mating for 12 days in laboratory reared *An. funestus*.

A prerequisite to obtain the highest number of mated *An. funestus* females for subsequent experiments was to determine the number of days required for the maximum number of females

to be inseminated —an indication of mating success rate. To do this, newly emerged males and females were combined in a cage at a 1:1 (male; female) ratio. Adults were allowed to mate for either 4, 8, 10, 12, 16 or 20 days. To determine the mating success rate, spermathecae were dissected after the required number of days and observed for the presence of spermatozoa that appear as thread-like structures around the perimeter of the spermatheca (Figure 3.18). The mean mating success rate for three biological replicates was calculated by dividing the total number of mated females by the total number of females dissected for each time point.

After 4 days of mating the mating success rate was 25.6 ± 5.1%. After 8 days the success rate increased to 42.2 ± 1.9%. After 10 days of mating the rate increased to 48.1 ± 2%. The mean mating success rate increased further to 62.2 ± 3.9% after 12 days of mating, thereafter a plateaux was reached (59.7 ± 2.6% after 16 days and 61.8 ± 2.6% after 20 days) (Figure 3.19). The largest significant difference was observed between day 4 and day 10 as well as day 4 and day 12 ($p<0.0001$), however a significant difference was also observed between day 10 and day 12 ($p<0.01$) indicating that mosquitoes needed to be combined for more than 10 days to achieve the maximum mating success rate. No significant differences were observed after 12 days of mating ($p>0.05$). The mean optimal mating success rate in laboratory reared *An. funestus* with an equal ratio of males to females is 62.2% after 12 days. As this results in the largest sample size of mated females, 12 days were subsequently used for fecundity and fertility assays.

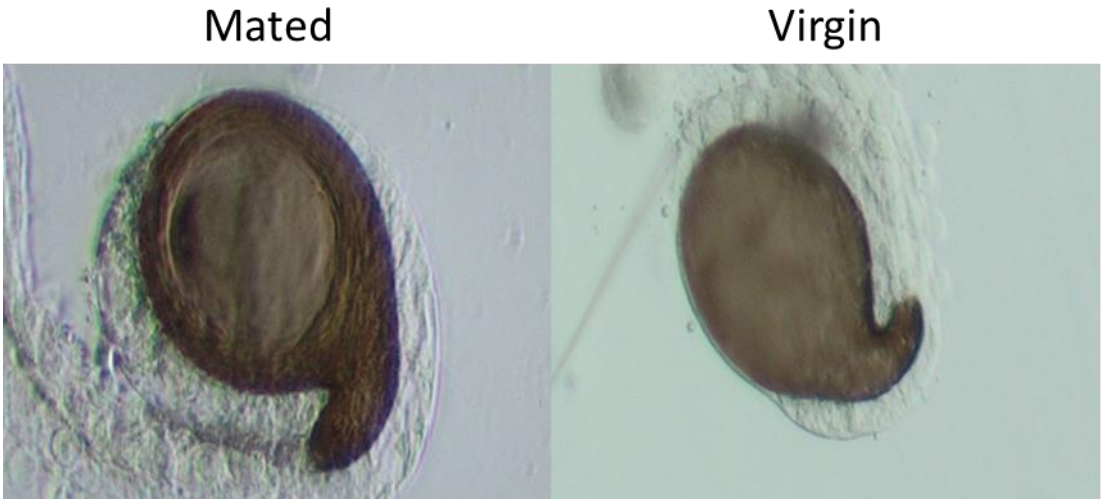


Figure 3.18: Differences in the spermatheca of mated and virgin *An. funestus* females. Spermatozoa that resemble darkened thread like structures were observed around the perimeter of the spermatheca of a mated female (left) whereas an empty spermatheca was observed in a virgin *An. funestus* female (right).

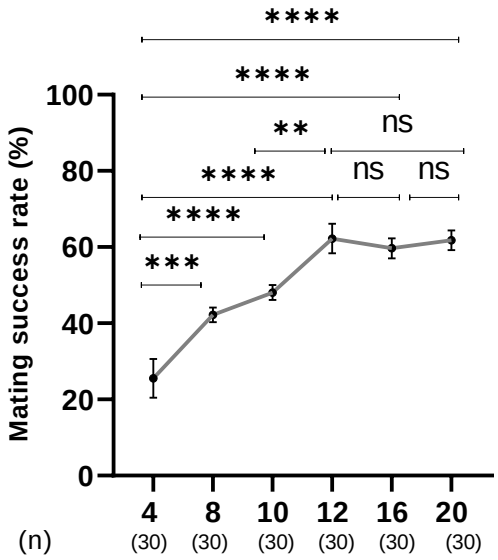


Figure 3.19: The highest mating success rate was achieved when *An. funestus* males and females are combined for 12 days after which no further increases are observed. The percentage mating success rate increased progressively until it reached its highest value of 62.2% after 12 days of mating. After this point, the mating success rate reached a plateau until day 20. Statistical significance was calculated using one-way ANOVA with Tukey's *post hoc* analysis to correct for multiple comparison. Data represents the means of 3 biological replicates. Error bars represent standard deviation of means. ns= not statistically significant $p>0.05$; **=$p<0.01$; ***=$p<0.001$; ****=$p<0.0001$. (n) = number of females per time point across 3 biological replicates.

3.3.2 Oviposition in *An. funestus* was not affected by the number of blood meals ingested

As some *Anopheles* females require several blood meals as a prerequisite of oviposition (Briegel and Hörler, 1993), the number of blood meals *An. funestus* females require for oviposition was determined. One or two blood meals were offered to *An. funestus* females aged 10 to 12 days old. Eggs were counted *en masse* and the average number of eggs per female in each treatment group was determined in mated females. The average number of eggs oviposited per female was 14 ± 4.18 after one blood meal and 23 ± 1.06 after two blood meals, however this difference was not significant ($p>0.05$) (Figure 3.20). One blood meal was subsequently used in further experiments that required fecundity and fertility to be calculated due to the simpler methodology behind it, i.e. the injection of ds*EcR* or ds*GFP* before every blood meal was not required.

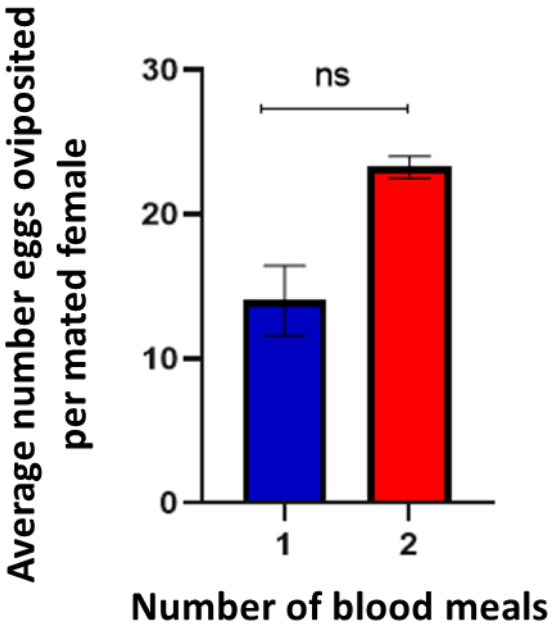


Figure 3.20: Oviposition in *An. funestus* females was not dependent on the number of blood meals ingested. No significant difference was observed between the average eggs oviposited per female after one or two blood meals. Significance was calculated using unpaired student's t test ($p>0.05$). Data is indicative of two biological replicates. Error bars represent standard deviation. ns= not statistically significant $p>0.05$.

3.3.3 Nanoinjection induced mortality was not influenced by *An. funestus* age.

The optimal mating success rate was achieved at 12 days of mating (Figure 3.19) and maximum *EcR* knockdown was achieved 48 hours post injection with ds*EcR* (Figure 3.13). Mosquitoes would therefore need to be injected 48 hours prior to the optimal mating success time i.e. at 10 days after males and females were combined for ds*EcR* to take effect after a blood meal. Moreover, older females would need to be injected with a good survival rate to continue with subsequent assays. To determine if the age of mosquitoes affects their survivability after nanoinjection, 1 day old (control), 5 day old, 10 day old and 12 day old mosquitoes were injected and mortality was subsequently monitored. The percentage survival 10 days after nanoinjection was 66.7% for 1 day old *An. funestus* females, 62.2% for 5 day old *An. funestus* females, 57.8% for 10 day old *An. funestus* females and 66.7% for 12 day old *An. funestus* females with no significant differences observed between the treatment groups (Figure 3.21). It was therefore confirmed that mosquito age does not significantly influence mortality after nanoinjection. The design for fecundity and fertility assays was therefore as follows: males and

females were combined for 12 days, females were injected at 10 days old and returned to the cage with males after injection to continue mating for another 2 days. Blood feeding then commenced when females were 12 days of age so that *EcR* depletion was highest when blood feeding takes place.

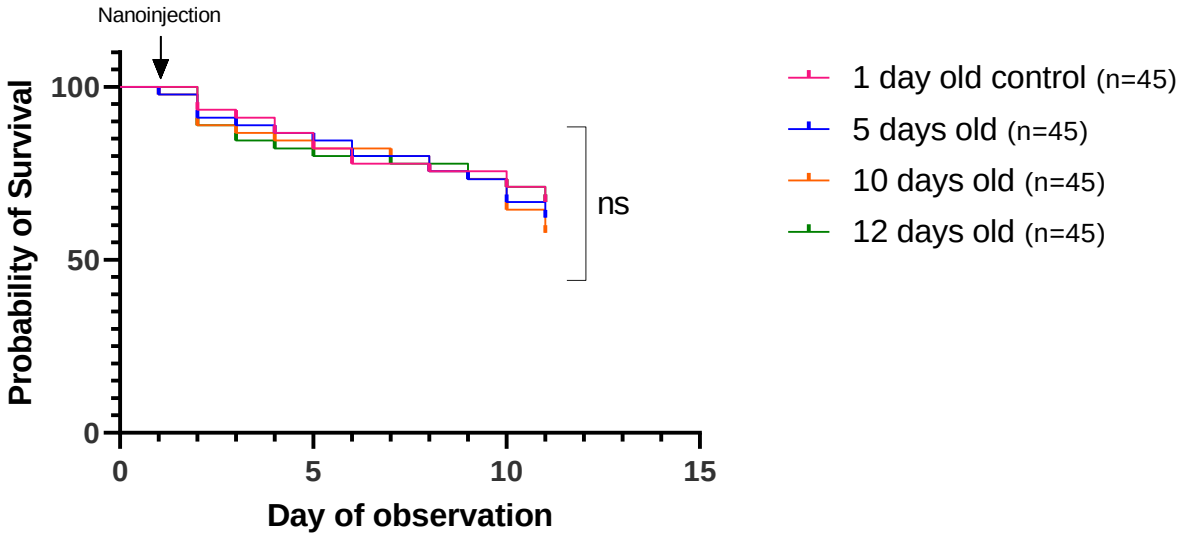


Figure 3.21: Mortality of *An. funestus* females at different age groups was not influenced by nanoinjection. Survival analysis indicated no difference in age related mortality subsequent to nanoinjection. The arrow indicated day of injection. No statistical significance was observed between experimental groups (Log rank test, $\chi^2 = 0.83$, DF = 3, $p>0.05$). Data is indicative of three biological replicates. ns= not statistically significant $p>0.05$.

3.3.4 The *EcR* was significantly knocked down in *An. funestus* females injected with ds*EcR*

Anopheles funestus females were injected with ds*EcR* and compared with ds*GFP* and uninjected controls to determine the impact of *EcR* knockdown on fecundity and fertility. A subset of *An. funestus* females were used from the fertility and fecundity assays to confirm *EcR* knockdown. Total RNA was extracted and the RNA integrity and purity were assessed. RNA samples with A_{260}/A_{280} ratios above 1.7 and the presence of a 1,923 base pair 18S RNA fragment (Figure S4) indicated that samples were pure (Table S3) and were suitable for use for cDNA synthesis and qPCR. Specificity in qPCR was confirmed as melt peaks contained a single specific peak for each gene product and the no template controls did not amplify non-specific products. (Figure S5).

Relative expression results from qPCR indicated that *EcR* was significantly downregulated in ds*EcR* injected mosquito samples with an expression of 0.05 ± 0.06 when compared to an *EcR* expression of 1 in ds*GFP* injected and uninjected control samples ($p<0.0001$) (Figure 3.22). This translated to a 95% knockdown of *EcR* in ds*EcR* injected *An. funestus* females. No significant difference in *EcR* expression was observed between the ds*GFP* and uninjected treatment groups ($p>0.05$), showing that the injection procedure does not affect *EcR* expression. Therefore, administering ds*EcR* resulted in a significant knockdown of *EcR* in *An. funestus*. The expression levels of selected reproductive genes in these ds*EcR* females were subsequently measured.

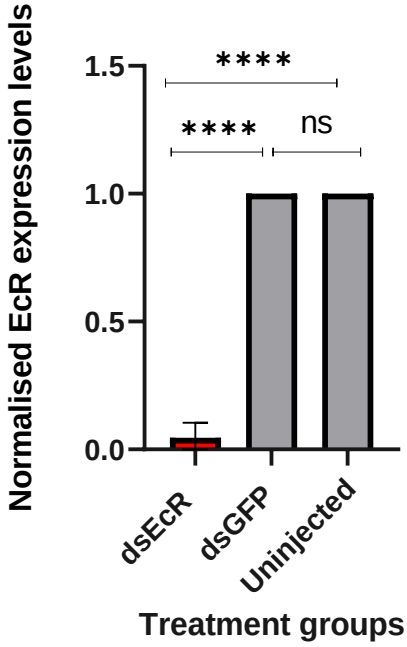


Figure 3.22: Relative *EcR* expression in ds*EcR* injected *An. funestus* females was reduced when compared to ds*GFP* injected and uninjected *An. funestus* females. A significant difference was observed in the expression levels of *EcR* in ds*EcR* injected mosquitoes compared to ds*GFP* and uninjected control mosquitoes ($p<0.0001$). There was no significant difference in *EcR* expression between ds*GFP* and uninjected control groups ($p>0.05$). Data is indicative of six biological replicates. Error bar represents standard deviation. ****= $p<0.0001$; ns= not statistically significant $p>0.05$.

3.3.5 Lipophorin and vitellogenin receptor genes involved in mosquito reproduction were downregulated when *EcR* was knocked down

Relative expression analysis of *Lp* and *VgR* genes in ds*EcR* injected females were compared to that of the ds*GFP* and uninjected control *An. funestus* females. Mean expression levels indicated that both *Lp* (0.17 ± 0.19 ($p<0.0001$)) and *VgR* (0.22 ± 0.27 ($p<0.0001$)) were significantly downregulated when *EcR* was knocked down (Figure 3.23). This translated to an 83% and a 78% reduction in *Lp* and *VgR* expression respectively. Relative *Lp* and *VgR* expression did not differ between ds*GFP* and uninjected control groups ($p>0.05$), suggesting that the injection procedure did not influence *Lp* and *VgR* expression. These results confirm that EcR regulates *Lp* and *VgR* expression. This also suggests that knocking down *EcR* could result in phenotypic changes due to the additional reduced expression of the *Lp* and *VgR* genes which are responsible for YPP synthesis as well as YPP and lipid transport to ovaries and developing oocytes.

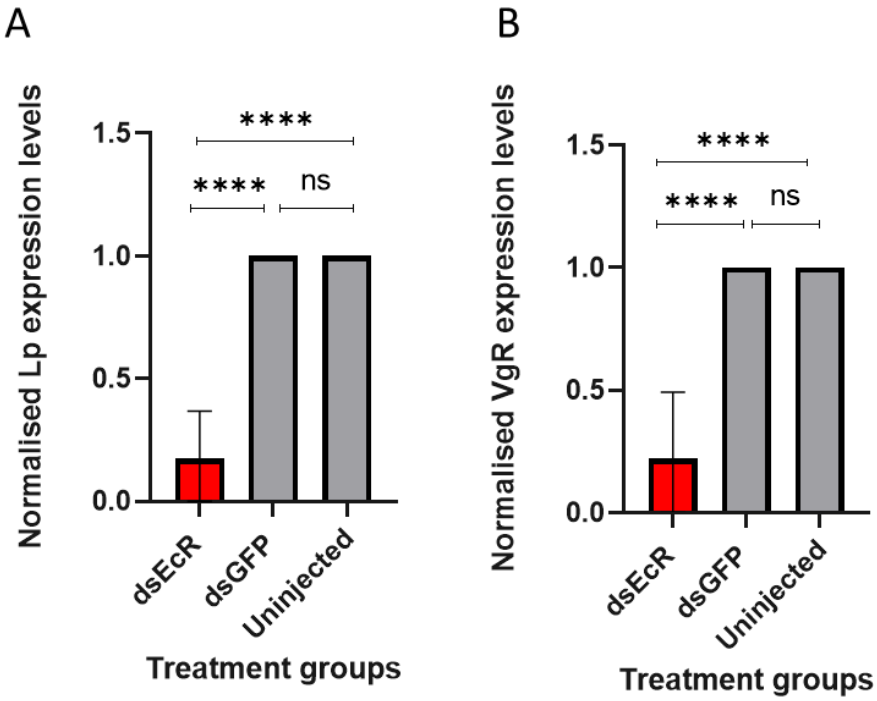


Figure 3.23: Relative *Lp* and *VgR* expression in ds*EcR* injected *An. funestus* females was reduced when compared to ds*GFP* injected and uninjected *An. funestus* females. A significant decrease in reproduction involved genes *Lp* (A) and *VgR* (B) was observed in ds*EcR* injected *An. funestus* females compared to ds*GFP* control and uninjected control females ($p<0.0001$). Data is indicative of six biological replicates. Error bars represent standard deviation of means. ****= $p<0.0001$; ns= not statistically significant $p>0.05$.

3.3.6 Ecdysone receptor knockdown reduced total fecundity in *An. funestus*

As the 20E signalling pathway facilitates a large part of mosquito reproduction, the effect of silencing *EcR* on mosquito fecundity was investigated. The *EcR* was knocked down in 10 day old females, 48 hours before offering a blood meal. Subsequent to the blood meal, fecundity was observed in mated females. The number of eggs oviposited were counted in females to determine the oviposition rate. Spermathecae were dissected in these females subsequent to oviposition to determine their mating status. Females that had not oviposited 7 days after imbibing a blood meal were dissected to determine their mating status and if mated, determine the number of eggs developed (retained) or the absence of eggs by examining their ovaries.

No significant difference in the number of eggs oviposited per female was observed between treatment groups with medians of 37, 52.5 and 36.5 eggs obtained in ds*EcR*, ds*GFP* and uninjected groups respectively ($p>0.05$) (Figure 3.24A; Table S5). Results suggested that knocking down *EcR* did not have an impact on the number of eggs oviposited when compared with control groups. As a lower sample size of ds*EcR* injected *An. funestus* females were found to have oviposited when compared to ds*GFP* and uninjected *An. funestus* females, the average oviposition rate across six biological replicates was calculated to determine if knocking down *EcR* disrupted the ability of *An. funestus* females' to oviposit. The mean percentage oviposition was determined to be 16.5% in ds*EcR* injected *An. funestus* females, 29.8% in ds*GFP* injected *An. funestus* females and 31.3% in uninjected *An. funestus* females, however these differences were not statistically significant among all treatment groups ($p>0.05$), indicating that ds*EcR* did not have an effect on mosquito oviposition rate (Figure 3.24B). Thereafter, the total number of eggs (both oviposited and retained in ovaries) in mated females was examined to determine if any changes in total fecundity are present in *An. funestus* females with *EcR* knockdown compared to control groups. Interestingly, the total egg count in mated females was significantly decreased in ds*EcR* injected *An. funestus* females with a median of 0 eggs compared with medians of 37 in ds*GFP* injected *An. funestus* females and 36 in uninjected *An. funestus* females ($p<0.0001$) (Figure 3.24C). No significant difference was observed between ds*GFP* and uninjected control groups ($p>0.05$), showing that the injection procedure did not affect the total egg count. This indicated that knocking down *EcR* reduced total fecundity in a developmental manner where oviposition was not affected. Moreover, the majority of ovaries of ds*EcR* injected mated *An. funestus* females closely resembled that of virgin *An. funestus* females, containing immature and undifferentiated oocytes whereas ds*GFP* injected and

uninjected control groups contained mature egg cells (Figure 3.25). This suggests that ds*EcR* injected *An. funestus* females typically failed to develop eggs compared to controls. One reason for this could be impairment of oogenesis and vitellogenesis resulting from the downregulation of *Lp* and *VgR* genes (Figure 3.23) which facilitate the above two processes by regulating YPP transport to developing oocytes. Together these results substantiate that knocking down *EcR* had a deleterious effect on oogenesis, not by reducing oviposition rates but by preventing the development of oocytes into mature egg cells and significantly reducing fecundity in *An. funestus*.

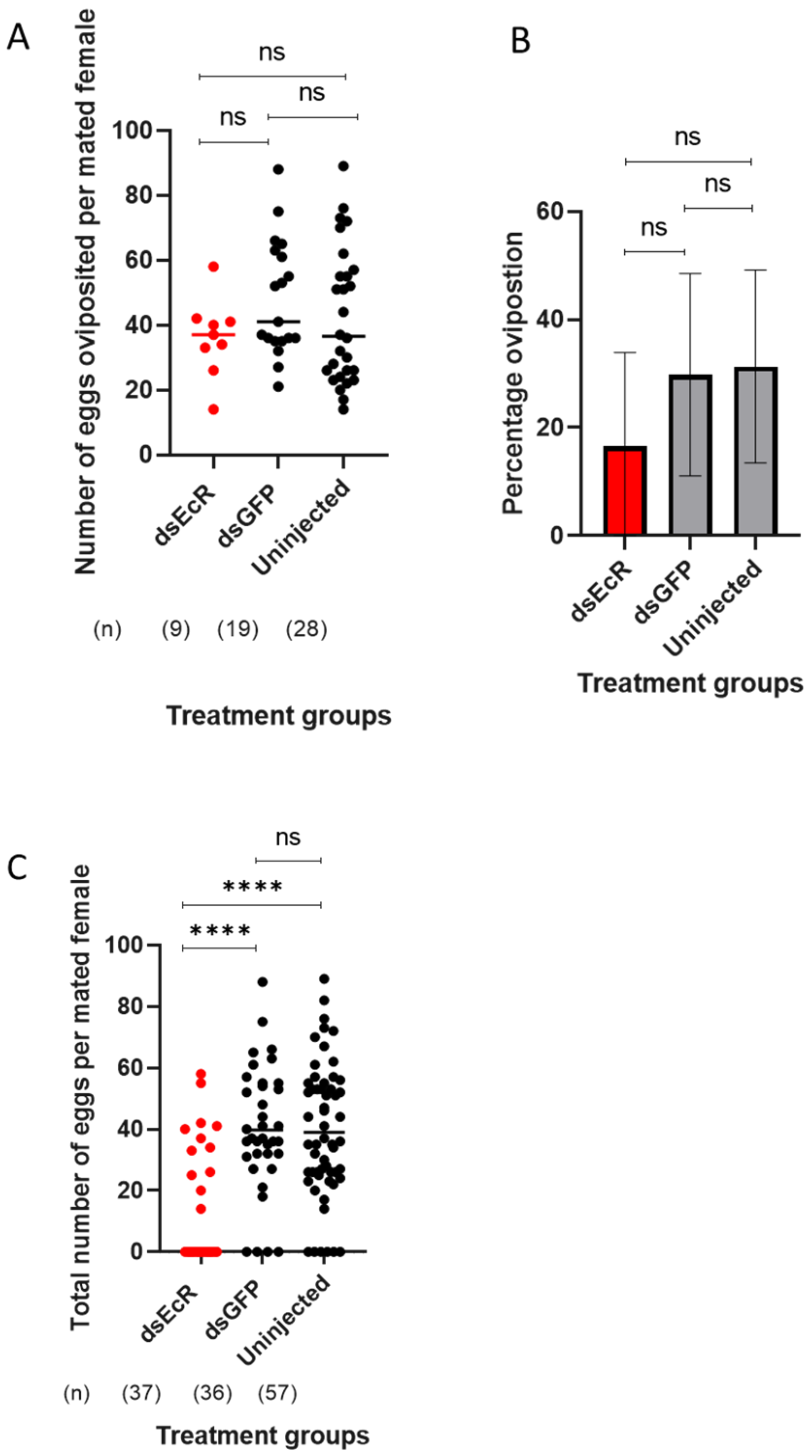


Figure 3.24: Fecundity was reduced in ds*EcR* injected females by their ability to develop eggs but not by their oviposition ability. The median number of eggs oviposited did not differ between ds*EcR*, ds*GFP* and uninjected groups respectively ($p>0.05$) (A). The mean oviposition rate was similar in ds*EcR*, ds*GFP* and uninjected treatment groups respectively ($p>0.05$) (B). The total number of eggs developed in mated females was significantly decreased in ds*EcR* injected *An. funestus* females compared to ds*GFP* and uninjected *An. funestus* females ($p<0.0001$) (C). All data are indicative of six biological replicates. Error bars represent standard deviation of means. ****= $p<0.0001$; ns= not statistically significant $p>0.05$.

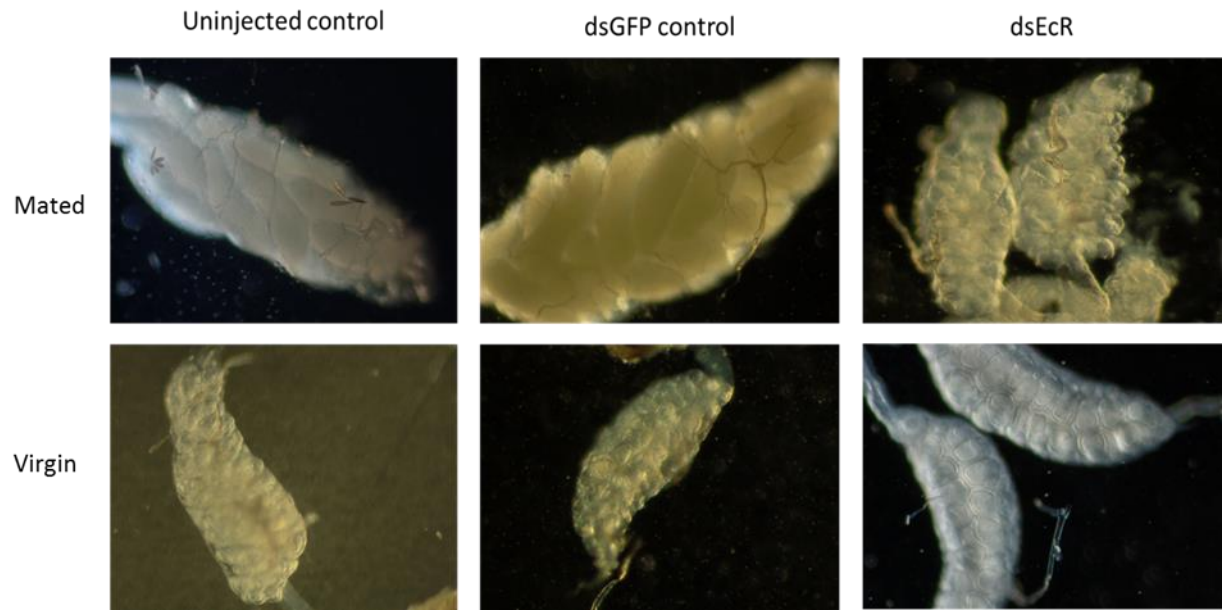


Figure 3.25: The development of eggs differed between mated uninjected and ds*GFP* controls and mated ds*EcR* treated *An. funestus* females. Mature, developed eggs (ovoid shape) were observed in mated uninjected and ds*GFP* treated *An. funestus* females. Contrastingly, ds*EcR* treated *An. funestus* females contained immature and undeveloped oocytes (spheroid shaped) in their ovaries that more closely resembled the ovaries of virgin *An. funestus* females of all treatment groups.

3.3.7 Fertility was reduced when *EcR* was knocked down in *An. funestus*

Investigating another component of mosquito reproduction that could effectively influence vector density, fertility in females was examined. The fertility rates were calculated in each treatment group by determining the number of hatchlings per female divided by the total number of eggs oviposited per female. The percentage fertility per female was 69% in ds*EcR* injected *An. funestus* females, 86% in ds*GFP* injected *An. funestus* females and 84% in uninjected *An. funestus* females ($p<0.05$) (Figure 3.26; Table S5). The fertility of ds*EcR* injected *An. funestus* females was significantly decreased by 19% compared to an average of control samples. It was clear that EcR played a role in fertility and that knocking down *EcR* had an adverse effect on mosquito fertility when compared to control *An. funestus* females.

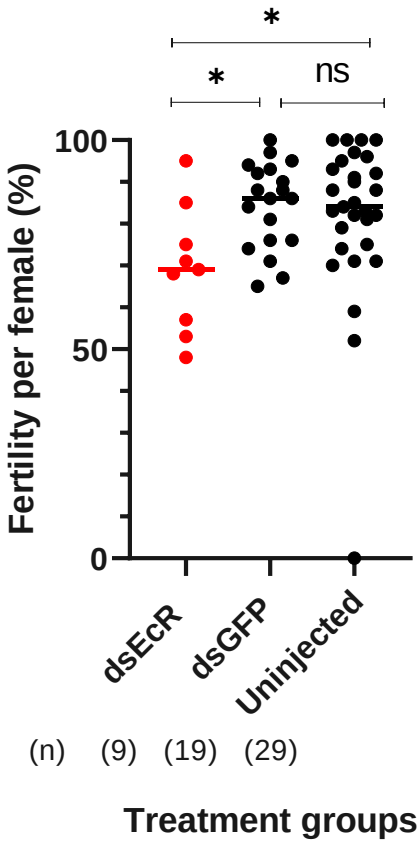


Figure 3.26: Reduced fertility was observed in *An. funestus* females treated with ds*EcR*. The median fertility of ds*EcR* treated *An. funestus* females was significantly lower compared to ds*GFP* and uninjected control groups ($p<0.05$). Data is indicative of six biological replicates. *= $p<0.05$; ns= not statistically significant $p>0.05$.

3.3.8 The blood feeding rates did not influence the reductions in fecundity and fertility in female *An. funestus*

To exclude the possibility of differences in blood feeding rates among *An. funestus* treatment groups potentially influencing mosquito fecundity and fertility, the blood feeding rates in each biological replicate were recorded and analysed. The mean blood feeding rates were 50.5 ± 23.11%, 57.17 ± 6.33% and 66.0 ± 11.58% in ds*EcR*, ds*GFP* and uninjected *An. funestus* females respectively (Figure 3.27). No significant differences ($p>0.05$) existed between treatment groups and therefore differences in blood feeding rates did not affect the differences in fecundity and fertility between ds*EcR* treated and control groups.

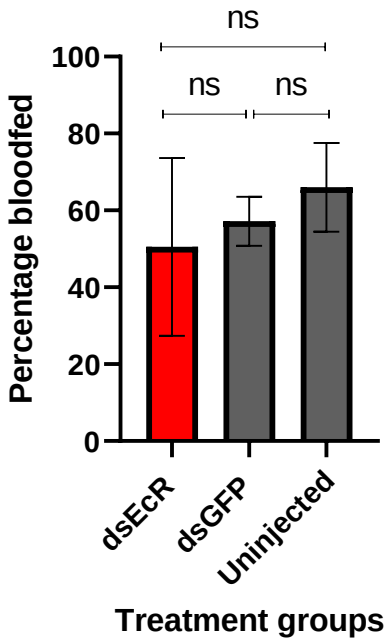


Figure 3.27: Blood feeding rates did not differ between treatment groups. Insignificant differences amongst treatment groups confirmed that the blood feeding rates did not influence any changes observed in the phenotypes of ds*EcR* treated *An. funestus* females ($p>0.05$). Error bars represent standard deviation. ns= not statistically significant $p>0.05$.

3.4 *Anopheles funestus* susceptibility to *P. falciparum*

To determine the role of EcR in *An. funestus* susceptibility to *P. falciparum*, *EcR* was knocked down in 10 day old females. A subset of females were removed 24 hours after injection for RNA extraction and qPCR analysis, while the rest of the females were fed on *P. falciparum* infected blood. Double stranded *GFP* and uninjected controls were also included and analysed accordingly.

3.4.1 The *EcR* was significantly knocked down in ds*EcR* injected *An. funestus* females

Anopheles funestus females were injected with ds*EcR* and compared with ds*GFP* and uninjected controls to determine the extent of *EcR* knockdown. Total RNA was extracted from a subset of *An. funestus* females to evaluate RNA integrity and purity. The presence of a single 1,923 base pair 18S RNA fragment (Figure S6) and A_{260}/A_{280} ratios above 1.7, indicated integrity and purity in samples respectively (Table S4). All RNA samples were therefore

considered acceptable for use in cDNA synthesis and qPCR. Additionally, melt peaks contained a single specific peak for each specific gene product and the no template controls did not amplify non-specific products, confirming that the qPCR was specific (Figure S7).

Relative *EcR* expression 24 hours after knockdown (to confirm *EcR* expression at the time of *P. falciparum* infection) was determined in ds*EcR*, ds*GFP* and uninjected treatment groups using qPCR. Data indicated that *EcR* was significantly downregulated in ds*EcR* injected mosquito samples with an expression of 0.16 ± 0.20 when compared to an *EcR* expression of 1 in ds*GFP* injected and uninjected control samples ($p<0.0001$) (Figure 3.28). This translated to an 84% knockdown of *EcR* in ds*EcR* injected *An. funestus* females. No significant difference in *EcR* expression was observed between the ds*GFP* and uninjected treatment groups ($p>0.05$), showing that the injection procedure did not affect *EcR* expression. Therefore the administration of ds*EcR* resulted in a significant knockdown of *EcR* in *An. funestus*.

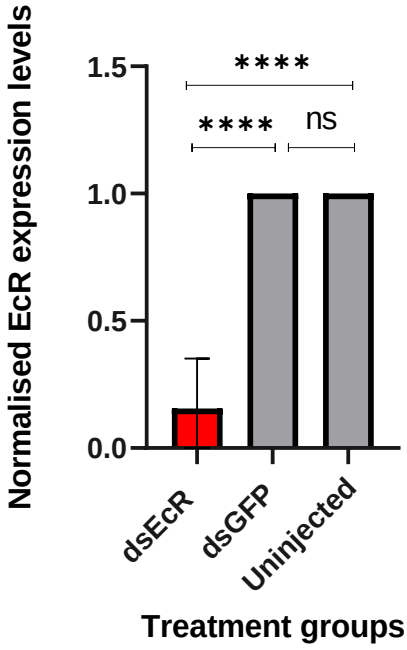


Figure 3.28: Relative *EcR* expression in ds*EcR* injected *An. funestus* females was reduced when compared to ds*GFP* injected and uninjected *An. funestus* females. A significant reduction in *EcR* expression was observed in ds*EcR* treated mosquitoes compared to controls ($p<0.0001$). Data is indicative of five biological replicates. Error bar represents standard deviation. ****= $p<0.0001$; ns= not statistically significant $p>0.05$.

3.4.2 Immune gene: *LRIM9* was downregulated when *EcR* was knocked down

Leucine rich immune protein 9 is known to be regulated by EcR and functions to kill *P. berghei* in the mosquito vector (Upton *et al.*, 2015). To confirm that *LRIM9* was regulated by *EcR* in *An. funestus*, relative expression analysis in ds*EcR*, ds*GFP* and uninjected treatment groups was conducted. Mean expression levels indicated that *LRIM9* was downregulated to 0.38 ± 0.18 in ds*EcR* treated, uninfected *An. funestus* females ($p<0.0001$) (Figure 3.29). This translated to a 62% reduction in *LRIM9* expression. These results confirmed that *EcR* regulates *LRIM9* expression.

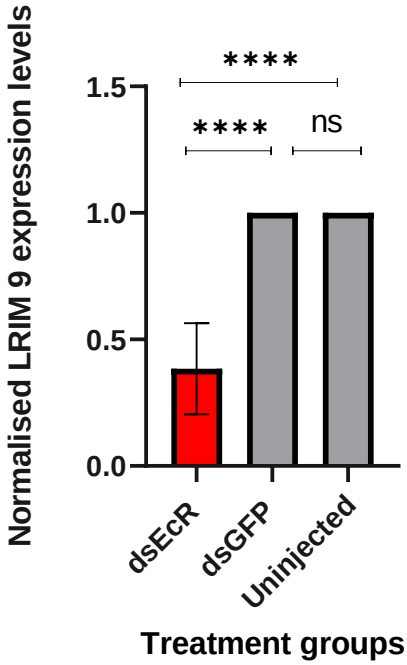


Figure 3.29: Relative *LRIM9* expression in ds*EcR* injected *An. funestus* females was significantly reduced when compared to ds*GFP* injected and uninjected *An. funestus* females. Data is indicative of five biological replicates ($p<0.0001$). Error bar represents standard deviation. ****= $p<0.0001$; ns= not statistically significant $p>0.05$.

3.4.3 Ecdysone receptor knockdown decreased oocyst numbers in *P. falciparum* infected *An. funestus* females

Double stranded *EcR*, ds*GFP* and uninjected treated *An. funestus* females infected with *P. falciparum* were dissected to determine oocyst intensity and ascertain if any phenotypical changes occurred due to the downregulation of *EcR* and *LRIM9*. Surprisingly, oocyst intensity

was significantly decreased by 44% in ds*EcR* treated *An. funestus* females with a median of 2 ± 7.47 oocysts per midgut compared to ds*GFP* treated and uninjected *An. funestus* females with medians of 4 ± 6.81 ($p<0.05$) and 5 ± 3.23 ($p<0.01$) oocysts per midgut respectively (Figure 3.30; Table S6). Furthermore, the mean prevalence of infected *An. funestus* females was 62.9% ± 49 in ds*EcR* injected *An. funestus* females, 77% ± 42.4 in ds*GFP* injected *An. funestus* females and 84.2% ± 36.8 in uninjected *An. funestus* females (Figure 3.30). Statistical significance was not observed between ds*EcR* and ds*GFP* as well as ds*GFP* and uninjected *An. funestus* females ($p>0.05$), however prevalence in ds*EcR* and uninjected *An. funestus* females was significantly different ($p<0.05$). Interestingly, observation of ds*EcR* midguts revealed oocysts that appeared to have an increased size compared to ds*GFP* and uninjected controls (Figure 3.31), however as oocyst size was not measured across all biological replicates, statistical significance could not be calculated. Therefore this size difference remains a hypothesis until further studies are conducted in *An. funestus*. These results confirmed that *EcR* knockdown decreased the intensity of *P. falciparum* oocysts and that this effect was due to an unidentified mechanism which may or may not be due to the downregulation of *LRIM9*.

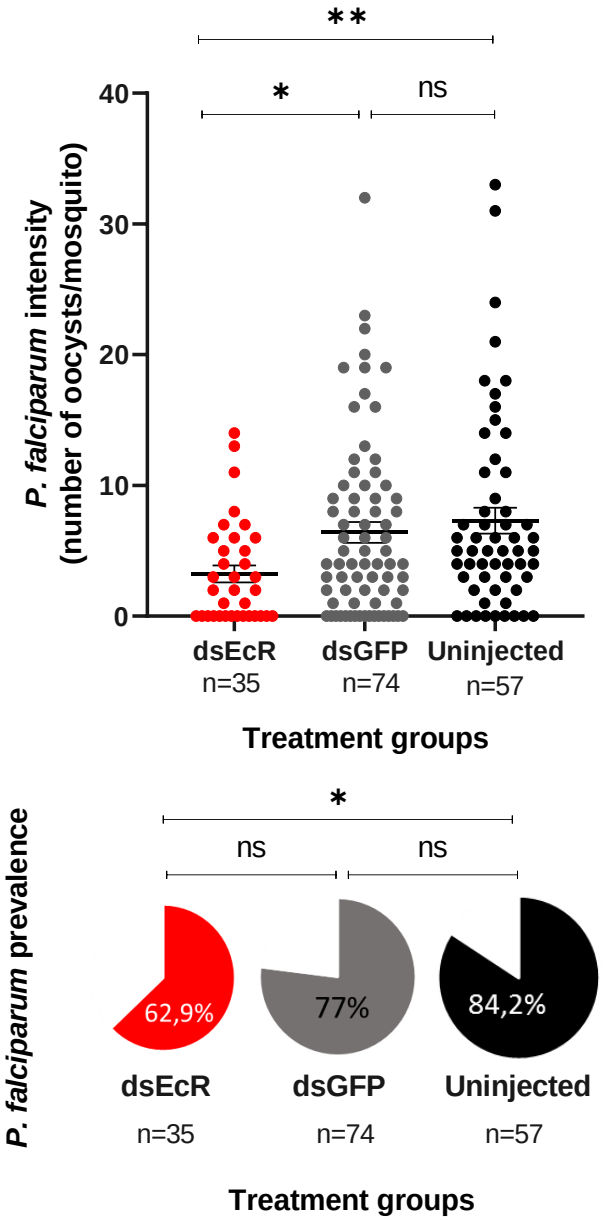


Figure 3.30: Reduced oocyst intensity was observed in *An. funestus* females treated with ds*EcR*. The median number of oocysts from ds*EcR* treated *An. funestus* females was significantly decreased compared to ds*GFP* ($p<0.05$) and uninjected control groups ($p<0.01$). The prevalence of infection was only significant between ds*EcR* injected *An. funestus* females and uninjected *An. funestus* females ($p<0.05$). Data is indicative of five biological replicates. Error bars represent SEM. *=$p<0.05$; **= $p<0.01$; ns= not statistically significant $p>0.05$.

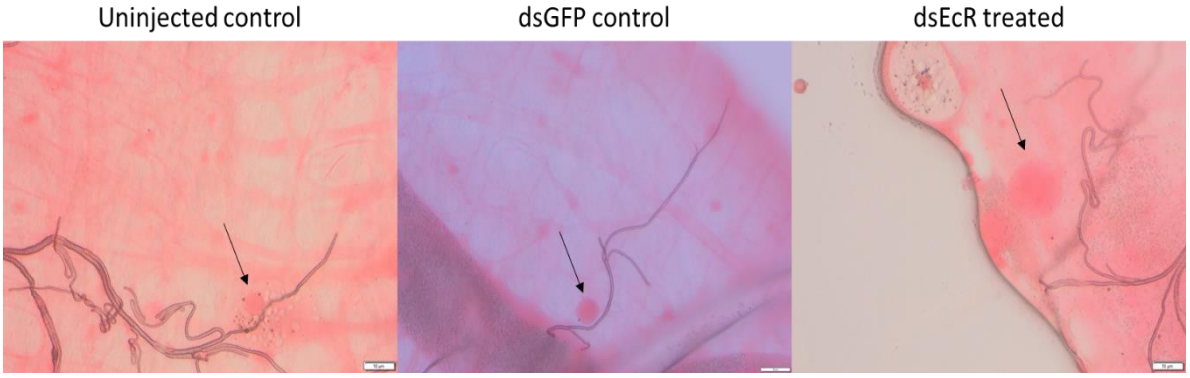


Figure 3.31: Oocyst size appeared to differ between ds*EcR* treated and ds*GFP* and uninjected control groups. Oocysts (indicated by arrows) in ds*EcR* treated *An. funestus* females appeared larger than oocysts in ds*GFP* and uninjected *An. funestus* females at 400X magnification. Scale bar is equivalent to 10 µm.

3.4.4 *Anopheles funestus* TBA and TRA differed between ds*EcR* treated *An. funestus* females and control *An. funestus* females

The TBA is the percentage inhibition in the prevalence of infected mosquitoes and the TRA is the percentage inhibition in the mean oocyst number per infected mosquito. Together these two parameters measure the effectiveness of a treatment in the reduction of *Plasmodium* infection in malaria vectors (Miura *et al.*, 2016).

The TRA and TBA was compared in ds*EcR*, ds*GFP* and uninjected treatment groups. The TBA of ds*EcR* treated females compared to the ds*GFP* control was 11%, ds*EcR* compared to the uninjected control was 24% and the ds*GFP* control compared to the uninjected control was 15% (Table 3.4). A small but significant difference (p=0.03) was observed in ds*EcR* treated females compared to the uninjected control (Table 3.4).

The TRA of ds*EcR* treated females compared to the ds*GFP* control was 49%, ds*EcR* treated females compared to the uninjected control was 53% and the ds*GFP* control compared to the uninjected control was 27% (Table 3.4). Significant differences were observed between ds*EcR* treated *An. funestus* females and both ds*GFP* (p=0.02) and uninjected controls (p=0.002), however no significant difference was observed between ds*GFP* and uninjected control groups. These results substantiated and strengthened the finding that *P. falciparum* transmission is reduced in ds*EcR* treated *An. funestus* females. Taken together these results indicated that *EcR* knockdown did not reduce *An. funestus* susceptibility to *P. falciparum* but did reduce the intensity of *P. falciparum* infection.

Table 3.4: The TBA and TRA of ds*EcR* treated *An. funestus* females compared to ds*GFP* control and uninjected control *An. funestus* females.

Sample	TBA	TRA
ds*EcR* vs ds*GFP*	11% ^{ns}	49% *
ds*EcR* vs uninjected	24% *	53% **
ds*GFP* vs uninjected	15% ^{ns}	27% ^{ns}

*= p< 0.05; **= p< 0.01; ns= not statistically significant p>0.05.

3.4.5 The blood feeding rate did not contribute to changes in phenotype in infected *An. funestus* females

To confirm that changes in oocyst intensity were not influenced by the blood feeding rate between ds*EcR*, ds*GFP* and uninjected treatment groups, the average blood feeding rate from five biological replicates was calculated. The mean feeding rates were 18.38 ± 18.92% in ds*EcR* treated *An. funestus* females, 26.25 ± 17.90% in ds*GFP* treated *An. funestus* females and 19.62 ± 10.98% in uninjected *An. funestus* females with no significant difference between treatment groups (p>0.05) (Figure 3.32). This substantiated that changes in phenotype were due to the knockdown of *EcR* and downregulation of *LRIM9* and not due to differences in the blood feeding rates.

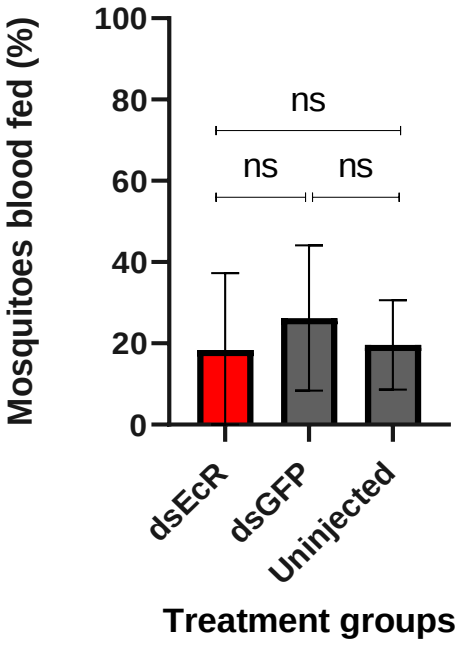


Figure 3.32: Blood feeding rates were similar between ds*EcR* treated and ds*GFP* and uninjected control groups. No significant difference was observed between the percentages of blood fed *An. funestus* females in the different treatment groups ($p>0.05$). Data is representative of five biological replicates. Error bars represent standard deviation of means. ns= not statistically significant $p>0.05$.

4 DISCUSSION

4.1 Decreased longevity in ds*EcR* treated *An. funestus*

Understanding how vector longevity is regulated is of utmost importance for the development of novel vector control methods as it ultimately affects malaria transmission. A decrease in longevity negatively impacts vector density, causing a reduction in the mosquito to human ratio. Decreased longevity also reduces the likelihood of *Plasmodium* infected vectors ingesting a second blood meal and spreading malaria. Much attention has been given to the 20E signalling pathway as a novel method to reduce vector longevity (Childs *et al.,* 2016; Brown *et al.,* 2020), however before the current study, EcRs (an important component of this pathway) contribution to vector longevity still remained unexplored.

The current study therefore focused on determining the function of EcR on *An. funestus* longevity by using ds*RNA* to knockdown *EcR*. This study is currently the first account of decreased longevity resulting from *EcR* knockdown in *An. funestus* females. Nanoinjection with ds*EcR* depleted the EcR transcript by 96% and thus affected the phenotypes of ds*EcR* treated mosquitoes. Consequently, longevity in ds*EcR* treated females was reduced by 57% while the probability of survival was reduced to only 14% at 16 days post nanoinjection.

In the current study, targeting *EcR* by knockdown was studied using nanoinjection as opposed to other ds*RNA* introduction methods such as ingestion and topical application. This is because nanoinjection is the most consistent method to deliver accurate and precise concentrations of dsRNA into the mosquitoes (Walshe *et al.*, 2009; Sampath and Puttaraju, 2012; Pridgeon *et al.*, 2014). However, one limitation of using nanoinjection in this study included a need for the optimisation of several RNAi parameters to minimise the mortality rate from injection induced injuries as there were no previous records of *An. funestus* nanoinjection in the literature to present knowledge. The parameters optimised included determining the appropriate age of *An. funestus* females for injection and confirmation of gene knockdown after nanoinjection. Optimising these factors led to the development of a nanoinjection protocol —suitable for *An. funestus*— that was used throughout with some minor modifications amongst objectives as required. The limitation of mortality resulting from injuries was overcome with the inclusion of a ds*GFP* control to ensure that the change in survival observed was due to *EcR* knockdown and not due to the nanoinjection procedure.

As observed in this study, depletion of the *EcR* transcript resulted in decreased longevity. Longevity affects the extrinsic incubation period (EIP) required for *Plasmodium* maturation and transmission in the vector and hence vector competence (Ohm *et al.,* 2018). The EIP is essentially the period in which gametocytes mature into infectious sporozoites in the mosquito and are capable of being transmitted to vertebrate hosts (reveiwed by Ohm *et al.*, 2018). Malaria transmission can be impaired by vectors not surviving long enough for *Plasmodium* to mature into infectious sporozoites (Shaw and Catteruccia, 2018). In WRIM laboratory reared *An. funestus* females, the approximate EIP is 16 days post infectious blood meal. At 16 days after nanoinjection, *An. funestus* females treated with ds*EcR* had a considerably low survival rate and lived for approximately 20 days compared to control treated *An. funestus* females that survived over a month. In the field, *Anopheles* mosquitoes do not survive as long, living approximately 10 to 30 days (Gillies and De Meillon, 1968). Although, the EIP is influenced by longevity, it can also be impacted by several factors such as temperature, vector species, parasite species, vector nutrition and survival (reveiwed by Ohm *et al.,* 2018). Defining the duration is therefore very difficult, however it typically ranges from 12 to 16 days (WHO, 1975; Vaughan *et al.,* 1992; Ohm *et al.,* 2018). Knocking down *EcR* in *An. funestus* females could therefore decrease longevity to a point where the EIP cannot be completed in the field, remarkably reducing malaria transmission.

Although EcRs effect on longevity has not been studied in other malaria vectors, it has previously been investigated in several insect species such as *D. melanogaster* (Simon *et al.*, 2003; Simon *et al.*, 2006; Tricoire *et al.*, 2009), *N. lugens* (Yu *et al.*, 2014), *Sitobion avenae* F. (*S. avenae* F.) (Yan *et al.*, 2016), *Grapholita molesta* (*G. molesta*) (Reinke and Barrett, 2007) amongst others. Heterozygous *D. melanogaster* mutants generated by a deletion in the ligand binding domain of *EcR* showed increased longevity compared to controls (Simon *et al.*, 2003). In a subsequent study, a more gradual aging process in the same male and female mutants was evident compared to control *D. melanogaster* adults (Simon *et al.*, 2006). Although the mutants generated by Simon (2003; 2006) had impaired *EcR* functioning, much like the current study where *EcR* was knocked down, results were not in agreement due to differences in the phenotypes observed. The contradiction in results between the above studies and current study could arise due to several reasons, firstly, heterozygote advantage where the wildtype allele shows overdominance could be a possibility (reviewed by Charlesworth and Willis, 2009). Alternate reasons could include a difference in treatments such as generating *EcR* mutants

(Simon *et al.*, 2003; Simon *et al.*, 2006) compared to knocking down *EcR* with ds*EcR* and/or a difference in the biological material compared i.e. *D. melanogaster* compared to *An. funestus*.

Interestingly, in another study involving *D. melanogaster* adults, Tricoire *et al.* (2009) discovered a sex specific response to inactivated *EcR* using ds*EcR*. Male *D. melanogaster* showed increased longevity with moderate *EcR* inactivation but a decrease in longevity with low and high inactivation of *EcR*. *Drosophila melanogaster* females on the other hand, showed decreased longevity irrespective of the level of *EcR* inactivation (Tricoire *et al.*, 2009). The decrease in longevity in *D. melanogaster* females after *EcR* inactivation is similar to the decrease in longevity observed in the current study after *EcR* was knocked down in *An. funestus* females. The effect of ds*EcR* on adult males was not investigated in this study. It would be interesting to determine if *EcR* exhibits sex specific regulation of longevity in *An. funestus* similar to that in *D. melanogaster*. In a recent study Zengenene *et al.* (2021) showed that *An. funestus* males live longer than females (approximately 60 days). Reducing longevity in both males and females will assist in reducing vector population size and consequently malaria transmission and therefore it will be important to determine if *EcR* affects male and female *An. funestus* longevity differentially.

Additionally, based on results obtained by Tricoire *et al.* (2009) it could be possible that *EcR* expression levels influence longevity differentially and normal lifespan critically relies on a moderate biological level of EcR. This reveals a shortcoming of the current study as only one concentration of ds*EcR* was used to examine longevity. Investigating the effect of several different concentrations of ds*EcR* on *An. funestus* longevity could have provided in-depth information about *EcR*s regulation of longevity.

Interestingly, studies involving *N. lugens* and *S. avenae F.* used a ds*EcR* based approach to study longevity in these insects. A 44% to 66% decrease in *N. lugens* survival was observed after nymphs were fed on transgenic crops containing ds*EcR* (Yu *et al.*, 2014). Similarly, *S. avenae F.* showed a concentration dependent decrease in longevity when fed with transgenic crops containing ds*EcR* (Yan *et al.*, 2016). Results obtained by Yan *et al.* (2016) and Yu *et al.* (2014) are consistent with current results demonstrating a decrease in *An. funestus* longevity with *EcR* knockdown.

Moving away from EcR and focusing more broadly on the 20E pathway, an approach used to study longevity focuses on the use of 20E agonists. 20-hydroxyecdysone agonists mimic the structure of the 20E hormone and in this manner are able to bind to EcR resulting in increased

20E signalling (reviewed by Dhadialla *et al.*, 1998). The 20-hydroxyecdysone agonist, methoxyfenozide, when applied on surfaces decreased the longevity of *G. molesta* (Reinke and Barrett, 2007). Importantly, studies involving the use of 20E agonists have been undertaken with several malaria vector species. Childs *et al.* (2016) demonstrated that applying the 20E agonist methoxyfenozide topically to *An. gambiae* decreased its longevity in a dose dependent manner. Likewise, when methoxyfenozide was applied topically to *An. funestus, An. gambiae, An. coluzzii* and a hybrid of *An. gambiae* and *An. coluzzii*, all mosquito strains —except for *An. funestus*— showed a decrease in longevity (Brown *et al.*, 2020). However, when further experiments tested the tarsal application of methoxyfenozide on the above mosquito strains, all strains, including *An. funestus*, showed decreased longevity (Brown *et al.*, 2020). These results are promising as control interventions such as LLINs and IRS focus on tarsal contact with insecticides to eliminate mosquitoes.

Compared to the current study, Reinke and Barrett (2007), Childs *et al.* (2016) and Brown *et al.* (2020) all had similar decreases in longevity, however this was due to increased 20E signalling unlike the decreased *EcR* expression and hence decreased 20E signalling presently. Comparing the current study with the study by Brown *et al.* (2020), it appears that ds*EcR* reduces longevity to a greater extent than methoxyfenozide as noted by a difference in the average survival time between treated and control groups of 15 days in the current study compared to 6 days observed by Brown *et al.* (2020). This ties back to the theory that *EcR* expression levels influence longevity differentially. Literature has indicated that manipulating the 20E signalling pathway by elevating or reducing its activity produces deleterious effects on longevity (reviewed by Ekoka *et al.*, 2021). Therefore it will be interesting to determine how longevity in *An. funestus* adults is affected with different levels of *EcR* silencing or manipulation of the 20E signalling pathway.

Collectively, these results offer new and compelling information about malaria vector longevity. It is evident that longevity is regulated by EcR in *An. funestus* and that silencing *EcR* results in decreased longevity in these vectors. The results obtained in this study validate that EcR may be used to develop novel vector control strategies; therefore substantiating the importance of targeting *EcR* to combat malaria transmission by reducing vector density and competence. Current laboratory results have been promising and consequently future research should focus on and confirm if *EcR* regulates longevity in wild caught adults from malaria endemic countries. Moreover the EcR is a known transcriptional factor that regulates the expression of several early and subsequently late genes (Koelle *et al.*, 1991). Longevity in *An.*

funestus is most likely a very complex process and various unidentified genes and pathways might be involved in its regulation. In future, it would be interesting to delve further into the pathway regulating longevity to determine which EcR regulated genes are responsible for facilitating longevity.

4.2 Decreased fecundity and fertility in ds*EcR* treated *An. funestus*

Fecundity and fertility are two reproductive processes that affect vector density and thus malaria transmission (Shaw and Catteruccia, 2018). Moreover, ingestion of a blood meal (a prerequisite for mosquito vitellogenesis and oogenesis) increases the risk of *Plasmodium* transmission (Shaw and Catteruccia, 2018). Reducing vector density and malaria transmission by targeting mosquito reproduction is key in the fight against malaria. Reproduction in the mosquito is largely regulated by 20E signalling (Pierceall *et al.*, 1999; reviewed by Ekoka *et al.*, 2021). The current study investigated the effect that *EcR* knockdown has on reproduction in *An. funestus*. Expectedly, it was confirmed that EcR regulates reproduction in *An. funestus*.

In this study, ds*EcR* treated females had a 95% reduction in *EcR* expression. As a result of *EcR* depletion, *Lp* and *VgR* expression was consequently reduced by 83% and 78% respectively. The reduction of *EcR*, *Lp* and *VgR* transcripts subsequently resulted in a phenotype with impaired reproduction. In the mosquito, Lp and Vg are two important proteins involved in lipid transport and the uptake of Vg proteins required for developing oocytes respectively (Raikhel, 1992; Sun *et al.*, 2000). The *VgR* gene investigated in this study is essential for the function of Vg where it mediates the uptake of Vg to ensure developing oocytes are supplied with essential nutritional compounds (Sappington *et al.*, 1995). The VgR therefore assists in the functioning of Vg in vitellogenesis. Total fecundity (observed by total eggs developed) in ds*EcR* treated females was greatly reduced due to impaired oogenesis whereas fertility in ds*EcR* treated females was reduced by 16% when compared to controls. To current knowledge, this is the first study determining the function of EcR on fertility in *Anopheles* mosquitoes. Overall it was discovered that *EcR* knockdown resulted in adverse effects on vector reproduction, substantiating EcR's regulation of this process.

As many reproductive processes in laboratory reared *An. funestus* such as optimal mating time, blood feeding and oviposition differ greatly from the more extensively studied *An. gambiae* complex species (Baldini *et al.*, 2013; Childs *et al.*, 2016; Werling *et al.*, 2019), optimization

was necessary to design differential experimental methods from those developed for use in *An. gambiae*. The optimal mating success time used in several studies involving *An. gambiae* was significantly shorter (4 days) than the optimal time of 12 days for *An. funestus* (Gabrieli *et al.*, 2014; Childs *et al.*, 2016; Marcenac *et al.*, 2020). It is unknown if optimization was conducted in the other studies to optimize the mating success rate, however in the current study the maximum mating success rate was approximately 62.2% obtained after 12 days. Since the highest mating success rate was achieved after 12 days this was subsequently used as the period to combine male and female *An. funestus* mosquitoes to obtain a suitable sample size and reliable results. While the current optimal mating rate may seem low, it is known that *An. funestus* is refractory to colonisation due to its low mating success (Koekemoer *pers comm*). This highlighted the importance of studying the *An. funestus* mating success rate.

To ensure the ds*RNA* exhibited maximum effects on reproduction, blood feeding was carried out when *EcR* expression was at its lowest i.e. 48 hours after nanoinjection. This ensured that the expression of *EcR* was lower than control *An. funestus* females during blood feeding, preventing *EcR* levels in ds*EcR* treated *An. funestus* females from peaking to *EcR* levels in control *An. funestus* females. Since a blood meal increases *EcR* expression and therefore *Lp* and *Vg* expression (Fallon *et al.*, 1974; Hagedorn *et al.*, 1975; Cho *et al.*, 1995; Sun *et al.*, 2000; Kokoza *et al.*, 2001; Martín *et al.*, 2001) this optimisation was necessary to achieve accurate results. However, for more scientifically sound results, the expression levels in ds*EcR* treated and control *An. funestus* females after blood feeding should be confirmed in future studies.

Naturally, following mating and blood feeding is ovipositioning. *Anopheles* females' preference of an oviposition site varies depending on species and is usually influenced by chemical and physical composition of the site as well as light intensity and substrate type (Blackwell and Johnson, 2000; Huang *et al.*, 2005; Huang *et al.*, 2006; Lindh *et al.*, 2015). Glass vials containing moistened filter paper (Munhenga *et al.*, 2011) were initially used for oviposition but were determined to be unfavourable as no oviposition took place. Laboratory oviposition plates with dark backgrounds were tested next and a moderate level of oviposition was observed however this method was excluded as it resulted in an average egg count, prevented the determination of the fecundity and fertility per female and assumed all females that were mated had oviposited. As *Anopheles* females seem to prefer a dark background for oviposition (Bates, 1940; Huang *et al.*, 2005), individual cups with dark backgrounds were used to produce optimal oviposition as well as obtain individual results per mated female.

These methods of optimisation were definitely necessary as they allowed for *An. funestus* specific methods as well as precise and accurate results in both fecundity and fertility assays.

Although the study was optimised to a great extent, several limitations appeared throughout. Although the sample size was appropriate for statistical analyses, it was nevertheless reduced due to the majority of *An. funestus* females' reluctance to ingest an artificial blood meal. *Anopheles funestus* is highly anthropophilic, preferring human blood (Gillies and De Meillon, 1968) to bovine blood that was currently used. Supplementing bovine with human blood could perhaps increase the sample size of blood fed females in future experiments conducted with *An. funestus*. Additionally, oviposition rates in females were considerably low in all treatment groups, although the oviposition medium was optimised. An approximate mean of 30% of blood fed females oviposited currently compared to an oviposition rate of greater than 70% in a study by Choi *et al.* (2014), indicating the need for greater optimisation. Huang *et al.* (2006) demonstrated that *Anopheles* females prefer to oviposit in a natural substrate containing water from a known oviposition site instead of distilled water. It is highly likely that the artificial feeding system impacted oviposition in *An. funestus* in the present study. Choi *et al.* (2014) provided glass vials with moistened filter paper as an oviposition medium for *An. funestus* females and observed successful oviposition, however, females were provided with blood directly from a vertebrate host unlike the current study. Modifying the blood type, oviposition substrate and water source in future experiments could thus improve the accuracy and reliability of results in future fecundity and fertility studies with *An. funestus*.

The regulation of fecundity by EcR has been studied in *D. melanogaster*. The generation of *EcR* mutant *D. melanogaster* adults with an impaired efficiency of 20E to bind EcR (Simon *et al.*, 2003) and ds*EcR* treated *D. melanogaster* adults (Tricoire *et al.*, 2009) both resulted in phenotype exhibiting decreased fecundity. These results are consistent with current results as knockdown of *EcR* also resulted in reduced fecundity in *An. funestus*. In a study published after initiation of the present investigation, the effect of knocking down *EcR* to study fecundity was examined in *An. gambiae* (Werling *et al.*, 2019). The development of eggs was reduced by 34% in ds*EcR* treated females compared to controls. This concurs well with current results obtained in *An. funestus*, suggesting that fully functional EcR is required for normal egg development and maturation.

Two important proteins required for egg development: *Lp* and *Vg* are regulated by the 20E signalling pathway, consistent with a number of studies in mosquitoes (Sun *et al.*, 2000;

Kokoza *et al.*, 2001; Baldini *et al.*, 2013; Werling *et al.*, 2019). Consequently, silencing *EcR* decreased *Vg* and *Lp* expression in *An. gambiae* (Werling *et al.*, 2019), corresponding with results obtained presently. The resulting phenotype of mosquitoes with depleted *Lp* and *Vg* was an elevated lipid content in the midgut, suggesting impaired vitellogenesis and decreased transport of lipids to the fat body and ovaries by Vg and Lp respectively (Werling *et al.*, 2019). The effect of this was also evident when silencing *Lp* resulted in fewer eggs developed due to insufficient lipid transport to developing oocytes (Werling *et al.*, 2019). Interestingly, although Lp and Vg play a similar role in ensuring oocyte maturation, *Lp* was found to regulate this process to a larger extent than *Vg* (Rono *et al.*, 2010). A downside of the present methodology was that *Lp* and *Vg*/ *VgR* silencing was not studied in *An. funestus*, however this could be conducted in future to provide more information about the functions of these genes. As in *EcR* knockdown, disrupting the 20E signalling pathway also results in faulty reproductive processes from impaired Lp and Vg functioning.

20-hydroxyecdysone agonists have been widely employed to study the effects of disrupting 20E signalling on reproduction. Brown *et al*. (2020) demonstrated that topical application of methoxyfenozide resulted in a lower number of eggs developed in treated *An. funestus*, *An. gambiae* and *An. coluzzii* females whereas tarsal application produced a similar effect in *An. funestus* females (Brown *et al.*, 2020). As mentioned previously, tarsal application of 20E agonists mirrors conditions in the field where mosquitoes come into contact with insecticidal nets and IRS tarsally. This is promising for vector control. The reduction in the number of eggs observed by Brown *et al.* (2020) is similar to the current study where a minority of developed eggs as opposed to underdeveloped eggs were observed in ds*EcR* treated females. In another study, topical application of methoxyfenozide reduced oviposition in females up to 89%, decreased the number of eggs oviposited, impaired oogenesis by preventing yolk deposition as well as reduced the number of mated females by up to 65% (Childs *et al.*, 2016). Deleterious effects were more pronounced in the study by Childs *et al.* (2016) than currently, noted by an additional decrease in oviposition and a reduction in the number of mated females. This could however be attributed to the difference in signalling disruption methods compared i.e. 20E agonists compared to knockdown with ds*EcR* or the difference in mosquito species studied.

Other than oviposition and oogenesis, mating is also influenced by 20E signalling. Intriguingly, a study demonstrated that injection of 20E into virgin *An. gambiae* females prevented them from subsequent matings (Gabrieli *et al.*, 2014). This phenomenon was discovered to be due to the formation of a ‘plug’ in the atrium that prevented females from receiving another mating

plug from males typically containing spermatheca, proteins and the 20E hormone (Gabrieli *et al.*, 2014). Moreover, 20E injections into virgin females induced the oviposition of sterile eggs (Gabrieli *et al.*, 2014). Together these results demonstrate that 20E signalling is responsible for initiating oviposition as well as preventing *An. gambiae* females from mating multiple times. It would therefore be interesting to determine if the same effects are observed in *An. funestus* as this will add to the knowledge used to develop novel vector control methods.

It is interesting to note that besides blood, females also obtain 20E from males during mating as discussed previously (Gabrieli *et al.*, 2014). In addition to regulating the transport of nutrients to developing oocytes, EcR induced MISO is responsible for facilitating the release of 20E from the mating plug and modulating the effects of 20E thereafter (Baldini *et al.*, 2013). Silencing *MISO* reduced oviposition rates and reduced fecundity by impairing oocyte development due to decreased *Lp* expression and hence a decreased nutrient content (Baldini *et al.*, 2013). This evidences another EcR regulated gene controlling reproductive processes in *An. gambiae* and possibly another gene to study potentially contributing to vector control in *An. funestus*.

It is clear that knocking down *EcR* has deleterious effects on *An. funestus* fecundity as discussed above. In the current study *EcR* knockdown significantly reduced fertility, however a major source of uncertainty arises from the small sample size. This experiment should therefore be repeated after optimisation in future to provide more clarity. Nevertheless, results from the current study are noteworthy; a heme peroxidase: HPX15 was found to control fertility in *An. gambiae* (Shaw *et al.*, 2014). This enzyme is regulated by EcR and requires 20E for normal functioning, evidencing that EcR does in fact influence fertility (Shaw *et al.*, 2014). Silencing HPX15 was found to decrease fertility in females over multiple gonotrophic cycles (Shaw *et al.*, 2014). Additionally, as peroxidases do, HPX15 was discovered to reduce oxidative stress in the spermatheca, protecting spermatozoa in this process (Shaw *et al.*, 2014). There is currently a gap in the knowledge of EcRs regulation of anopheline fertility however Baldini *et al.* (2013) demonstrated that silencing the EcR regulated *MISO* gene had no effect on *An. gambiae* fertility. This suggests that MISO is a simply a regulator of oogenesis and is not involved in regulating fertility like HPX15 is, exhibiting EcR's pleiotropic effects.

The current study aimed to determine if EcR regulated reproduction in *An. funestus*. As a decrease in fecundity and fertility was noted in ds*EcR* treated females, it is unmistakable that *EcR* plays a significant role in the regulation of vector reproduction. Currently, *Lp* and *VgR*

gene depletion was only determined after *EcR* knockdown to confirm that they are regulated by EcR. However, in future studies it will be beneficial to silence these genes to determine to what extent they regulate reproduction in *An. funestus*. Furthermore, *Lp* and *VgR* are only two of the many genes involved in regulating vector reproduction. Future studies should focus on RNA sequencing in which a full transcript profile is obtained to determine the reproduction genes regulated by EcR. This study is the first step towards increasing the understanding of EcRs regulation of reproduction in *An. funestus*. It has therefore paved the way for future experiments in *An. funestus* such as determining EcRs effect on mating success and refractoriness to mating to expand the insight on future EcR targeted vector control methods.

4.3 Decreased intensity of *P. falciparum* in ds*EcR* treated *An. funestus*

Reducing vector competence by targeting vector immunity against *Plasmodium* parasites is promising to reduce malaria transmission. Recent studies have shown that the 20E signalling pathway is involved in the regulation of mosquito immune responses combating *Plasmodium* infection (Childs *et al.*, 2016; Reynolds *et al.*, 2020). Upon initiation of the current study, no published data confirming EcRs involvement in vector susceptibility to *P. falciparum* existed. The current study therefore focused on determining the function of EcR in *An. funestus*' susceptibility to *P. falciparum*. Recently, EcRs regulation of *P. falciparum* infection has been investigated in *An. gambiae* (Werling *et al.*, 2019). The latter study confirms the current finding that EcR plays a role in regulating *P. falciparum* infection in *Anopheles* mosquitoes.

In the present study, *EcR* transcripts were reduced by 84% in ds*EcR* treated females 24 hours after nanoinjection. Consequently, depletion of the *EcR* transcript reduced *LRIM9* expression by 62%. Phenotypically, females with reduced expression of *EcR* had decreased oocyst intensity with a 44% reduction in oocyst numbers in their midguts. The transmission reducing activity of *EcR* depletion was evident with a 49% and 53% reduction in *P. falciparum* oocysts between ds*EcR* treated and ds*GFP* and uninjected controls respectfully. Surprisingly, the prevalence of infection did not differ greatly between treatment groups and a small significant difference was solely observed between ds*EcR* and uninjected females with a TBA of 24%.

The discrepancy in the prevalence of *P. falciparum* infection between ds*GFP* and uninjected controls when compared to ds*EcR* treated mosquitoes was not anticipated in the current study. Statistical significance was not observed between ds*EcR* and ds*GFP An. funestus* females but

was observed between ds*EcR* and uninjected *An. funestus* females. Due to the small significant difference in differences between ds*EcR* and uninjected mosquitoes, it is possible to attribute this to a decrease in sample size of ds*EcR* treated females. The decreased sample size could have occurred due to reductions in lifespan caused by ds*EcR* treatment or a high amount of injuries during the nanoinjection procedure. Additionally, Werling *et al.* (2019) did not observe a difference in *P. falciparum* infection prevalence between ds*EcR* and ds*GFP* treated *An. gambiae* females. It is therefore unlikely that ds*EcR* treated *An. funestus* females are less susceptible to infection with *P. falciparum*.

Importantly, the *LRIM9* gene is involved in regulating *P. berghei* infection in *An. gambiae* mosquitoes (Upton *et al.*, 2015). Upton *et al.* (2015) confirmed that *LRIM9* is regulated by the 20E signalling pathway, observed by upregulation of *LRIM9* after injection of the 20E hormone. Therefore in the current study, *LRIM9* expression was examined after *EcR* knockdown to determine if it is in fact EcR in the 20E signalling pathway that regulates LRIM9 expression. Subsequently, downregulation of *LRIM9* resulting from *EcR* knockdown was observed, confirming that EcR regulates the expression of *LRIM9* in *An. funestus*. These studies indicate that *LRIM9* is most likely an EcR regulated late gene, explained by its regulation in response to changes in the 20E signalling pathway. Moreover, LRIM9 has been implicated in the killing of *Plasmodium* parasites in the mosquito (Upton *et al.*, 2015).

Decreasing *LRIM9* expression by using dsRNA against *LRIM9* resulted in increased *P. berghei* oocyst intensity and a decrease in the number of melanised oocysts in *Plasmodium* refractory mosquitoes compared to controls (Upton *et al.*, 2015). These results suggest that LRIM9 functions as an immune regulator in the mosquito and functions to kill *Plasmodium* parasites using melanisation. Although melanisation was not studied currently, it will be advantageous to determine the role of *EcR* and *LRIM9* silencing on melanisation in future studies. In contrast with findings by Upton *et al.* (2015), a decrease in *LRIM9* expression due to *EcR* knockdown did not increase *P. falciparum* oocyst numbers. On the contrary, a lower number of oocysts was observed in ds*EcR* treated mosquitoes compared to controls in the present study. This result is interesting and unexpected as increased oocysts were expected in ds*EcR* injected *An. funestus* females due to *LRIM9* downregulation. This discrepancy could presumably be due to a variance in the activity of LRIM9 against different *Plasmodium* species studied. Additionally, it could be attributed to differences in the immune systems and regulation of *Plasmodium* infection between *An. gambiae* and *An. funestus*. Immune genes of *An. funestus* are genetically more similar to the Asian malaria vector *An. stephensi* than *An. gambiae* due to evolutionary

divergences in these vectors (Kamali *et al.*, 2014; Couto *et al.*, 2016; Mitri *et al.*, 2020). The contradiction in these results suggest a different mechanism is involved in decreasing the intensity of *P. falciparum* oocysts when *EcR* is knocked down in *An. funestus*. Similar to LRIM9, LRIM1 was also found to decrease oocysts by melanisation, however it is not regulated by EcR (Osta *et al.*, 2004; Povelones *et al.*, 2009; Upton *et al.*, 2015). This indicates that the pathway that regulates *Plasmodium* infection in vectors is undoubtedly a very complex one. Many genes that have not yet been identified could be involved in this process, and it will be important to study more genes to elucidate how this pathway functions.

Several other factors influenced by EcR regulation or the 20E signalling pathway have been established to affect *Plasmodium* infection intensity and prevalence. Methoxyfenozide: a 20E agonist, was topically applied to *An. gambiae* and reduced the prevalence of *P. falciparum* oocysts by 87% however it did not affect oocyst intensity (Childs *et al.*, 2016). These results demonstrate that methoxyfenozide has *Plasmodium* transmission blocking potential. Another 20E agonist confirmed that *Plasmodium* survival is affected by the 20E signalling pathway; halofenozide reduced *P. berghei* oocyst intensity and prevalence in *An. gambiae* by killing the ookinete stage of the parasite (Reynolds *et al.*, 2020). Surprisingly, although halofenozide's action is mediated by EcR, it does not employ the same pathway used by 20E to control infection, i.e. the EcR induced cecropin genes are not involved in the *Plasmodium* killing immune response adopted by halofenozide (Reynolds *et al.*, 2020). In the current study, *EcR* silencing had no significant TBA but instead had TRA as oocyst intensity but not prevalence of infection was affected. Similarly, using ds*EcR* in *An. gambiae* created substantial changes by reducing *P. falciparum* oocyst intensity but not prevalence (Werling *et al.*, 2019) much like the current study. Although the current findings are in agreement with a decreased oocyst intensity noted when 20E agonists were used, there exists a discrepancy in oocyst prevalence in these studies. The discrepancy in *Plasmodium* prevalence between studies using 20E agonists and having a difference in oocyst prevalence and those using ds*EcR* with no difference in oocyst prevalence is most likely due to the differential methods used to alter the 20E signalling pathway. As mentioned previously, 20E agonists result in heightened 20E signalling whereas knockdown of EcR decreases 20E signalling, and differences in oocyst prevalence could arise due to this.

There are currently a couple of known EcR induced genes mediating the immune response against *Plasmodium* in the anopheline mosquitoes. Exceptionally, these genes, *Lp* and *Vg* also regulate reproduction in mosquitoes. Oocyst intensity was reduced when *Lp* and *Vg* were

silenced individually or in combination in *An. gambiae*, suggesting that Lp and Vg promote *Plasmodium* survival. However Vg promotes *Plasmodium* survival more so than Lp, due to a higher reduction in oocyst intensity when *Vg* was knocked down (Rono *et al.*, 2010). The mechanism behind Vg's and Lp's promotion of parasite survival was discovered to be due to their antagonistic action towards TEP1. The oocyst killing activity of TEP1 was previously determined when silencing *TEP1* resulted in an increase of oocysts (Blandin *et al.*, 2004; Dong *et al.*, 2006; Rono *et al.*, 2010). The parasite killing efficiency of TEP1 was heightened when expression of *Lp* and *Vg* genes were low, furthermore it was discovered that Lp and Vg hindered the ability of TEP1 to bind to and kill *Plasmodium* parasitic forms (Rono *et al.*, 2010). Decreased expression of *Lp* and *VgR* due to *EcR* knockdown presently resulted in decreased oocyst intensity much like the experiments carried out by Rono *et al.* (2010). A postulation could certainly be made that the decrease in oocyst intensity was due to the parasitic killing action of TEP1, however further studies will certainly have to corroborate this theory.

Besides altering oocyst intensities in vectors, Lp was also found to have additional functions in mosquito immunity. Lipophorin was determined to influence the expression of Vg (Rono *et al.*, 2010). Therefore in the study by Rono *et al.* (2010) the oocyst reduction noted in mosquitoes with *Lp* knockdown could possibly be due to decreased expression of *Vg* due to *Lp* depletion. This could possibly implicate only Vg in reducing the activity of TEP1, providing the basis for a future study to confirm this hypothesis.

Notably, mating which is regulated by 20E signalling could function as a regulator of *Plasmodium* infection in the mosquito vector. As 20E is introduced into female mosquitoes by males during mating and contributes to refractoriness to further mating (Gabrieli *et al.*, 2014). Dahalan *et al.* (2019) injected 20E into virgin *An. coluzzii* female mosquitoes to simulate the physiological changes in mated females. A higher oocyst intensity and prevalence was observed in the 20E treated females and the conclusion was made that males contribute to malaria transmission in this way and that this difference was not affiliated with an increase in Lp or Vg (Dahalan *et al.*, 2019). A subsequent study determined the opposite; no significant differences were observed in oocyst intensity between mated and virgin females (Marcenac *et al.*, 2020). Moreover silencing of the EcR induced gene *MISO* revealed a decrease in oocytes when mosquitoes ingested blood with a high gametocyte content, control mosquitoes on the other hand showed an increase in both oocytes and oocysts with the same blood (Marcenac *et al.*, 2020). These results suggest that MISO is solely responsible for governing reproduction and not *Plasmodium* survival. As these studies are very recent, it is difficult to determine

whether or not mating does affect *Plasmodium* survival. More studies are therefore required to confirm this interesting concept.

Review of literature revealed another interesting discovery about *Plasmodium* infection. Examination of oocysts by Werling *et al.* (2019) lead to the discovery of striking results; ds*EcR* treated females contained oocysts that although reduced in number were larger in size to control oocysts. *Plasmodium* oocysts require lipids for growth and internalise Lp for their nutritional requirements (Atella *et al.*, 2009). Silencing *Lp* resulted in a reduction in oocyst size in several studies (Rono *et al.*, 2010; Costa *et al.*, 2018; Werling *et al.*, 2019). This was attributed to the decrease of nutrients, specifically lipids transported by Lp to developing oocysts (Rono *et al.*, 2010; Costa *et al.*, 2018; Werling *et al.*, 2019).

Subsequent to *Lp* silencing, lipids derived from a blood meal accumulate in the midgut where the blood is digested as they cannot sufficiently be transported to developing oocysts hence the decrease in oocyst size (Costa *et al.*, 2018). Due to the fact that EcR regulates *Lp* expression it is surprising that *Lp* levels were higher in ds*EcR* treated mosquitoes than control mosquitoes following a blood meal (Werling *et al.*, 2019). Concurrent with this finding, larger oocysts were observed in ds*EcR* treated mosquitoes (Werling *et al.*, 2019). This suggests that the increase in *Lp* may provide additional nutrients when *EcR* is silenced which results in faster *Plasmodium* growth in the mosquito. It would be interesting to confirm if in the presence of *P. falciparum*, Lp is upregulated in ds*EcR* treated *An. funestus* which results in larger oocysts. This would address the current hypothesis that knocking down *EcR* results in larger oocysts in *An. funestus*. Interestingly, when Werling *et al*. (2019) silenced both *EcR* and *Lp* simultaneously, the increase in oocyst size was reversed, confirming that *Lp* is responsible for the alteration of oocyst size.

Lipophorin is not the only factor affecting rapidly growing *Plasmodium* parasites. Larger oocysts in ds*EcR* treated females supported accelerated *P. falciparum* growth leading to an earlier EIP of 10 days due to the rapid maturation of sporozoites that are able to infect human hepatocytes (Werling *et al.*, 2019). Moreover, it was recently discovered that the ingestion of additional blood meals also increase oocyst size and contribute to the rapid maturation of *Plasmodium* infectious sporozoites (Shaw *et al.*, 2020). Due to these findings, it is risky to conclude that ds*EcR* has beneficial TRA and that knockdown of *EcR* could reduce the risk of malaria transmission due to decreased oocyst intensity in the current study. In the study by Werling *et al.* (2019) decreased oocyst intensity correlated with faster maturing sporozoites.

Moreover, in the field, mosquitoes imbibe multiple blood meals and therefore the study by Shaw *et al*. (2020) represents a more accurate representation of conditions in malaria endemic areas. This unveils a limitation of the current study, demonstrating the importance of determining the EIP and examining *Plasmodium* sporozoite infectivity and the effect of multiple blood meals on *Plasmodium* infection in future studies.

Evidently, results obtained presently demonstrate a definite role of EcR in the regulation of *P. falciparum* susceptibility in *An. funestus*. Interestingly, EcR seems to promote *P. falciparum* survival, noted by a decrease in oocyst intensity when *EcR* was knocked down. It was also determined that EcR regulates *Lp, VgR* and *LRIM9* genes in *An. funestus*. These genes have been implicated in mosquito immunity against *Plasmodium* in the literature. It would therefore be advantageous to further study the functions of these and other EcR regulated genes and how they regulate *An. funestus* susceptibility to *Plasmodium.* This will thereby allow for the unravelling of EcRs mode of action in the regulation of *Plasmodium* infection. Literature has also demonstrated that it is risky to presuppose the function of *EcR* presently as even though oocyst intensity was decreased currently and in other studies, sporozoites became infectious to human cells sooner than controls in other studies. This should unquestionably be confirmed in *An. funestus*. Overall, this study established that EcR does influence immunity to *P. falciparum* in *An. funestus* and lays the foundation for further studies focusing on the development of novel vector control methods.

5 CONCLUSION AND FUTURE PERSPECTIVES

As a transcriptional regulator of several genes, the pleiotropic effects of EcR and the 20E signalling pathway on anopheline longevity, reproduction and immunity against *Plasmodium* have been observed in the current study (Figure 4.1) as well several other studies (Rono *et al.*, 2010; Childs *et al.*, 2016; Costa *et al.*, 2018; Werling *et al.*, 2019; Brown *et al.*, 2020). Lipophorin and Vg were discovered to both be involved in delivering nutrients to growing oocytes and oocysts with a positive correlation between the two noted (Rono *et al.*, 2010; Costa *et al.*, 2018; Werling *et al.*, 2019). In *D. melanogaster*, a postulation was made that genes governing reproduction are also responsible for longevity (Tricoire *et al.*, 2009).

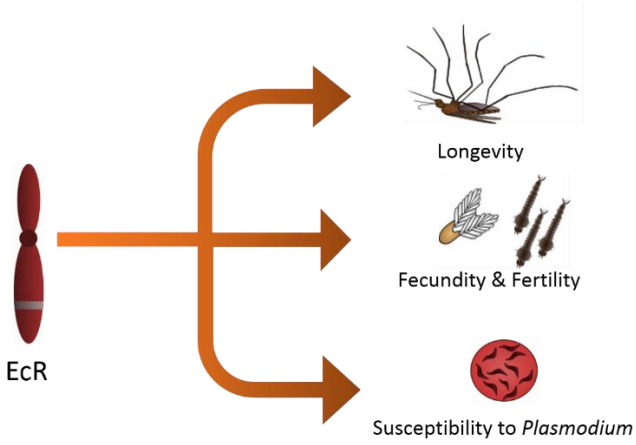


Figure 4.1: Schematic diagram showing the pleiotropic functions of the *EcR* gene. Several physiological functions in *An. funestus* females have been linked to *EcR*. The *EcR* is responsible for facilitating longevity, fecundity, fertility and susceptibility to *Plasmodium* in *An. funestus*.

As EcR appears to be responsible for the regular beneficial, physiological functions in the mosquito and other organisms it was hypothesised that disrupting these functions would result in a series of deleterious effects. This was evident in the present study where longevity and reproduction were decreased in *An. funestus* after *EcR* knockdown. Strikingly, a decrease in *P. falciparum* oocyst intensity was observed- an ideal situation for potentially reducing malaria transmission. To postulate that *EcR* would be an ideal candidate gene to knockdown for novel vector control is risky. Review of the literature has shown that even though a reduction in parasite growth is evident in ds*EcR* mosquitoes, it is also coupled with faster maturing sporozoites and hence a shorter EIP that may circumvent the reduction in longevity (Werling *et al.*, 2019; reviewed by Ekoka *et al.*, 2021). It is therefore of utmost importance that this phenomenon be confirmed in *An. funestus* both in field and laboratory settings before

confirming this as a vector control strategy. If it is found to be true that depleting *An. funestus EcR* in any way increases parasite infectivity, gene drives, paratransgenesis, TBVs or simply any form of gene modification cannot be considered for vector control as it will mimic the above effects.

Fortunately, decreasing *EcR* levels is only one of the possibilities to target ecdysone signalling to reduce malaria transmission. Nonsteroidal 20E agonists are also considered a possible solution to mitigate the spread of malaria. 20-hydroxyecdysone agonists share structural similarities with 20E, hence they are able to competitively bind to the EcR-USP complex, amplifying 20E signalling and all of its effects (reveiwed by Dhadialla *et al.*, 1998). Five 20E agonists, namely chromafenozide, fufenozide, halofenozide, methoxyfenozide and tebufenozide are currently available as insecticides targeting agricultural pests (Nakagawa, 2005; Smagghe *et al.*, 2012). These 20E agonists are promising as potential malaria vector control strategies as they exhibit low toxicity to non-target organisms and penetrate the mosquito cuticle (Schneider *et al.*, 2004; Nakagawa, 2005; Smagghe *et al.*, 2012). The efficacy of some of these compounds have recently been demonstrated against several *Anopheles* vectors. Methoxyfenozide applied topically reduced mating success, fecundity and susceptibility to *P. falciparum* in *An. gambiae* (Childs *et al.*, 2016). Similarly, methoxyfenozide decreased longevity and fecundity insecticide resistant strains of *An. funestus*, *An. gambiae* and *An. coluzzii* when applied topically and tarsally (Brown *et al.*, 2020). Another study demonstrated the effectiveness of halofenozide in decreasing *P. berghei* oocyst intensity and infection prevalence (Reynolds and Smith, 2020).

Unfortunately, it is probable that compounds exerting a fitness cost could result in the development of resistant organisms. Resistance to ecdysone agonists has not yet been characterised in *Anopheles* mosquitoes, however it is likely that such resistance —if it occurs— will be based on the upregulation of detoxification enzymes, behavioural changes (Table 1.1) or possibly conformational changes in the ligand binding domain of EcR. Strikingly, studies in other invertebrates showing resistance to 20E agonists have developed phenotypes associated with reduced fitness parameters such as a reduction in longevity, fecundity, fertility, mating success and growth defects (Cao and Han, 2006; Tang *et al.*, 2011; Sun *et al.*, 2012; Rehan and Freed, 2015; Shah *et al.*, 2017). This resistance to 20E agonists is however reversed upon the removal of the compound (Rehan and Freed, 2014), making this promising for counteracting current insecticide-based vector control strategies. While the above findings could be likely in *Anopheles* vectors, it should be confirmed in future studies. Studies in pyrethroid, carbamate

and DDT resistant *An. gambiae* and pyrethroid and DDT resistant *An. funestus* strains confirmed that the upregulation of P450 enzymes, involved in pyrethroid resistance, did not confer any form of resistance to 20E agonist methoxyfenozide (Yunta *et al.*, 2016; Brown *et al.*, 2020). These studies demonstrate the potential of these compounds to be used in the field against insecticide resistant populations evading current insecticide-based vector control interventions.

The current study defined the function of *EcR* in *An. funestus* as a regulator of longevity, fecundity, fertility and immunity against *P. falciparum*. RNAi was used as a functional genomics tool to demonstrate that *EcR* maintains longevity, promotes the normal functioning of fecundity and fertility through the regulation of *Lp* and *VgR* and is involved in immunity against *Plasmodium* albeit through an undetermined pathway in *An. funestus*. This study is merely a stepping stone but has demonstrated that *EcR*'s regulation of several physiological processes in the mosquito forms the foundation for the research and development of novel vector control strategies. Further research is required to determine the mode of action of and genes involved in EcRs regulation of pathways governing longevity, reproductive success and importantly *Plasmodium* infectivity in *An. funestus*. For example, the complex interaction of EcR and the 20E signalling pathway can further be elucidated through next generation RNA sequencing. This will allow for the identification of the complete profile of early and late genes regulated by EcR, providing a holistic overview of this pathway. These genes can thereafter be examined to determine their functions in regulating mosquito physiological processes that potentially target vector density and competence. Once this has been achieved, studies in field settings will be essential to confirm laboratory based experiments. Success in both laboratory and field based aspects of this research can subsequently result in the approval of EcR based vector control methods that will potentially reduce malaria transmission.

6 REFERENCES

Ahmed, A. *et al.* (1999) 'Genomic structure and ecdysone regulation of the prophenoloxidase 1 gene in the malaria vector Anopheles gambiae', *Proceedings of the National Academy of Sciences*, 96(26): 14795–14800.

Ahmed, M. A. and Cox- Singh, J. (2015) 'Plasmodium knowlesi–an emerging pathogen', *ISBT science series*, 10(S1): 134–140.

Airs, P. M. and Bartholomay, L. C. (2017) 'RNA Interference for mosquito and mosquito-borne disease control', *Insects*, 8(1): 4.

Alphey, L. *et al.* (2010) 'Sterile-insect methods for control of mosquito-borne diseases: an analysis', *Vector-Borne and Zoonotic Diseases*, 10(3): 295–311.

Alphey, L. (2014) 'Genetic control of mosquitoes', *Annual review of entomology*, 59: 205–224.

Amenya, D. A. *et al.* (2008) 'Over expression of a cytochrome P450 (CYP6P9) in a major African malaria vector, Anopheles funestus, resistant to pyrethroids', *Insect molecular biology*, 17(1): 19–25.

Andriessen, R. *et al.* (2015) 'Electrostatic coating enhances bioavailability of insecticides and breaks pyrethroid resistance in mosquitoes', *Proceedings of the National Academy of Sciences*, 112(39): 12081–12086.

Arango Duque, G. and Descoteaux, A. (2014) 'Macrophage cytokines: involvement in immunity and infectious diseases', *Frontiers in immunology*, 5: 491.

Arrow, K. J.Panosian, C.and Gelband, H. (2004) 'Antimalarial drugs and drug resistance', in *Saving Lives, Buying Time: Economics of Malaria Drugs in an Age of Resistance*, 252–300.

Atella, G. C.Bittencourt-Cunha, P. R.Nunes, R. D.Shahabuddin, M.and Silva-Neto, M. A. C. (2009) 'The major insect lipoprotein is a lipid source to mosquito stages of malaria parasite', *Acta tropica*, 109(2): 159–162.

Attardo, G. M.Hansen, I. A.and Raikhel, A. S. (2005) 'Nutritional regulation of vitellogenesis in mosquitoes: implications for anautogeny', *Insect biochemistry and molecular biology*, 35(7): 661–675.

Badenhorst, P. *et al.* (2005) 'The Drosophila nucleosome remodeling factor NURF is required for Ecdysteroid signaling and metamorphosis', *Genes and development*, 19(21): 2540–2545.

Baldini, F.Gabrieli, P.South, A.Valim, C.Mancini, F.and Catteruccia, F. (2013) 'The interaction between a sexually transferred steroid hormone and a female protein regulates oogenesis in the malaria mosquito Anopheles gambiae', *PLoS biology*, 11(10): e1001695.

Bartoloni, A. and Zammarchi, L. (2012) 'Clinical aspects of uncomplicated and severe malaria', *Mediterranean journal of hematology and infectious diseases*, 4(1): 2012026.

Bates, M. (1940) 'Oviposition Experiments with Anopheline Mosquitoes1', *The American Journal of Tropical Medicine and Hygiene*, 1(4): 569–583.

Beach, R. (1979) 'Mosquitoes: biting behavior inhibited by ecdysone', *Science*, 205(4408): 829–831.

Beckstead, R. *et al.* (2001) 'Bonus, a Drosophila homolog of TIF1 proteins, interacts with nuclear receptors and can inhibit βFTZ-F1-dependent transcription', *Molecular cell*, 7(4): 753–765.

Beier, J. C.Müller, G. C.Gu, W.Arheart, K. L.and Schlein, Y. (2012) 'Attractive toxic sugar bait (ATSB) methods decimate populations of Anopheles malaria vectors in arid environments regardless of the local availability of favoured sugar-source blossoms', *Malaria journal*, 11(1): 31.

Berg, J. M. (1989) 'DNA binding specificity of steroid receptors', *Cell*, 57(7): 1065–1068.

Bernstein, E.Caudy, A. A.Hammond, S. M.and Hannon, G. J. (2001) 'Role for a bidentate ribonuclease in the initiation step of RNA interference', *Nature*, 409(6818): 363.

Bhatt, S. *et al.* (2015) 'The effect of malaria control on Plasmodium falciparum in Africa between 2000 and 2015', *Nature*, 526(7572): 207–211.

Blackwell, A. and Johnson, S. N. (2000) 'Electrophysiological investigation of larval water and potential oviposition chemo-attractants for Anopheles gambiae ss', *Annals of Tropical Medicine and Parasitology*, 94(4): 389–398.

Blandin, S. *et al.* (2004) 'Complement-like protein TEP1 is a determinant of vectorial capacity in the malaria vector Anopheles gambiae', *Cell*, 116(5): 661–670.

Bohm, M. K.Behan, M.and Hagedorn, H. H. (1978) 'Termination of vitellogenin synthesis by

mosquito fat body, a programmed response to ecdysterone', *Physiological Entomology*, 3(1): 17–25.

Briegel, H. (1975) 'Excretion of proteolytic enzymes by Aedes aegypti after a blood meal', *Journal of insect physiology*, 21(10): 1681–1684.

Briegel, H. and Hörler, E. (1993) 'Multiple blood meals as a reproductive strategy in Anopheles (Diptera: Culicidae)', *Journal of Medical Entomology*, 30(6): 975–985.

Brooke, B.Koekemoer, L.Kruger, P.Urbach, J.Misiani, E.and Coetzee, M. (2013) 'Malaria vector control in South Africa', *South African Medical Journal*, 103(10): 784–788.

Brown, F.Paton, D. G.Catteruccia, F.Ranson, H.and Ingham, V. A. (2020) 'A steroid hormone agonist reduces female fitness in insecticide-resistant Anopheles populations', *Insect Biochemistry and Molecular Biology*, 121: 103372.

Brown, M. R. *et al.* (1998) 'Identification of a steroidogenic neurohormone in female mosquitoes', *Journal of Biological Chemistry*, 273(7): 3967–3971.

Brown, M. R. *et al.* (2008) 'An insulin-like peptide regulates egg maturation and metabolism in the mosquito Aedes aegypti', *Proceedings of the National Academy of Sciences*, 105(15): 5716–5721.

Bunnik, E. M. and Le Roch, K. G. (2013) 'An introduction to functional genomics and systems biology', *Advances in wound care*, 2(9): 490–498.

Cao, G. and Han, Z. (2006) 'Tebufenozide resistance selected in Plutella xylostella and its cross- resistance and fitness cost', *Pest Management Science*, 62(8): 746–751.

Carney, G. E. and Bender, M. (2000) 'The Drosophila ecdysone receptor (EcR) gene is required maternally for normal oogenesis', *Genetics*, 154(3): 1203–1211.

Carter, R. (2001) 'Transmission blocking malaria vaccines', *Vaccine*, 19(17–19): 2309–2314.

Carter, R. and Chen, D. H. (1976) 'Malaria transmission blocked by immunisation with gametes of the malaria parasite', *Nature*, 263(5572): 57–60.

CDC (2019) *CDC - Malaria - About Malaria - Biology*. Available at: https://www.cdc.gov/malaria/about/biology/index.html (Accessed: 15 April 2020).

Chaccour, C.Lines, J.and Whitty, C. J. M. (2010) 'Effect of ivermectin on Anopheles gambiae mosquitoes fed on humans: the potential of oral insecticides in malaria control', *The Journal*

of infectious diseases, 202(1): 113–116.

Charlesworth, B. and Willis, J. H. (2009) 'Nature reviews. Genetics', *Nature Reviews Genetics*, 10(3): 195–205.

Chaturvedi, N.Bharti, P. K.Tiwari, A.and Singh, N. (2016) 'Strategies and recent development of transmission-blocking vaccines against Plasmodium falciparum', *The Indian journal of medical research*, 143(6): 696.

Cherbas, L.Lee, K.and Cherbas, P. (1991) 'Identification of ecdysone response elements by analysis of the Drosophila Eip28/29 gene.', *Genes and development*, 5(1): 120–131.

Childs, L. M. *et al.* (2016) 'Disrupting mosquito reproduction and parasite development for malaria control', *PLoS pathogens*, 12(12): e1006060.

Cho, W.-L. *et al.* (1999) 'Mosquito cathepsin B-like protease involved in embryonic degradation of vitellin is produced as a latent extraovarian precursor', *Journal of Biological Chemistry*, 274(19): 13311–13321.

Cho, W.-L.Deitsch, K. W.and Raikhel, A. S. (1991) 'An extraovarian protein accumulated in mosquito oocytes is a carboxypeptidase activated in embryos', *Proceedings of the National Academy of Sciences*, 88(23): 10821–10824.

Cho, W.-L.Kapitskaya, M. Z.and Raikhel, A. S. (1995) 'Mosquito ecdysteroid receptor: analysis of the cDNA and expression during vitellogenesis', *Insect biochemistry and molecular biology*, 25(1): 19–27.

Choi, K. S. *et al.* (2014) 'Insecticide resistance and role in malaria transmission of Anopheles funestus populations from Zambia and Zimbabwe', *Parasites and Vectors*, 7(1): 464.

Christian, R. N.Strode, C.Ranson, H.Coetzer, N.Coetzee, M.and Koekemoer, L. L. (2011) 'Microarray analysis of a pyrethroid resistant African malaria vector, Anopheles funestus, from southern Africa', *Pesticide biochemistry and physiology*, 99(2): 140–147.

Christophides, G. K. *et al.* (2002) 'Immunity-related genes and gene families in Anopheles gambiae', *Science*, 298(5591): 159–165.

Christophides, G. K.Vlachou, D.and Kafatos, F. C. (2004) 'Comparative and functional genomics of the innate immune system in the malaria vector Anopheles gambiae', *Immunological reviews*, 198(1): 127–148.

Clayton, R. B. (1964) ‘The utilization of sterols by insects’, *Journal of lipid research*, 5(1): 3–19.

Clements, A. N. and Potter, S. A. (1967) ‘The fine structure of the spermathecae and their ducts in the mosquito Aedes aegypti’, *Journal of Insect Physiology*, 13(12): 1825–1836.

Cohuet, A.Simard, F.Toto, J. C.Kengne, P.Coetzee, M.and Fontenille, D. (2003) ‘Species identification within the Anopheles funestus group of malaria vectors in Cameroon and evidence for a new species.’, *The American journal of tropical medicine and hygiene*, 69(2): 200.

Collins, F. H. *et al.* (1986) ‘Genetic selection of a Plasmodium-refractory strain of the malaria vector Anopheles gambiae’, *Science*, 234(4776): 607–610.

Cooper, D. J. *et al.* (2020) ‘Plasmodium knowlesi malaria in Sabah, Malaysia, 2015–2017: ongoing increase in incidence despite near-elimination of the human-only Plasmodium species’, *Clinical infectious diseases*, 70(3): 361–367.

Costa, G. *et al.* (2018) ‘Non-competitive resource exploitation within mosquito shapes within-host malaria infectivity and virulence’, *Nature communications*, 9(1): 1–11.

Couto, J.Ferrolho, J.de la Fuente, J.and Domingos, A. (2016) ‘Anopheles gambiae and A. stephensi immune response during Plasmodium berghei infection uncovered by sialotranscriptomic analysis’, *International Trends in Immununology*, 4: 58–72.

Coy, M. R. *et al.* (2012) ‘Gene silencing in adult Aedes aegypti mosquitoes through oral delivery of double- stranded RNA’, *Journal of applied entomology*, 136(10): 741–748.

Cruz, F. E. DelaKirsch, D. R.and Heinrich, J. N. (2000) ‘Transcriptional activity of Drosophila melanogaster ecdysone receptor isoforms and ultraspiracle in Saccharomyces cerevisiae’, *Journal of molecular endocrinology*, 24(2): 183–192.

Dahalan, F. A.Churcher, T. S.Windbichler, N.and Lawniczak, M. K. N. (2019) ‘The male mosquito contribution towards malaria transmission: Mating influences the Anopheles female midgut transcriptome and increases female susceptibility to human malaria parasites’, *PLoS pathogens*, 15(11): e1008063.

Devarakonda, S.Harp, J. M.Kim, Y.Ożyhar, A.and Rastinejad, F. (2003) ‘Structure of the heterodimeric ecdysone receptor DNA- binding complex’, *The EMBO journal*, 22(21): 5827–5840.

Dhadialla, T. S.Carlson, G. R.and Le, D. P. (1998) ‘New insecticides with ecdysteroidal and juvenile hormone activity’, *Annual review of entomology*, 43(1): 545–569.

Dhara, A. *et al.* (2013) ‘Ovary ecdysteroidogenic hormone functions independently of the insulin receptor in the yellow fever mosquito, Aedes aegypti’, *Insect biochemistry and molecular biology*, 43(12): 1100–1108.

DiBello, P. R.Withers, D. A.Bayer, C. A.Fristrom, J. W.and Guild, G. M. (1991) ‘The Drosophila Broad-Complex encodes a family of related proteins containing zinc fingers.’, *Genetics*, 129(2): 385–397.

Dinglasan, R. R. *et al.* (2007) ‘Disruption of Plasmodium falciparum development by antibodies against a conserved mosquito midgut antigen’, *Proceedings of the National Academy of Sciences*, 104(33): 13461–13466.

Djimdé, A. *et al.* (2001) ‘A molecular marker for chloroquine-resistant falciparum malaria’, *The New England journal of medicine*, 344(4): 299–302.

Dobens, L.Rudolph, K.and Berger, E. M. (1991) ‘Ecdysterone regulatory elements function as both transcriptional activators and repressors.’, *Molecular and Cellular Biology*, 11(4): 1846–1853.

Dong, Y.Aguilar, R.Xi, Z.Warr, E.Mongin, E.and Dimopoulos, G. (2006) ‘Anopheles gambiae immune responses to human and rodent Plasmodium parasite species’, *PLoS pathogens*, 2(6): e52.

Dong, Y.Manfredini, F.and Dimopoulos, G. (2009) ‘Implication of the mosquito midgut microbiota in the defense against malaria parasites’, *PLoS pathogens*, 5(5): e1000423.

Dong, Y.Simões, M. L.Marois, E.and Dimopoulos, G. (2018) ‘CRISPR/Cas9 -mediated gene knockout of Anopheles gambiae FREP1 suppresses malaria parasite infection’, *PLOS Pathogens*, 14(3): e1006898.

Doudna, J. A. and Charpentier, E. (2014) ‘The new frontier of genome engineering with CRISPR-Cas9’, *Science*, (6213): 346.

Drexler, A. L.Vodovotz, Y.and Luckhart, S. (2008) ‘Plasmodium development in the mosquito: biology bottlenecks and opportunities for mathematical modeling’, *Trends in parasitology*, 24(8): 333–336.

Dufour, C. *et al.* (2003) 'TNF-α and IFN-γ are overexpressed in the bone marrow of Fanconi anemia patients and TNF-α suppresses erythropoiesis in vitro', *Blood*, 102(6): 2053–2059.

Durand, R.Jafari, S.Vauzelle, J.Delabre, J.-F.Jesic, Z.and Le Bras, J. (2001) 'Analysis of pfcrt point mutations and chloroquine susceptibility in isolates of Plasmodium falciparum', *Molecular and biochemical parasitology*, 114(1): 95–102.

Eckstein-Ludwig, U. *et al.* (2003) 'Artemisinins target the SERCA of Plasmodium falciparum', *Nature*, 424(6951): 957–961.

Ekoka, E.Maharaj, S.Nardini, L.Dahan-Moss, Y.and Koekemoer, L. L. (2021) '20-Hydroxyecdysone (20E) signaling as a promising target for the chemical control of malaria vectors', *Parasites and Vectors*, 14(1): 86.

Fallon, A. M.Hagedorn, H. H.Wyatt, G. R.and Laufer, H. (1974) 'Activation of vitellogenin synthesis in the mosquito Aedes aegypti by ecdysone', *Journal of Insect Physiology*, 20(9): 1815–1823.

Filipowicz, W. (2005) 'RNAi: the nuts and bolts of the RISC machine', *Cell*, 122(1): 17–20.

Fire, A.Xu, S.Montgomery, M. K.Kostas, S. A.Driver, S. E.and Mello, C. C. (1998) 'Potent and specific genetic interference by double-stranded RNA in Caenorhabditis elegans', *nature*, 391(6669): 806.

Fleige, S. and Pfaffl, M. W. (2006) 'RNA integrity and the effect on the real-time qRT-PCR performance', *Molecular aspects of medicine*, 27(2–3): 126–139.

Fraiture, M. *et al.* (2009) 'Two mosquito LRR proteins function as complement control factors in the TEP1-mediated killing of Plasmodium', *Cell host and microbe*, 5(3): 273–284.

Fujiwara, H.Jindra, M.Newitt, R.Palli, S. R.Hiruma, K.and Riddiford, L. M. (1995) 'Cloning of an ecdysone receptor homolog from Manduca sexta and the developmental profile of its mRNA in wings', *Insect biochemistry and molecular biology*, 25(7): 845–856.

Gabrieli, P. *et al.* (2014) 'Sexual transfer of the steroid hormone 20E induces the postmating switch in Anopheles gambiae', *Proceedings of the National Academy of Sciences*, 111(46): 16353–16358.

Gaddelapati, S. C.Dhandapani, R. K.and Palli, S. R. (2020) 'CREB-binding protein regulates metamorphosis and compound eye development in the yellow fever mosquito, Aedes aegypti',

Biochimica et Biophysica Acta (BBA)-Gene Regulatory Mechanisms, 194576.

Geering, K. (1975) 'Lipase and unspecific esterase activity in the fat body of Aedes aegypti L.', *Acta tropica*, 32(3): 273.

Geering, K. and Oberlin, U.-P. (1975) 'The esterase patterns in the ovaries and the embryonated eggs of Aedes aegypti L.', *Acta tropica*, 32(1): 48–56.

Gething, P. W. *et al.* (2012) 'A long neglected world malaria map: Plasmodium vivax endemicity in 2010', *PLoS neglected tropical diseases*, 6(9): e1814.

Ghurye, J. *et al.* (2019) 'A chromosome-scale assembly of the major African malaria vector Anopheles funestus', *GigaScience*, 8(6): giz063.

Gilbert, L. I.Rybczynski, R.and Warren, J. T. (2002) 'Control and biochemical nature of the ecdysteroidogenic pathway', *Annual review of entomology*, 47(1): 883–916.

Gillies, M. T. and Coetzee, M. (1987) 'A supplement to the Anophelinae of Africa South of the Sahara', *Publications of the South African Institute for medical research*, 55: 1–143.

Gillies, M. T. and De Meillon, B. (1968) 'The Anophelinae of Africa south of the Sahara (Ethiopian zoogeographical region).', *The American Journal of Tropical Medicine and Hygiene*.

Gleave, K.Lissenden, N.Richardson, M.Choi, L.and Ranson, H. (2018) 'Piperonyl butoxide (PBO) combined with pyrethroids in insecticide-treated nets to prevent malaria in Africa', *Cochrane Database of Systematic Reviews*, (11).

Gwadz, R. W. (1976) 'Successful immunization against the sexual stages of Plasmodium gallinaceum', *Science*, 193(4258): 1150–1151.

Gwadz, R. W.Kaslow, D.Lee, J.-Y.Maloy, W. L.Zasloff, M.and Miller, L. H. (1989) 'Effects of magainins and cecropins on the sporogonic development of malaria parasites in mosquitoes.', *Infection and immunity*, 57(9): 2628–2633.

Hagedorn, H. H. and Fallon, A. M. (1973) 'Ovarian control of vitellogenin synthesis by the fat body in Aedes aegypti', *Nature*, 244(5411): 103–105.

Hagedorn, H. H.O'Connor, J. D.Fuchs, M. S.Sage, B.Schlaeger, D. A.and Bohm, M. K. (1975) 'The ovary as a source of alpha-ecdysone in an adult mosquito.', *Proceedings of the National Academy of Sciences*, 72(8): 3255.

Hammond, A. M. and Galizi, R. (2017) ‘Gene drives to fight malaria: current state and future directions’, *Pathogens and global health*, 111(8): 412–423.

Hansen, I. A.Attardo, G. M.Rodriguez, S. D.and Drake, L. L. (2014) ‘Four-way regulation of mosquito yolk protein precursor genes by juvenile hormone-, ecdysone-, nutrient-, and insulin-like peptide signaling pathways’, *Frontiers in physiology*, 5: 103.

Hays, A. R. and Raikhel, A. S. (1990) ‘A novel protein produced by the vitellogenic fat body and accumulated in mosquito oocytes’, *Roux’s archives of developmental biology*, 199(2): 114–121.

Healy, S. A. *et al.* (2020) ‘Pfs230 yields higher malaria transmission-blocking vaccine activity than Pfs25 in humans but not mice’, *medRxiv*, 2020.11.19.20234922. Available at: http://medrxiv.org/content/early/2020/11/22/2020.11.19.20234922.abstract.

Hu, X.Cherbas, L.and Cherbas, P. (2003) ‘Transcription activation by the ecdysone receptor (EcR/USP): identification of activation functions’, *Molecular endocrinology*, 17(4): 716–731.

Huang, J.Walker, E. D.Giroux, P. Y.Vulule, J.and Miller, J. R. (2005) ‘Ovipositional site selection by Anopheles gambiae: influences of substrate moisture and texture’, *Medical and Veterinary Entomology*, 19(4): 442–450.

Huang, J.Walker, E. D.Otienoburu, P. E.Amimo, F.Vulule, J.and Miller, J. R. (2006) ‘Laboratory tests of oviposition by the African malaria mosquito, Anopheles gambiae, on dark soil as influenced by presence or absence of vegetation’, *Malaria Journal*, 5(1): 1–5.

Huch, S.Fleige, S.and Pfaffl, M. W. (2005) ‘Determination of RNA quality and its influence on the quantitative real-time RT-PCR’.

Hunt, P. *et al.* (2010) ‘Experimental evolution, genetic analysis and genome re-sequencing reveal the mutation conferring artemisinin resistance in an isogenic lineage of malaria parasites’, *BMC genomics*, 11(1): 499.

Hunt, R. H.Brooke, B. D.Pillay, C.Koekemoer, L. L.and Coetzee, M. (2005) ‘Laboratory selection for and characteristics of pyrethroid resistance in the malaria vector Anopheles funestus’, *Medical and veterinary entomology*, 19(3): 271–275.

Ibrahim, S. S. *et al.* (2015) ‘Allelic variation of cytochrome P450s drives resistance to bednet insecticides in a major malaria vector’, *PLoS genetics*, 11(10): e1005618.

Ibrahim, S. S.Ndula, M.Riveron, J. M.Irving, H.and Wondji, C. S. (2016) 'The P450 CYP 6Z1 confers carbamate/pyrethroid cross-resistance in a major African malaria vector beside a novel carbamate-insensitive N485I acetylcholinesterase-1 mutation', *Molecular ecology*, 25(14): 3436–3452.

Jaramillo-Gutierrez, G.Rodrigues, J.Ndikuyeze, G.Povelones, M.Molina-Cruz, A.and Barillas-Mury, C. (2009) 'Mosquito immune responses and compatibility between Plasmodium parasites and anopheline mosquitoes', *BMC microbiology*, 9(1): 1–11.

Jayachandran, G. and Fallon, A. M. (2000) 'Evidence for expression of EcR and USP components of the 20-hydroxyecdysone receptor by a mosquito cell line', *Archives of insect biochemistry and physiology*, 43(2): 87–96.

Jinek, M.Chylinski, K.Fonfara, I.Hauer, M.Doudna, J. A.and Charpentier, E. (2012) 'A programmable dual-RNA–guided DNA endonuclease in adaptive bacterial immunity', *science*, 337(6096): 816–821.

Joung, J. K. and Sander, J. D. (2013) 'TALENs: a widely applicable technology for targeted genome editing', *Nature reviews Molecular cell biology*, 14(1): 49–55.

Kamali, M. *et al.* (2014) 'Multigene phylogenetics reveals temporal diversification of major African malaria vectors', *PloS one*, 9(4): e93580.

Kamareddine, L.Nakhleh, J.and Osta, M. A. (2016) 'Functional Interaction between Apolipophorins and Complement Regulate the Mosquito Immune Response to Systemic Infections', *Journal of Innate Immunity*, 8(3): 314–326.

Kapulu, M. C. *et al.* (2015) 'Comparative assessment of transmission-blocking vaccine candidates against Plasmodium falciparum', *Scientific reports*, 5(1): 1–15.

Karim, F. D. and Thummel, C. S. (1992) 'Temporal coordination of regulatory gene expression by the steroid hormone ecdysone.', *The EMBO Journal*, 11(11): 4083–4093.

Karlson, P. (1963) 'Chemistry and biochemistry of insect hormones', *Angewandte Chemie International Edition in English*, 2(4): 175–182.

Khaligh, F. G.Jafari, A.Silivanova, E.Levchenko, M.Rahimi, B.and Gholizadeh, S. (2021) 'Endectocides as a complementary intervention in the malaria control program: a systematic review', *Systematic Reviews*, 10(1): 30.

Khvorova, A.Reynolds, A.and Jayasena, S. D. (2003) ‘Functional siRNAs and miRNAs exhibit strand bias’, *Cell*, 115(2): 209–216.

Killiny, N.Hajeri, S.Tiwari, S.Gowda, S.and Stelinski, L. L. (2014) ‘Double-stranded RNA uptake through topical application, mediates silencing of five CYP4 genes and suppresses insecticide resistance in Diaphorina citri’, *PloS one*, 9(10): e110536.

Kim, W. *et al.* (2004) ‘Ectopic expression of a cecropin transgene in the human malaria vector mosquito Anopheles gambiae (Diptera: Culicidae): effects on susceptibility to Plasmodium’, *Journal of medical entomology*, 41(3): 447–455.

King-Jones, K. and Thummel, C. S. (2005) ‘Nuclear receptors—a perspective from Drosophila’, *Nature Reviews Genetics*, 6(4): 311–323.

Knipling, E. F. (1955) ‘Possibilities of insect control or eradication through the use of sexually sterile males’, *Journal of Economic Entomology*, 48(4): 459–462.

Knols, B. G. J. *et al.* (2016) ‘Eave tubes for malaria control in Africa: an introduction’, *Malaria journal*, 15(1): 404.

Kobylinski, K. C. *et al.* (2010) ‘The effect of oral anthelmintics on the survivorship and re-feeding frequency of anthropophilic mosquito disease vectors’, *Acta tropica*, 116(2): 119–126.

Kobylinski, K. C.Sylla, M.Chapman, P. L.Sarr, M. D.and Foy, B. D. (2011) ‘Ivermectin mass drug administration to humans disrupts malaria parasite transmission in Senegalese villages’, *The American journal of tropical medicine and hygiene*, 85(1): 3–5.

Koelle, M. R.Talbot, W. S.Segraves, W. A.Bender, M. T.Cherbas, P.and Hogness, D. S. (1991) ‘The Drosophila EcR gene encodes an ecdysone receptor, a new member of the steroid receptor superfamily’, *Cell*, 67(1): 59–77.

Kokoza, V. A.Martin, D.Mienaltowski, M. J.Ahmed, A.Morton, C. M.and Raikhel, A. S. (2001) ‘Transcriptional regulation of the mosquito vitellogenin gene via a blood meal-triggered cascade’, *Gene*, 274(1–2): 47–65.

Kokoza, V.Ahmed, A.Shin, S. W.Okafor, N.Zou, Z.and Raikhel, A. S. (2010) ‘Blocking of Plasmodium transmission by cooperative action of Cecropin A and Defensin A in transgenic Aedes aegypti mosquitoes’, *Proceedings of the National Academy of Sciences*, 107(18): 8111–8116.

Kwiatkowski, D.Cannon, J. G.Manogue, K. R.Cerami, A.Dinarello, C. A.and Greenwood, B. M. (1989) 'Tumour necrosis factor production in Falciparum malaria and its association with schizont rupture.', *Clinical and experimental immunology*, 77(3): 361.

Kyrou, K. *et al.* (2018) 'A CRISPR–Cas9 gene drive targeting doublesex causes complete population suppression in caged Anopheles gambiae mosquitoes', *Nature biotechnology*, 36(11): 1062.

Lal, A. A. *et al.* (2001) 'Anti-mosquito midgut antibodies block development of Plasmodium falciparum and Plasmodium vivax in multiple species of Anopheles mosquitoes and reduce vector fecundity and survivorship', *Proceedings of the National Academy of Sciences*, 98(9): 5228–5233.

Lamikanra, A. A.Theron, M.Kooij, T. W. A.and Roberts, D. J. (2009) 'Hemozoin (malarial pigment) directly promotes apoptosis of erythroid precursors', *PloS one*, 4(12).

Layez, C. *et al.* (2005) 'Plasmodium falciparum rhoptry protein RSP2 triggers destruction of the erythroid lineage', *Blood*, 106(10): 3632–3638.

Lea, A. O. (1967) 'The medial neurosecretory cells and egg maturation in mosquitoes', *Journal of insect physiology*, 13(3): 419–429.

Lemos, F. J. A.Cornel, A. J.and Jacobs-Lorena, M. (1996) 'Trypsin and aminopeptidase gene expression is affected by age and food composition in Anopheles gambiae', *Insect biochemistry and molecular biology*, 26(7): 651–658.

Lengeler, C. (2004) 'Insecticide-treated bed nets and curtains for preventing malaria.', *Cochrane Database of systematic reviews*, (2): 1–46.

Li, C.Kapitskaya, M. Z.Zhu, J.Miura, K.Segraves, W.and Raikhel, A. S. (2000) 'Conserved molecular mechanism for the stage specificity of the mosquito vitellogenic response to ecdysone', *Developmental Biology*, 224(1): 96–110.

Lindh, J. M. *et al.* (2015) 'Discovery of an oviposition attractant for gravid malaria vectors of the Anopheles gambiae species complex', *Malaria journal*, 14(1): 1–12.

Liu, C.Jason Pitts, R.Jonathon, D. B.Patrick, L. J.Wang, G.and Laurence, J. Z. (2010) 'Distinct olfactory signaling mechanisms in the malaria vector mosquito', *Anopheles gambiae PLoS Biol*, 8.

Livak, K. J. and Schmittgen, T. D. (2001) ‘Analysis of relative gene expression data using real-time quantitative PCR and the 2− ΔΔCT method’, *methods*, 25(4): 402–408.

Luxemburger, C.Ricci, F.Nosten, F.Raimond, D.Bathet, S.and White, N. J. (1997) ‘The epidemiology of severe malaria in an area of low transmission in Thailand’, *Transactions of the Royal Society of Tropical medicine and Hygiene*, 91(3): 256–262.

Macharia, R. W.Ombura, F. L.and Aroko, E. O. (2015) ‘Insects’ RNA profiling reveals absence of “hidden break” in 28S ribosomal RNA molecule of onion thrips, Thrips tabaci’, *Journal of nucleic acids*, 2015: 965294.

MacPherson, G. G.Warrell, M. J.White, N. J.Looareesuwan, S.and Warrell, D. A. (1985) ‘Human cerebral malaria. A quantitative ultrastructural analysis of parasitized erythrocyte sequestration.’, *The American journal of pathology*, 119(3): 385.

Makarova, K. S.Grishin, N. VShabalina, S. A.Wolf, Y. I.and Koonin, E. V (2006) ‘A putative RNA-interference-based immune system in prokaryotes: computational analysis of the predicted enzymatic machinery, functional analogies with eukaryotic RNAi, and hypothetical mechanisms of action’, *Biology direct*, 1(1): 7.

Mangelsdorf, D. J. *et al.* (1995) ‘The nuclear receptor superfamily: the second decade’, *Cell*, 83(6): 835.

Marcenac, P. *et al.* (2020) ‘A mating-induced reproductive gene promotes Anopheles tolerance to Plasmodium falciparum infection’, *PLoS pathogens*, 16(12): e1008908.

Martín, D.Wang, S.-F.and Raikhel, A. S. (2001) ‘The vitellogenin gene of the mosquito Aedes aegypti is a direct target of ecdysteroid receptor’, *Molecular and cellular endocrinology*, 173(1–2): 75–86.

Mendes, A. M. *et al.* (2008) ‘Conserved mosquito/parasite interactions affect development of Plasmodium falciparum in Africa’, *PLoS pathogens*, 4(5): e1000069.

Menon, V. *et al.* (2018) ‘Assessment of antibodies induced by multivalent transmission-blocking malaria vaccines’, *Frontiers in immunology*, 8: 1998.

Meshnick, S. R.Thomas, A.Ranz, A.Xu, C.-M.and Pan, H.-Z. (1991) ‘Artemisinin (qinghaosu): the role of intracellular hemin in its mechanism of antimalarial action’, *Molecular and biochemical parasitology*, 49(2): 181–189.

Michel, K. and Kafatos, F. C. (2005) ‘Mosquito immunity against Plasmodium’, *Insect biochemistry and molecular biology*, 35(7): 677–689.

Milazzo, G. *et al.* (2020) ‘Histone Deacetylases (HDACs): Evolution, Specificity, Role in Transcriptional Complexes, and Pharmacological Actionability’, *Genes*, 11(5): 556.

Mitri, C. *et al.* (2020) ‘Gene copy number and function of the APL1 immune factor changed during Anopheles evolution’, *Parasites and Vectors*, 13(1): 1–12.

Mittal, P. K. (2003) ‘Biolarvicides in vector control: challenges and prospects’, *Journal of vector borne diseases*, 40: 20–32.

Miura, K. *et al.* (2016) ‘Transmission-blocking activity is determined by transmission-reducing activity and number of control oocysts in Plasmodium falciparum standard membrane-feeding assay’, *Vaccine*, 34(35): 4145–4151.

Moiroux, N. *et al.* (2012) ‘Changes in Anopheles funestus biting behavior following universal coverage of long-lasting insecticidal nets in Benin’, *The Journal of infectious diseases*, 206(10): 1622–1629.

Mojica, F. J. M.García-Martínez, J.and Soria, E. (2005) ‘Intervening sequences of regularly spaced prokaryotic repeats derive from foreign genetic elements’, *Journal of molecular evolution*, 60(2): 174–182.

Moonasar, D. *et al.* (2013) ‘What will move malaria control to elimination in South Africa?’, *South African Medical Journal*, 103(10): 801–806.

Müller, G. C.Junnila, A.and Schlein, Y. (2010) ‘Effective control of adult Culex pipiens by spraying an attractive toxic sugar bait solution in the vegetation near larval habitats’, *Journal of medical entomology*, 47(1): 63–66.

Munhenga, G. *et al.* (2011) ‘Evaluating the potential of the sterile insect technique for malaria control: relative fitness and mating compatibility between laboratory colonized and a wild population of Anopheles arabiensis from the Kruger National Park, South Africa’, *Parasites and Vectors*, 4(1): 208.

Nakagawa, Y. (2005) ‘Nonsteroidal ecdysone agonists’, *Vitamins and Hormones*, 73: 131–173.

Nakhleh, J.Christophides, G. K.and Osta, M. A. (2017) ‘The serine protease homolog CLIPA14 modulates the intensity of the immune response in the mosquito Anopheles

gambiae', *Journal of Biological Chemistry*, 292(44): 18217–18226.

Neafsey, D. E. *et al.* (2013) 'The evolution of the Anopheles 16 genomes project', *G3: Genes, Genomes, Genetics*, 3(7): 1191–1194.

Nikolaeva, D.Draper, S. J.and Biswas, S. (2015) 'Toward the development of effective transmission-blocking vaccines for malaria', *Expert review of vaccines*, 14(5): 653–680.

Ohm, J. R. *et al.* (2018) 'Rethinking the extrinsic incubation period of malaria parasites', *Parasites and vectors*, 11(1): 1–9.

Okoye, P. N.Brooke, B. D.Koekemoer, L. L.Hunt, R. H.and Coetzee, M. (2008) 'Characterisation of DDT, pyrethroid and carbamate resistance in Anopheles funestus from Obuasi, Ghana', *Transactions of the Royal Society of Tropical Medicine and Hygiene*, 102(6): 591–598.

Õmura, S. and Crump, A. (2004) 'The life and times of ivermectin - A success story', *Nature Reviews Microbiology*, 2(12): 984–989.

Oro, A. E.McKeown, M.and Evans, R. M. (1990) 'Relationship between the product of the Drosophila ultraspiracle locus and the vertebrate retinoid X receptor', *Nature*, 347(6290): 298–301.

Osta, M. A.Christophides, G. K.and Kafatos, F. C. (2004) 'Effects of Mosquito Genes on Plasmodium Development', *Science*, 303(5666): 2030–2032.

Patil, D. R.Nikumbh, S. D.Parulekar, A.and Roplekar, K. (2015) 'Multiorgan dysfunction in Plasmodium vivax malaria: a prospective study', *Internation Journal of Scientific Study*, 3(5): 155–162.

Pearson, W. R. (2013) 'An introduction to sequence similarity ("homology") searching', *Current protocols in bioinformatics*, 42(1): 1–3.

Peters, W. (1970) 'Chemotherapy and drug resistance in malaria.', *Chemotherapy and drug resistance in malaria.*, 1(2): 876.

Pierceall, W. E.Li, C.Biran, A.Miura, K.Raikhel, A. S.and Segraves, W. A. (1999) 'E75 expression in mosquito ovary and fat body suggests reiterative use of ecdysone-regulated hierarchies in development and reproduction', *Molecular and cellular endocrinology*, 150(1–2): 73–89.

Pillai, A. B. *et al.* (2017) 'RNA interference in mosquito: understanding immune responses, double-stranded RNA delivery systems and potential applications in vector control', *Insect molecular biology*, 26(2): 127–139.

Pluess, B.Tanser, F. C.Lengeler, C.and Sharp, B. L. (2010) 'Indoor residual spraying for preventing malaria', *Cochrane database of systematic reviews*, (4): CD006657.

Pondeville, E.Maria, A.Jacques, J.-C.Bourgouin, C.and Dauphin-Villemant, C. (2008) 'Anopheles gambiae males produce and transfer the vitellogenic steroid hormone 20-hydroxyecdysone to females during mating', *Proceedings of the National Academy of Sciences*, 105(50): 19631–19636.

Povelones, M.Waterhouse, R. M.Kafatos, F. C.and Christophides, G. K. (2009) 'Leucine-rich repeat protein complex activates mosquito complement in defense against Plasmodium parasites', *Science*, 324(5924): 258–261.

Price, R. N. *et al.* (1999) 'The pfmdr1 gene is associated with a multidrug-resistant phenotype in Plasmodium falciparumfrom the western border of Thailand', *Antimicrobial agents and chemotherapy*, 43(12): 2943–2949.

Pridgeon, J. W.Zhao, L.Becnel, J. J.Strickman, D. A.Clark, G. G.and Linthicum, K. J. (2014) 'Topically applied AaeIAP1 double-stranded RNA kills female adults of Aedes aegypti', *Journal of medical entomology*, 45(3): 414–420.

Raghavendra, K.Barik, T. K.Reddy, B. P. N.Sharma, P.and Dash, A. P. (2011) 'Malaria vector control: from past to future', *Parasitology research*, 108(4): 757–779.

Raikhel, A. S. (1992) 'Vitellogenesis in mosquitoes', in *Advances in Disease Vector Research*, 1–39.

Raikhel, A. S.Miura, K.and Segraves, W. A. (1999) 'Nuclear receptors in mosquito vitellogenesis', *American zoologist*, 39(4): 722–735.

Readio, J.Peck, K.Meola, R.and Dahm, K. H. (1988) 'Corpus allatum activity (in vitro) in female Culex pipiens during adult life cycle', *Journal of insect physiology*, 34(2): 131–135.

Rehan, A. and Freed, S. (2014) 'Resistance selection, mechanism and stability of Spodoptera litura (Lepidoptera: Noctuidae) to methoxyfenozide', *Pesticide Biochemistry and Physiology*, 110: 7–12.

Rehan, A. and Freed, S. (2015) ‘Fitness cost of methoxyfenozide and the effects of its sublethal doses on development, reproduction, and survival of Spodoptera litura (Fabricius)(Lepidoptera: Noctuidae)’, *Neotropical entomology*, 44(5): 513–520.

Reinke, M. D. and Barrett, B. A. (2007) ‘Fecundity, fertility and longevity reductions in adult oriental fruit moth (Lepidoptera: Tortricidae) exposed to surfaces treated with the ecdysteroid agonists tebufenozide and methoxyfenozide’, *Journal of Entomological Science*, 42(4): 457–466.

Ren, X.Hoiczyk, E.and Rasgon, J. L. (2008) ‘Viral paratransgenesis in the malaria vector Anopheles gambiae’, *PLoS pathogens*, 4(8): e1000135.

Reynolds, R. A.Kwon, H.and Smith, R. C. (2020) ‘20-Hydroxyecdysone Primes Innate Immune Responses That Limit Bacterial and Malarial Parasite Survival in Anopheles gambiae’, *Msphere*, 5(2): e00983-19.

Reynolds, R. A. and Smith, R. C. (2020) ‘The 20-hydroxyecdysone agonist, halofenozide, primes anti-Plasmodium immunity in Anopheles gambiae via the ecdysone receptor’, *bioRxiv*, 3(10): 1–9.

Riehle, M. A. and Brown, M. R. (2002) ‘Insulin receptor expression during development and a reproductive cycle in the ovary of the mosquito Aedes aegypti’, *Cell and tissue research*, 308(3): 409–420.

Riehle, M. A. and Jacobs-Lorena, M. (2005) ‘Using bacteria to express and display anti-parasite molecules in mosquitoes: current and future strategies’, *Insect biochemistry and molecular biology*, 35(7): 699–707.

Riehle, M. M. *et al.* (2006) ‘Natural malaria infection in Anopheles gambiae is regulated by a single genomic control region’, *Science*, 312(5773): 577–579.

Riveron, J. M. *et al.* (2013) ‘Directionally selected cytochrome P450 alleles are driving the spread of pyrethroid resistance in the major malaria vector Anopheles funestus’, *Proceedings of the National Academy of Sciences*, 110(1): 252–257.

Riveron, J. M. *et al.* (2014a) ‘A single mutation in the GSTe2 gene allows tracking of metabolically based insecticide resistance in a major malaria vector’, *Genome biology*, 27.

Riveron, J. M. *et al.* (2014b) ‘The highly polymorphic CYP6M7 cytochrome P450 gene partners with the directionally selected CYP6P9a and CYP6P9b genes to expand the pyrethroid

resistance front in the malaria vector Anopheles funestus in Africa', *BMC genomics*, 817.

Riveron, J. M.Tchouakui, M.Mugenzi, L.Menze, B. D.Chiang, M.-C.and Wondji, C. S. (2018) 'Insecticide resistance in malaria vectors: an update at a global scale', *Towards malaria elimination-a leap forward*, 9(12): 645.

Rono, M. K.Whitten, M. M. A.Oulad-Abdelghani, M.Levashina, E. A.and Marois, E. (2010) 'The major yolk protein vitellogenin interferes with the anti-plasmodium response in the malaria mosquito Anopheles gambiae', *PLoS biology*, 8(7): e1000434.

Rosenfeld, M. G. and Glass, C. K. (2001) 'Coregulator codes of transcriptional regulation by nuclear receptors', *Journal of Biological Chemistry*, 276(40): 36865–36868.

Sampath, K. S. and Puttaraju, H. P. (2012) 'Improvised microinjection technique for mosquito vectors', *The Indian journal of medical research*, 136(6): 971.

Sappington, T. W.Hays, A. R.and Raikhel, A. S. (1995) 'Mosquito vitellogenin receptor: purification, developmental and biochemical characterization', *Insect biochemistry and molecular biology*, 25(7): 807–817.

Saralamba, S. *et al.* (2011) 'Intrahost modeling of artemisinin resistance in Plasmodium falciparum', *Proceedings of the national academy of sciences*, 108(1): 397–402.

Schneider, M. I.Smagghe, G.Pineda, S.and Vinuela, E. (2004) 'Action of insect growth regulator insecticides and spinosad on life history parameters and absorption in third-instar larvae of the endoparasitoid Hyposoter didymator', *Biological Control*, 31(2): 189–198.

Schwarz, D. S.Hutvágner, G.Du, T.Xu, Z.Aronin, N.and Zamore, P. D. (2003) 'Asymmetry in the assembly of the RNAi enzyme complex', *Cell*, 115(2): 199–208.

Shah, R. M.Shad, S. A.and Abbas, N. (2017) 'Methoxyfenozide resistance of the housefly, Musca domestica L.(Diptera: Muscidae): cross-resistance patterns, stability and associated fitness costs', *Pest management science*, 73(1): 254–261.

Shaw, W. R. *et al.* (2014) 'Mating activates the heme peroxidase HPX15 in the sperm storage organ to ensure fertility in Anopheles gambiae', *Proceedings of the National Academy of Sciences*, 111(16): 5854–5859.

Shaw, W. R. *et al.* (2020) 'Multiple blood feeding in mosquitoes shortens the Plasmodium falciparum incubation period and increases malaria transmission potential', *PLoS Pathogens*,

16(12): e1009131.

Shaw, W. R. and Catteruccia, F. (2018) ‘Vector biology meets disease control: Using basic research to fight vector-borne diseases’, *Nature microbiology*, 4(1): 20–34.

Simon, A. F.Liang, D. T.and Krantz, D. E. (2006) ‘Differential decline in behavioral performance of Drosophila melanogaster with age’, *Mechanisms of ageing and development*, 127(7): 647–651.

Simon, A. F.Shih, C.Mack, A.and Benzer, S. (2003) ‘Steroid control of longevity in Drosophila melanogaster’, *Science*, 299(5611): 1407–1410.

Sinden, R. E. and Gilles, H. M. (2002) ‘The malaria parasites’, *Essential malariology*, 4: 8–34.

Smagghe, G.Gomez, L. E.and Dhadialla, T. S. (2012) ‘Bisacylhydrazine insecticides for selective pest control’, *Advances in Insect Physiology*, 43: 163–249.

Snow, R. W.Guerra, C. A.Noor, A. M.Myint, H. Y.and Hay, S. I. (2005) ‘The global distribution of clinical episodes of Plasmodium falciparum malaria’, *Nature*, 434(7030): 214–217.

Sougoufara, S. *et al.* (2014) ‘Biting by Anopheles funestus in broad daylight after use of long-lasting insecticidal nets: a new challenge to malaria elimination’, *Malaria journal*, 13(1): 125.

Spillings, B. L.Brooke, B. D.Koekemoer, L. L.Chiphwanya, J.Coetzee, M.and Hunt, R. H. (2009) ‘A new species concealed by Anopheles funestus Giles, a major malaria vector in Africa’, *The American journal of tropical medicine and hygiene*, 81(3): 510–515.

Sternberg, E. D. *et al.* (2016) ‘Eave tubes for malaria control in Africa: initial development and semi-field evaluations in Tanzania’, *Malaria journal*, 15(1): 447.

Stewart, Z. P.Oxborough, R. M.Tungu, P. K.Kirby, M. J.Rowland, M. W.and Irish, S. R. (2013) ‘Indoor application of attractive toxic sugar bait (ATSB) in combination with mosquito nets for control of pyrethroid-resistant mosquitoes’, *PLoS ONE*, 8(12): e84168.

Stowers, A. W.Keister, D. B.Muratova, O.and Kaslow, D. C. (2000) ‘A Region of Plasmodium falciparumAntigen Pfs25 That Is the Target of Highly Potent Transmission-Blocking Antibodies’, *Infection and immunity*, 68(10): 5530–5538.

Sun, G.Zhu, J.Li, C.Tu, Z.and Raikhel, A. S. (2002) ‘Two isoforms of the early E74 gene, an Ets transcription factor homologue, are implicated in the ecdysteroid hierarchy governing

vitellogenesis of the mosquito, Aedes aegypti', *Molecular and cellular endocrinology*, 190(1–2): 147–157.

Sun, J.Hiraoka, T.Dittmer, N. T.Cho, K.-H.and Raikhel, A. S. (2000) 'Lipophorin as a yolk protein precursor in the mosquito, Aedes aegypti', *Insect Biochemistry and Molecular Biology*, 30(12): 1161–1171.

Sun, J.Liang, P.and Gao, X. (2012) 'Cross-resistance patterns and fitness in fufenozide-resistant diamondback moth, Plutella xylostella (Lepidoptera: Plutellidae)', *Pest management science*, 68(2): 285–289.

Talbot, W. S.Swyryd, E. A.and Hogness, D. S. (1993) 'Drosophila tissues with different metamorphic responses to ecdysone express different ecdysone receptor isoforms', *Cell*, 73(7): 1323–1337.

Tang, B.Sun, J.Zhou, X.Gao, X.and Liang, P. (2011) 'The stability and biochemical basis of fufenozide resistance in a laboratory-selected strain of Plutella xylostella', *Pesticide biochemistry and physiology*, 101(2): 80–85.

Tarumi, T. *et al.* (1995) 'Interferon-alpha-induced apoptosis in human erythroid progenitors.', *Experimental hematology*, 23(12): 1310–1318.

Taylor, S.Wakem, M.Dijkman, G.Alsarraj, M.and Nguyen, M. (2010) 'A practical approach to RT-qPCR—publishing data that conform to the MIQE guidelines', *Methods*, 50(4): S1–S5.

Ter Kuile, F. O. *et al.* (1993) 'Halofantrine versus mefloquine in treatment of multidrug-resistant falciparum malaria', *The Lancet*, 341(8852): 1044–1049.

Timmons, L. and Fire, A. (1998) 'Specific interference by ingested dsRNA', *Nature*, 395(6705): 854.

Tiono, A. B. *et al.* (2018) 'Efficacy of Olyset Duo, a bednet containing pyriproxyfen and permethrin, versus a permethrin-only net against clinical malaria in an area with highly pyrethroid-resistant vectors in rural Burkina Faso: a cluster-randomised controlled trial', *The Lancet*, 392(10147): 569–580.

Tricoire, H.Battisti, V.Trannoy, S.Lasbleiz, C.Pret, A.-M.and Monnier, V. (2009) 'The steroid hormone receptor EcR finely modulates Drosophila lifespan during adulthood in a sex-specific manner', *Mechanisms of ageing and development*, 130(8): 547–552.

Tsai, C.-C.Kao, H.-Y.Yao, T.-P.McKeown, M.and Evans, R. M. (1999) 'SMRTER, a Drosophila nuclear receptor coregulator, reveals that EcR-mediated repression is critical for development', *Molecular cell*, 4(2): 175–186.

Tucker, M. S.Mutka, T.Patel, J.and Kyle, D. E. (2012) 'Phenotypic and genotypic analysis of in vitro-selected artemisinin-resistant progeny of Plasmodium falciparum', *Antimicrobial agents and chemotherapy*, 56(1): 302–314.

Tuschl, T.Zamore, P. D.Lehmann, R.Bartel, D. P.and Sharp, P. A. (1999) 'Targeted mRNA degradation by double-stranded RNA in vitro', *Genes and development*, 13(24): 3191–3197.

Uchida, K. (1998) 'Role of nutrition in initiation and promotion of ovarian development in the Japanese house mosquito, Culex pipiens pallens', *Medical Entomology and Zoology*, 49(2): 75–85.

Upton, L. M.Povelones, M.and Christophides, G. K. (2015) 'Anopheles gambiae blood feeding initiates an anticipatory defense response to Plasmodium berghei', *Journal of innate immunity*, 7(1): 74–86.

Urquhart, A. D. (1994) 'Putative pathophysiological interactions of cytokines and phagocytic cells in severe human falciparum malaria', *Clinical infectious diseases*, 19(1): 117–131.

Valzania, L.Mattee, M. T.Strand, M. R.and Brown, M. R. (2019) 'Blood feeding activates the vitellogenic stage of oogenesis in the mosquito Aedes aegypti through inhibition of glycogen synthase kinase 3 by the insulin and TOR pathways', *Developmental biology*, 454(1): 85–95.

Van Ekert, E.Powell, C. A.Shatters Jr, R. G.and Borovsky, D. (2014) 'Control of larval and egg development in Aedes aegypti with RNA interference against juvenile hormone acid methyl transferase', *Journal of insect physiology*, 70: 143–150.

Vandesompele, J. *et al.* (2002) 'Accurate normalization of real-time quantitative RT-PCR data by geometric averaging of multiple internal control genes', *Genome biology*, 3(7): 1–12.

Vaughan, J. A.Noden, B. H.and Beier, J. C. (1992) 'Population dynamics of Plasmodium falciparum sporogony in laboratory-infected Anopheles gambiae', *The Journal of parasitology*, 78(4): 716–724.

Vizioli, J. *et al.* (2000) 'Cloning and analysis of a cecropin gene from the malaria vector mosquito, Anopheles gambiae', *Insect molecular biology*, 9(1): 75–84.

Vlachou, D.Schlegelmilch, T.Christophides, G. K.and Kafatos, F. C. (2005) 'Functional genomic analysis of midgut epithelial responses in Anopheles during Plasmodium invasion', *Current Biology*, 15(13): 1185–1195.

Vogel, K. J.Brown, M. R.and Strand, M. R. (2015) 'Ovary ecdysteroidogenic hormone requires a receptor tyrosine kinase to activate egg formation in the mosquito Aedes aegypti', *Proceedings of the National Academy of Sciences*, 112(16): 5057–5062.

Volz, J.Müller, H.-M.Zdanowicz, A.Kafatos, F. C.and Osta, M. A. (2006) 'A genetic module regulates the melanization response of Anopheles to Plasmodium', *Cellular Microbiology*, 8(9): 1392–1405.

Waite, J. L.Lynch, P. A.and Thomas, M. B. (2016) 'Eave tubes for malaria control in Africa: a modelling assessment of potential impact on transmission', *Malaria journal*, 15(1): 449.

Walshe, D. P.Lehane, S. M.Lehane, M. J.and Haines, L. R. (2009) 'Prolonged gene knockdown in the tsetse fly Glossina by feeding double stranded RNA', *Insect molecular biology*, 18(1): 11–19.

Wang, S.-F.Li, C.Sun, G.Zhu, J.and Raikhel, A. S. (2002) 'Differential expression and regulation by 20-hydroxyecdysone of mosquito ecdysteroid receptor isoforms A and B', *Molecular and cellular endocrinology*, 196(1–2): 29–42.

Wang, S.-F.Li, C.Zhu, J.Miura, K.Miksicek, R. J.and Raikhel, A. S. (2000) 'Differential expression and regulation by 20-hydroxyecdysone of mosquito ultraspiracle isoforms', *Developmental biology*, 218(1): 99–113.

Wang, S.-F.Miura, K.Miksicek, R. J.Segraves, W. A.and Raikhel, A. S. (1998) 'DNA binding and transactivation characteristics of the mosquito ecdysone receptor-Ultraspiracle complex', *Journal of Biological Chemistry*, 273(42): 27531–27540.

Wang, S.Ghosh, A. K.Bongio, N.Stebbings, K. A.Lampe, D. J.and Jacobs-Lorena, M. (2012) 'Fighting malaria with engineered symbiotic bacteria from vector mosquitoes', *Proceedings of the National Academy of Sciences*, 109(31): 12734–12739.

Wang, S. and Jacobs-Lorena, M. (2017) 'Paratransgenesis applications: Fighting malaria with engineered mosquito symbiotic bacteria', in *Arthropod Vector: Controller of Disease Transmission, Volume 1*, 219–234.

Warhurst, D. C. (2001) 'A molecular marker for chloroquine-resistant falciparum malaria', *The*

New England journal of medicine, 344(4): 299–302.

Weatherall, D. J. *et al.* (2002) 'Malaria and the red cell', *ASH Education Program Book*, 2002(1): 35–57.

White, K. P.Hurban, P.Watanabe, T.and Hogness, D. S. (1997) 'Coordination of Drosophila metamorphosis by two ecdysone-induced nuclear receptors', *Science*, 276(5309): 114–117.

White, N. J. (2004) 'Antimalarial drug resistance', *The Journal of clinical investigation*, 113(8): 1084–1092.

Whitten, M. M. A.Shiao, S.-H.and Levashina, E. A. (2006) 'Mosquito midguts and malaria: cell biology, compartmentalization and immunology', *Parasite immunology*, 28(4): 121–130.

WHO (1975) *Manual on practical entomology in malaria part II*.

WHO (2006) *Pesticides and their application: for the control of vectors and pests of public health importance*.

WHO (2007) 'Long-lasting insecticidal nets for malaria prevention: A manual for malaria programme managers'.

WHO (2011) *Global insecticide use for vector-borne disease control: a 10-year assessment [2000-2009]*.

WHO (2012) 'WHO Global malaria programme, Global plan for insecticide resistance management in malaria vectors (GPIRM)'.

WHO (2015) 'Global technical strategy for malaria 2016-2030'.

WHO (2017) 'The evaluation process for vector control products'.

WHO (2018a) 'Global report on insecticide resistance in malaria vectors: 2010–2016', 72.

WHO (2018b) 'WHO recommended insecticides for indoor residual spraying against malaria vectors'.

WHO (2019a) *Guidelines for Malaria Vector Control*.

WHO (2019b) 'World malaria report 2019'.

WHO (2020) *World malaria report 2020: 20 years of global progress and challenges.*

Wiebe, A. *et al.* (2017) 'Geographical distributions of African malaria vector sibling species and evidence for insecticide resistance', *Malaria Journal*, 16(1): 85.

Wilke, A. B. B. and Marrelli, M. T. (2015) 'Paratransgenesis: a promising new strategy for mosquito vector control', *Parasites and vectors*, 8(1): 1–9.

Winnebeck, E. C.Millar, C. D.and Warman, G. R. (2010) 'Why does insect RNA look degraded?', *Journal of Insect Science*, 10(1): 159.

Wondji, C. S.Dabire, R. K.Tukur, Z.Irving, H.Djouaka, R.and Morgan, J. C. (2011) 'Identification and distribution of a GABA receptor mutation conferring dieldrin resistance in the malaria vector Anopheles funestus in Africa', *Insect biochemistry and molecular biology*, 41(7): 484–491.

Wong, D. and Dorovini-Zis, K. (1992) 'Upregulation of intercellular adhesion molecule-1 (ICAM-1) expression in primary cultures of human brain microvessel endothelial cells by cytokines and lipopolysaccharide', *Journal of neuroimmunology*, 39(1–2): 11–21.

Wood, O. R.Hanrahan, S.Coetzee, M.Koekemoer, L. L.and Brooke, B. D. (2010) 'Cuticle thickening associated with pyrethroid resistance in the major malaria vector Anopheles funestus', *Parasites and vectors*, 3(1): 1–7.

Xue, R.-D.Ali, A.Kline, D. L.and Barnard, D. R. (2008) 'Field Evaluation of Boric Acid- and Fipronil-Based Bait Stations Against Adult Mosquitoes', *Journal of the American Mosquito Control Association*, 24(3): 415–418.

Xue, R.-D.Kline, D. L.Ali, A.and Barnard, D. R. (2006) 'Application of Boric Acid Baits to Plant Foliage for Adult Mosquito Control', *Journal of the American Mosquito Control Association*, 22(3): 497–500.

Xue, R.-D.Müller, G. C.Kline, D. L.and Barnard, D. R. (2011) 'Effect of Application Rate and Persistence of Boric Acid Sugar Baits Applied to Plants for Control of Aedes albopictus', *Journal of the American Mosquito Control Association*, 27(1): 56–60.

Yamanaka, N.Rewitz, K. F.and O'Connor, M. B. (2013) 'Ecdysone control of developmental transitions: lessons from Drosophila research', *Annual review of entomology*, 58: 497–516.

Yan, T.Chen, H.Sun, Y.Yu, X.and Xia, L. (2016) 'RNA interference of the ecdysone receptor genes EcR and USP in grain aphid (Sitobion avenae F.) affects its survival and fecundity upon feeding on wheat plants', *International journal of molecular sciences*, 17(12): 2098.

Yao, T.-P. *et al.* (1993) 'Functional ecdysone receptor is the product of EcR and Ultraspiracle genes', *Nature*, 366(6454): 476.

Yassine, H.Kamareddine, L.Chamat, S.Christophides, G. K.and Osta, M. A. (2014) 'A Serine Protease Homolog Negatively Regulates TEP1 Consumption in Systemic Infections of the Malaria Vector Anopheles gambiae', *Journal of Innate Immunity*, 6(6): 806–818.

Ye, J.Coulouris, G.Zaretskaya, I.Cutcutache, I.Rozen, S.and Madden, T. L. (2012) 'Primer-BLAST: a tool to design target-specific primers for polymerase chain reaction', *BMC bioinformatics*, 13(1): 134.

Yu, R. *et al.* (2014) 'The insect ecdysone receptor is a good potential target for RNAi-based pest control', *International journal of biological sciences*, 10(10): 1171.

Yunta, C. *et al.* (2016) 'Pyriproxyfen is metabolized by P450s associated with pyrethroid resistance in An. gambiae', *Insect biochemistry and molecular biology*, 78: 50–57.

Zelhof, A. C.Yao, T.-P.Chen, J. D.Evans, R. M.and McKeown, M. (1995) 'Seven-up inhibits ultraspiracle-based signaling pathways in vitro and in vivo.', *Molecular and cellular biology*, 15(12): 6736–6745.

Zengenene, M. P.Munhenga, G.G, C.and Koekemoer, L. L. (2021) 'Characterization of life-history parameters of an Anopheles funestus (Diptera: Culicidae) laboratory strain', *Journal of Vector Ecology*, 46(1): 1–7.

Zhu, J.Chen, L.and Raikhel, A. S. (2003a) 'Posttranscriptional control of the competence factor βFTZ-F1 by juvenile hormone in the mosquito Aedes aegypti', *Proceedings of the National Academy of Sciences*, 100(23): 13338–13343.

Zhu, J.Chen, L.Sun, G.and Raikhel, A. S. (2006) 'The competence factor βFtz-F1 potentiates ecdysone receptor activity via recruiting a p160/SRC coactivator', *Molecular and cellular biology*, 26(24): 9402–9412.

Zhu, J.Miura, K.Chen, L.and Raikhel, A. S. (2003b) 'Cyclicity of mosquito vitellogenic ecdysteroid-mediated signaling is modulated by alternative dimerization of the RXR homologue Ultraspiracle', *Proceedings of the National Academy of Sciences*, 100(2): 544–549.

7 APPENDIX

7.1 Appendix 1: RNAi and qPCR primer information

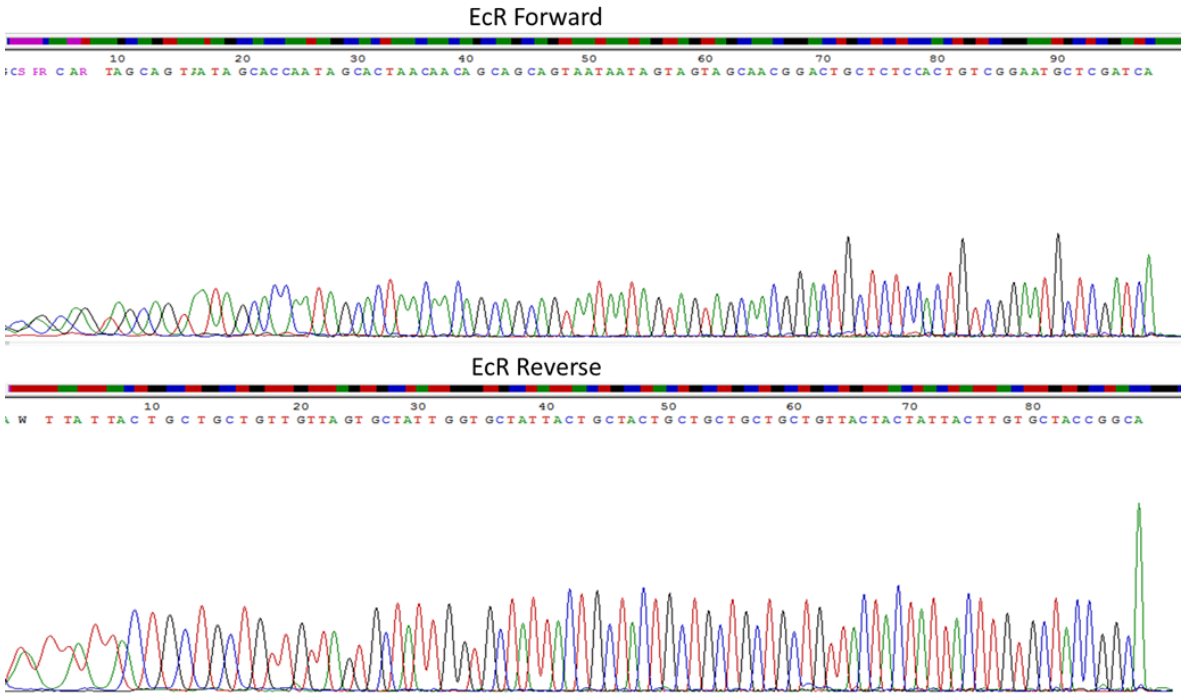
Table S1: RNAi and qPCR primer information.

Name	Sequence (5'-3')	Tm (˚C)	Amplicon size (base pairs)	Reference
An. funestus EcR (forward)	GAT TCT TCC GAC GTA GTG TG	60	484	Designed in this study
An. funestus EcR (reverse)	TCC TCG TTG GGT GAG TTA	60		
An. funestus T7-*EcR* (forward)	TAA TAC GAC TCA CTA TAG GGA GAG ATT CTT CCG ACG TAG TGT G	67	530	Designed in this study
An. funestus T7-*EcR* (reverse)	TAA TAC GAC TCA CTA TAG GGA GAT CCT CGT TGG GTG AGT TA	68		
T7-*GFP* (forward)	TAA TAC GAC TCA CTA TAG GGA GAA CGT AAA CGG CCA CAA GT	66.5	544	Designed by Ms. E. Ekoka (WRIM)
T7-*GFP* (reverse)	TAA TAC GAC TCA CTA TAG GGA GAG GGT GTT CTG GTA GTG	68.4		
qPCR *EcR* (forward)	GCC GGT AGC ACA AGT AAT AG	60	130	Designed in this study
qPCR *EcR* (reverse)	GAT CGA GCA TTC CGA CAG	60		

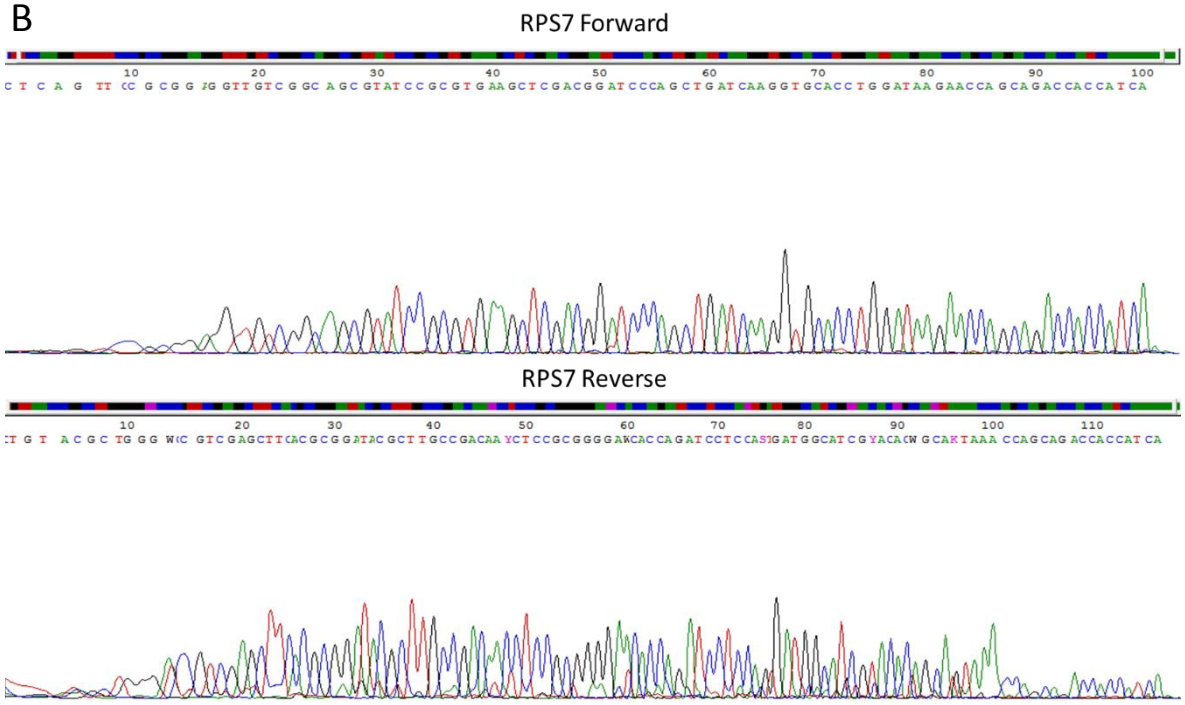
Name	Sequence (5'-3')	Tm (˚C)	Amplicon size (base pairs)	Reference
LRIM9 (forward)	CAG TTC TTC ACC GCA TAG TT	60	117	Designed in this study
LRIM9 (reverse)	TTG TCG TCC AGG TAG AGT T	60		
Lp (forward)	GCT TCG ACA AGG TGT TAG AG	60	104	Designed in this study
Lp (reverse)	AAG ACC AAG AGC GGT AGT	60		
VgR (forward)	TAC TTA CGG CGG GAC TTA T	60	147	Designed in this study
VgR (reverse)	GGA GCT GAT CCT GTA TGA TTG	60		
RPS7 (forward)	TTA CTG CTG TGT ACG ATG CC	60.4	134	Amenya *et al.*, 2008
RPS7 (reverse)	GAT GGT GGT CTG CTG GTT	62.3		
RPL19 (forward)	GAA ACA CCA ACT CCC GAC A	60.2	223	Spillings *et al.*, 2009
RPL19 (reverse)	TCA ACA GGC GAC GCA ACA CA	62.3		
RPS26 (forward)	GAT AAG GCA ATC AAG AAG TTC G	59	160	Spillings *et al.*, 2009
RPS26 (reverse)	TAC GGA CAA CCT TCG AGT GG	62.5		
GAPDH (forward)	GAC TGC CAC TCG TCC ATC	62.2	139	Spillings *et al.*, 2009
GAPDH (reverse)	CCT TGG TCT GCA TGT ACT TG	60.4		
18S (forward)	GTG TAC TTG GGC GTT ACT CTG TG	64.6	116	Spillings *et al.*, 2009
18S (reverse)	CTT TGA GCA CTC TAA TTT GTT CAA	59.7		

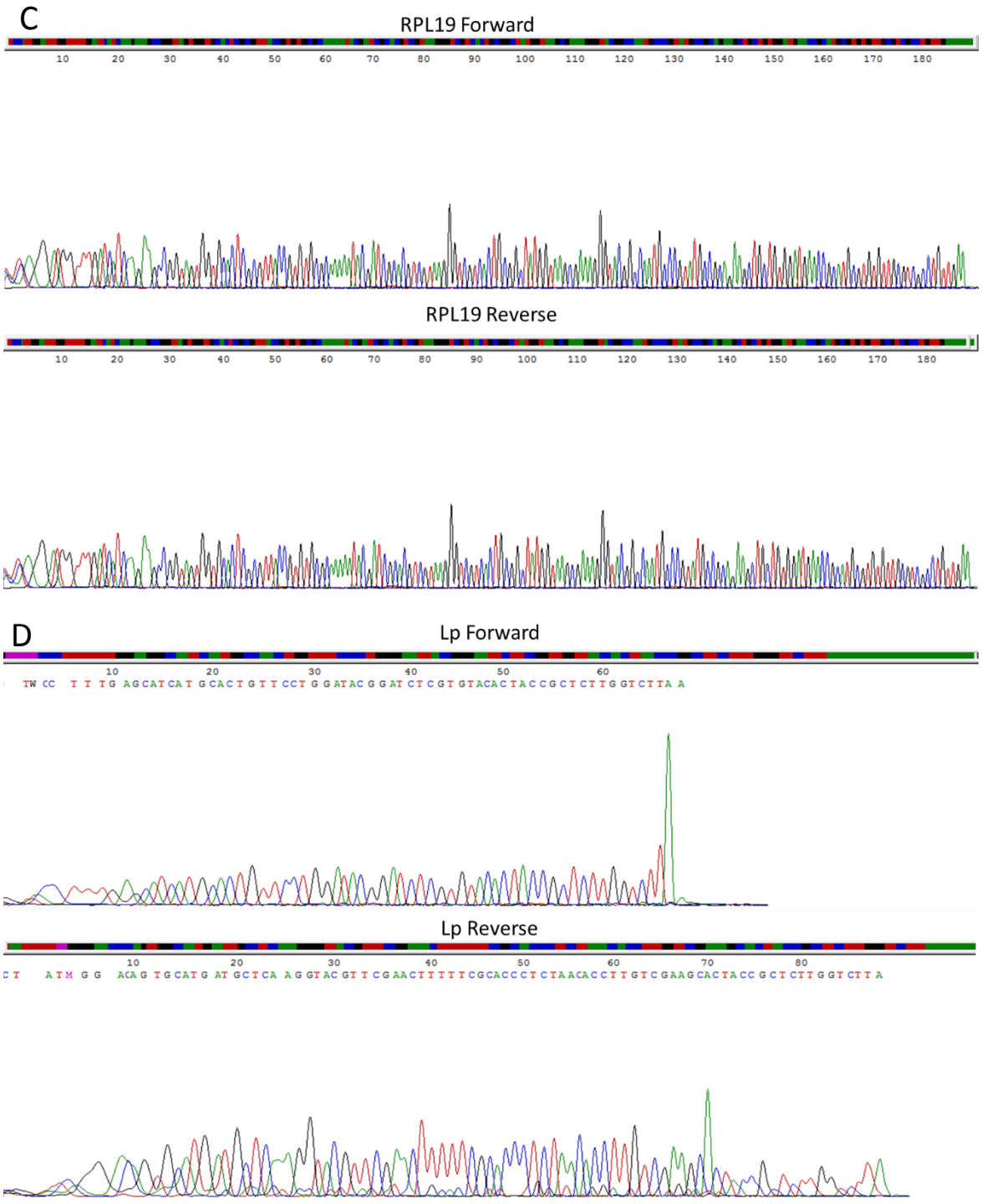
7.2 Appendix 2: Chromatograms of all genes sequenced to confirm primer specificity to respective genes

A



B




C
RPL19 Forward
10 20 30 40 50 60 70 80 90 100 110 120 130 140 150 160 170 180
RPL19 Reverse
10 20 30 40 50 60 70 80 90 100 110 120 130 140 150 160 170 180
D
Lp Forward
10 20 30 40 50 60
Lp Reverse
10 20 30 40 50 60 70 80

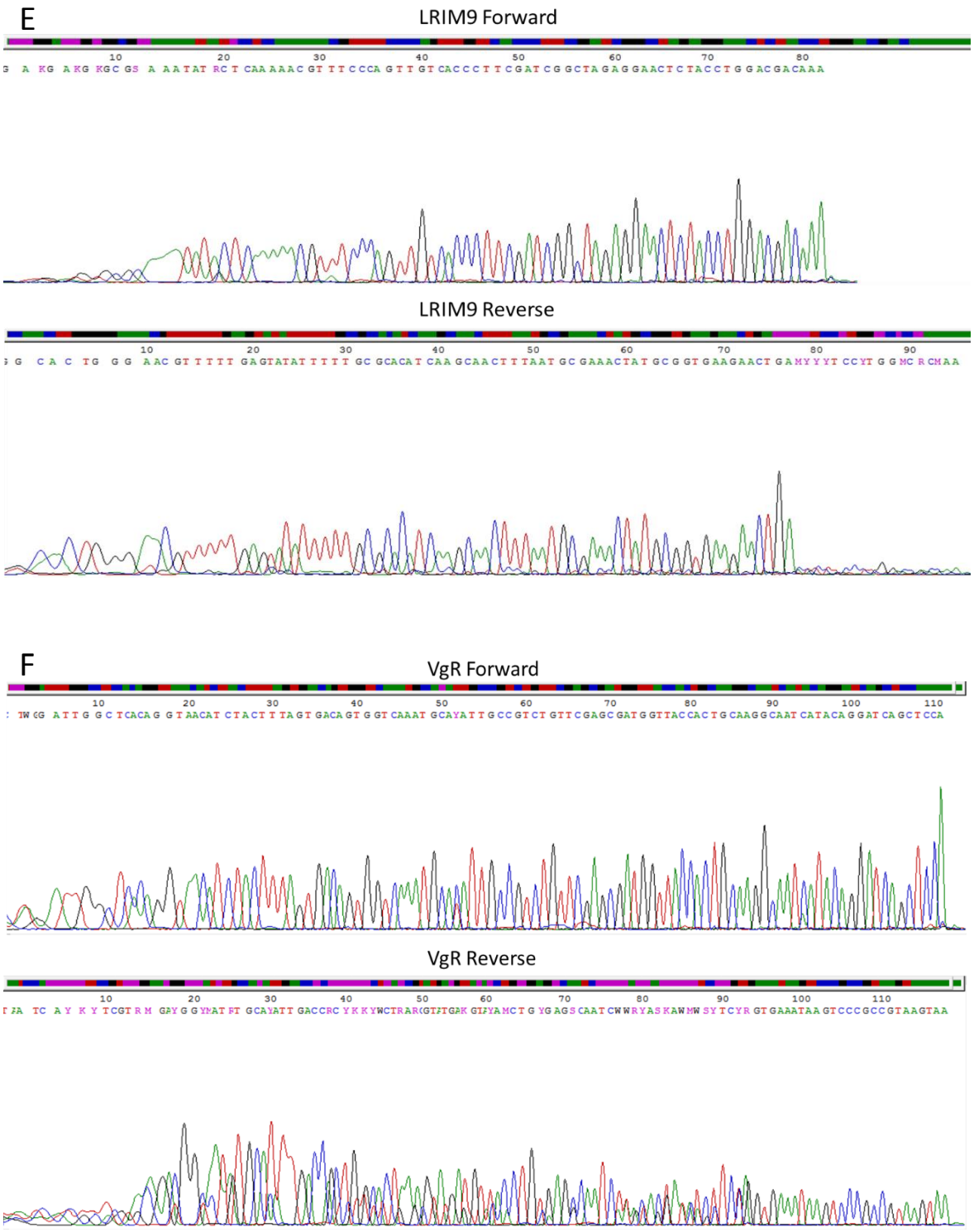


Figure S1: Chromatograms of all *An. funestus* qPCR products sequenced. Chromatograms containing forward and reverse Sanger sequences of *EcR* (A), *RPS7* (B), *RPL19* (C), *Lp* (D), *LRIM9* (E) and *VgR* (F).

7.3 Appendix 3: Agarose gel electrophoresis and spectrophotometry confirm tlRNA integrity and purity from ds*EcR*, ds*GFP* and uninjected *An. funestus* females used in Objective 1

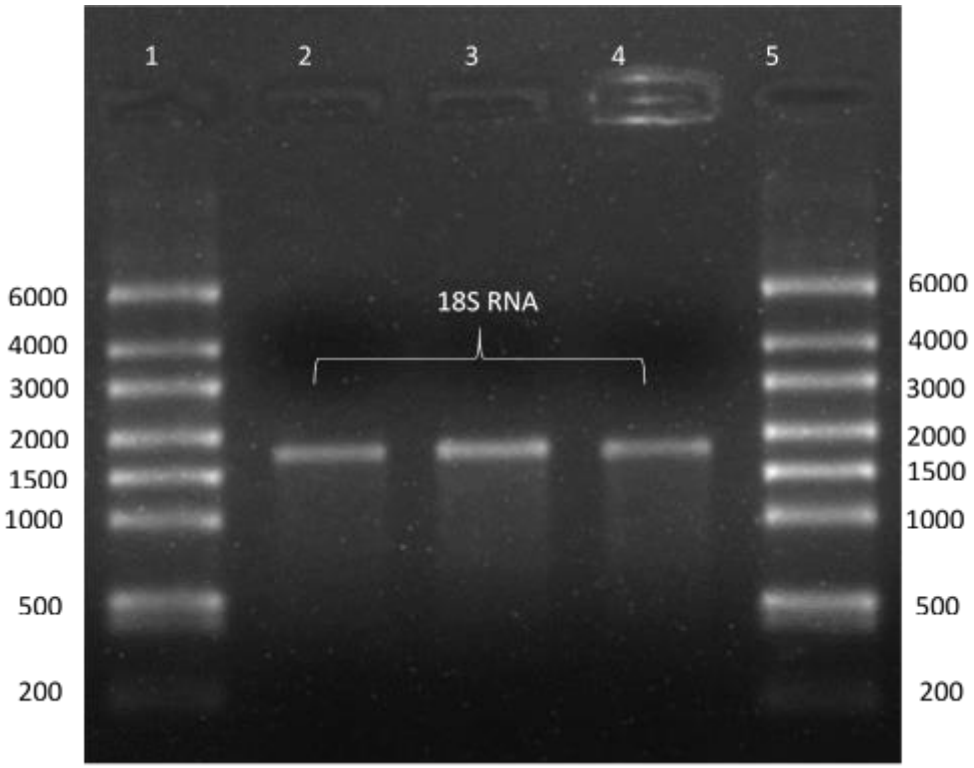


Figure S2: RNA gel electrophoresis confirms the presence of intact and good quality 18S RNA. RNA fragments sized with RiboRuler™ High Range RNA ladder SM 1821 (Lanes 1 and 5). RNA extracted from *An. funestus* females injected with ds*EcR* (Lane 2), ds*GFP* (Lane 3) or uninjected (Lane 4) were confirmed to have integrity, observed by a single intact fragment of 1,923 base pairs in size. This indicated that the RNA extracted was suitable for use in downstream reactions. Results are representative of three biological replicates.

Table S2: A_{260}/A_{280} Purity ratios of total RNA samples extracted from ds*EcR* treated, ds*GFP* treated and uninjected *An. funestus* females used in downstream reactions for objective one.

RNA sample	A_{260}/A_{280}
ds*EcR* 1	2.31
ds*GFP* 1	2.17
Uninjected control 1	2.33
ds*EcR* 2	2.46
ds*GFP* 2	2.20
Uninjected control 2	2.26
ds*EcR* 3	1.97
ds*GFP* 3	1.80
Uninjected control 3	1.84

*The number after the treatment group indicates the biological replicate from which the sample arises.

7.4 Appendix 4: Quantitative PCR results demonstrate specific amplification amongst samples amplified for longevity assay

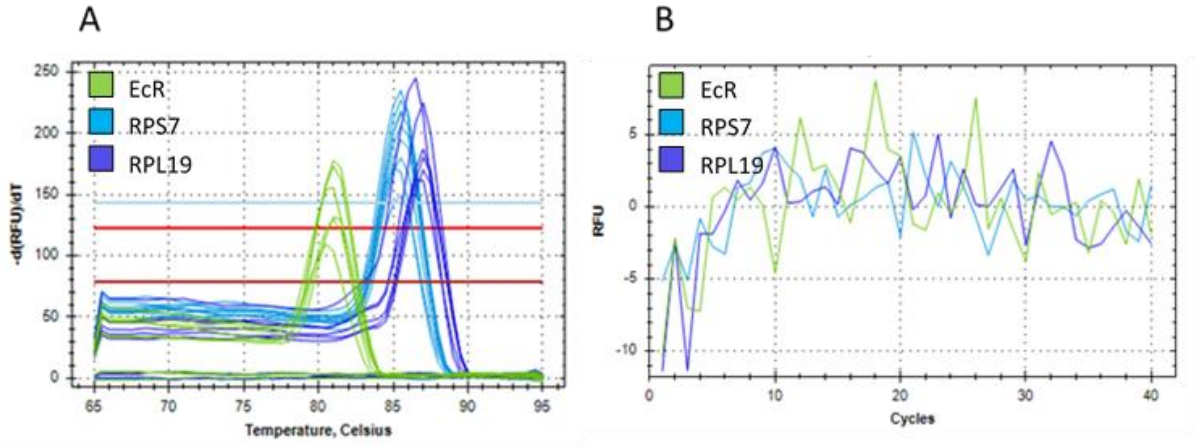


Figure S3: Melt curve and no template controls confirm specific amplification in qPCR. Single melt peaks were visible for each gene amplified validating amplification of a specific gene product amongst samples (A). No template controls did not amplify and confirmed ideal qPCR conditions and non-contaminated reagents (B). Specific amplification of samples ensured accuracy of gene expression analysis. Data is representative of 3 biological replicates.

7.5 Appendix 5: Agarose gel electrophoresis and spectrophotometry confirm tlRNA integrity and purity from ds*EcR*, ds*GFP* and uninjected *An. funestus* females used in Objective 2

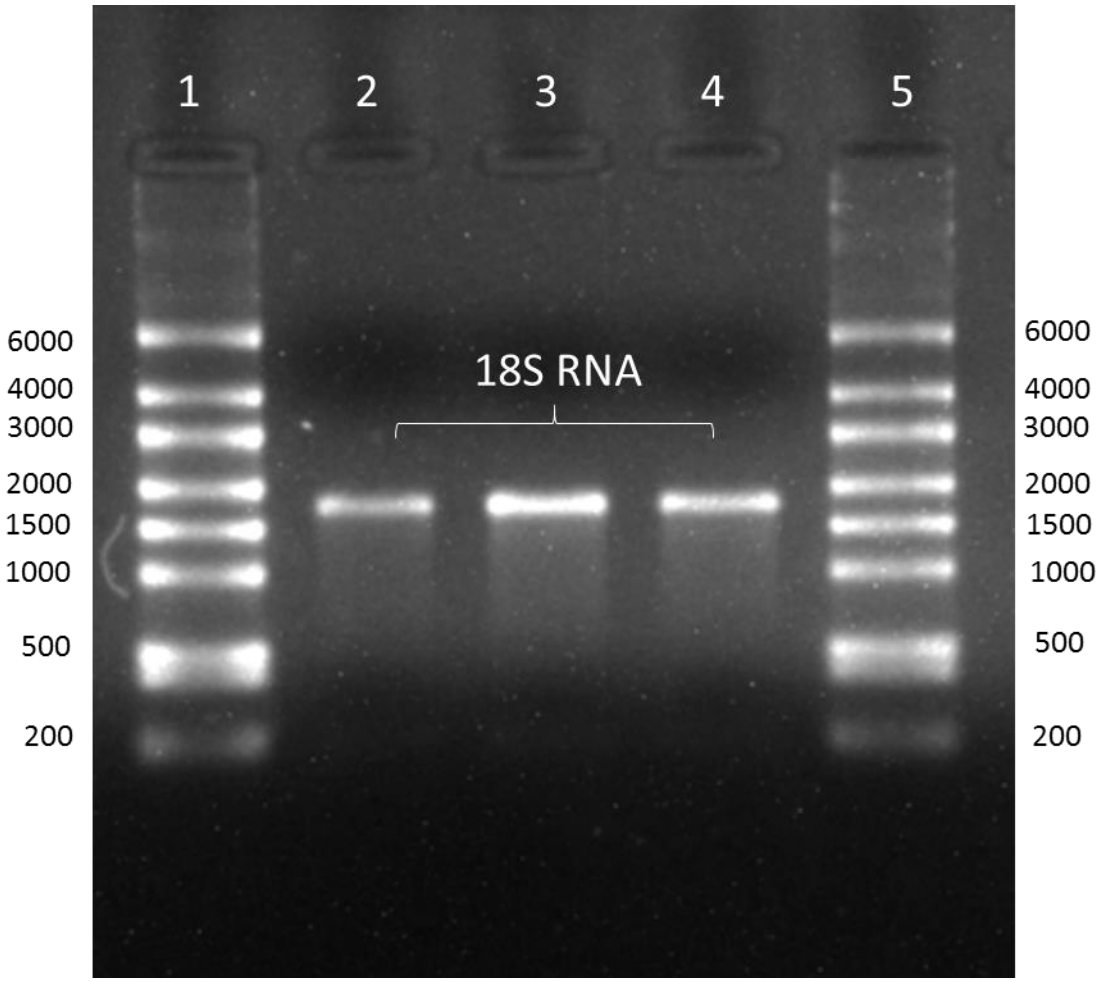


Figure S4: RNA gel electrophoresis confirms the presence of intact and good quality 18S RNA. RNA fragments sized with RiboRuler™ High Range RNA ladder SM 1821 (Lanes 1 and 5). RNA extracted from *An. funestus* females injected with ds*EcR* (Lane 2), ds*GFP* (Lane 3) or uninjected (Lane 4) were confirmed to be good quality and were not denatured, observed by a single intact fragment of 1923 base pairs in size. This indicated that the RNA extracted was suitable for use in downstream reactions. Results are representative of six biological replicates.

Table S3: A_{260}/A_{280} Purity ratios of total RNA samples extracted from ds*EcR* treated, ds*GFP* treated and uninjected *An. funestus* females used in downstream reactions for objective two.

RNA sample	A_{260}/A_{280}
ds*EcR* 1	1.79
ds*GFP* 1	1.88
Uninjected control 1	1.85
ds*EcR* 2	1.75
ds*GFP* 2	1.83
Uninjected control 2	1.82
ds*EcR* 3	1.80
ds*GFP* 3	1.84
Uninjected control 3	1.84
ds*EcR* 4	1.78
ds*GFP* 4	1.94
Uninjected control 4	1.88
ds*EcR* 5	1.86
ds*GFP* 5	1.83
Uninjected control 5	1.84
ds*EcR* 6	1.80
ds*GFP* 6	1.85
Uninjected control 6	1.83

* The number after the treatment group indicates the biological replicate from which the sample arises.

7.6 Appendix 6: Quantitative PCR results demonstrate specific amplification amongst samples amplified for fecundity and fertility assays

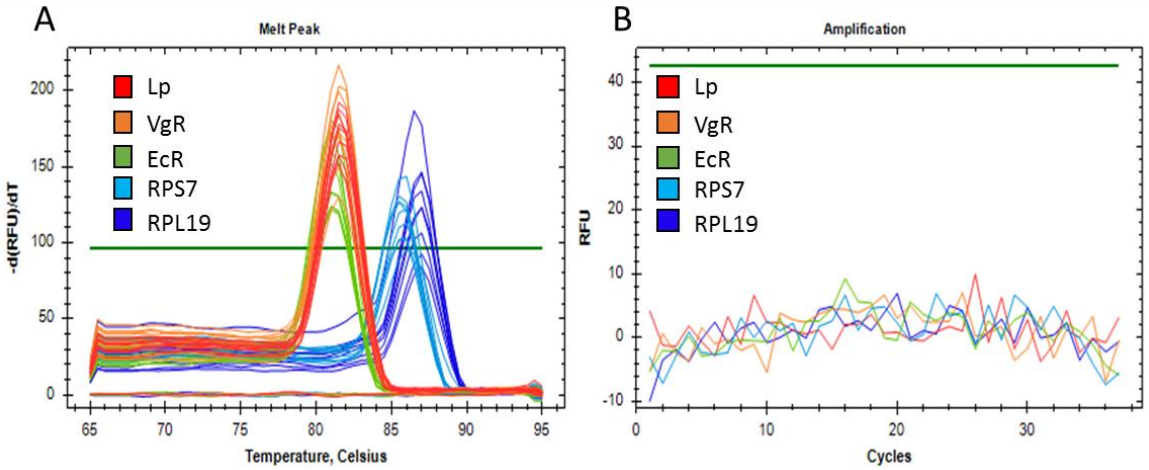


Figure S5: Melt curve and no template controls confirm specific amplification in qPCR. Single melt peaks were observed for the *Lp*, *VgR*, *EcR*, *RPS7* and *RPL19* genes amplified confirming amplification of a specific gene product amongst samples (A). No template controls did not amplify and confirmed ideal qPCR conditions and non-contaminated reagents (B). Specific amplification of samples ensured accuracy of gene expression analysis. Data is representative of six biological replicates.

7.7 Appendix 7: Agarose gel electrophoresis and spectrophotometry confirm tlRNA integrity and purity from ds*EcR*, ds*GFP* and uninjected *An. funestus* females used in Objective 3

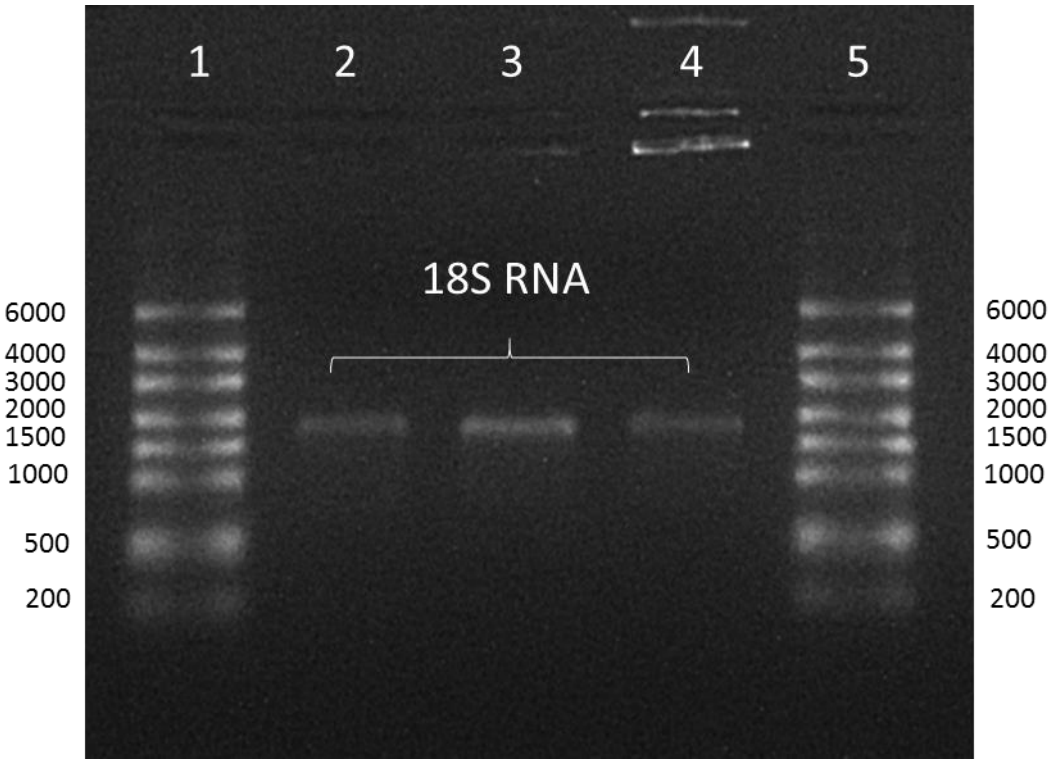


Figure S6: RNA gel electrophoresis confirms the presence of intact and good quality 18S RNA. RNA fragments sized with RiboRuler™ High Range RNA ladder SM 1821 (Lanes 1 and 5). RNA extracted from *An. funestus* females injected with ds*EcR* (Lane 2), ds*GFP* (Lane 3) or uninjected (Lane 4) were confirmed to be of good quality and were not denatured, observed by a single intact fragment of 1,923 base pairs in size. This indicated that the RNA extracted was suitable for use in downstream reactions. Results are representative of five biological replicates.

Table S4: A_{260}/A_{280} Purity ratios of all RNA samples used in downstream reactions for objective three.

RNA sample	A_{260}/A_{280}
ds*EcR* 1	1.83
ds*GFP* 1	1.90
Uninjected control 1	1.84
ds*EcR* 2	1.73
ds*GFP* 2	1.74
Uninjected control 2	1.85
ds*EcR* 3	1.84
ds*GFP* 3	1.91
Uninjected control 3	1.88
ds*EcR* 4	1.71
ds*GFP* 4	1.75
Uninjected control 4	1.95
ds*EcR* 5	1.74
ds*GFP* 5	1.88
Uninjected control 5	1.84

* The number after the treatment group indicates the biological replicate from which the sample arises.

7.8 Appendix 8: Quantitative PCR results demonstrate specific amplification amongst samples amplified for *P. falciparum* infection assay

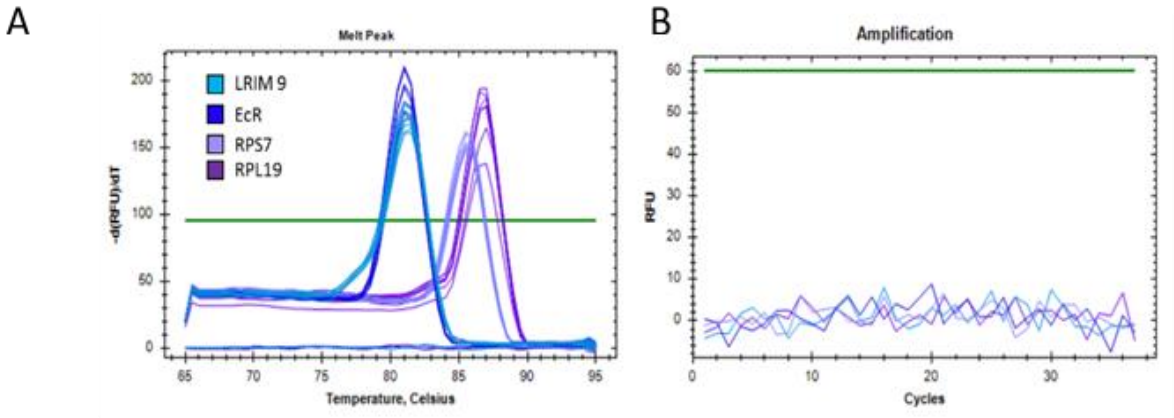


Figure S7: Melt curve and no template controls confirm specific amplification in qPCR. Single melt peaks were observed for the *LRIM9*, *EcR*, *RPS7* and *RPL19* genes amplified confirming amplification of a specific gene product amongst samples (A). No template controls did not amplify which confirmed ideal qPCR conditions and non-contaminated reagents (B). Specific amplification of samples ensured accuracy of gene expression analysis. Data is representative of five biological replicates.

7.9 Appendix 9: *Anopheles funestus* fecundity assay data

Table S5: Raw data obtained from *An. funestus* fecundity assay.

Treatment	n fed	% mated (n)	% unmated (n)	% oviposited (n)	% did not oviposit (n)
ds*EcR* 1	8	88 (7)	13 (1)	38 (3)	62 (5)
ds*EcR* 2	3	60 (2)	40 (1)	0 (0)	100 (3)
ds*EcR* 3	9	88 (8)	12 (1)	12 (1)	88 (8)
ds*EcR* 4	3	66.7 (2)	33.3 (1)	0 (0)	0 (0)
ds*EcR* 5	18	66.7 (12)	33.3 (6)	11 (2)	89 (16)
ds*EcR* 6	8	87.5 (7)	12.5 (1)	37.5 (3)	62.5 (5)
ds*GFP* 1	12	67 (8)	33 (4)	42 (5)	58 (7)
ds*GFP* 2	6	50 (3)	50 (3)	33 (2)	67 (4)
ds*GFP* 3	9	67 (6)	33 (3)	22 (2)	78 (7)
ds*GFP* 4	10	40 (4)	60 (6)	0 (0)	0 (0)
ds*GFP* 5	15	60 (9)	40 (6)	26.7 (4)	73.3 (11)
ds*GFP* 6	9	55.6 (5)	44.4 (4)	55.6 (5)	44.4 (4)
Uninjected 1	15	74 (11)	26 (4)	40 (6)	60 (9)
Uninjected 2	15	60 (9)	40 (6)	27 (4)	73 (11)
Uninjected 3	19	58 (11)	42 (8)	47 (9)	53 (10)
Uninjected 4	9	55.6 (5)	44.4 (4)	11 (1)	89 (8)
Uninjected 5	9	55.6 (5)	44.4 (4)	11 (1)	89 (8)
Uninjected 6	17	76.5 (13)	23.5 (4)	9 (53)	8 (47)

*The number after the treatment group indicates the biological replicate from which the sample arises.

7.10 Appendix 10: *Anopheles funestus* infection with *P. falciparum* data

Table S6: Raw data obtained from *An. funestus* infection with *P. falciparum*.

Treatment	Sample size (n) after injection	% fed (n)	% dissected (n)	% infected (n)
ds*EcR* 1	57	36.8 (21)	12.3 (7)	8.8 (5)
ds*EcR* 2	88	5.7 (5)	2.3 (2)	1.1 (1)
ds*EcR* 3	35	0 (0)	0 (0)	0 (0)
ds*EcR* 4	49	26.5 (13)	22.4 (11)	14.3 (7)
ds*EcR* 5	72	55.6 (15)	20.8 (15)	12.5 (9)
ds*GFP* 1	68	38.2 (26)	30.9 (21)	2.5 (17)
ds*GFP* 2	91	15.4 (14)	11.0 (10)	4.4 (4)
ds*GFP* 3	88	9.0 (8)	4.5 (4)	4.5 (4)
ds*GFP* 4	78	52.7 (41)	30.8 (24)	24.4 (19)
ds*GFP* 5	83	16.9 (14)	18.1 (15)	15.7 (13)
Uninjected 1	98	33 (32)	15.3 (15)	14.3 (14)
Uninjected 2	87	14.9 (13)	8.0 (7)	5.7 (5)
Uninjected 3	93	16.1 (15)	7.5 (7)	7.5 (7)
Uninjected 4	79	20.3 (16)	13.9 (11)	11.4 (9)
Uninjected 5	93	23.7 (22)	18.3 (17)	14.0 (13)

*The number after the treatment group indicates the biological replicate from which the sample arises.

7.11 Appendix 11: Ethics waiver

ANIMAL RESEARCH ETHICS COMMITTEE

Registration number: AREC-101210-002

Date: July 1, 2019

Certificate reference: 20190701-7O
Category: O
Re: Waiver from the Animal Research Ethics Committee of the University of the Witwatersran

Reference : Animal Ethics to complete
Re: Waiver from the Animal Research Ethics Committee of the University of the Witwatersrand
HoD applicant : Lizette Koekemoer
Staff number : 09700304
Degree : PhD/Msc Candidates
Study Title : "Studies on malaria vectors".
Department: Wits Research Institute for Malaria;
laboratory
Supervisor: Lizette Koekemoer, Givemore Munhenga, Yael Dahan-Moss, Shune Oliver, Basil Brooke and Maria Kaiser
Email: lizette.koekemoer@wits.ac.za
Address: 7 York Road, Parktown, Johannesburg, 2001
Tel: + 011-717 2486;
Full clearance certificate from the AREC of the University of the Witwatersrand is NOT required.
Reason: This study uses mosquitoes (invertebrates).
Comment/Notes :

1) This is a General Waiver for the PI and listed Supervisors.
2) Individual researchers and MSc & PhD candidates may require Ethics Clearance in the own name according to applicable rules of the Post-Graduate and other Committees.
3) Feeding of the mosquitos should be specified.

Please contact me should you require further information.

GP Candy

Geoffrey Candy PhD
Chair : Animal Research Ethics Committee

Geoffrey P Candy PhD
Professor, Department of Surgery, Faculty of Health Sciences, University of the Witwatersrand, *7 York Road Parktown 2193, Johannesburg; Tel: 27-11-717-2574; Email: geoffrey.candy@wits.ac.za*

7.12 Appendix 12: Bioethics clearance certificate

UNIVERSITY OF THE WITWATERSRAND, JOHANNESBURG

Research Office

INSTITUTIONAL BIOSAFETY COMMITTEE
(R 14/16)

CLEARANCE CERTIFICATE **PROTOCOL NUMBER: 20180402Lab**

BRIEF DESCRIPTION OF APPLICATION:

Laboratory situated in room 10M02 10th Floor, Wits Research Institute for Malaria, Medical School

APPLICANT: Professors M/LL Coetzee and Koekemoer

SCHOOL/DEPARTMENT : Molecular Medicine and Haematology

DATE CONSIDERED: By Circulation 29 November 2018

DECISION OF COMMITTEE: Approved unconditionally

These laboratories are considered to meet the standards of the Institutional Biosafety Committee (IBC), for BSL2 approval, as specified in the IBC's published Standard Operating procedures.
Any change to the type of biohazardous agents being handled should be reported to the IBC
DAFF - Reg no 39.2/University of Witwatersrand - 18/041 expiry date 03 December 20-21

1. This clearance certificate expires on 03 December 2023 and may be renewed on application.

DATE OF APPROVAL: 03 December 2019

CHAIRPERSON: James F. S. Larkin 2019.04.15 12:07:53 +02'00'

(Professor J Larkin)

DECLARATION OF APPLICANT:

To be completed in duplicate and **one copy** returned to the University of the Witwatersrand, Faculty of Health Sciences, Research Office, Office 301, Phillip Tobias Building, 29 Princess of Wales Terrace, Parktown,2193.

1. I have read, understood and accepted the approval conditions above
2. I note that the University Safety Officer, or his/her representative, may at any reasonable time inspect my laboratory or trial site to ensure compliance with current Health and Safety legislation. I undertake to offer my full co-operation in any such inspection.
3. I have read, understood and will comply with the *recommended standard operating procedures for the handling of biohazardous materials* posted at http://intranet.wits.ac.za/academic/uro/Pages/Institutional-Biosafety-Committee-(IBC).aspx

Signed: Koekemoer **Date:** 1/1/2019

PLEASE QUOTE THE PROTOCOL NUMBER IN ALL ENQUIRIES

7.13 Appendix 13: Certificate for registration of facility

agriculture,
forestry & fisheries

Department:
Agriculture, Forestry and Fisheries
REPUBLIC OF SOUTH AFRICA

Genetic Resources, Department of Agriculture, Forestry and Fisheries
Private Bag X973, Pretoria 0001

Enquiries: Bathobile Mahlangu • **Tel**: 012 319 6165 • **Fax:** 012 319 6298 • **E-mail**: BathobileM@daff.gov.za •**Ref**: 39.2/University of Witwatersrand -18/019

Prof P B Arbuthnot
University of Witwatersrand
Faculty of Health Sciences
School of Pathology
Department of Molecular Medicine and Haematology
Wits Research Institute for Malaria
7 York Road
Parktown
2193

+27 (0) 11 717 2365 **(Tel)**
+27 (0) 11 717 2395/ +27 (0) 86 529 6833 **(Fax)**
Patrick.Arbuthnot@wits.ac.za **(E-mail)**

Dear Prof Arbuthnot

RE: REGISTRATION OF FACILITY

With reference to the application to register a facility, submitted in terms of the Genetically Modified Organisms Act, 1997 (Act No. 15 of 1997). Registration number **39.2/University of Witwatersrand -18/041.**

The facility is hereby registered; please find attached your certificate which serves as proof of registration. Please familiarize yourself with the Standard Operating Procedure approved for Regulation 2(2) to determine whether your current activities or any future activities would require an additional contained use permit or not.

Please consult the website of the Department at www.daff.gov.za (Branches, Agricultural Production, Health & Food Safety/ Genetic Resources/ Biosafety) for the latest application forms and the SOP document referred to in the above paragraph.

If any of the provisions of the Genetically Modified Organisms Act, 1997 (Act No. 15 of 1997), including any condition of any permit issued in terms of the GMO Act, is not complied with at all times, you will be subject to prosecution in terms of Section 21 of the GMO Act, 1997.

DIRECTORATE GENETIC RESOURCES
2018 -12- 03
PRIVATE BAG X973 PRETORIA 0001
REGISTRAR - GMO ACT

Yours sincerely

Ms N L Mkhonza
Registrar: Genetically Modified Organisms Act, 1997 (Act No. 15 of 1997)

7.14 Appendix 14: Turnitin report